AsCA'98

3rd Conference of the Asian Crystallographic Association

Hotel Equatorial, Bangi
MALAYSIA
13-15 October 1998

in association with

Universiti Kebangsaan Malaysia

Program and Abstracts

AsCA'98

3rd Conference of the
Asian Crystallographic Association
Hotel Equatorial Bangi
MALAYSIA
13-15 October 1998

in association with

Universiti Kebangsaan Malaysia

Program and Abstracts

Organisisng Committes

International Organising Committee

Prof. S.L. Chang	- *Chairman*	Taiwan
Prof. S.J. Chung		Korea
Prof. A.H. Othman		Malaysia
Prof. J. Simpson		New Zealand
Dr. M. Spackman		Australia
Prof. L.H. Lai		China
Dr. K. Lal		India
Prof. H. Toraya		Japan
Dr. K. Ogawa		Japan

International Program Committee

Prof. T. Yamanaka - *Chairman*	Japan
Dr. M. Guss	Australia
Prof. R. Cheary	Australia
Prof. S.W. Suh	Korea
Dr. G. Jameson	New Zealand
Prof.. H.K. Fun	Malaysia
Dr. R. Withers	Australia
Prof. Z. Zhang	China
Prof. M. Sakata	Japan
Prof. K. Ohsumi	Japan
Prof. K. Miki	Japan
Prof. Yu Wang	Taiwan

Local Organising Committee

Prof. A. Hamid Othman - *Chairman*
Dr. Chen Wei - *Secretary /Treasurer*
Dr. Yang Farina A. Aziz *Assistant Secretary*
Dr. Lo Kong Mun *Assistant Treasurer*
Prof. Bohari Mohd. Yamin
Prof. Fun. Hoong Kun
Dr. Musa Ahmad
Mr Mohammad Kassim

General Information

AsCA'98 is organised by the Asian Crystallographic Associantion in association with Universiti Kebangsaan Malaysia.

Conference Venue and Accommodation

The map inside the front cover shows the locations of the Hotel Equatorial, Kamsis Ibu Zain, Banks and Bangi Utama Shopping Centre. The Kamsis is about 7 km from Hotel Equatorial, the conference venue. Lectures will be at the Ballroom, Raya, and Melati 2 and 3 rooms. Posters will be in the lobby just outside the Ballroom. Trade exhibitors will be at the Chempaka room next to the Ballroom. The AsCA Secretariat will be at the Melati 1 room. The Tour and Souvenier desks will be at the Hotel Lobby.

Registration / Information Desk

Registration/Information Desk will be located at Hotel Equatorial Lobby and will remain open from 10.00 - 17.30 on Monday 12 October and from 07.30 – 12 noon on Tuesday October 13. From 13.00 the Registration/Information Desk will be at the Secretariat Desk located in the Melati 1 room and will remain open for the remainder of the Conference.

Name Badges

Name badges will be issued to all registrants during registration. Participants are kindly requested to wear their badges throughout the meetings and this will also help hotel staff for the purpose of indentifications. The following colour scheme will be used.

Active participants	Green
Accompanying persons	Yellow
Local Organising Committee/Secretariat	Red
Exhibitors	Blue
International Organising Committee and AsCA Council Members	Purple

Mail and Messages

Mail and messages for conference participants will be available from the Secretariat or Registration Desk.

Telephones

Telephones for outgoing International calls are available in rooms at Hotel Equatorial. For incoming calls, messages may be taken at the Hotel Equatorial front desk whilst scientific sessions are in progress, but it will NOT be possible to summon participants to take incoming calls.

Hotel Equatorial	Phone: 6 03 677 2222	Fax: 6 03 677 2888
Kamsis Ibu Zain	Phone: 6 03 8292601	Fax: 6 03 829 2600

Bangi Shopping Centre

The location of the shopping centre is shown in the map. The Warta supermarket is located in this shopping centre and a variety of goods and food are available. The shopping centre also houses a pharmacy and several popular fast-food outlets, a Chinese and a Japanese restaurant.

Banks

The locations of Bank Bumiputera Malaysia and Maybank are indicated in the map. Banking hours are from 9.30 – 15.30.

Meals and Refreshments

Morning and afternoon coffee

Morning and afternoon coffee with light snacks will be provided for full and student participants at the lobby of the lecture rooms.

Lunch

Lunches are provided free of charge for full and student participants and will be at the Coffee Garden Restaurant and the Golden Pheonix Chinese Restaurant. The lunches are sponsored **by Bruker AXS, ICDD and Marresearch**.

Society Meetings

Asian Crystallographic Association Committee
Tuesday, October 13. Venue and time will be announced.

Society of Crystallographers in Australia.
Thursday, October 15, 13.00-14.00. Melati 2 & 3.

IUCr Commission on Journals
Tuesday, October at 13:15. Raya room

Sponsors of AsCA'98

The Asian Crystallographic Association wishes to thank the following professional bodies and institutions for their contribution towards the funding and organisation of AsCA'98.

The International Union of Crystallography
The Crystallographic Society of Japan
The Society of Crystallographers in Australia
Universiti Kebangsaan Malaysia
Malaysia Airlines
Hotel Equatorial Bangi
Malaysian Tourist Development Corporation

The Asian Crystallographic Association also wishes to gratefully acknowledge genereous financial support from the following companies.

Rigaku International Japan
MAC Science
International Center for Diffraction Data
Bruker AXS
Marresearch

Last but not least thank you to those individuals who have worked tirelessly to make the AsCA'98 Conference a success.

Social Events

Welcoming Reception

A welcoming reception and get together will be held at the Poolside of the Hotel Equatorial from 20.00 on Monday October 12 for all registrants (full, student and accompanying persons). Refreshment and snacks will be served . The reception is sponsored by **MAC Science**

Farewell Banquet

A farewell banquet for all registrants (full, student and accompanying persons) will be held in the Ballroom on Wednesday, October 14 at 20.00. It will be a 8 course Chinese dinner. This banquet is sponsored by **Rigaku International Japan**

Local Tours

Participants are reminded that tours can be arranged daily at the tour desk. A minimum of 10 pax is required for each departure to commence. Please register a day earlier. Group tours are planned for Friday October 16, please fill in the required form and hand it over at the tour desk.

Opening Ceremony

The opening ceremony for AsCA'98 will be held in the Ballroom from at 8.30. The speakers will be:

Welcome by Prof. Abdul Hamid Othman, Chairman, Local Organising Committee

Prof. Shih-Lin, Chang	Chairman, International Organising Committee
Prof. Ze Zhang	President, Asian Crystallographic Association
Prof. Edward N. Baker	President, International Union of Crystallography
Prof. Mohd. Salleh Mohd. Yasin	Deputy Vice-Chancellor, Universiti Kebangsaan Malaysia

Scientific programme

The Scientific Program of AsCA'98 includes IUCr'50 anniversary symposium, 4 Plenary Lectures, 14 Microsymposium and Poster Sessions on wide scope crystallography.

I. IUCr 50 anniversary symposium

To celebrate the 50th Anniversary of the International Union of Crystallography, three IUCr'50 symposia will be held in the morning or afternoon session at the 1998 meetings of the Regional Associates ACA, AsCA and ECA. The IUCr'50 symposium was planned under the auspices of IUCr Executive Committee (EC).They are sponsored by the IUCr and each of them will consist of 4 lectures. AsCA'98 is willing to make a joint program with EC. The IUCr'50 Anniversary Symposium in the AsCA'98 Kulala Lumpur Meeting will be held in the morning on October 14 at the main hall.

Professor Edward N. Baker, President of the IUCr will be the symposium chairman. He will give a lecture about the history of the IUCr. The other three lectures will have a biocrystallography, a chemical and a physical flavor respectively.

THE HISTORY OF THE IUCr.
Professor Edward N. Baker (Massy University, New Zealand)
ASPECTS OF CRYSTALLOGRAPHIC SCALING IN CRYSTALS QUASICRYSTALS AND BIOMOLECULES
Professor Aloysio Janner (University of Nijmegen, Netherlands)
TOWARD A GRAMMAR OF CRYSTAL PACKING.
Professor Carolyn P. Brock (University of Kentucky, USA)
STRUCTURE AND FUNCTION OF MEMBRANE PROTEIN COMPLEX.
CYTOCHROME C OXIDE FROM BOVINE HEART.
Professor Tomitake Tsukihara (Osaka University, Japan)

II Plenary lecture

Four plenary lectures on new crystallographic progresses are addressed in the morning on October 13 and 15.

Spring-8 MOVES INTO USER OPERATION.
Dr Hiromichi Kamitsubo (Director of Spring-8, Japan)
DIRECT DETERMINATION OF X-RAY REFLECTION PHASES USING MULTIPLE DIFFRACTION: THEORY AND EXPERIMENT.
Professor Shin-Lin Chang (Department of Physics, Tsing Hua University, Taiwan)
REAL TIME IN SITU OBSERVATION OF CHEMICAL REACTIONS.
Professor Yuji Ohashi (Department of Chemistry Tokyo Institute of Technology, Japan)
DRUG DESIGN AGAINST SHIFTING TARGETS.
Professor Peter M. Colman (Division of Biomolecular Engineering, CSIRO, Australia)

III. Microsymposium

The following microsymposia will be organized by the convenors shown in the parenthesis. These symposia will be undertaken within 3 days, October 13~15. All symposia have one or two oral and poster sessions. All symposia have several oral presentations and will have parallel sessions.

MS-01. Diffraction theory (S.L. Chang)
MS-02. Synchrotron radiation (K. Ohsumi)
MS-03. Neutron diffraction (C.J. Howard)
MS-04. Electron diffraction (R. L. Withers)
MS-05. Structure refinement by powder diffraction (B.H. O'Connor)
MS-06. Aperiodic structures and incommensurate phases (A. Yamamoto)
MS-07. Biocrystallography and protein structure (S.W. Suh)
MS-08. Structural studies of coordination and organometallic compounds
Structural studies of organic and drug-related compounds (G. B.Jameson)
MS-09. Inorganic compounds and mineral (T. Yamanaka)
MS-10. Materials Chemistry (Y. Ohashi)
MS-11. Phase transitions (S.W. Wilkins)
MS-12. Charge density (Y. Wang)
MS-13. Diffraction under the extreme condition (O. Shimomura)
MS-14. Instrumentation and Other category

Program Schedule

Oral Presentation

Room	Ballroom	Melati	Raya	Lobby
October 13	**Tuesday**			
9:00- 9:50	PL-1	PL-2		
10:00-12:00	13A1(MS-07(I))	13B1(MS-02)	13C1(MS-12)	
13:30-16:00				Poster-1
16:00-18:00	13A2(MS-08(I)	13B2 (MS-05)	13C2(MS-04)	
October 14	**Wednesday**			
9:00- 9:50	IUCr'50			
10:00-12:00	IUCr'50			
13:30-16:00				Poster-2
16:00-18:00	14A2(MS-09)	14B2(MS-01,14)	14C2(MS-06)	
October 15	**Thursday**			
9:00- 9:50	PL-3	PL-4		
10:00-12:00	15A1(MS-08(II))	15B1(MS-10)	15C1(MS-03)	
13:30-16:00				Poster-3
16:00-18:00	15A2(MS-07(II)	5B2 (MS-11)	15C2	

IV. Poster session

There will be four poster sessions in AsCA'98 Science program. Poster sessions will run from 1:30 to 4:00pm on the days listed. Posters should be hung between 9:00am and 1:00pm and should be removed by 7:00pm. The poster halls will be open for viewing all day long. The odd numbered posters should be presented in the first half poster time and the even numbered in the last half.

Poster Presentation and Date

Room : Lobby 13:30 - 16:00

Date	Microsymposium
October 13 Poster-1	MS-01,14, MS-05, MS-07(I), MS-08(I), MS-09(I), MS-12
October 14 Poster-2	MS-02, MS-04, MS-06, MS-07(II), MS-08(II), MS-11
October 15 Poster-3	MS-03, MS-07(III), MS-08(III), MS-09(II), MS-10

Program Schedule

October 13 Tuesday

Plenary Talk

room: Ballroom

Chairman A.H. Othman

9:00-9:50 PL-1	SPring-8 MOVES INTO USER OPERATION. H. Kamitsubo

room:Melati

Chairman T. Tsukihara

9:00-9:50 PL-2	DRUG DESIGN AGAINST SHIFTING TARGETS. P. M. Colman

Oral session

13A1. room:Ballroom

MS-07 (I) Biocrystallography and Protein Structure

Chairman S. W. Suh Co-chairman E. N. Baker

10:00-10:20 13A1-1	A PROLINE-SPECIFIC AMINOPEPTIDASE WITH A DINUCLEAR MANGANESE CENTRE. M.C. Wilce, C.S. Bond, N.E. Dixon, H.C. Freeman, J.M. Guss, P.E. Lilley and J.A. Wilce
10:20-10:40 13A1-2	CRYSTALLOGRAPHIC STUDIES OF RETROVIRAL MATRIX ANTIGENS FROM SI MLV AND EIAV. Z. Rao
10:40-11:00 13A1-3	STRUCTURE OF PHYSALIS MOTTLE VIRUS. S. S. Krishna, S.K. Munshi, C.N. Hiremath, S. Suryanarayana, A.N.K. Jacob, M. Shastri, H.S. Savithri and M.R.N. Murthy
11:00-11:20 13A1-4	CRYSTAL STRUCTURE OF PHOSPHOENOLPYRUVATE CARBOXYLASE FROM ESCHERICHIA COLI. Y. Kai, H. Matsumura, T. Inoue, K. Terada, Y. Nagara, T. Yoshinaga, A. Kihara, K. Tsumura and K. Izui
11:20-11:40 13A1-5	CRYSTAL STRUCTURE OF HEMOPEXIN: A UNIQUE HEME BINDING SITE FORMED BY TWO β-PROPELLER DOMAINS. M. Paoli, H. M. Baker, E.N. Baker and B. F. Anderson
11:40-12:00 13A1-6	THE CRYSTAL STRUCTURE OF THE ENDONUCLEASE DOMAIN OF COLICIN E7 COMPLEXED WITH ITS INHIBITOR Im7. T.P.Ko, W.Y. Ku, S.S. Chern and H. S. Yuan, C-C. Liaw and K-F. Chak

13B1. room:Melati

MS-02 Synchrotron Radiation

Chairman K. Ohsumi Co-chairman S. Sasaki

10:00-10:15 13B1-1	PHASE-RETRIEVAL X-RAY DIFFRACTOMETRY: A TOOL FOR UNAMBIGUOUS CHARACTERIZATION OF CRYSTALLINE MATERIALS. A.Y. Nikulin
10:15-10:30 13B1-2	THREE-WAVE GRAZING INCIDENT X-RAY DIFFRACTION:A METHOD FOR DIRECT PHASE DETERMINATION OF SURFACE IN-PLANE REFLECTION Y.S. Haung, S.L.Chang, C.H.Chao, M.T. Tang, and Y.P. Stetsko
10:30-10:45 13B1-3	MAGNETIC STRUCTURE OF Fe/Gd MULTILAYERS DETERMINED BY X-RAY MAGNETIC SCATTERING. H. Hashizume, N. Hosoito, N.I shimatsu and G. Srajer
10:45-11:00 13B1-4	INFLUENCE OF SITE-SELECTIVE IRON IONS ON THE MAGNETIC CIRCULAR X-RAY DICHROISM IN Fe[NixFe2-x]O4 F. Saito, T. Toyoda, T. Mori, M. Tanaka, K. Hirano and S. Sasaki
11:00-11:15 13B1-5	CRYSTAL STRUCTURE ANALYSIS OF THE SUPERCONDUCTING PrBa2Cu3Ox COMPOUND J. Ye, Z. Zou, K. Oka, Y. Nishihara, A. Matsushita and T. Matsumoto
11:15-11:30 13B1-6	SYNCHROTRON X-RAY DIFFRACTION STUDIES ON INTER-PLANETARY DUST PARTICLES: L2005AE6 AND L2005AG17. K. Ohsumi and M.E. Zolensky

October 13 Tuesday

11:30-11:45 13B1-7	LOCAL DISTORTION OF LiNiO2, Li(Ni,Co)O2 AND LiMn2O4 WITH LiDEINTERCALATION IN CATHODE MATERIALS OF RECHARGEABLE Li BATTERIES, STUDIED BY IN SITU X-RAY ABSORPTION FINE STRUCTURE ANALYSIS. I. Nakai, Y. Shiraishi and F. Nishikawa
11:45-12:00 13B1-8	HIGH-RESOLUTION POWDER DIFFRACTION EXPERIMENTS USING SYNCHROTRON RADIATION AT BEAMLINE BL02B1 IN SPring-8. H. Okudera, Y. Kubota, H. Hibino, M. Yamakata, H. Toraya and Y. Noda

13C1. room:Raya

MS-12 Charge Density

Chairman Yu. Wang Co-chairman N. Ishizawa

10:00-10:20 13C1-1	INTERMOLECULAR INTERACTION ENERGIES FROM ACCURATE X-RAY DIFFRACTION DATA. M.A. Spackman and A.S. Mitshell
10:20-10:40 13C1-2	4f-ELECTRON DENSITY ANALYSIS IN RARE-EARTH CRYSTALS TAKING INTO ACCOUNT SPIN-ORBIT INTERACTION. K. Tanaka and Y. Onuki
10:40-11:00 13C1-3	CHARGE DENSITIES OF CRYSTALLINE MATERIALS BY THE MAXIMUM ENTROPY METHOD. M. Sakata
11:00-11:15 13C1-4	X-RAY IMAGING OF ELECTRON DENSITY UNDER MAGNETIC FIELDS. V. Streltsov and D. Du Boulay
11:15-11:30 13C1-5	A CHARGE DENSITY STUDY OF THE POLYMORPHS OF P-NITROPHENOL. P. Kumaradhas,G.U. Kulkarni and C.N.R. Rao
11:30-11:45 13C1-6	CHANGE DENSITIES AT 10 K-A COMPARISON OF SYNCHROTRON AND CONVENTIONAL DATA. P.A. Reynolds
11:45-12:00 13C1-7	CHARGE DENSITY STUDIES AND TOPOLOGICAL ANALYSIS OF METAL SQUARATES. Y. Wang,C.R.Lee,C.C. Wang and G.H. Lee

13A2. room:Ballroom

MS-08 (II) Structural studies of coordination and organomrtsllic compounds

Chairman G. B. Jameson Co-chairman

16:00-16:20 13A2-1	CRYSTAL STRUCTURE ANALYSES OF MICRO CRYSTALS OF ORGANIC COMPOUNDS AT SPring-8. M. Yasui, N. Akiyama, M. Suzuki, M. Sudou, D. Hashizume and F. Iwasaki
16:20-16:40 13A2-2	CRYSTAL STRUCTURE ANALYSES OF ORGANIC COMPOUNDS AT LIQUID HELIUM TEMPERATURE. D.Hashizume, H. Sto, M., Yasui, F. Iwasaki, A. Sato and H. Kobayashi
16:40-17:00 13A2-3	HIRSHFELD SURFACES: A NEW TOOL FOR VISUALIZING AND EXPLORING MOLECULAR CRYSTALS. J.J. McKinnon, A.S. Mitshell and M.A. Spackman
17:00-17:20 13A2-4	CRYSTAL STRUCTURE OF HYDROGEN-BONDED CHARGE TRANSFER (CT) COMPLEXES OF CYANANILIC ACID WITH TETRATHIAFULVALENES (TTFs). B. Zaman, K. Nakasuji, J. Toyoda and Y. Morita
17:20-17:40 13A2-5	STRUCTURE OF DIMAGNESIUM CATION SPECIES $[Mg_2Cl_3(THF)_6]^+$ IN GRIGNARD REAGENTS. K.Yamaguchi, S. Sakamoto, H. Tsuruta and T. Imamoto
17:40-18:00 13A2-6	CRYSTAL AND MOLECULAR STRUCTURE OF AN ANTHRACENE DERIVATIVE. M.N. Ponnuswamy, M.S. Kumar, R. Sugadev and K.K. Chacko

13B2. room:Melati

MS-05 Structure refinement by Powder Diffraction

Chairman B.H. O'Connor Co-chairman H. Toraya

16:00-16:30 13B2-1	X-RAYS OR NEUTRONS OR X-RAYS AND NEUTRONS? STRUCTURAL REFINEMENTS OF METAL OXIDES. B.J. Kennedy
16:30-16:50 13B2-2	CRYSTAL STRUCTURE STUDIES OF ORGANIC COMPOUNDS FROM POWDER DIFFRACTION DATA. Y.D. Xiao, L.H. Wei, R. Chen, R.X. Shen, J.B. Zhang, C.M. Lai and S.F. Lin
16:50-17:10 13B2-3	THE INFLUENCE OF CARBAMIDE PEROXIDE AND STANNOUS FLUORIDE ON CRYSTALLITE SIZE AND MICROSTRAIN OF TOOTH ENAMEL. M. Hikam and R. Tjandrawinata
17:10-17:30 13B2-4	IMPROVEMENT OF THE ACCURACY OF STRUCTURAL PARAMETERS IN RIETVELD REFINEMENTS USING A NEW WEIGHT FUNCTION. H. Toraya
17:30-17:50 13B2-5	STUDIES OF INCLUSION COMPLEXES VIA POWDER REFINEMENTS AND COMPUTER SIMULATIONS. T.N. Gurn Row
17:50-18:10 13B2-6	APPLICATION OF CRYSTALLOGRAPHIC DATABASES TO MATERIALS J. Faber, R. Jenkins and R. Snyder

13C2. room:Raya

MS-04 Electron Diffraction

Chairman R.L. Withers Co-chairman N. Yamamoto

16:00-16:30 13C2-1	ELECTRON MICROSCOPY AND ITS APPLICATION TO ADVANCED MATERIALS. N. Yamamoto
16:30-17:00 13C2-2	MAXIMUM ENTROPY AND BAYESIAN METHODS FOR SOLVING CRYSTAL STRUCTURES USING ELECTRON DIFFRACTION DATA C.J. Gilmore
17:00-17:15 13C2-3	HIGH RESOLUTION ELECTRON MICROSCOPY STUDY OF INTERFACE STRUCTURE OF MULTILAYERS WITH GIANT MANETORESISTANCE. Z. Zhang
17:150-17:30 13C2-4	THE DETERMINATION OF AN UNKNOWN OXYGEN ATOM POSITION IN RARE-EARTH ZIRCONATE PYROCHLORES BY SYSTEMATIC ROW CBED. Y. Tabira and R. L. Withers
17:30-17:45 13C2-5	TEM CHARACTERIZATION OF STRAINED QUATERNARY MULTIPLE QUANTUM WELL STRUCTURES. I.K. Ng and C. B. Boothroyd
17:45-18:00 13C2-6	STUDY OF CHARGE-ORDERED STATES IN $LaSr_2Mn_2O_7$ BY LOW-TEMPERATURE ELECTRON DIFFRACTION. J.Q. Li, Y. Matsui, T. Kimura, R. Kumai and Y. Tokura

October 14 Wednesday

IUCr'50 Anniversary Symposium
room: Ballroom

Chairman E.N. Baker Co-Chairman M. Tanaka

October 14

9:00 - 9:40 IUCR-1	THE HISTORY OF THE IUCr. E.N. Baker
9:40-10:20 IUCr-2	ASPECTS OF CRYSTALLOGRAPHIC SCALING IN CRYSTALS QUASICRYSTALS AND BIOMOLECULES. A. Janner
coffee break	
10:40-11:20 IUCr-3	TOWARDS A GRAMMAR OF CRYSTAL PACKING. C.P. Brock
11:20-12:00 IUCr-4	STRUCTURE AND FUNCTION OF MEMBRANE PROTEIN COMPLEX, CYTOCHROME C OXIDASE FROM BOVINE HEART. T. Tsukihara

Oral Session
14A2. room:Ballroom
MS-09 Inorganic Compounds and Minerals

Chairman T. Yamanaka Co-chairman S.J. Chung

16:00-16:20 14A2-1	GRAPHS REPRESENTING CRYSTAL STRUCTURES. S.J. Chung
16:20-16:40 14A2-2	GROWTH AND CHARACTERIZATION OF A SINGLE CRYSTAL $Bi_2Sr_2PrCu_2O_y$. T.J. Lee, T.S. Lin, C.Y. Wan, T.I. Hsu and H.C. Ku
16:40-17:00 14A2-3	THE BOND CHARACTER OF MO2 (M=Si,GE,Sn,Pb) RUTILE STRUCTURE DETERMINED BY K-REFINEMENT AND MOLECULAR ORBITAL CALCULATION. T. Yamanaka, R. Kurashima, T. Tsuchiya and J. Mimaki
17:00-17:15 14A2-4	INTERACTION OF CROWN ETHER WITH LANTHANIDES:A COMPARATIVE STUD BY X-ray CRYSTALLOGRAPHY AND PM3 AND MOLECULAR MECHANICS METHODS. Z. Arifin, S.M. Zain and N.A. Rahman
17:15-17:30 14A2-5	CRYSTAL STRUCTURE STUDIES OF $CeAlO_3$ UNDER LOW TEMPERATURE. M. Tanaka, H. Horiuchi, T. Shishido and T. Fukuda
17:30-17:45 14A2-6	CRYSTAL STRUCTURE OF RELAXOR FERROELECTRIC $Pb(Zn_{1/3}Nb_{2/3})O_3$. H.M. Park and S.J. Chung
17:45-18:00 14A2-7	TEMPERATURE DEPENDENCE OF INTERATOMIC DISTANCES IN THE SUPERCONDUCTIVE TRANSITIONS OF Hg-1212 AND Tl-2212 SUPERCONDUCTORS. K. Yamawaki, S. Sasaki, M. Kakihana and M. Tanaka

14B2. room:Melati
MS-01 Diffraction Theory
MS-14 Diffraction and Spectroscopic Technology

Chairman S. L. Chang Co-chairman A.Y. Nikulin

16:00-16:20 14B2-1	DYNAMICAL DIFFRACTION AT GRAZING INCIDENCE. A. Authier
16:20-16:40 14B2-2	UNIQUENESS OF THE COMPLEX DIFFRACTION AMPLITUDE IN X-RAY BRAGG DIFFRACTION A.Y. Nikulin
16:40-17:00 14B2-3	COMPUTER SIMULATION AS A TOOL FOR THE ANALYSIS OF DIFFUSE SCATTERING. T.R. Welberry
17:00-17:20 14B2-4	STRUCTURE-PROPERTY RELATIONSHIP OF GIANT MAGNETORESISTIVE MULTILAYERS. K.Y. Kok and J. A. Leake
17:20-17:40 14B2-5	CORRELATED INTERFACE STRUCTURES IN Si1-xGexSi SUPERLATTICES DETERMINED BY X-RAY SCATTERING. Y. Yamaguchi and H. Hashizume, N. Usami and Y. Shiraki

17:40-18:00 USE OF THE CCD AREA DETECTOR FOR LARGE SCALE SURVEYS OF MICROFIBRIL ANGLE IN WOOD SAMPLES.
14B2-6 R. Kadirvelraj, A. Hussain, I. D. Cave, G. Smith and W. T. Robinson

14C2. room:Raya

MS-06 Aperiodical and Incommensurate Structure

Chairman A. Yamamoto Co-chairman M.Onoda

16:00-16:20 COMPOSITE MODURATED STRUCTURES IN WIDE-RANGE SOLID SOLUTIONS.
14C2-1 S Schmid, J.G. Thompson and R.L.Withers

16:20-16:40 THE STRUCTURES OF QUASICRYSTALS AND THEIR RELATED CRYSTALLINE PHASES.
14C2-2 K. Hiraga

16:40-17:00 MODULATED STRUCTURE ANALYSIS OF INCOMMENSURATE COMPOSITE CRYSTAL, $(SnS)_{1.17}NbS_2$.
14C2-3 Y. Gotoh, J. Akimoto, Y. Oosawa and M. Onoda

17:00-17:20 STRUCTURE STUDIES OF QUASICRYSTAL BY THE CONVERGENT-BEAM ELECTRON DIFFRACTION AND HIGH-ANGLE ANNULAR DARK-FIELDS.
14C2-4 K. Saitoh, K.Tsuda, M.T anaka and A.P. Tsai

17:20-17:40 PERIODIC NODAL SURFACES, ATOMIC MODULATION FUNCTIONS AND THE THREE-DIMENSIONAL INCOMMENSURABLY MODULATED (1- x)Bi2O3.xNb_2O_5, $0.06<x<0.23$, SOLID SOLUTION.
14C2-5 R.L.Withers, C.D. Ling, S. Schmid and J.G. Thompson

October 15 Thursday

Plenary Talk
room: Ballroom

Chairman J.W. White

9:00-9:50 DIRECT DETERMINATION OF X-RAY REFLECTION PHASES USING MULTIPLE
PL-3 DIFFRACTION: THEORY AND EXPERIMENTS.
S.L. Chang

room:Melati

Chairman S.M. Peng

9:00-9:50 REAL TIME IN SITU OBSERVATION OF CHEMICAL REACTIONS.
PL-4 Y. Ohashi

Oral session
15A1. room: Ballroom
MS-08 (I) Structural studies of organic and drug-related compounds

Chairman G. B. Jameson Co-chairman

10:00-10:15 THE POSSIBILITIES FOR HOMOMETRIC STRUCTURES IN A HEXAGONAL LATTICE.
15A1-1 A.D. Rae

10:15-10:30 CLATHRATION AND CRYSTAL STRUCTURES OF SOME COORDINATION POLYMERS.
15A1-2 X.M. Chen and M.L. Tong

10:30-10:45 SINGLE CRYSTAL X-RAY ANALYSIS OF SUCCESSIVE ISOMERIZATION ON A COBALT
15A1-3 ATOM OF AN ALKYL GROUP.
A. Sekine, M. Yoshiike and Y. Ohashi

10:45-11:00 THE CRYSTAL AND MOLECULAR STRUCTURES OF DI-μ-HYDROXY-BIS(DI-2-
15A1-4 PYRIDYLAMINE)DINITRATODI-COPPER(II) AND AQUA-μ-FORMATO-
TRIFORMATO-BIS(DI-2-PYRIDYLAMINE) DICOPPER(II) MONOHYDRATE.
S. Youngme, W. Somjitsripunya, K. Chinnakali, S. Chantrapromma and H.K. Fun

11:00-11:15 CRYSTAL STRUCTURE OF 1,11-UNDECANEDIOL.
15A1-5 N. Nakamura, S. Setodoi and T. Ikeya

11:15-11:30 HYDROTHERMAL SYNTHESIS AND CRYSTAL STRUCTURE OF 1-DIMENSIONAL CHAIN
15A1-6 CLUSTER $[H_2en]_2[Mo_{8.5}V_{5.5}O_{38}(H_2PO_4)]_6H_2O$.
W.M.B u, G.Y. Yang, Q.Zhen, L.Ye, J.Q.Xu and Y.G.Fan

11:30-11:45 TETRANUCLEAR IRON-OXYGEN CLUSTERS IN ORGANICALLY TEMPLATED IRON
15A1-7 PHOSPHATES.
K.H. Lii

11:45:12:00 DIMOLYBDENUM TRIS (μ-THIOLATO) COMPLEXES.
15A1-8 K.W. Muir, F.Y. Petillon and P. Schollhammer

15B1. room:Melati
MS-10 Material Chemistry

Chairman Y. Ohashi Co-Chairman K. Okuyama

10:00-10:20 CRYSTAL STRUCTURES AND DEFORMATION ELECTRON-DENSITY-DISTRIBUTIONS OF
15B1-1 TEMPORADICALS SHOWING MAGNETIC INTERACTIONS.
F. Iwasaki, E. Kannari, D. Hashizume and M. Yasui

10:20-10:40 MATERIALS DESIGN USING SUPRA- AND SUPER-MOLECULAR ASSEMBLY
15B1-2 I.D. Williams, S.S-Y. Chui, S. M-F. Lo AND H. H.-Y. Sung

10:40-11:00 CRYSTAL STRUCTURE CHANGE FOR THE THERMOCHROMY OF N-
15B1-3 SALICYLIDENEANILINES.THE FIRST OBSERVATION BY X-RAY DIFFRACTION.[1].
K. Ogawa,Y. Kasahara,Y. Ohtani and J. Harada

11:00-11:20 THE CRYSTAL STRUCTURES OF DIDENZYLDIAZA-18-CROWN-6 COMPLEXES WITH Cu-
15B1-4 AND Ce-THIOCYANATES.
S. A. Talipov,M.I. Saleh, A. Salhin,and B. Saad

11:20-11:40 GROWTH OF HIGHLY ORDERED SILICATE-ORGANIC COMPOSITE FILMS AT THE
15B1-5 AIR-WATER INTERFACE.
P.A. Reynolds, A.S. Brown, S.A. Holt, J.L.Ruggles and J.W. White

11:40-12:00 15B1-6	FROM METAL STRING COMPLEXES TO MOLECULAR METALWIRES. S.M.Peng

15C1. room:Raya

MS-03 Neutron Diffraction

Chairman C. J. Howard Co-chairman Y. Fujii

MS-03

10:00-10:20 15C1-1	MAGNETIC NEUTRON DIFFRACTION AND COVALENCE. P.A. Reynolds
10:20-10:40 15C1-2	NEUTRON AND X-RAY SCATTERING STUDY OF INORGANIC SPIN-PEIERLS COMPOUNDS. Y. Fujii, H. Nakao, K. Ohwada, T. Yoshihama, N. Takesue, M. Nishi, K. Kakurai, M. Isobe and Y. Ueda
10:40-11:00 15C1-3	TORSION, MIGRATION AND DISORDER: VARIABLE TEMPERATURE NEUTRON DIFFRACTION STUDIES OF HYDROGEN ATOM THERMAL PARAMETERS. C.C. Wilson
11:00-11:20 15C1-4	AN NEUTRON IMAGING PLATE AND ITS APPLICATION TO NEUTRON DIFFRACTOMETRY. N. Niimura and Y. Karasawa
11:20-11:40 15C1-5	NEUTRON POWDER DIFFRACTION DETERMINATION OF OXYGEN POSITIONS IN METAL OXIDES. C.J. Howard
11:40-12:00	To be advised

15A2. room:Ballroom

MS-07 (II) Biocrystallography and Protein Structure

Chairman S. W. Suh Co-chairman J. M. Guss

16:00-16:15 15A2-1	STRUCTURAL BASIS OF INTRASTERIC AND ALLOSTERIC CONTROLS OF PHENYLALANINE HYDROXYLASE. B. Kobe, I. G. Jennings, C. M. House, B. J. Michell, R. G. H. Cotton and B. E. Kemp
16:15-16:30 15A2-2	CRYSTAL STRUCTURE OF A *SACCHAROMYCES CEREVISIAE* PROTEIN TYROSINE PHOSPHATASE AT 2.2 Å RESOLUTION. H.J. Ahn, H.K. Song, H. Cho and S.W. Suh
16:30-16:45 15A2-3	THREE DIMENSIONAL STRUCTURE OF THE HUMAN IMMUNOGLOBULIN G RECEPTOR-FcγRII K.F. Maxwell, M.S. Powell, D. Emmanouilidis, M.D. Hulett, P.M. Hogarth and T. P.J. Garrett
16:45-17:00 15A2-4	CRYSTAL STRUCTURE OF 20S PROTEASOME FROM BOVINE LIVER. M. Unno, Y. Tomisugi, T. Mizushima, Y. Mori,oto, J. Yasuoka, K. Tanaka and T. Tsukihara
17:00-17:15 15A2-5	THE REFINED STRUCTURES OF THE FULLY OXIDIZED AND THE FULLY REDUCED CYTOCHROME C OXIDASE FROM BOVINE HEART. M. Yao, N. Inoue, T. Mizushima, E. Yamashita, H. Yamaguchi, T. Tomizaki, T. Tsukihara, R. Nakashima, H. Shinzawa-Itoh, R. Yaono, P. L. Clare and S. Yoshigawa
17:15-17:30 15A2-6	STRUCTURE OF SHEEP LIVER CYTOSOLIC ALDEHYDE DEHYDROGENASE AT 2.35Å RESOLUTION. S.A. Moore, T.J. Blythe, K.E. Kitson, T.M. Kitson, H.M. Baker and E.N. Baker
17:30-17:45 15A2-7	CLUES AS TO DENATURATION DETECTED BY THE TEMPERATURE JUMP-LAUE METHOD IN 3-ISOPROPYLMALATE DEHYDROGENASE. T.Hori, H. Moriyama, N. Tanaka and T. Oshima
17:45-18:00 15A2-8	MEMBRANE ION TRANSPORT BY ANTIBIOTICS AND TOXINS. W.L. Duax, B.M. Burkhart, D. Ghosh, N.Li and V. Pletnev

October 15 Thursday

15B2. room:Melati

MS-11 Phase Transition

Chairman S.W. Wilkins Co-chairman

16:00-16:20 15B2-1	PRESSURE-INDUCED PHASE TRANSITION IN RELAXOR $Pb(In_{1/2}Nb_{1/2})O_3$.	K. Nomura, T. Shingai, S. Ishino, N. Yasuda, H. Ohwa and H. Terauchi
16:20-16:40 15B2-2	ATOMIC AND MAGNETIC SHORT-RANGE ORDER INPT-8.8 AT. % MN SPIN-GLASS ALLOY.	K. Ohshima, M.T akahashi and S. Yoshimi
16:40-17:00 15B2-3	LOW TEMPERATURE MAGNETIC PROPERTY AND HEAT CAPACITY OF $LiNiO_2$.	O. Fujishima, H. Kawaji, M. Takematsu, T. Atake, A. Hirano and R. Kanno
17:00-17:20 15B2-4	CHARACTERISTICS OF ORDER-MESOSCOPIC PHASE TRANSFORMATION IN COMPOUND SEMICONDUCTER In_2Te_3.	S. Abe, Y. Nakamura and O. Nittono
17:20-17:40 15B2-5	INCOMMENSURATE CHARGE ORDERING IN $La_{0.5}Ca_{0.5}MnO_3$.	S. Mori.
17:40-18:00 15B2-6	ANOMALOUS-X-RAY SCATTERING ASSOCIATED WITH THE ORDER-DISORDER TRANSFORMATION IN $Al_{70}Ni_{15}Co_{15}$ QUASICRYSTAL.	H. Abe, N.Tamura, J.Bai, D.Le Bolloc'h, S.C. Moss and Y. Matsuo
18:00-18:20 15B2-7	THERMOCHROMIC PHASE TRANSITIONS IN CRYSTALS : SINGLE CRYSTAL X-RAY INVESTIGATIONS.	B. Narayanan and M.M. Bhadbhade

October 13 13:30-16:00
Poster Session room: Lobby and Malati 1

MS-01 and MS-14

13P1	PHASE DETERMINATION OF FORBIDDEN REFLECTIONS. J. Kokubun, M. Kuribayashi, K. Ishida and V.E. Dmitrienko, A.V.Shubnikov
13P2	A MODEL WITH P1 SYMMETRY, WHICH SHOWS CUBIC SYMMETRY m3m IN DIFFRACTION. T. Matsumoto and S. Hashimoto
13P3	RECENT X-RAY CRYSTAL STRUCTURE ANALYSIS BY NEW DIFFRACTOMETER USING A CYLINDRICAL IMAGING PLATE. H. Uekusa and Y. Ohashi
13P4	ON-LINE AND IN SITU X-RAY DIFFRACTION ANALYSIS OF THE CRYSTALLISATION OF IMPORTANT PHAMACEUTICAL MATERIALS. S. Hastings and K. Roberts
13P5	CIFSIEVE: QUICK CREATION OG CIF INTERFACES. J. Hester and F. P. Okamura
13P6	XTAL3.6: NEW VERSION OF Xtal TO BE RELEASED. D.du Boulay and S. Hall
13P7	STRUCTURAL PROPERTIES INDUCED BY ANEALING IN Al-N-M(M:Co,Fe) FILMS. PREPARAD BY REACTIVE SPUTTERING A.G. Roy and O. Nittono
13P8	SPECTROSCOPIC INVESTIGATION OF LASER DYES IN SOLID MATRICES. A.F.Farooqui and Z.H. Zaidi
13P9	X-RAY OPTICAL ACTIVITY AND X-RAY BIREFRINGENCE MEASURED WITH POLARIZATION-SWITCHING OPTICS. Y. Ueji, K. Okitsu, K. Sato and Y. Amemiya

MS-05

13P10	BOTH CALCULATION OF SHIFT AND INTENSITY OF X-RAY DIFFRACTION PEAK, AND DETERMINATION OF KIND OF RESPONSE FUNCTION AND ITS PARAMETERS BY MODE ROSA IN X-RAY PROFILE BROADENING ANALYSIS. P.O. Verkhovodov
13P11	RAPID AND ROUTINE STRUCTURE SOLUTION OF HIGHLY FLEXIBLE MOLECULAR CRYSTAL STRUCTURES FROM POWDER DIFFRACTION DATA. K. Shankland and W.I.F. David
13P12	CRYSTAL STRUCTURES OF A-SITE DEFICIENT PEROVSKITES LixLa$_{1/3}$NbO$_3$. R.A. Dilanian and F. Izumi
13P13	RAPID STRUCTURE SOLUTION OF IBUPROFEN FROM POWDER DIFFRACTION DATA BY THE APPLICATION OF A GENETIC ALGORITHM COMBINED WITH CONFORMATIONAL ANALYSIS. L. McBride, K. Shankland, W. I. F. David and T. Csoka
13P14	PHYSICAL INTERPRETATION OF THE MARTH FUNCTION r-PARAMETER IN POWDER DIFFRACTION RIETVELD MODELLING OF PREFERRED ORIENTATION. H. Sitepu, B.H. O'Connor and D.Y. Li
13P15	STRUCTURAL PROPERTIES OF DOPED SYSTEMS: $PrBa_{2-x}Ca_xCu_3O_y$ and $PrBa_2Cu_{3-x}Ag_xO_y$. Z. Zou, J. Ye, H. Kawanaka, T. MInawa, H. Bando and Y. Nishihara
13P16	STRUCTURAL MODIFICATION OF BORON CARBIDE INDUCED BY INDUCTION PLASMA TREATMENT. T. Tanaka, X. Fan and T. Ishigaki

MS-07 (I)

13P17	EXPRESSION, PURIFICATION AND CRYSTALLIZATION OF BACTERIAL CMP-Neu5Ac CITIDYLYLTANSFERASES. J.A. Carmichael, R.K. Scopes, T.P.J. Garrett,G.G.Lilley, M.Z. Lou and P.A. Pilling
13P18	STRUCTURES OF PENICILLOPEPSIN IN COMPLEX WITH CYCLIC AND ACYCLIC PEPTIDE INHIBITORS. A.R. Khan, J. Parrish, M.E. Fraser, A. Deacon and M.N.G. James

October 13 13:30-16:00

Poster Session room: Lobby and Malati 1

13P19	PROTEIN STRUCTURRE IN ORGANIC MEDIA. Q. Huang, Z. Wang, M. Qian, G. Zhu and Y.T ang
13P20	PROTEIN DATA BANK ACTIVITIES AT THE INSTITUTE FOR PROTEIN RESEARCH, OSAKA UNIVERSITY, JAPAN. M. Kusunoki, R. Igarashi, S. Suzuki, M. Okamoto and G. Kurisu
13P21	STRUCTURE OF A DOUBLE-HEADED SERINE PROTEASE INHIBITOR AND ITS ENZYME INTERACTION. D. Mukhopadhyay, S. Ravichandran, U. Sen, A. Podder, C.Chakrabarti and J.K. Dattagupta
13P22	THE CRYSTAL STRUCTURE OF THE OPEN-FORM *E.COLI* TYROSINE AMINO-TRANSFERASE BOUND WITH A COFACTOR PYRIDOXAL 5'-PHOSPHATE T.P. Ko, W.Z. Yang and H.S. Yuan
13P23	TIME-RESOLVED STRUCTURAL ANALYSIS FOR SOLID-STATE POLYMERIZATION OF DIACETYLENE DERIVATIVES. T. Maruo, E. Mochizuki, N. Kanehisa and Y. Kai
13P24	INTEGRATED DIRECT METHODS WITH ANORMALOUS SCATTERING AND ISOMORPHOUS REPLACEMENT METHOD-JOINT AND CONDITIONAL PROBABILITY DISTRIBUTIONS OF THE TRIPLET,QUARTET AND SEXTET IN THEIR FIRST NEIGHBOURHOOD. D. Velmurugan and S. Banuumathi
13P25	LIGAND BINDING BY AND STABILITY OF GENTIC VARIATS OF BOVINE β-LACTOGLOBULIN. B.Y. Qin, L.K. Creamer, E. N. Baker and G.B. Jameson
13P26	NOVEL PLASTOCYANIN WITH π–π STACKING INTERACTION AS THE KEY FACTOR FOR A CIDIC ENDURANCE. T. Inoue, T. Kohzuma, F. Yoshizaki, M. Gotowda and Y. Kai
13P27	INTEGRATED DIRECT METHODS FOR MACROMOLECULAR PHASING S. Parthasarthy and D. Velmurugan
13P28	CONPUTER MODELLING OF INTERACTIONS OF a WITH HIV-1 REVERSE TRANSCRIPTASE AND ITS DRUG-RESISTANT VARIANTS V.K. Ganesh and D. Velmurugan
13P29	HIGHER RESOLUTION STRUCTURE OF A DNA DODECAMER OF d(CGCGmo6AATCCGCG) CONTAINING N6-METHOXY-ADENOSINE T. Chatake, A. Ono, Y. Ueno, A. Matsuda and A. Takenaka
MS-08 (I)	
13P30	WELL, HOW DO CRYSTAL PACKING EFFECTS INFLUENCE MOLECULAR GEOMETRY IN ORGANOTIN SYSTEMS? E.R.T. Tiekink
13P31	THE SYNTHESIS AND DEVELOPMENT OF METAL-ION ACTIVATED MOLECULAR RECEPTOR MOLECULES S.F. Lincoln, C.B. Smith, M.R.T aylor, K.P. Wainwright and K.S. Wallwork
13P32	CRYSTAL AND MOLECULAR STRUCTURE OF "BIS[DIAQUA(1H-CYCLOPENT A(2,1-b:3,4-b') (DIPYRIDINE -2,5-DIONE)NICKEL(II)]MONOHYDRATE. G.Y.S.K. Swamy and K. Ravikumar
13P33	SEVEN CRYSTAL STRUCTURES AND CONFORMATIONS OF DRUG INTERMEDIATES OF DILTIAZEM. K.A. Nirmala, P. Kumaradhas and N. Kalyanam
13P34	CRYSTAL STRUCTURE ANALYSIS OF 4-PHENYL 5-CHLOROPHENYL 1,2,4-TRIAZOLE-3-THIONE. K. Puviarasan and D. Velmurugan
13P35	CRYSTAL AND MOLECULAR STRUCTURE DETERMINATION OF 2,4-(BIS) 0-TOLYL-3-METHYL-3-AZABICYCLO(3.3.1)NONAN-9-ONE. L. Vijayalakshmi, V. Parthasarathi, R. Jayaraman and M. Venkatraj
13P36	CONFORMATIONAL ASPECTS OF SOME PIPERIDINONE DERIVATIVES. M.N. Ponnuswamy and D. Kumaran

October 13 13:30-16:00
Poster Session room: Lobby and Malati 1

13P37	CRYSTAL STRUCTURE AND CONFORMATION OF THE DIPEPTIDE tboc-Aib-Ile-OMe. M. Nilofarnissa, and D. Velmurugan
13P38	CRYSTAL STRUCTURE OF TWO CARBAZOLE DERIVATIVES. L. Govindasamy and D. Velmurugan
13P39	CRYSTAL AND MOLECULAR STRUCTURE OF AN ACRIDINEDIONE. M.S. Kumar, D.Kumaran, M.N.Ponnuswamy, P.Murugan and V.T. Ramakrishnan
13P40	CRYSTAL AND MOLECULAR STRUCTURE OF PIPERAZINE DERIVATIVES. M.S. Kumar, D. Kumaran, M.N. Ponnuswamy, K. Chinnakali and H.K. Fun
13P41	SOLID-STATE PHOTOISOMERIZATION OF COBALOXIME COMPLEXES WITH A BULKY SUBSTITUENT IN THE EQUATORIAL LIGANDS. G. Iketani, A. Sekine, H. Uekusa and Y. Ohashi
13P42	RACEMIZATION PROCESS OF CHIRAL COBALOXIME COMPLEXES BY PHOTOIRRADIATION. H. Sato and Y. Ohashi
13P43	EFFECT OF SIDE CHAIN LENGTH ON MOLECULAR ASSEMBLY MODES OF CHOLIC ACID DERIVATIVES. M. Sugahara, K. Sada and M. Miyata
13P44	CRYSTAL STRUCTURE OF ω-[4-(4-METHOXYPHENOXY-CARBONYL) PHENOXYCARBONYL] ETHYL 4-FERROCENYLBENZOATE. N. Nakamura and S. Setodoi
13P45	SOLID STATE PHOTORACEMIZATION OF COBALOXIMES IN HOST-GUEST COMPLEXES. N. Sugimoto, H. Uekusa, A. Sekine and Y. Ohashi
MS-09 (I)	
13P46	X-RAY ABSORPTION FINE STRUCTURE STUDY IN $FeTiO_3$. R. M. F. Hsu and L.Y. Jang
13P47	A REVISED DESCRIPTION OF SOME 'FLUORITE-RELATED' BINARY BISMUTH OXIDE PHASES BASED ON THE CRYSTAL STRUCTURES OF TWO BISMUTH TANTALATES. C.D. Ling, R.L. Withers, S. Schmid and J.G. Thompson
13P48	SITE OCCUPANCY OF Ba AND Sm ON THE MICROWAVE DIELECTRIC $Ba_{6-3x}Sm_{8+2x}Ti_{18}O_{54}(x=0.5)$ SOLID SOLUTION. H. Ohsato, M. Imaeda, A.Komura and T.Okuda
13P49	SINGLE CRYSTAL STUDY OF THE HYDROXYAPATITE TRANSFORMED FROM CHLORAPATITE BY THE SOLID STATE ION EXCHANGE UNDER HYDROTHERMAL CONDITIONS. H. Takase, N. Ishizawa, I. Sugiura, S. Oishi, J.C. Rendon-Angeles and K. Yanagisawa
13P50	THERMAL BEHAVIOR OF MODULATION IN Co-ÅKERMANITE AT ELEVATED TEMPERATURES. K. Kusaka, K. Hagiya, N. Haga and M. Ohmasa
13P51	SITE PREFERENCE OF TRANSITION-METAL IONS IN FERRITES DETERMINED BY SINGLE-CRYSTAL DIFFRACTION METHODS. T. Mizobuchi, K. Matsumoto and S. Sasaki
13P52	POSITIONAL DISODER OF Y AND Ca ATOMS IN A MELILITE-TYPE Ce^{3+}-DOPED $YCaAl_3O_7$. M. Hayatsu, N. Ishizawa and N. kodama
13P53	X-RAY STRUCTURAL STUDY WITH THE SINGLE CRYSTAL OF A (Hg,Pb)-1223 SUPERCONDUCTOR. N. Kita, K. Yamawaki, S. Sasaki, S.R. Lee and H. Yamauchi
13P54	SITE PREFERENCE OF CATIONS AND STRUCTURAL VARIATION IN $MgAl_{2-x}Ga_xO_4$ $(0 \leqq x \leqq 2)$ SOLID SOLUTION WITH SPINEL STRUCTURE. T.I to, A.Yoshiasa, A. Nakatsuka, T. Yamanaka and H. Maekawa
13P55	STRUCTURAL STUDY OF PEROVSKITE-TYPE $PbZn_{1/3}Nb_{2/3}O_3$. Y. Matsushima, N. Ishizawa, N. Wakiya and N. Mizutani

MS-12

13P56	DEVELOPMENT OF VACUUM CAMERA X-RAY IMAGEPLATE METHOD. EXAMPLE: ELECTRON DENSITY INVESTIGATION OF $KNiF_3$ CRYSTAL. E.A. Zhurova, V.V.Zhurov and K.Tanaka
13P57	METAL ATOM DISPLACEMENTS IN 1T-TYPE $(V,Ta)S_2$. N.Ishizawa, K.Suda, S.Tsubouchi and M.Wakihara
13P58	REEXAMINATION OF ELECTRON DENSITY DISTRIBUTION IN FAYALITE BY SYNCHROTRON RADIATION. F.Marumo, Y.Tabira, M.Okui, N.Ishizawa and H.Takei
13P59	ELECTRON DENSITY IN KDP USING 60keV X-RAYS. J. Hester, Y.Shiozaki, E.Suzuki and F.P.Okamura
13P60	ELECTRON DENSITY DISTRIBUTION IN THE HIGH TEMPERATURE PHASE OF Fe_3O_4 H.Okudera

October 14 13:30-16:00
Poster Session room: Lobby and Malati 1

MS-02

14P1 THREE DIMENSIONAL DIFFRACTION PHENOMENON AT A 90 DEGREE BRAGG REFLECTION.
A.Y.Nikulin, J. R. Davis and D. J. Cookson

14P2 ENERGY DEPENDENCE OF ATS REFLECTIONS FOR PYRITE AND MAGNETITE.
J. Kokubun, K. Hagiwara, K. Horie, M. Kuribayashi and K.Ishida

14P3 SITE-SELECTIVE EXAMINATION OF MCXD PRE-EDGE PEAKS IN TRANSITION-METAL FERRITES USING SYNCHROTRON X-RAY RESONANT SCATTERING.
T.Hanashima, F. Saito, K. Matsumoto, S. Sasaki, T. Mori and K. Hirano

14P4 CHARACTERIZATION OF CHEMICAL VAPOR DEPOSITION DIAMONDS BY THE MICRO-REGION LAUE METHOD.
T.Osaka, Y. Mitsuda and K. Ohsumi

14P5 STRUCTURE ANALYSIS OF SODIUM PARADODECA-TANGSTATE USING SPring-8 BL02B1 BEAMLINE.
T.Ozeki

14P6 PHASE TRANSITION AND CHARGE ORDERING OF MAGNETITE EXAMINED BY THE VALENCE-DIFFERENCE CONTRAST METHOD.
T.Toyoda, S. Sasaki and M. Tanaka

14P7 CATION DISTRIBUTION IN Mn-Zn-Fe FERRITE DETERMINED BY THE TWO-WAVELENGTHS ANORMALOUS DISPERSION METHOD.
Y.Konoike, F. Saito, S. Sasaki and H. Koinuma

14P8 THE STRUCTURAL STUDY OF γ-ALUMINA (AL2O3) WITH SYNCROTRON RADIATION.
Y.Nakakita, T. Ushiro, C. Numako, K. Koto, T. Osaka, K. Osumi

14P9 DIRECT OBSERVATION OF ANISOTROPIC X-RAY FLOURESCENCE IMAGES FROM SOLID SAMPLES.
C.K.Chen, S.L. Chang, T.S. Gau, Y.F. Hung, Y.N. Hung, J.M. Chen, R.G. Liu and M.T. Tang

14P10 CRYSTALLOGRAPHIC STUDIES OF BIOMINERALS COMPOSING PEARL AND MARINE SHELLS.
C. Numako,T. Minomura, K. Ohsumi and K. Koto

14P11 ENERGY-DIPERSIVE TOPOGRAPHIC OBSERVATION OF InAs LATTICE-MISMATCHED HETEROEPITAXIAL LAYER ON GaAs USING SYNCHROTRON X-RADIATION.
Y. Suzuki, H. Kii, M. Yoshida and Y. Chikaura

14P12 COMPUTER SIMULATION STUDY ON X-RAY DYNAMICAL PENETRATION DEPTH FOR LARGE LATTICE-MISMATCHED InAs HETEROEPITAXIAL LAYER ON GaAs.
M. Yoshida, Y. Suzuki and Y. Chikaura

MS-04

14P13 HIGH RESOLUTION ELECTRON MICROSCOPY WORK ON SOL-GEL DERIVED COBALT SUBSTITUTED BARIUM FERRITE.
G.B.Teh and D. A. Jefferson

MS-06

14P14 A 5-DIMENSIONAL MODEL OF DODECAGONAL Ta-Te QUASICRYSTALS.
A.Yamamoto

14P15 LONG-RANGE ORDER AT THE SURFACE IN A MAGNETIC FLUID:AN X-RAY REFRECTIVITY STUDY UNDER MAGNETIC FIELD.
K.Ueda and I.Takahasi

14P16 COMMON PROJECTION OF INCOMMENSURATE COMPOSITE CRYSTAL $Sr_{1.145}TiS_3$ OBSERVED BY HIGH-RESOLUTION ELECTRON MICROSCOPY
M.Onoda, G-Y Yang, M Saeki and Y. Bando

14P17 SUPERSPACE GROUP APPROACH OF THE ROOM-TEMPERATURE PHASE OF Cu_8GeSe_6
M.Onoda, M.Ishii, K. Shibata and A. Yamamoto

October 14 13:30-16:00
Poster Session room: Lobby and Malati 1

14P18	QUASICRYSTAL STRUCTURE AND CONDUCTIVITY OF DENTAL ENAMEL AND SPECIAL PORCELAIN ENEMEL Nguyen Van Tri
MS-07 (II)	
14P19	CRYSTALLIZATION AND PRELIMINARY CRYSTALLOGRAPHIC STUDIES ON NON-PHOTOSYNTHETIC FERREDOXINS. G.Kurisu, R. Igarashi, M. Kusunoki and T. Hase
14P20	CRYSTAL STRUCTURE OF O6-METHYLGUANINE-DNA METHYLTRANSFERASE FROM *PYROCOCCUS KODAKARAENSIS* STRAIN KODI H. Hashimoto, M. Nishioka, T. Matsumoto, T. Yuasa, T. Inoue, S. Fujiwara, M. Takagi, T. Imanaka and Y. Kai
14P21	THE DEVERAPMENT OF AN EMPIRICAL PEPTIDE DRUG DESIGN SYSTEM H.Ishida, T. Shirai, Y. Matsui, Y. Kato and T. Yamane
14P22	STRUCTURE OF COAGULATION FACTOR IX-BINDING PROTEIN AT 2.6A RESOLUTION. H. Mizuno, Z. Fujimoto, M. Koizumi, H. Kano, H. Atoda and T. Moria
14P23	FLAVOCETIN-HAS A NOVAL TETRAMERIC STRUCTURE OF C-TYPE DOMAIN HETERODIMERS. K.Fukuda, H. Mizuno, Z. Fujimoto, H. Aoda and T. Morita
14P24	CRYSTALIZATION AND PRELIMINARY X-RAY ANALYSIS OF THERMOSTABLE ASPARTATE AMINOTRANSFEREASE FROM A THERMOPHILIC CTYNOBACTERIUM K.Hamada, K. Nozawa, H. Shibata and Y. Sawa
14P25	MIRO-OAS: A PROGRAM SYSTEM FOR PROTEIN STRUCTURE DETERMINNATION WITH GUI. K.Hamada, K. Kakoi, N. Tanaka, H. Moriyama and N. Kamiya
14P26	PRELINMINARY X-RAY CRYSTALLOGRAPHIC STUDIES OF A NOVEL ANTIOXIDANT PROTEIN FROM *Amphibacillus xylanus* K.Kitano, Y.Niimura, Y. Nishiyama, and K. Miki
14P27	TRIPLE-HELICAL STRUCTURE OF COLLAGEN MODEL POLYPEPTIDES. K.Okuyama, V. Nagarajan, G. Aizawa, C. Hongo and S. Kamitori
14P28	MEASUREMENT OF CRYSTAL GROWTH RATE OF TETRAGONAL HEN EGG WHITE LYSOZYME WITH ATOMIC FORCE MICROSCOPY. L.Rong, T. Yamane and N. Nimura
14P29	CRYSTAL STRUCTURE ANALYSIS OF ß-AMYLASE FROM BACILLUS POLYMYXA M. Akita, H. Tasaki, F.Matsumoto, A. Suzuki, T. Yamane, T. Ashida and N. Uozumi
14P30	CRYSTAL STRUCTURE OF AZINE BOUND CYTOCHROME C OXIDASE AT 2.9Å RESOLUTION FROM BOVINE M. Fei, E.Y amasita, N. Inoue,T. Mizushima,H. Aoyama,T. Tomisaki, T.Tsukihara, K. Shinzawa-itoh, R. Nakashima, R. Yaono and S. Yoshikawa
14P31	PRELIMINARY X-RAY CRYSTALLOGRAPHIC STUDIES OF FARNESYL DIPHOSPHATE SYNTHASE FROM BACILLUS STEAROTHERMOPHILUS M. Fujihashi, T. Koyama and K. Miki
MS-08 (II)	
14P32	POLYMORPHISM OF A Co(III)-SALEN SCHIFF BASE COMPLEX. S.Sato, T.Fukuda, K.Ishii, Y.Nakano and Y.Fujii
14P33	STRUCTURAL STUDIES OF SOME CLONIDINE DERIVATIVES. E.M.Elssfah, H.K.Fun, K.Chinnakali, I.W.Mathison, E.K.Gan, T.W.Sam, C.Y.Tan and M.Zubaid
14P34	CONFORMATIONAL STUDIES ON TWO XANTHENE DERIVATIVES TO CORRELATE THE STRUCTURE WITH THEIR FUNCTION. J.Jeyakanthan, D.Velmurugan, S.S.S.Raj and H.K.Fun
14P35	CRYSTAL STRUCTURE OF (IR, 2S)-2-(N-METHYL-N-TOLUENESULFONYL)AMINO-1-PHENYL-1-PROPANOL. K.Chinnakali, H.K.Fun, K.Sriraghavan and V.T.Ramakrishnan

October 14 13:30-16:00
Poster Session room: Lobby and Malati 1

14P36	THE FIRST EXAMPLE OF THE *mer*-Oh GEOMETRY IN A SIX-COORDINATE TRIORGANOTIN COMPOUND: TRIFLUOROACETATOTRIPHENYLTIN 3,4,7,8-TETRAMETHYL-1,10-PHENANTHROLINE(1/1). N.S.Weng
14P37	CRYSTAL STRUCTURE DETERMINATION OF PLATYPHYLLINE. S.Ozturk, H.K.Fun, S.Ide and B.Sener
14P38	THE STRUCTURE OF GOSSYPOL 1:2 HOST-GUEST COMPLEX WITH TROPOLONE. S.A.Talipov, Y.Ohashi, B.T.Ibragimov, J.Harada, M.I.Saleh and B.Saad
14P39	CRYSTAL STRUCTURE OF A MONOMERIC PALLADIUM (II) COMPLEX. K.Panneerselvam, T.H.Lu, S.F.Tung, V.K.Jain and S.Narayan
14P40	STRUCTURAL CHEMISTRY OF dppe-BRIDGING DICATION $[\{(\eta^5\text{-}C_5H_5)Fe(CO)_2\}_2(\mu-\ \eta^1{:}\eta^1\text{-}dppe)^{2+}]$. L.K.Liu, Y.S.Wen, C.Peng and O.Adeyemi
14P41	CRYSTAL AND MOLECULAR STRUCTURE OF 9-3,4,6,7,9,10-HEXAHYDRO-3,3,6,6-TETRAMETHYL-1,8(2H,5H)-ACRIDINE-DIONE. R.Sankaranarayanan, D.Velmurugan, S.S.S.Raj and H.K.Fun
14P42	INVESTIGATION OF THE HYDROQUINONE CRYSTALLIZATION AT DIFFERENT TEMPERATURES AND CRYSTAL STRUCTURE OF THE NEW HYDROQUINONE - ACETONE COMPLEX. SIMULTANEOUSCRYSTALLIZATION OF THE α-, β-, γ-HYDROQUINONES FROM ONE SOLUTION. K.K.Makhkamov, B.T. Ibragimov, K.M.Beketov and G.B.Nazarov
14P43	CRYSTAL STRUCTURES OF TWO COPPER(II) COMPLEXES. S.Chantrapromma, S.Youngmee, K.Poopasit, K.Chinnakali and H.K.Fun
14P44	A FRAMEWORK ARCHITECTURE VIA COORDINATION AND π-π INTERACTIONS: $[(VO)_2(OH)_2(C_4O_4)(Phen)_2.H_2O]_n$. K.J. Lin
14P45	PROTONATION AND OLIGOMERIZATION OF TETRAALKYLAMMONIUM DECAVANADATES. S.Nakamura and T.Ozeki
14P46	THE CHEMISTRY AND STRUCTURAL PROPERTIES OF PALLADIUM-OSMIUM MIXED-METAL CARBONYL CLUSTERS. W.T.Wong
14P47	SYNTHESIS AND CRYSTAL STRUCTURE OF A NEW MOLYBDENUM OXALATE COMPLEX $K6[Mo_2(\mu\text{-}O)(\mu\text{-}S)O_2(ClPO_3)_2(C_2O_4)_2]\ 3H_2O$ Y.-H.Xing, W.M.Bu, L.Ye, Y.G.Fan, J.Q.Xu
MS-11	
14P48	CRYSTAL STRUCTURES OF DABCO SALTS WITH LONG ALKYL CHAINS-ANALYSES OF THE HIGH TEMPERATURE PHASE USING POWDER X-RAY DIFFRACTION DATA. M.Sudo, H.Sato, D.Hashizume, M.Yasui and F.Iwasak
14P49	CRITICAL BEHAVIOR ON $SrTiO_3$(001) SURFACE WITH THE STRUCTURAL PHASE TRANSITION. S.Doi and I.Takahashi
14P50	CO DOPING EFFECT ON THE STRUCTURE AND MAGNETIC PROPERTIES OF $La_{0.7}Sr_{0.3}Mn_{1-x}Co_xO_3$ SYSTEM. T.J. Lee, C.Y. Wan, H.C. Ku, X.-G.Li, W.B. Wu, X.J.Fan and G.Ji
14P51	PYRENE II←→PYRENE I : THE HIGH-RESOLUTION VIEW. N.Shankland,K.S.Knight,K.Shankland,S.W.Love and C.S.Frampton
14P52	STRUCTURAL PHASE TRANSITIONS IN TRIAMMONIUM HYDROGEN DISULFATE. K.Sooryanayana and T.N.Guru Row
14P53	CRYSTAL STRUCTURE OF SPINEL $CuIr_2S_4$ AT LOW TEMPERATURE. H. Ishibashi, K.Tanioka, K.Nakahigashi,and R. Oshima

October 15 13:30-16:00
Poster Session room: Lobby and Malati I

MS-07 (III)	
15P1	IMPROVEMENT OF CRYSTAL HABIT FOR X-RAY DIFFRACTION OF MALTOOLIGOSYL TREHALOSE SYNTHASE BY REDUCTIVE METHYLATION OF LYSINE RESIDUES. M.Kobayashi, M. Kubota, and Y. Matsuura
15P2	THREE-DIMENSIONAL STRUCTURE OF GLUTATHIONE S-TRANSFERASE FROM *ESCHERICHIA COLI.* M.Nishida, S. Harada, Y. Satow, H. Inoue and K. Takahashi
15P3	THE CRYSTAL STRUCTURE OF 1-AMINOCYCLOPROPANE-1-CARBOXYLIC ACID DEAMINASE FROM YEAST. M.Yao, T. Sugimoto, A. Horiuchi, T. Ose, A. Nakagawa, I. Tanaka, S. Wakatsuki, D. Yokoi, T. Murakami and M. Honma
15P4	CRYSTALLOGRAPHIC STUDY OF PHOSPHOLIPASE D FROM *STREPTOMYCES ANTIBIOTICUS.* A. Suzuki, K. Kakuno, Y. Iwasaki, T. Yamane and T. Yamane
15P5	CRYSTALLOGRASPHIC ANALYSIS OF THE CATALYTIC MECHANISM OF L-2-HALOACID DEHALOGENASE. Y. Hata, Y-F. Li, T. Fujii, T. Akutagawa and N. Esaki
15P6	THE CRYSTAL STRUCTURE OF FOLYLPOLYGLUTAMATE SYNTHETASE TO 2.4Å RESOLUTION: STRUCTURAL HOMOLOGIES WITH ATP- AND FOLATE-BINDING ENZYMES. C.A. Smith, X. Sun, E. N. Baker and A. L. Bognar
15P7	DIRECT PHASE DETERMINATION FOR MACROMOLECULAR CRYSTALS BY STEREOSCOPIC MULTI-BEAM IMAGING. C.H. Chao, Y. S. Huang, F. J. Liang, H. C. Chien, C. K. Chen, S. L. Chang, Y. C. Jean, H. S. Sheu and H. S. Yuan
15P8	CRYSTALLOGRAPHIC STUDY OF A PORCINE HEMOGLOBN AT 1.8Å RESOLUTION - A POTENTIAL ARTIFICIAL HUMAN BLOOD. T-H. Lu, K. Panneerselvam, Y-C. Liaw, C-M. Tsai, P. Kan and C-J. Lee
15P9	PROTEIN CRYSTALLIZATION AND LAB. AUTOMATION. F. Han
15P10	THE STRUCTURE OF THE FIRST 3 DOMAINS OF THE TYPE 1 IGF RECEPTOR. T.P.J. Garrett, N.M. McKern, M. Lou, M.J. Frenkel, J.D. Bentley, G.O. Lovrecz, T.C. Elleman, L. J. Cosgrove and C. W. Ward
15P11	CRYSTAL STRUCTURE OF RIBULOSE 1,5-BISPHOSPHATE CARBOXYLASE/OXYGENASE FROM A RED ALGA, GALDIERIA PARTITA, WITH HIGH SPECIFICITY FACTOR. H.Yamamoto, H. Sugawara, N. Shibata, C. Miyake, A. Yokota and Y. Kai
MS-08 (III)	
15P12	CRYSTAL STRUCTURE OF COPPER COMPLEXES AND ITS HYDROGEN BONDINGS. T.Nemoto, S.Terada, T.Ogawa, S.Isoda and T.Kobayashi
15P13	CRYSTAL STRUCTURE OF 4-METHYL-(2-FORMYL-6-MORPHOLINO-1-YL-METHYL) PHENOL (I) AND BIS [2-HYDROXY-3-(MORPHOLINO-1-YL-METHYL)-5-METHYLBENZYL] ETHYLENEDIIMINE(II). S.S.S. Raj, R. Thirumurugan, G. Shanmugam, and H. K. Fun
15P14	FERROCENIUM TETRABROMOTIN STRUCTURAL STUDY OF A COMPLEX OF FERROCENIUM AND TETRABROMOTIN. I.A.Razak, H.K.Fun and B. M. Yamin
15P15	HYDROTHERMAL SYNTHESIS AND CRYSTAL STRUCTURE OF A CLUSTER $[Co(en)_3][Co(en)_2(H_2O)_2][Mo_8V_8O_{40}(HAsO_4)]$. W.M.Bu, G.Y.Yang, Q.Zeng, L.Ye, J.Q.Xu and Y.G.Fan
15P16	HYDROTHERMAL SYNTHESIS AND CRYSTAL STRUCTURE OF A SUPERMOLECULAR INORGANIC-ORGANIC CLUSTER $[Co(enMe)_2]_3[As_6V_{15}O_{42}(H_2O)]2H_2O$. W.M.Bu,G.Y.Yang, Q.Zeng, L.Ye, J.Q.Xu and Y.G.Fan
15P17	HYDROTHERMAL SYNTHESIS AND CRYSTAL STRUCTURE OF SUPERMOLECULAR INORGANIC-ORGANIC CLUSTER $[Ni(en)_2][Ni_2(en)_4As_8V_{14}O_{42}(HPO_3)]_5H_2O$. W.M. Bu, G.Y. Yang, L.C. Chen, L.Ye, J.Q.Xu and Y.G.Fan

October 15 13:30-16:00
Poster Session room: Lobby and Malati 1

15P18 COMPLEXES OF DIMETHYLTIN(IV) DICHLORIDE WITH HYDRAZONE AND AZINE LIGANDS -THE CRYSTAL STRUCTURES OF [Sn(Me)$_2$(Ph$_2$CNNC(Me)(C$_5$H$_4$N)Cl$_2$] AND [PhNHHNC(Me)(C$_5$H$_4$N)][Me$_2$SnCl$_3$].
R.B.Hitam, M.A.Affan, M.B.Shansuddin, B.M.Yamin, F.H.Kun and A.R.Ibrahim

15P19 STRUCTURES OF CALIX[n]ARENES.
Y.J.Park, B.H.Lee and S.H.Cho

15P20 STRUCTURE OF TETRACYCLO-μ-(*N*-ETHYLENETHIOUREA)-TRIS(IODOCOPPER(I)) MONOHYDRATE.
Y.Thanyasirikul, C.Pakawatchai, S.Pansook and T.Saepae

15P21 STRUCTURES OF COPPER(I) AND SILVER(I) NITRATES WITH ETHYLENETHIOUREA.
C.Pakawatchai and W.Ratchawee

15P22 THE STRUCTURAL CHARACTERIZATION OF [L$_2$CdI$_2$] COMPLEXES.
F.Fariati, S.I. Rahayu, B. W. Skelton and A.H. White

15P23 IMPROVING THE RATE OF CRYSTALLIZATION OF CONFECTIONERY FATS.
S.D.MaCmillan and K.J.Roberts

15P24 N-H...π(INDOLE) INTERMOLECULAR INTERACTION IN 3,3' DI INDOLYL PHENYL METHANE.
R. Krishna and D.Velmurugan

15P25 CRYSTAL AND MOLECULAR STRUCTURES OF DIAZAPINES.
M.S. Kumar, D. Kumaran, M.N. Ponnuswamy, K.Chinnakali and H.K. Fun

15P26 CONFORMATIONAL ANALYSIS OF AZA AND DIAZA BICYCLIC RING SYSTEMS.
D. Kumaran, M.N. Ponnuswamy, G. Shanmugam, K.Sivakumar and H.K. Fun

MS-09 (II)

15P27 GROWYH OF HOKUTOLITE CRYSTAL WITH FLUX PROCESSES AND ITS INPLICATIONS.
S.C. Yu and H.R. Wang

15P28 CRYSTAL STRUCTURE OF A MIXED-VALENCE COPPER CHLORIDE COMPLEX WITH TRIETHANOLAMINE.
L.A. Kovbasyuk-Mokhir, O.Y. Vassilyeva, V.N. Kokozay, I. Bernal and H. Chun

15P29 PHASE ANALYSIS OF NIOBIUM DOPED HEXAGONAL POTASSIUM TUNGSTEN BRONZES.
A. Hussain and A.U. Monir

15P30 NEW HIGH PRESSURE PHASE OF FeGeO$_3$ CLINOPYROXENE.
T. Hattori, G. Yagyu, T. Nagai, T. Yamanaka, S. Werner and H. Schulz

15P31 A STUDY ON ZSM-5 ZEOLITES SYNTHSISED WITH AND WITHOUT THE AID OF TEMPLATE
F. Seyedeyn-Azad and D. Zhang

15P32 POLYMORPHISM, TWINNING, STRUCTURAL MODULATION, AND CHEMISTRY OF SARTORITE, PbAs$_2$S$_4$(?).
T.Ozawa and Tachikawa

15P33 INFLUENCES OF DOPED-MATERIALS ON STRUCTURES AND PROPERTIES OF THE SnO$_X$-THIN FILMS.
V. Vong and N-T. Huong

15P34 CRYSTAL MORPHOLOGY OF Y$_3$Fe$_5$O$_{12}$ GROWN BY TSSG TECHNIQUE AND BY LPE METHOD.
S.J. Chung, H.M. Park and D.Y. Choi

15P35 TWINNING AND ORIENTATION CHARACTERISTICS OF HTSC EPITAXIAL THIN FILMS
I.K. Bdkin

15P36 STRUCTURAL CHARACTERIZATION OF SOME NEW IONIC AND MIXED CONDUCTORS BASED ON Li$_4$GeO$_4$.
R.P. Gunawardane, M.A.K.L. Dissanayake and H.H. Sumathipala

15P37 INTERATOMIC INTERACTION OF THE RUTILE-TYPE DIFLUORIDES OF FIRST-ROW TRANSITION METALS BY EXTENDED X-RAY ABSORPTION FINE STRUCTURE
K. Murai, A. Yoshiasa, O. Kamishima, K. Nakajima and T. Yamanaka

October 15 13:30-16:00
Poster Session room: Lobby and Malati 1

MS-10

15P38	STRUCTURAL STUDIES OF SOME INCLUSION COMPLEXES INVOLVING ß-CYCLODEXTRIN AND ALKYL(AQUA) COBALOXIME. H.K.Fun ,K.Chinnakali,X.Ping,Y.Chen and H.L.Chen
15P39	CLATHRATE COMPOUNDS OF MONOALKYLTRIMETHYL-AMMONIUM SALT AND NON-LANAR AROMATIC MOLECULES. K.Noguchi,Y.Sumimoto and K.Okuyama
15P40	COMPLEX FORMATIONS BETWEEN SURFACTANT AND AROMATIC COMPOUNDS WITH HETERO-RING. K.Sawada, and Y.Ohashi
15P41	CRYSTAL STRUCTURES OF PHENANTHRIDINE AND ACRIDINE DERIVATIVES WITH MAGNETIC INTERACTIONS. M.Suzuki,D.Hashizume,M.Yasui,T.Ishida,T.Nogami, and F.Iwasaki
15P42	STUDY ON A NEW TETRAGONAL PHASE OF NB-DOPED $PB(ZR_XTI_{1-X})O_3$ BY SYNCHROTRON X-RAY POWDER DIFFRACTION. H.C. Liu and H.Toraya
15P43	SYNTHESIS AND STRUCTURES OF POLYNUCLEAR COPPER(II)-LANTHANOID(III) COMPLEXES WITH CARBOXYLATE-BRIDGES. Y.Y. Yang,Y-L.Wu and X-M.Chen
15P44	SOLVOTHERMAL CRYSTALLIZATION OF METAL COORDINATION POLYMERS. S.M.F.Lo,Stephen S-Y.Chui,Herman.H-Y.Sung and Ian D.Williams
15P45	DIMENSIONAL CONTROL OF INORGANIC SOLIDS:1-D,2-D AND 3-D ORGANO-TEMPLATED ZrPOS. H.Y.Sung,Jihong Yu and Ian D.Williams
15P46	CRYSTAL ENGINEERING OF NLO PROPERTIES OF ORGANIC CRYSTALS USING SACCHARIDE MOIETIES. J.A.K.Cha,Kin-ning Hui,Vivian M-F.Chen and Ian D.Williams
15P47	(BEDT-TTF)-BASED ORGANIC CONDUCTOR SURFACES CHARACTERIZED BY STM. K. Hashimoto, T.Nakayama, N.Yoshimoto, M. Yoshizawa, M. Hara, M. Aono and I. Yamaguchi

MS-03

15P48	NEUTRON DIFFRACTION STUDY OF 3-1 PHOTOISOMERIZATION OF THE 3-CYANOPROPYL GROUP IN A COBALOXIME COMPLEX. T.Ohhara, J. Harada, Y. Ohashi, I. Tanaka, S. Kumazawa and N. Niimura
15P49	NEW 4-CIRCLE NEUTRON DIFFRACTOMETER AT JRR3M. Y.Noda, A. Kojima, H. Sawa, H. Yoshizawa and Y. Morii
15P50	INTERMOLECULAR HYDROGEN BRIDGES AND INTERMOLECULAR INTERACTIONS. U. Englert, G. Heger, E. Kuemmerle and R. Wang
15P51	$Ni_2[(m\text{-}S)CH_2CH_2NC(CH_3)CHC(CH_3)NH]_2$ DIMER: AN UNEXPECTED N-DEALKYLATION REACTION PRODUCT Kenneth J. Haller, T. Tuntulani and B. Tomapatanaget

Scientific Abstracts

IUCr'50-1

THE HISTORY OF THE IUCr.

E.N.Baker, University of Auckland, New Zealand.

This year sees the 50th anniversary of the first General Assembly and Congress of the IUCr, held at Harvard University from 28 July to 3 August, 1948. The rationale for what was considered to be a relatively small but clearly focused Scientific Union was advanced Professor Paul Ewald and Sir Lawrence Bragg after much discussion among crystallographers. A key aspect was the desire to establish an international journal for crystallography. The first issue of *Acta Crystallographica* appeared in April 1948, and preparations for *International Tables* were already in hand. For an account of this early history, see Kamminge, H. (1989) *Acta Cryst.* A 45, 581-601.

Since 1948 the activities of the Union have grown enormously, as has the science of crystallography. The initial group of four countries represented at the first Congress has grown to more than 40, from all parts of the world, and the 1997 World Directory of Crystallographers lists around 8000 names, from 74 countries. The publishing activities have expanded to now include six journals, new volumes of *International Tables* and a number of books. These support a variety of initiatives, from support for young scientists at meetings to the development of new electronic media. Many famous papers have been published in IUCr journals or presented at IUCr meetings. Present trends point to new challenges ahead, for our journals and for the IUCr in structural informatics, in the explosive growth of biological crystallography, and in the emergence of crystallography in developing nations.

ASPECTS OF CRYSTALLOGRAPHIC SCALING IN CRYSTALS QUASICRYSTALS AND BIOMOLECULES

A.Janner Institute for Theoretical Physics, University of Nijimegen

Crystallographic linear and planar scaling symmetries are observed in snow crystals, in decagonal, octagonal, icosahedral quasicrystals and in a number of biomolecules (in the axial projection of their rotational symmetry) like DNA, single-stranded DNA binding protein (GVP) and coat protein (GVIIIP) super-helices of filamentous bacteriophages, light-harvesting protein (LH2), cholera toxin B and others.

Typically, these symmetries are revealed by structural relations involving edges and intersection points of regular star polygons, expressible in terms of integral invertible nxn-matrices generating a crystallographic scale-rotational point group of infinite order. In 3 dimensions, one then often has corresponding scale-rotational screw transformations.

Peculiar is that not all atomic positions of the given structure are involved (in proteins only part of the C-alpha's in the polypeptide chains) and not necessarily those of a same atomic species. This gives rise to the concept of basic structural sites, as a subset of scale-rotational equivalent points of ideal atomic positions (or of holes, also), more or less deviating from the observed positions. Indeed, the scale-rotational symmetries are always broken and have a local character. They only occur within an intermediate scale region delimited by a maximal and a minimal distance.

All these aspects allow an incredible wealth in the realization of different structures with a given scale-rotational point group symmetry, even for a same set of equivalent points, and explain the difficulty of relating symmetry and structure.

TOWARDS A GRAMMAR OF CRYSTAL PACKING

C. P. Brock, Department of Chemistry, University of Kentucky, USA

It is no longer difficult to determine the locations of atoms in crystals even if the unit cell is large. It is far harder, however, to predict how a given molecule, even a simple molecule, will crystallize. Rational design of molecular crystals remains a challenge.

Even weak, probabilistic rules for predicting structures of molecular crystals are useful for scientists trying to design solid-state materials (as for optical or electronic applications). Such rules can be discovered and/or verified by investigating patterns found in the structural databases. Examples of rules we have discovered will be discussed (see references below). Work of others will be reviewed.

Brock, C. P. & Minton, R. P. (1989). *J. Am. Chem. Soc.*, **111**, 4586-4593.

Brock, C. P., Schweizer, W. B. & Dunitz, J. D. (1991). *J. Am. Chem. Soc.*, **113**, 9811-9820.

Brock, C. P. & Duncan, L. L. (1994). *Chem. Mater.*, **6**, 1307-1312.

Brock, C. P. & Dunitz, J. D. (1994). *Chem. Mater.*, **6**, 1118-1127.

Brock, C. P. (1996). *J. Res. Natl. Inst. Stand. Technol.*, **101**, 321-325.

Lloyd, M. A. & Brock, C. P. (1997). *Acta Cryst.*, **B53**, 780-786.

STRUCTURE AND FUNCTION OF MEMBRANE PROTEIN COMPLEX, CYTOCHROME C OXIDASE FROM BOVINE HEART

T. Tsukihara*, E. Yamashita*, N. Inoue*, M. Yao*, M. J. Fei*, T. Mizushima*, C. Peters Libeu%, H. Yamaguchi*, and T. Tomizaki*, K. Shinzawa-Itoh%, R. Nakashima%, R. Yaono%, S. Yoshikawa%,
*Institute for Protein Research, Osaka University, Suita, Osaka, Japan,
%Department of Life Science, Himeji Institute of Technology, Kanaji, Kamigori, Hyogo, Japan.

Cytochrome c oxidase catalyzes reduction of dioxygen to water coupled with proton pumping. The crystal structures of an eukaryotic and a prokaryotic cytochrome c oxidases was reported at 2.8 A resolution in 1995 (1, 2) and the whole structure of the bovine heart enzyme was reported in 1996 (3). For the proton pumping function of cytochrome c oxidase driven by the dioxygen reduction, an acidic group in the protein must be accessible only to one of the two bulk water phases on both sides of the mitochondrial membrane in a certain oxidation state of the enzyme, and the accessible side must be switched to the other side by change in the oxidation state, concomitantly with a significant change in pK of the acidic group.

Here we report crystal structures of the fully oxidized form at 2.30 A resolution, and the fully reduced form at 2.35 A resolution, showing significant redox coupled conformational changes in the segment containing Asp51 of subunit I and at CuB site (4). The crystal structures reveal new aspects for the enzymatic mechanism. In the fully oxidized state, Asp51 is completely buried inside the protein and is connected with the matrix surface by a hydrogen bond network. The residue migrates to the cytosolic surface upon reduction, disrupting the hydrogen bond network. The movement indicates a novel proton pumping mechanism.

1. T.Tsukihara et al., Science, 269, 1069(1995).
2. S.Iwata et al., Nature, 376, 660(1995).
3. T.Tsukihara et al., Science, 272, 1136(1996).
4. S. Yoshikawa et al., Science, 280, 1723(1998).

Pleanry-1

SPring-8 MOVES INTO USER OPERATION

H.Kamitsubo
SPring-8/JASRI (Japan Synch-rotron Radiation research Institute)

SPring-8 is one of the world's brightest synchrotron radiation source in the X-ray region of the spectrum. The facility consists of a 1GeV linac, an8GeV synchrotron and an 8GeV storage ring. SPring-8 has been in operation since October 1997 and the design goals of an emittance of 7nmrad and a stored current of 100mA with a lifetime longer than 40 hours were achieved.

The storage ring can accommodate 38 insertion devices (ID) and various types of IDs are developed at SPring-8. Now SPring-8 is providing researchers with high-brilliance ID radiation from 0.5 keV to 300 keV at 16 beamlines. In addition, 20 beamlines are under construction. An overview of the facility and some of the results will be presented.

DRUG DESIGN AGAINST SHIFTING TARGETS

P M Colman, J N Varghese, T J Blick, A Sahasrabudhe, J L McKimm-Breschkin, Biomolecular Research Institute.

Inhibitors of the influenza virus neuraminidase have been shown to be effective antiviral agents in humans. Several studies have reported the selection of novel influenza strains when the virus is cultured with neuraminidase inhibitors *in vitro*. These resistant viruses have mutations either in the neuraminidase or in the viral haemagglutinin. The neuraminidase variant Arg292→Lys is modified in one of three arginine residues that encircle the carboxylate group of the substrate. The structure of this variant in complex with the inhibitor used for its selection, and with other Neu5Ac2en analogues, has been determined. The results provide evidence that a general strategy for drug design when the target has a high mutation frequency is to design the inhibitor to be as closely related as possible to the natural ligands of the target.

13A1-1

A PROLINE-SPECIFIC AMINOPEPTIDASE WITH A DINUCLEAR MANGANESE CENTRE

M.C.J. Wilce[1], C.S. Bond[1], N.E. Dixon[2], H.C. Freeman[3], J.M.Guss[1], P.E. Lilley[1] and J.A. Wilce[1]. [1]Department of Biochemistry and [3]School of Chemistry, University of Sydney; [2]Research School of Chemistry, Australian National University.

Aminopeptidases are enzymes which catalyse the cleavage of the amino acid from the amino terminal residue of a peptide substrate. The specificity of a particular enzyme may either be for the N-terminal residue or the penultimate residue. Proline aminopeptidases (E.C. 3.4.11.9) specifically cleave the Xaa-Pro... bonds of oligopeptides. Prolidases are proline aminopeptidases which are specific for dipeptides.

We have solved and refined the structure of the proline aminopeptidase (AMPP) (Wilce *et al.*, 1998) from *Escherichia coli*. Crystals of the holo-enzyme grown at pH 8.5, near the optimum value for enzyme activity, are hexagonal, space-group $P6_422$ with a = 178.4 Å, c = 95.6 Å. Crystals of a low pH inactive form are tetragonal, space-group $I4_122$ with a = 139.7 Å, c = 230.9 Å. The structure of the hexagonal crystal form was solved by multiple isomorphous replacement. The phases were improved by solvent flattening which benefited from a volume fraction of solvent which exceeded 72%. The active site of the enzyme contains a dinuclear Mn(II) centre bridged by carboxyl groups of the protein and a hydroxide ion. The structure of a complex of AMPP with the inhibitor dipeptide Pro-Leu suggests a possible mechanism for the enzyme.

Wilce, M.C.J., Bond, C.S., Dixon, N.E., Freeman, H.C., Guss, J.M., Lilley, P.E. & Wilce, J.A. (1998). *Proc. Natl. Acad. Sci. USA*, **95**, 3472-3477.

CRYSTALLOGRAPHIC STUDIES OF RETROVIRAL MATRIX ANTIGENSFROM SIV,MLV,AND EIAV

Z.Rao ; Laboratory of Molecular Biophysics, Oxford University, OX1 3QU, UK & School of Life Scoences, Tsinghua University, Beijing, 100084,China

Retroviral matrix poteins (MAs) perform key roles in viral assembly, envelope incorporation and nuclear import. Detailed understanding of these functions, from the high resolution crystal structures are critical to the rational design of gene delivery vectors and retroviral disease treatments.
Crystal structure of SIV matrix protein (SIV-MA) solved to 2.1A resolution by m.i.r methods both at 100K and 249K. In the crystal, this protein forms a trimmer stabilized by inter-molecular hydrogen bounds and presents a broad flat and charged surface to the inner region of the virion membrane. The organization is consistent with the observed architecture of the SIV virion and explains a number of the biological properties. Anti-AIDS drug design work based on the structure has carried out in collaboration with Dr. Ian Jones group(Virology, Oxford). It is therefore necessary to study a selection of relevant retroviruses in order to provide a comprehensive understanding of MA function. Collaborations with Kingsman's group(Biochemistry, Oxford) and Dr. Jones on the murine leukemia virus matrix protein (MLV-MA) and the equine infectious anemia virus matrix protein (EIAV-MA), have led to crystals being obtained. A 2.5A resolution structure of EIAV-MA has been solved.

STRUCTURE OF PHYSALIS MOTTLE VIRUS

S. Sri Krishna[1], S.K.Munshi[1], C.N.Hiremath[1], S.Suryanarayana[2], A.N.K.Jacob[2], M. Sastri[2], H.S.Savithri[2] and M.R.N.Murthy[1]

[1]Molecular Biophysics Unit and [2]Biochemistry Department

Indian Institute of Science, Bangalore 560 012, India

Physalis mottle virus (PhMV) is a highly infectious plant virus that belongs to the T=3 tymovirus group. It has a particle diameter of about 300 Å. The coat protein consists of 180 subunits, each of 21 kDa, surrounding a single-stranded positive sense RNA genome of size 6 kb. PhMV, purified from infected plant tissue, was crystallized by vapor diffusion using the sitting drop method. Crystals obtained belonged to either R3 or P1 space group, although there are two forms (Form I and Form II) of P1 appearing under identical crystallization conditions. The unit cell edges and interaxial angles of all the crystal forms are of the order of 290 Å and 60°, respectively. X-ray diffraction data to 3.8 Å resolution have been recorded on films by screenless oscillation photography for R3 crystals. Diffraction data on crystals of Form I and Form II have been collected on a MAR imaging plate to 4.0 Å and 3.5 Å, respectively. A preliminary solution for all the structures has been obtained by molecular replacement using the coordinates of the related turnip yellow mosaic virus with which PhMV coat protein shares 32% amino acid sequence identity. These structures are currently being refined using X-PLOR.

13A1-4

CRYSTAL STRUCTURE OF PHOSPHOENOLPYRUVATE CARBOXYLASE FROM *ESCHERICHIA COLI*

Y. Kai[a], H. Matsumura[a], T. Inoue[a], K. Terada[b], Y. Nagara[a], T. Yoshinaga[c], A. Kihara[b], K. Tsumura[b], K. Izui[b] [a]Dept. of Materials Chemistry, Osaka University, [b]Dept. of Applied Biosciences, Kyoto University, [c]Dept. of Public health, Kyoto University

Phosphoenolpyruvate carboxylase (PEPC) [EC 4.1.1.31] is one of the most important enzymes in photosynthesis, since it contributes to 50% of photosynthetic carbon fixation on the earth. The crystal structure of PEPC from *Escherichia coli* was determined at 2.8 Å resolution by multiple isomorphous replacement method. Crystallographic R and R_{free} factors are 21.9% and 25.9%, respectively. As *E. coli* PEPC is very similar to plant PEPC in the primary structure, the result can be directly applied to plant PEPC. PEPC is composed of four identical subunits that take a "dimer-of-dimers" structure with respect to subunit contact and an overall square arrangement. The tertiary structure of each subunit consists of a $(\beta/\alpha)^8$ barrel with the active site located at the carboxy terminus of the strands of the barrel. The barrel is very large (containing 491 residues) relative to many other $(\beta/\alpha)^8$ proteins, since all of the 8 β-strands are widely dispersed on the primary structure. The allosteric inhibitor site for L-aspartate is located ~20 Å away from the active site within the same monomer. The Arg587 identified as a catalytically essential residue (Yano *et al.*, 1995) interacts with L-aspartate through hydrogen-bonds, providing a novel mechanism for allosteric regulation.

1) Yano, M. *et al.* (1995) *J. Biochem*, **117**, 1196-1200

13A1-5

CRYSTAL STRUCTURE OF HEMOPEXIN: A UNIQUE HEME BINDING SITE FORMED BY TWO β-PROPELLOR DOMAINS

M.Paoli, H.M.Baker, E.N.Baker (University of Auckland, New Zealand) and B.F.Anderson (Massey University, New Zealand).

Hemopexin is a serum glycoprotein that binds heme with the highest affinity of any known protein. Its biological role is to bind the heme that is released during hemoglobin breakdown and to transport it to the liver for release via specific receptors. To understand these properties of heme binding and release we have determined the three-dimensional structure of hemopexin by X-ray crystallography, using three different crystal forms, and both glycosylated and deglycosylated forms of the protein.

The protein is folded into two domains, joined by a flexible linker peptide. Both domains have a fourfold β-propellor fold, with the edge of one packing against the face of the other. The heme occupies a unique site in a pocket between the interdomain connecting peptide and the junction of the two domains. Heme recognition depends on an exquisite network of hydrogen bonds from conserved protein sidechains to the buried heme propionates, together with packed aromatic sidechains. The structure also suggests a mechanism for heme release, by receptor-mediated disruption of the packing of the two β-propellor domains. This may be assisted by flexibility in the central portion of the connecting peptide, which may act as a "hot spot" to initiate release. The association of the two β-propellor domains further shows how these modules, which are common in multi-domain proteins, such as collagenases, G proteins and other proteins with modular repeats, can mediate both protein-protein and protein-ligand interactions.

THE CRYSTAL STRUCTURE OF THE ENDONUCLEASE DOMAIN OF COLICIN E7 COMPLEXED WITH ITS INHIBITOR Im7

T.P. Ko, W.Y. Ku, S.S. Chern, and H. S. Yuan, Institute of Molecular Biology, Academia Sinica, Taipei, Taiwan, ROC. Chen-Chun Liaw and Kin-Fu Chak, Institute of Biochemistry, Yang-Ming University, Taipei, Taiwan, ROC.

Plasmid encoded colicins are a group of antibiotic-like bacteriocins which kill sensitive bacteria in different ways, such as formation of ion channel, and exhibiting either DNase or RNase activity. Colicin E7 (ColE7) contains an endonuclease domain and it kills other bacteria by cleaving their DNA. In order to protect the host cell, immediately after production, ColE7 forms a complex with an inhibitor protein, Im7, resulting in neutralization of colicin's toxicity. How Im7 interacts specifically with ColE7 and how it inhibits the endonuclease activity after the formation of the complex are not fully understood.

The crystal structure of Im7 has been determined at 1.8 Å resolution and possible colicin-interacting surfaces have been identified (*Proc. Natl. Acad. Sci. USA* 1996, 93, 6437-6442 and *EMBO J.* 1997, 16, 1444-1454). Now we report the crystal structure of the endonuclease domain of ColE7 complexed with Im7 at 2.3 Å resolution. The endonuclease domain of ColE7 has an α/β fold that interacts with Im7 mostly via an α-helix. Putative endonuclease active site is proposed in the structure that is partially blocked by Im7.

13B1-1

PHASE-RETRIEVAL X-RAY DIFFRACTOMETRY: A TOOL FOR UNAMBIGUOUS CHARACTERISATION OF CRYSTALLINE MATERIALS.

A. Y . Nikulin

Department of Physics, Monash University, Clayton, Vic 3168, Australia.

A novel experimental-analytical technique is developed for model-independent and non-destructive characterisation of crystalline materials, Nikulin, Zaumseil & Petrashen' (1996), (1997), Nikulin (1998). The method relies on the retrieval of the phase of a scattered x-ray wave from its intensity profile via a logarithmic dispersion relation, Petrashen' & Chukhovskii (1989). The crystal structure factor can then be determined via a Fourier transform. Practical examples of the applicability together with examined problems of the developed technique are discussed, Nikulin & Petrashen' (1997), Nikulin & Zaumseil (1997).

Nikulin, A. Yu. (1998). *Phys. Rev. B*57, 11178-11183.

Nikulin, A. Yu. & Petrashen', P. V. (1997) *J. Appl. Phys.* **82**, 989-993.

Nikulin, A. Yu. & Zaumseil, P. (1997) *Phys. Stat. Sol. (a)* **163**, 305-312.

Nikulin, A. Yu., Zaumseil, P. & Petrashen', P. V. (1996) *J. Appl. Phys.* **80**, 6683-6688.

Nikulin, A. Yu., Zaumseil, P. & Petrashen', P. V. (1997) *J. Phys. D.: Appl. Phys.* **30**, 2373-2378.

Petrashen', P. V. & Chukhovskii, F. N. (1989) *Sov. Phys. Dokl.* **34**, 957-959.

13B1-2

THREE-WAVE GRAZING INCIDENT X-RAY DIFFRACTION : A METHOD FOR DIRECT PHASE DETERMINATION OF SURFACE IN-PLANE REFLECTION

Y.S. Huang[*], S.L. Chang[*], C.H. Chao[*], M.T. Tang[#], AND Y. P. Stetsko[$],
[*]Department of Physics, National Tsing Hua University, Hsinchu, Taiwan
[#]Synchrotron Radiation Research Center, Hsinchu, Taiwan, R.O.C.
[$]Chernovtsy State University, Chernovtsy, Ukraine

Three-wave grazing incidence x-ray diffraction is realized by tuning the x-ray photon energy to match the incident wave vector with the coplanar momentum transfers of crystal surface in-plane reflections. Near the resonance energy, the observed specularly diffracted intensities decreasing at lower energies and increasing at higher energies or vice versa reveal the effects of reflection phases due to the coherent interaction of x-ray surface waves. This experiment thus provides a new way of direct phase determination for surface in-plane reflections.

13B1-3

MAGNETIC STRUCTURE OF Fe/Gd MULTILAYERS DETERMINED BY X-RAY MAGNETIC SCATTERING

H. Hashizume (Materials and Structure Laboratory, Tokyo Institute of Technology), N. Hosoito (Inst. of Chem. Research, Kyoto Univ.), N. Ishimatsu (TIT) and G. Srajer (Advanced Photon Source, Argonne National Laboratory)

Fe/Gd multilayers are known to take aligned and twisted magnetic structures depending on temperature (T) and the strength of in-pane magnetic field applied parallel to the surface. In the twisted state antiferromagnetically coupled Fe and Gd moments make large in-plane angles to the field direction to minimize the magnetic energy. We used the resonant X-ray magnetic scattering technique to map out the distributions of the magnitudes and the orientations of the magnetic moments over the 50 nm thickness of the Gd layers. Photon energy was tuned to the Gd absorption edge at a third-generation synchrotron source. The resonant magnetic scattering was measured by flipping the helicity of a circularly polarized X-ray beam with a diamond phase plate. In both the high-T aligned state and the low-T twisted state, the Gd layers are more strongly magnetized in the interface regions close to the Fe layers than at the film centers. The twist angles are also non-uniform over the depth of the Gd films. At Ts close to the compensation temperature (170 K), only the near-interface regions have twisted magnetizations. The twist angle increases at lower temperatures and the magnetic moments at the Gd film center are directed nearly perpendicular to the applied field at 140 K.

13B1-4

INFLUENCE OF SITE-SELECTIVE IRON IONS ON THE MAGNETIC CIRCULAR X-RAY DICHROISM IN $\mathrm{Fe[Ni_xFe_{2-x}]O_4}$

E. Saito, T. Toyoda, T. Mori*, M. Tanaka*, K. Hirano* and S. Sasaki, Materials and Structures Laboratory, Tokyo Institute of Technology, Nagatsuta, Midori-ku, Yokohama, Japan; *Institute of Materials Structure, High Energy Acceleration Research Organization, Oho, Tsukuba, Japan.

Magnetic circular X-ray dichroism (MCXD) experiments for the ferrimagnetic Ni ferrites with different Ni concentration were performed using the phase shifter of a thin diamond crystal and rare-earth magnets at the Faraday arrangement with the magnetic field of 0.58 T.

The quantities determined in the MCXD experiment were the difference in the absorption coefficients for right- and left-circularly polarized synchrotron X-rays at the Fe *K* absorption edge with spin parallel and antiparallel in the direction of light travel. The samples investigated in this study were $[\mathrm{Fe^{3+}}]^A\,[\mathrm{Ni^{2+}}_x\mathrm{Fe^{3+}}_{2-x}]^B\mathrm{O_4}$ (x = 0, 0.16, 0.33, 0.52, 0.71 and 0.93), having the complete inverse-spinel structure of the space group $Fd\,\bar{3}m$. This study aims at examining the origin of the magnetic moments in Ni ferrites which are strongly affected how the constituent cations occupy the crystallographically-independent A and B sites.

In the MCXD spectra obtained for all samples, dispersion-type signals and bell-type peaks appeared at the pre-edge and main-edge regions of the Fe *K* edge, respectively. The signals of bell-type peaks increased with the decreasing of the Ni concentration in the B sites, although the height of the pre-edge peaks did not change significantly. Thus, our result strongly suggests that the main-edge peaks originate in the Fe ions occupying the B sites, which are deeply related to the production of the magnetic moments of Ni ferrites.

CRYSTAL STRUCTURE ANALYSIS OF THE SUPERCONDUCTING $PrBa_2Cu_3O_x$ COMPOUND

J. Ye[1], Z. Zou[2], K. Oka[2], Y. Nishihara[2,3], A. Matsushita[1], and T. Matsumoto[1]
[1]National Research Institute for Metals, Tsukuba, Ibaraki, Japan
[2]Electrotechnical Laboratory, Tsukuba, Ibaraki, Japan
[3]Faculty of Science, Ibaraki University, Mito, Japan

Crystal structure of the superconducting $PrBa_2Cu_3O_x$ compound was investigated at both of ambient and high pressures. The compound, which was known as the exceptional material being non-superconducting among $RBa_2Cu_3O_x$ (R= rare earth), has become superconductive for the crystals specially prepared [1-3]. To make clear the origin of the superconductivity, accurate crystal structure analyses of the compound were carried out using X-ray diffraction with conventional MoKα and synchrotron radiation. The structure of the superconducting Pr123 grown by TSFZ method was revealed to be essentially isostructural to that of R123, with a slight modification, such as longer *c*-axis coming from the expansion of the two CuO_2 planes. The details of the structural parameters, including ordering state of Pr and Ba will be reported. Moreover, as a means to help understanding of the superconducting mechanism, pressure effects on the T_c and structure of the compound were investigated using a cubic anvil cell high pressure apparatus and a diamond anvil cell. An unusually large T_c enhancement ($T_{c(zero)}$ =105 K at 9.3 GPa) has been observed, while the lattice parameters of Pr123 were found to be compressed linearly as a function of pressure. The facts contradict with the consideration of widely accepted "hybridization model".

[1] Z. Zou, K. Oka, T. Ito, and Y. Nishihara (1997). Jpn. J. Appl. Phys. **36**, L18-L20.

[2] Z. Zou, J. Ye, K. Oka, and Y. Nishihara (1998). Phys. Rev. Lett. **80**, 1074-1077.

[3] J. Ye, Z. Zou, A. Matsushita, K. Oka, Y. Nishihara, and T. Matsumoto (1998). Phys. Rev. B. R., in press.

13B1- 6

SYNCHROTRON X-RAY DIFFRACTION STUDIES ON INTERPLANETARY DUST PARTICLES : L2005AE6 AND L2005AG17

K.Ohsumi (Inst. Materials Structure Science, High Energy Accelerator Research Organization) and M.E.Zolensky (NASA/Johnson Space Center)

The equipment for obtaining diffraction patterns from submicrometer-sized specimen and micrometer area of a larger sample was developed employing the imaging plate for two dimensional detector at the beamline 4B1 of the Photon Factory, KEK. It has been applied to the interplanetary dust particles with the sizes of 6 μm(L2005AE6) and 17 μm(L2005AG17).

1) Analysis of chondritic interplanetary dust particle L2005 AE6

The chemical formula of this sample is determined as Fe0.89Ni0.02S analyzed with an electron prove micro analyzer (EPMA). The Laue pattern was obtained by a 30 minute exposure with the average ring current of 297 mA under the ring operation of 2.5GeV. The experiment was carried out in vacuum of 6x10-2 Torr..

More than 40 Laue spots were recorded on the imaging plate. An important feature of the Laue pattern is that some satellite reflections accompanied with missing main spots are observed. Indices of the missing spots with the pair of satellites are 1-2 2, 1-2 1, 1-2-1, 1-2-2 and 1-2-4. This type of pyrrhotite is classified into the NA type, and its *c*-axis is three times of that of the niccolite (NiAs) type subcell. The pairs of satellites indicate twinning of the NA type. From the positions of satellite reflections, the periodicity of the *a*-axis is estimated to be 41.84 times (N = 41.84) longer than that of the niccolite type FeS subcell.

2) Analysis of the chondritic interplanetary dust particle L2005 AG17

The chemical formula is determined as Fe0.83S by the method mentioned above. Laue pattern of 1.6 μm ϕ area of the sample was obtained by 15 min. exposure with the average ring current of 291mA. Diffuse streaks are observed along the zone. In order to clarify the diffuse streaks, six oscillation patterns were also taken by monochromatic synchrotron radiation (1.0005A) with an oscillation range of 30 degrees for each to cover 180 degrees. Most of the diffuse diffractions peaks can be indexed based on the 3C type pyrrhotite. Four weak but distinct powder lines are also observed in all oscillation patterns; these lines correspond to those of magnetite (Fe3O4). This sample is thus revealed to be composed of 3C-pyrrhotite and magnetite.

LOCAL DISTORTION OF $LiNiO_2$,, $Li(Ni,Co)O_2$, AND $LiMn_2O_4$ WITH Li DEINTERCALATION IN CATHODE MATERIALS OF RECHARGEABLE Li BATTERIES, STUDIED BY IN SITU X-RAY ABSORPTION FINE STRUCTURE ANALYSIS

I.Nakai, Y.Shiraishi ; Dept. of Applied Chemistry, Faculty of Science, Science Univ. of Tokyo, and F.Nishikawa; Battery Development Laboratory, Asahi Chemical Industry, Co., Ltd.

Structural changes accompanying the electrochemical Li deintercalation of the title compounds were studied by the transmission XAFS technique using an in situ X-ray cell of original design and synchrotron radiation. Our results revealed that the Jahn-Teller distortion of the Ni-O octahedra found in $LiNiO_2$ decreased as the Li ion was removed from the cathode. The observed XANES spectra of $Li_{1-x}NiO_2$ and $Li_{1-x}CoO_2$ as a function of x are consistent with the phase transitions found by powder-diffraction studies. The Ni-O, Co-O and Ni-Ni interatomic distances decreased almost linearly to x=0.8 as the Li content decreased, while the Co-Co distance slightly decreased to x=0.5 and increased up to x=0.8.

The electronic structures of Ni and Co in a solid solution $Li_{1-x}(Ni_{0.5}Co_{0.5})O_2$ are clarified as a function of x. XAFS analysis discloses that oxidation of the Ni ion in $Li_{1-x}(Ni_{0.5}Co_{0.5})O_2$ occurs immediately when the cell is charged, then stops at x=0.5, whereas the oxidation of Co continues slowly to x=0.8. The Jahn-Teller distortion of the NiO_6 octahedra in $Li(Ni_{0.5}Co_{0.5})O_2$ decreases with the Li deintercalation. It is found that, when the solid solution is used as a cathode of the battery, the Ni ions play a principle role in the initial stage of the charging process.

The dynamical structural behavior of Mn in $Li(Mn_{1.93}Li_{0.07})O_4$, and $Li(Mn_{1.85}Li_{0.15})O_4$ as a function of both excess Li content and the Li deintercalation was revealed using the in situ cell. The analysis disclosed the coexistence of two MnO_6-coordination polyhedra with different Mn-O distances for the Mn^{3+} and Mn^{4+} ions at the 16d site of the spinel structure. Because the charge-discharge process accompanies the oxidation-reduction of the Mn ions, this size difference causes an unfavorable lattice distortion for the electrode materials, which can cause a loss of cell capacity after cyclic use of the cell. A partial substitution of Li for Mn will diminish this effect and will be favorable for the battery material.

HIGH-RESOLUTION POWDER DIFFRACTION EXPERIMENTS USING SYNCHROTRON RADIATION AT BEAMLINE BL02B1 IN SPRING-8

H. Okudera[1)], Y. Kubota[2)], H. Hibino[1)], M. Yamakata[3)], H. Toraya[1)], and Y. Noda[4)]. 1) Ceramics Research Laboratory, Nagoya Institute of Technology, Gifu,
2) Department of Natural Science, Osaka Women's University, Osaka,
3) SPring-8, Hyogo, 4) Research Institute for Scientific Measurements, Tohoku University, Miyagi, Japan

Powder diffraction experiments were conducted by using a seven-axes diffractometer at the beam line BL02B1 in SPring-8, which is a new synchrotron radiation facility in Japan. The aim of the present experiments was to examine beam quality and instrumental resolution in powder diffraction using the diffractometer presently available.

A flat-specimen geometry was employed by using a rotating powder specimen of NIST SRM 640b Si or SRM 674a CeO_2. Crystal planes of monochromator used were Si(111) and Si(311). A second cyrstal of the monochromator was sagitally focused for converging the beam at a sample position in some experiments. The analyzer, mounted on a detector arm of the diffractometer, was a Si(220) flat crystal.

The observed reflections had well-resolved nearly symmetric profile shapes. The minimum FWHM's of 0.0127° and 0.0136° in 2θ were obtained for CeO_2 and Si, respectively, by using Si(311) plane of monochromator and incident beam of $\lambda = 0.5$Å. Diffraction intensity was much increased with the monochromator plane of Si(111) without increasing the profile width. In both cases, the profiles were not largely broadened with increasing 2θ.

Three results were obtained for Si powder by using monochromator crystals of sagitally focused Si (311) and Si(111), and flat Si(111), and incident beam of $\lambda = 1.0$Å. The FWHM's were 0.015°, 0.014°, and 0.015° at the minimum for respective monochromator crystals. In the high-angle region, FWHM's for the respective monochromator crystals were 0.05°, 0.09°, and 0.064° at $2\theta = 129°$. The best resolution was obtained if we use Si(311) crystal, whereas obtained intensity was weak. Diffraction intensity was increased with Si(111) plane, and the combination of flat Si(111) and a narrower vertical slit yielded the same resolution and much more intensitiy in comparison with the use of sagitally focused Si(311) crystal.

INTERMOLECULAR INTERACTION ENERGIES FROM ACCURATE X-RAY DIFFRACTION DATA

M.A. Spackman and A.S. Mitshell
Division of Chemistry, University of New England, Armidale, Australia

Although it is a decade since the first comprehensive attempt was made to extract meaningful interaction energies from x-ray data for molecular crystals (Spackman, Weber & Craven, 1988), still very few studies report intermolecular energies following a multipole refinement procedure. In part this is due to the limited availability of appropriate programs, and in part due to the limited appreciation of the physical meaning of the results - in particular, the energy obtained is the classical electrostatic interaction between polarized molecules, and this is not quite comparable with the true binding energy. In recent work we have utilized a simpler algorithm for computing these electrostatic energies (Stone, 1997) which enables accurate error analysis for the first time, and applied it to the calibration of these energies using simple dimeric systems.

Model data sets have been computed for the systems $(HF)_2$, $(H_2O)_2$, $(HCN)_2$ and $(HCONH_2)_2$ - both sums of non-interacting monomers as well as hydrogen-bonded dimers - and these have been fitted with conventional multipole models. The resulting electrostatic energies have been compared with the outcomes of an energy decomposition scheme (Morokuma & Kitaura, 1976; 1981) in order to illuminate what can, and what cannot, be obtained with confidence from high-quality x-ray diffraction data. Results obtained from both theoretical and experimental data for molecular crystals will also be presented.

Morokuma, K. & Kitaura, K. (1976) *Int. J. Quantum Chem.*, **10**, 325.
Morokuma, K. & Kitaura, K. (1981) in *Chemical Applications of Atomic and Molecular Electrostatic Potentials*, eds P. Politzer & D.G. Truhlar (Plenum, NY) p 215.
Spackman, M.A., Weber, H.P. & Craven, B.M. (1988) *J. Am. Chem.Soc.*, **110**, 775.
Stone, A.J. (1997) *The Theory of Intermolecular Forces* (Oxford).

13C1-2

4f-ELECTRON DENSITY ANALYSIS IN RARE-EARTH CRYSTALS TAKING INTO ACCOUNT SPIN-ORBIT INTERACTION

K. Tanaka, Dept. Mat. Sc. and Eng., Nagoya Inst. Tech., Japan and Y. Onuki, Phys. Dept., Osaka Univ., Japan

The 4f-electron density distribution(EDD) of CeB_6 at 165K was measured by avoiding multiple diffraction. It was analyzed based on the crystal filed theory confirming that the peaks around Ce were due to the 4f-electrons on the T_{1u} state. In order to evaluate the effect of anharmonic thermal vibration on EDD it was further measured at 100K, 230K and 298K. The anharmonic vibration effect on EDD was not significant but the analyses based on crystal field theory revealed inconsistent results. The t_{2u} orbitals were populated significantly at the three temperatures and the 4f orbitals were significantly contracted.

The analysis of EDD assuming that the spin-orbit interaction dominates the crystal field effect(weak field model) showed that four Γ_8 orbitals with J=5/2 were populated and two Γ_7 orbitals (J=5/2) are not occupied except at 298K. The 4f-orbitals showed no contraction. Therefore it becomes evident that analyses based on the weak field model explain the experiments much better. X-ray diffraction experiment is accurate enough to analyze the 4f-EDD since theory tells that weak filed model is more appropriate for 4f-electrons..

The peaks around Ce on the deformation densities at 230K and 165K are 0.8e Å^{-3} and 2.0e Å^{-3}, respectively. However those at 100K are unexpectedly small, 0.2e Å^{-3}, though the electron population on Γ_8 orbitals are the same within the experimental error. The intensity measurements at 115K and 85K for CeB_6 and for LaB_6, will be carried out to see the reasons for the strange temperature dependence of EDD.

13C1-3

CHARGE DENSITIES OF CRYSTALLINE MATERIALS BY THE MAXIMUM ENTROPY METHOD

M. Sakata, Department of Applied Physics, Nagoya University,
Chikusa-ku, Nagoya, JAPAN

Fourier theory tells us that charge densities of crystalline materials are calculated only if all the structure factors are known. It is exactly identical to know all of the structure factors and to know all the details of charge density distribution of a crystalline material. In reality, it is not practically possible to collect all of the structure factors of materials by any type of X-ray diffraction experiment. Besides the observed Bragg integrated intensities have some ambiguities. Here we encounter two infinite problems, i. e. impossibility of measuring infinite number of Bragg integrated intensities and impossibility of measuring a Bragg intensities with infinitesimal error. This two kinds of impossibilities leads to impossibilities of knowing 'truth'. As long as the limited number of Bragg reflection data is used, such an essential difficulties can not be avoided whatever analytical methods are employed, e.g. least squares refinement, Fourier or difference Fourier transformation and the Maximum Entropy Method(MEM).

What MEM can do is to restore a charge density distribution which is consistent with observed data and least biased with respect to unobserved data from a limited number of structure factors. It can be also proved from mathematical expression of Entropy that MEM is favorable to restore lower electron density distribution rather than higher density distribution. In other words, MEM is a good way to study distributions of electrons which differs from a free atoms or free ions model, such as covalent bond electrons, lone pair electrons, hydrogen bond electrons etc.. In such a case, it is very important to collect an accurate integrated intensities of low angle Bragg reflections, because bonding electrons mainly contribute to low angle Bragg reflections and rapidly decay as diffraction angle increase. On this point, careful powder experiments may have an advantage

be analyzed by MEM in order to see bond electrons etc.. In the talk,many examples will be shown including fullerene compounds after brief introduction of theory.

13C1-4

X-RAY IMAGING OF ELECTRON DENSITY UNDER MAGNETIC FIELDS.

V. Streltsov and D. du Boulay, *Crystallography Centre, The University of Western Australia.*

Synchrotron X-radiation diffraction experiments have been performed with applied external magnetic fields to measure structural and electron density changes in magnetostrictive intermetallics RFe_2 (R=rare earth) and haematite, α-Fe_2O_3. A relatively simple attachment to the Photon Factory BL14-A 4-circle diffractometer has been designed, which generates magnetic field of order 0.07 T at the sample position, without limiting the diffractometer driving angles.

Some cubic RFe_2 compounds derive their giant magnetostriction from their large anisotropic 4*f* electron charge density. Impressive changes to the structure and the electron distribution in $TbFe_2$ take place when the field is applied. This material undergoes positive strain by elongating along a cubic body diagonal, resulting in rhombohedral distortion.

Haematite is an imperfect antiferromagnet, with a weak ferromagnetic moment. Although the structural symmetry of α-Fe_2O_3 is rhombohedral, the magnetic symmetry is monoclinic. Under magnetic fields, the lattice is expected to magnetostrictively deform matching the magnetic symmetry. Haematite subjected to a magnetic field shows a strong distortion of electron density. No statistically significant displacement of the Fe atom from its rhombohedral position has so far been observed under a field of strength 0.07 T.

13C1-5

A CHARGE DENSITY STUDY OF THE POLYMORPHS OF P-NITROPHENOL,

G.U.Kulkarni, P.Kumaradhas and C.N.R.Rao ; Chemistry and Physics of Materials Unit, Jakkur, Bangalore-560 064, India.

A careful investigation of the structures and charge densities of the β- and α- polymorphs of p-nitrophenol has been carried out. Though the two forms crystallize in different monoclinic cells, the crystal densities are similar. There are several differences in the intramolecular structural features in the two forms, including the C-C-O bond angles as well as the N-O distances. The a form exhibits a large number of intermolecular hydrogen contacts, an observation which is related to its thermodynamic stability. More importantly, a detailed charge density analysis of the β and α forms has brought out significant differences in the charge distribution in both the intra-and ntermolecular hydrogen bonding regions. Deformation density maps reveal many differences in the bonding regions of the molecule in the two forms. Charge migration from the phenolic part of the molecule to the nitro group region occurs as the structure changes from the β to the α form. Relief maps of the negative Laplacians in the plane of the intermolecular hydrogen bonds show polarization of the oxygen lone-pair electrons towards hydrogen. The molecular dipole moments in the solid state derived from the pseudoatomic charges in the β and α structures are much larger (~ 22 Debye) than that in the free molecule.

13C1- 6

CHARGE DENSITIES AT 10 K - A COMPARISON OF SYNCHROTRON AND CONVENTIONAL DATA

P.A.Reynolds, Research School of Chemistry, Australian National University.

Lowering the temperature of a charge density determination from ca. 100 K to ca. 10 K minimises systematic, and effectively uncorrectable, errors due to thermal diffuse scattering and anharmonicity. We illustrate this by the cases of $(ND_4)_2Cu(D_2O)_6(SO_4)_2$ and $(ND_4)_2Fe(D_2O)_6(SO_4)_2$.

Simultaneous very low temperatures and the requirement for area detection require specialised synchrotron based diffractometers, such as on X3 at NSLS Brookhaven. We compare extensive ($\sin\Theta/\lambda<1.77Å^{-1}$) high quality data sets obtained for $Th(S_2PMe_2)_4$ on this machine and on a conventional displex-equipped diffractometer- both at short wavelengths (0.394 and 0.560 Å respectively) to minimise absorption, extinction and anomalous scattering effects.

120,154 synchrotron reflection data were collected in 3 days compared to 5,826 in 40 days with the conventional diffractometer. The extreme redundancy in the synchrotron data , averaging 19 reflections per unique reflections, was vital since present techniques produce 5-10% of spurious outliers which can only be rejected by statistical comparison. However when this is done *all* reflection intensity classes in the synchrotron data - not only the very weak- become superior to the conventional data. This is indicated for example by a final R(F) of 0.011 for synchrotron data compared to 0.022 for the conventional. With this technique bonding studies in heavy metal complexes become both feasible and reasonable. In this case we show that the Th-S bonding is unexpectedly ionic, and that the thorium core is significantly angularly polarised. The latter conclusion relies on the low temperature where the zero-point thorium motion is small (U of 0.002-0.003 $Å^2$) and all motions are harmonic.

Iversen, B.B., Larsen F.K., Pinkerton, A.A., Martin, A., Darovsky, A. & Reynolds, P.A. (1998). *Acta Cryst.*, **B**, in press.

13C1-7

CHARGE DENSITY STUDIES AND TOPOLOGICAL ANALYSIS OF METAL SQUARATES

C. R. Lee, C. C. Wang, G. H. Lee and Y. Wang, Department of Chemistry, National Taiwan University, Taipei, Taiwan, R. O. C.

Tetraaqua metal squarate complexes, $M(C_4O_4)(H_2O)_4$, (M = Fe, Co, Ni, Zn), are known to have a polymeric chain structure with $C_4O_4^{2-}$ served as a bridge (μ-2) ligand between two metal ions at *trans*-position. Each metal ion is bonded to two $C_4O_4^{2-}$ and four water molecules. They are all isostructural with space group *C*2/*c*. Carefully measured intensities at 120K are used to investigate the detailed electron density distribution in order to understand the chemical bonding and the *d*-orbital splitting of the metal ions subjected in such ligand field. Results on the electron density distribution will be presented in the form of deformation density and of Laplacian maps. Theoretical MO calculation of Ni complex is performed both with HF and DFT method. The interesting bent bond feature on the four-membered ring ligand $C_4O_4^{2-}$ is explicitly demonstrated. The asphericity in electron density distribution around the metal ion is also clearly illustrated in these compounds. The comparison on the series of 3*d*-transition metal complexes will be made not only by the deformation density distribution and by the Laplacian of the density but also by the d-orbital population and by the associated topological properties of the bond critical point. The total number of *d*-electrons from the experiments are 6.05, 6.88, 7.89, 8.40 respectively for Fe(II), Co(II), Ni(II), Zn(II) ions in these compounds. A comparison between experiment and theory is made on the Ni complex.

13A2-1

CRYSTAL STRUCTURE ANALYSES OF MICRO CRYSTALS OF ORGANIC COMPOUNDS AT SPRING-8

M. Yasui, N. Akiyama, M. Suzuki, M. Sudou, D. Hashizume, and F. Iwasaki
Dept. of Applied Physics and Chemistry, The University of Electro-Communications, JAPAN

Crystal structure determinations are essential for many studies. The size of single crystals, however, required with the conventional X-ray source is about a few hundred mm. In the case of crystals of charge-transfer complexes especially grown electrolytically, their dimensions tend to be very small and their shape may be thin plates or fine needles so that the structure analyses of these crystals were often very difficult. The high flux X-ray beam from SPring-8, the third generation of the synchrotron ring, will make possible the structure factor measurement of small crystallites. In this study, three kinds of organic microcrystals, $C_{38}H_{17}N_3O_3$: 230 x 130 x 50mm; $C_{16}H_{10}S_{12}I_3$: 200 x 80 x 30mm; $C_{31}H_{64}N_2Br_2$: 110 x 40 x 2.5mm, were subjected to the measurement of diffraction data using the vacuum camera equipped at BL02B1 of SPring-8. By the conventional X-ray generator, the measurements of diffraction data were failed due to their small size. The wavelength was corrected by the K edge of Zr (17.998keV) and set to 17.5keV (0.7085Å). Diffraction patterns were recorded on the cylindrical Imaging Plates (with radius of 75mm) using the oscillation method. The ring current was ranged from 17.0 to 19.0mA. The Bragg spots up to 2q of about 55° were clearly seen in each exposure. Brief results on the validity of the measured data and the crystal structure analyses using these data will be presented.

13A2-2

CRYSTAL STRUCTURE ANALYSES OF ORGANIC COMPOUNDS AT LIQUID HELIUM TEMPERATURE

D. Hashizume,[a] H. Sato,[a] M. Yasui,[a] F. Iwasaki,[a] A. Sato,[b] and H. Kobayashi[b]

[a]Department of Applied Physics and Chemistry, The University of Electro-Communications

[b]Institute for Molecular Science

Conventional experiments on the X-ray diffraction for organic compounds have been carried out above the liquid nitrogen temperature. Some interesting properties of materials, however, appear below the liquid nitrogen temperature. For this reason, it is necessary to elucidate the structures below liquid nitrogen temperature to understand the origins of their properties. We will report the structures of the magnetic materials, 4-benzylideneamino-TEMPO radical and dibromobis(pyrimidine)cobalt(II), at 7K, and the procedure of the measurements of diffraction data at liquid helium temperature.

The crystal was mounted on the gold wire which was connected with a brass tube through a copper wire. The system was covered with a cap made by carbon fibers. Then the inner of the cap was vacuumed by rotary pump. The liquid helium, as a coolant, were flowed in the brass tube to make the crystal cooled by thermal conduction. The data were collected by the Weissenberg camera using the imaging plate as a film. The resolution and the accuracy of the data were quite good. The analyses were finished without any problems.

13A2-3

HIRSHFELD SURFACES: A NEW TOOL FOR VISUALISING AND EXPLORING MOLECULAR CRYSTALS

J.J. McKinnon, A.S. Mitshell and M.A. Spackman
Division of Chemistry, University of New England, Armidale, Australia

A remarkable new way of exploring molecular crystals is afforded by smooth, non-overlapping molecular surfaces arising from a novel partitioning of crystal space (Spackman & Byrom, 1997). These molecular Hirshfeld surfaces, so named because they derive from Hirshfeld's stockholder partitioning (Hirshfeld, 1977), are constructed by partitioning the crystal into regions where the promolecule exceeds the procrystal. Initial investigations (McKinnon, Mitchell & Spackman, 1998) suggest that the Hirshfeld surface clearly reflects the proximity of nearest neighbours, and hence intermolecular interactions, in a novel visual manner, offering a hitherto unseen picture of molecular shape in a crystalline environment.

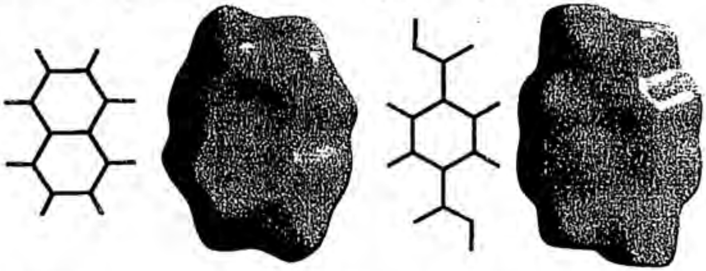

The figure illustrates Hirshfeld surfaces of naphthalene and terephthalic acid, clearly showing the differences in molecular packing within the crystals. Applications of this new tool to a variety of molecular crystals will be presented, including 3D isosurface pictures as well as a number of quantitative measures of molecular size and global shape. Current work on the utilisation of local descriptors such as curvature will also be outlined.

Hirshfeld, F.L. (1977). *Theor. Chim. Acta* , **44**, 129.

McKinnon, J.J., Mitchell, A.S. & Spackman, M.A. (1998). *Chem. Eur. J.*, **4**, in press.

Spackman, M.A. & Byrom, P.G. (1970). *Chem. Phys. Lett.*, **267**, 215-220.

13A2-4

CRYSTAL STRUCTURE OF HYDROGEN-BONDED CHARGE TRANSFER (CT) COMPLEXES OF CYANANILIC ACID WITH TETRATHIAFULVALENES (TTFs)

Md. B. Zaman, Department of Applied Chemistry and Chemical Technology, University of Dhaka, Dhaka, Bangladesh

K. Nakasuji, J. Toyoda and Y. Morita,. Graduate School of Science, Osaka University, Osaka, Japan

Considerable interest has been shown in using complementary hydrogen-bonded interections as a part of the design strategy for the development of solid-state conducting, electronic, magnetic and optical materials. Recently, we have exploited cyananilic acid (H_2CNAL) as a new acceptor and analyzed the crystal structure as hydrogen-bonded counter ion with TMTTF (tetramethyltetrathiafulvalene) in semiconducting CT complex (1). We report here the crystal structures of cyananilic acid and TTFs CT complexes of $(ET)_2(HCNAL)$ [ET=bis(ethylenedithio)tetrathiafulvalene, HCNAL=monoanion] and $(OMTTF)_3(HCNAL)(CNAL)$ [OMTTF=octa-methylenetetrathiafulvalene, HCNAL=monoanion CNAL=dianion). In the ET complex, ET forms a twisted columnar stacking of dimers which face-to-face overlap of the π-system and the monoanion HCNAL forms hydrogen-bonded ribbons. In the OMTTF complex, monoanion HCNAL and dianion CNAL form hydroen-bonded networks having cavities. The cavities are occupied by the trimeric OMTTFs of which ionicity are estimated as -1 by the length of central double bonds of OMTTF.

1. Zaman, M. B., Morita, Y., Toyoda, J., Yamochi, H., Saito, G., Yoneyama, N., Enoki, T., and Nakasuji, K. (1997) *Chem. Letts* 8, 729-730.

13A2-5

STRUCTURE OF DIMAGNESIUM CATION SPECIES $[Mg_2Cl_3(THF)_6]^+$ IN GRIGNARD REAGENTS

K. Yamaguchi, S. Sakamoto, Chemical Analysis Center, Chiba University, Yayoi-cho, Inage-ku, Chiba, 2635822, Japan and H. Tsuruta and T. Imamoto, Department of Chemistry, Faculty of Science, Chiba University, Yayoi-cho, Inage-ku, Chiba, 2635822, Japan

The structure of a cationic dimagnesium cluster, $[Mg_2Cl_3(THF)_6]^+$, possessing a short Mg–Mg contact in Grignard reagents is shown. This Mg–Mg interaction was observed in crystalline state obtained from PhMgCl and *t*-BuMgCl in tetrahydrofuran solution at room temperature. Slow evaporation of a THF solution of PhMgCl or *t*-BuMgCl under argon in Schlenk tube afforded crystalline solids. The highly unstable crystals were analyzed at 100K using rapid X-ray analysis system equipped with two–dimensional image plate detector.

We determined the crystal structure of $2Mg_2Cl_3(THF)_6 \cdot Ph_4Mg_2Cl_2$ (a=13.326, b=13.36, c=13.30Å, α=109.96, β=113.04, γ=85.75°, SG=P1, R=0.115) obtained from PhMgCl, and $Mg_2Cl_3(THF)_6 \cdot t\text{-}BuMgCl_2(THF)$ (a=14.99, b=15.829, c=9.39Å, α=96.65, β=105.98, γ=93.54°, SG=P1, R=0.092) from *t*-BuMgCl.

The detection of the dimagnesium species in Grignard reagents suggests that the important constitution including magnesium clusters might exist in the Schlenk equilibrium.

13A2- 6

CRYSTAL AND MOLECULAR STRUCTURE OF AN ANTHRACENE DERIVATIVE

M.N.Ponnuswamy, M.Suresh Kumar, R.Sugadev and K.K.Chacko
Department of Crystallography and Biophysics, University of Madras, Guindy Campus, Chennai – 600 025, India.

Anthracene is a naturally occuring compound found in coal-tar and formed during the incomplete combustion of organic compounds. Anthracene has high acute and chronic toxicity to aquatic life and birds. The compound is a pale yellowish crystlline material with a bluish fluorescence. It is used in dye stuffs, insecticides and wood preservatives. The crystal structure of [bis-9,10-(3,3′-diphenyl-3″-hydroxy-1-propyne)] anthracene has been determined by crystallographic methods.

Transparent and yellowish brown coloured crystals were obtained by slow evaporation method in DMSO solvate. The crystal belongs to monoclinic space group $P2_1/n$ with the cell constants $a = 16.296(3)$, $b = 11.837(2)$, $c = 19.426(4)$Å and $\beta = 104.11(3)^\circ$. The structure was solved by direct methods and refined by full-matrix least-squares procedures. The anthracene moiety is planar and is extended up to the propyne group. The phenyl rings are mutually perpendicular to each other. The molecules are stabilized by O-H...O and C-H...O type of hydrogen bonds in addition to the van der Waals forces.

13B2-1

X-RAYS OR NEUTRONS OR X-RAYS AND NEUTRONS? STRUCTURAL REFINEMENTS OF METAL OXIDES.

B.J. Kennedy, School of Chemistry, The University of Sydney

The spectacular improvements in powder diffractometers over the past decade, coupled with the even more dramatic advances in computing, allow us to tackle crystallographic problems of ever increasing complexity. Ab-initio structural determination from powder diffraction data, whilst not quite routine, is at least commonplace. Nevertheless the vast majority of structures derived from powder diffraction studies are refined using the Rietveld method. But even then as the structural complexity increases the type and amount of data required for a precise structural refinement also increases. In this presentation I will describe the strategies employed by the Sydney University group in our recent studies of different metal oxides structures. In particular I will address the question of if, and when, is it necessary to combine neutron diffraction data with high quality x-ray diffraction data.

Specific examples to be discussed include Pb-Bi disorder in $PbBi_2Nb_2O_9$ using anomalous dispersion x-ray diffraction data, static disorder in $Bi_3Sb_2AlO_{11}$ using variable temperature neutron diffraction data and the tetragonal-cubic phase transition in $CuRh_2O_4$.

13B2-2

CRYSTAL STRUCTURE STUDIES ON ORGANIC COMPOUNDS FROM POWDER DIFFRACTION DATA

Y.D. Xiao, L.H. Wei, R. Chen, R.X. Shen, J.B. Zhang, C.M.Lai and S.F. Lin
Centre Laboratory, Nankai University, Tianjin, 300071, P.R. China

It is the purpose of this paper to present two methods one is based on the combined use of molecular mechanics and crystal structural resolution, another is maximum entropy directly to determinate the crystal structure of organic or organo-metallic compounds. In former approach, the limited energy minimization configurations obtained by molecular mechanics calculation are independent of powder diffraction data, and then the relative trial structure is generated with cell parameters derived from experiment data. In the latter case, maximum entropy technique is used to refine the intensity of indexes in an extended range, and the trial structure can be gotten using the program of SHELXS86 from these indexes.These methods were illustrated by the solution of the crystal structure of ethyl hydrazodicarboxylate ($C_6H_{12}N_2O_4$) and (15-crown-5) manganese (II) di-isothiocyanate ($C_{12}H_{2}0MnN_{2}O_{5}S_{2}$), individually.

In general, mostly it is used to determine the structure of inorganic compound from powder diffraction data. Here, the molecular mechanics method and the maximum entropy technique are successfully introduced to the system. Molecular mechanics energy minimization can give the atomic coordinates of the interesting molecule and maximum entropy technique is used to refine the intensity of indexes in a wide range either measurable or not. The final structure was generated by the Rieveld technique. From the examples given above, we can conclude that the methods presented here have a high performance for organic compound. The limited structures by molecular mechanics or maximum entropy technique and comparing to the experimental diffraction data can help us obtain the good starting model. It simplified the procedure of the determination. We considered that these approaches have significant characteristics for rigid and small size compounds or these compounds with heavy atoms.

13B2-3

THE INFLUENCE OF CARBAMIDE PEROXIDE AND STANNOUS FLUORIDE ON CRYSTALLITE SIZE AND MICROSTRAIN OF TOOTH ENAMEL

M. Hikam and R. Tjandrawinata, Department of Physics, Faculty of Mathematics and Science, University of Indonesia, Depok 164224 Indonesia.

The purpose of this experiment was to study the influence of 10% carbamide peroxide and 0.4% stannous fluoride on crystallites of hydroxyapatite in tooth enamel, by using x-ray powder diffraction. Hydrogen peroxide solution and aquadest were used as controls. The materials were applied for 8 hours in an incubator operating at 37(C and 100% humidity. The crystallite size and the lattice parameters were calculated from the diffraction pattern, and the structure was then refined by Rietveld analysis. It was concluded that the carbamide peroxide and stannous fluoride influence microstrain in the tooth enamel, but not the crystallite size or lattice parameters.

13B2-4

IMPROVEMENT OF THE ACCURACY OF STRUCTURAL PARAMETERS IN RIETVELD REFINEMENTS USING A NEW WEIGHT FUNCTION

H.Toraya, Ceramics Research Laboratory, Nagoya Institute of Technology, Asahigaoka,Tajimi 507-0071, Japan

The Rietveld method is an indispensable technique for structure refinement using powder diffraction data. The accuracy of refined structural parameters was, however, not enough for detailed crystal chemical discussion even of simple structures like α-SiO_2. A new weight function in a form $w = 1/Y_o^e$ with $e \sim 2$ (Y_o = observed profile intensity) has been introduced into the minimization function used in Rietveld refinement 1). It has been tested by using profile intensity data sets of several inorganic materials measured with laboratory x-ray and synchrotron radiation sources.

The new weight function gives heavier weights on weak (higher order) reflections than those by the currently used weight function in a form $w = 1/Y_o$ in Rietveld refinement. Its validity was proved by 1) uniform distributions of $<w\,(Y_o - Y_c)^2>$ (Y_c= calculated profile intensity) against the groups of Y_o and 2) flat difference plots by $w^{1/2}(Y_o - Y_c)$. On the other hand, the conventional weight function by $1/Y_o$ more heavily weights the reflections with medium and strong intensities, although it accords with the statistical theory and gives a better overall fit between the Y_o and Y_c.

It was demonstrated that the average deviation of refined positional parameters of Mg_2SiO_4 from single crystal values was reduced to 0.002Å by using 1.2Å high-resolution synchrotron radiation data. The accuracy comparable to that obtained by a single crystal technique is attainable by the use of high-resolution powder diffraction data under the proper weighting on profile intensity. Several examples of application of the new weight function will be described in this paper.

1. H. Toraya, (1998). J. Appl. Cryst., 31 (in press).

13B2-5

STUDIES ON INCLUSION COMPLEXES VIA POWDER REFINEMENTS AND COMPUTER SIMULATIONS

T.N.Guru Row
Solid State and Structural Chemistry Unit , Indian Institute of Science.

The application of the Rietveld method using X-ray powder diffraction data for refinements of small molecules based on models derived from known structures or from ab-initio approaches is well established. Methods for the refinement of diffraction data from inclusion complexes are currently being investigated. Most often, the model of the host molecule is available based on earlier studies and essentially the guest molecule needs to be positioned in the constrained media provided by the host molecule. The interactions involved are generally weak and render the guest molecule to be in more than one configuration at a given temperature. The basic idea is to locate the guest molecule using molecular dynamic simulations at that temperature and identify the resulting electron density distribution on a difference Fourier map generated based on the powder diffraction data.

APPLICATION OF CRYSTALLOGRAPHIC DATABASES TO MATERIALS

J. Faber, R. Jenkins and R.L. SnyderThe international Centre for Diffraction Data (ICDD), 12 Campus Boulevard, Newtown Square, PA 19073, USA.

There are a number of data bases available to the diffraction community. Two of the more important of these are the Powder Diffraction File (PDF) maintained by the ICDD, and the Inorganic Crystal Structure Database (ICSD) maintained by the Fachsinformationzentrum (FIZ, Karlsruhe). In application, the PDF has been used as an indispensable tool in phase identification of unknowns. The ICSD database has extensive and explicit reference to the structures of compounds: atomic coordinates, space group and thermal vibration parameters. These databases are often used as independent sources of information. However, little thought has been given on how to exploit the combined properties of structural database tools. A recently completed agreement between ICDD and FIZ provides a first step in mutual use of the PDF and ICDD databases. The focus of this paper (as indicated below) is to examine ways of exploring the combined properties of both data bases.

In 1996, there were approximately 76,000 entries in the PDF and approximately 43,000 entire in the ICSD database. The latter is being used to calculate entries in the PDF. Thus, to derive d-spacing and peak intensity data requires the synthesis of full diffraction patterns, i.e., we use the structural data in the ICSD database and then add instrument resolution information. The combined data from PDF and ICSD can be effectively used in many ways. In this paper, we will show a number of examples that will focus on results obtained from multiple databases.

13C2-1

ELECTRON MICROSCOPY AND ITS APPLICATION TO ADVANCED MATERIALS

N.Yamamoto, Tokyo Institute of Technology, Oh-okayama, Meguro-ku, Tokyo 152, Japan

Transmission electron microscopy (TEM) has been applied to the wide range of materials as a useful tool for characterizing the structural properties on nanometer scale. There are special techniques in TEM such as dark-field imaging, high resolution imaging, and convergent beam electron diffraction, which unable us to analyze crystal structure and crystal symmetry of localized areas in the materials. We have observed domain structures and modulated structures formed by many types of phase transitions, such as ferroelectric phase transitions and incommensurate - commensurate phase transitions. In this paper the advantage of TEM will be shown in our recent research on the advanced materials, i.e., $Pb(Mg_{1/3}Nb_{2/3})O_3$ as relaxor ferroelectrics, manganese oxides with perovskite - type structure showing a charge-ordered phase transition, and Y_3TaO_7 showing ion conduction. The physical properties of these materials are concerned with the microdomain structures of nano-meter size, which change with temperature or annealing time. The microdomain structure in Y_3TaO_7 gives rise to diffuse scattering of a ring shape, and the crystal structure analysis of the microdomain region will be demonstrated.

13C2-2

MAXIMUM ENTROPY AND BAYESIAN METHODS FOR SOLVING CRYSTAL STRUCTURES USING ELECTRON DIFFRACTION DATA

C.J. Gilmore Department of Chemistry, University of Glasgow, Glasgow G12 8QQ, Scotland, UK.

The phasing of electron diffraction data poses considerable problems for traditional direct or heavy atom crystallographic methods since the data are incomplete, often at less than atomic resolution (i.e. 1.1Å), and subject to errors arising from dynamical scattering effects. The Bricogne formalism for phasing diffraction data using maximum entropy (ME) and Bayesian methods has proved especially useful in these situations[1] since it is stable irrespective of data resolution and completeness, and is robust with respect to errors on the measured diffraction intensities[2].

Successes with this formalism this include a wide range of structures including:

(1) The *ab initio* phasing of diketopiperazine $C_4H_6N_2O_2$[3].

(2) The structure solution of $CuCl_2.3Cu(OH)_2$[3].

(3) The *ab initio* phasing of two 2-D membrane data sets at *ca.* 6Å resolution without the use of image phases (Halorhodopsin and Omp F Porin[4]). In addition, we have had some success in phasing the 3-D data of bacteriorhodopsin at 6Å.

(4) 4-dimethylamino-3-cyanobiphenyl and other non-linear optical materials from electron diffraction data[5] .

(5) The surface structures of Si(111) 7x7[6]. Surface structures pose a particular problem since they are usually two-dimensional, weak and very incomplete (often <20 diffraction intensities!). In the Si case we can use image derived phases as a starting point, although the structure is solvable *ab initio*.

ME methods work so well in an electron diffraction environment because they use all the possible phase relationships correctly weighted simultaneously coupled with prior information (e.g. envelopes, forbidden zones), and thus can deal well with missing data, and it is also possible to utilise data variances in the calculations.

One major problem that arises at these resolutions is the verification of the structure: how does one know that the proposed structure is correct, given so little diffraction data which is so error prone? Is there a danger of choosing solutions which simply conform to our initial beliefs about the results?

1. G.Bricogne (1984). *Acta Cryst.* A40, 410-445.
2. G.Bricogne and C.J.Gilmore, *Acta Cryst,* (1990), A46, 284-297.
3. C.J.Gilmore, K.Shankland and G.Bricogne *Proc. Roy. Soc. Series A*, (1993), 442, 97-111.
4. C.J.Gilmore, W.V.Nicholson and D.L.Dorset *Acta Cryst.* (1996), A52, 937-946.

I.G.Voigt-Martin, Z.H.Zhang, U.Kolbe and C.J.Gilmore, *Ultramicroscopy* (1997) 68, 43-59. C.J.Gilmore, L. D. Marks, D. Grozea, C. Collazo, E. Landree andR.Twesten, *Surface Science* (1997) 381, 77-91.

13C2-3

HIGH RESOLUTION ELECTRON MICROSCOPY STUDY OF INTERFACE STRUCTURE OF MULTILAYERS WITH GIANT MANETORESISTANCE

Z. Zhang
Beijing Laboratory of Electron Microscopy, Center for Condensed Matter Physics 20 Chinese Academy of Sciences, P. O. Box 2724, Beijing 100080, China

The interfacial structure between magnetic and nonmagnetic layers plays an important role on Giant Magnetoresistance (GMR) effect in metallic magnetic multilayers. Since high resolution electron microscopy has its unique advancement in obtaining both diffraction and image information at atomic level, we have systematically investigated the interfacial microstructure of NiFe/Mo, Fe/Mo and NiFe/Cu magnetic multilayers by cross-sectional high resolution electron microscopy (XHREM).

For interface structure of [($Ni_{80}Fe_{20}$)1.4nm/Mox nm]30 magnetic multilayers (x=3D0.7, 1.6, 2.1), there are two types of orientation relationship between the fcc NiFe and bcc Mo layers: (110)Mo//(111)NiFe, [11]Mo// [10]NiFe and (110)Mo//(111)NiFe,[001]Mo//[10]NiFe. The NiFe/Mo interfaces are normally sharp with some region showing few atomic layer steps. The variation of lattice spacing at the interfacial region and the absence of the giant magnetic resistance effect have been discussed based on the structural characteristics of the multilayers.

In (Fe1.1nm/Moxnm)30 magnetic multilayers (x=3D0.6, 1.1, 2.2), each individual sub-layer is with polycrystalline phases. There are columnar bcc Fe and bcc Mo crystallites of 10(30 nm in width with epitaxy growth relation parallel to each other. The lattice in the columnar changes with the increase of the Mo layer thickness. It is suggested that the defects in the columnar is unfavorable to the magnetic resistance. A weak magnetic resistance effect in first MR peak of the Fe/Mo multilayer system should be result from the roughness of the multilayer.

Column crystallites of few nano-meters in width are found, for the first time, both in Fe/Mo and NiFe/Cu magnetic multilayers. Within a column crystallite, it is difficult to find out the lattice difference between the two different sub-layers due to the lattice relaxation of the ultrathin sub-layers. Elemental imaging results of Fe/Mo obtained from CM200-FEG equipped with GIF, show that the sub-layers are well recognized even though they could not be identified in the HREM images by taking the difference of the lattice spacing. From the view point of spin related free-path of electrons, the column structure of the multilayers may play a important role on the GMR effects in these systems.

13C2-4

THE DETERMINATION OF AN UNKNOWN OXYGEN ATOM POSITION IN RARE-EARTH ZIRCONATE PYROCHLORES BY SYSTEMATIC ROW CBED

Y. Tabira and R. L. Withers
Research School of Chemistry, Australian National University

Rare earth zirconate pyrochlores, ideal stoichiometry $Ln_2Zr_2O_7$ where Ln represents a lanthanide element, crystallize in space group Fd3m and can be described as $2 \times 2 \times 2$ cubic superstructures of an underlying fluorite–like parent structure. A large trivalent rare earth cation Ln and a smaller quadrivalent Zr cation order in the positions $16d(\frac{1}{2}, \frac{1}{2}, \frac{1}{2})$ and 16c(0,0,0) respectively. One oxygen, of seven per formula unit, occupies the $8b(\frac{3}{8}, \frac{3}{8}, \frac{3}{8})$ positions whilst the remaining six oxygens occupy the $48f(x, \frac{1}{8}, \frac{1}{8})$ positions. Solid solutions $Ln_yZr_{1-y}O_{2-y/2}(\approx 0.45 < y <\approx 0.55)$ have the pyrochlore structure for lanthanides ranging from La to Gd while a "defect fluorite" variant is found for compositions on either side of these pyrochlore solid solution fields. The unknown oxygen x parameter is difficult to determine from powder XRD data in the presence of the strongly scattering heavy metal atoms and has to date only been reported for Ln =La.

Taftø & Metzger(1985) introduced a large angle systematic row CBED technique for the measurement of high order kinematic structure factors. Such measurements were used to accurately determine unknown fractional coordinates. In this contribution we discuss the use of a similar systematic row CBED technique to determine the one unknown fractional coordinate of the 48f oxygen in a range of rare–earth zirconate pyrochlores. Results suggest that this x parameter can be determined to an accuracy of better than 0.005, although full dynamical calculations show that the 222 reflection is too strong and rule out kinematical data as obtained by Taftø & Metzger.

Reference

TAFTØ , J. & METZGER, T. H. (1985). *J. Appl. Cryst.* **18**, 110–113.

13C2-5

TEM CHARACTERIZATION OF STRAINED QUATERNARY MULTIPLE QUANTUM WELL STRUCTURES

I. K. Ng AND C. B. Boothroyd*, Malaysian Institute for Nuclear Technology Research (MINT). *Department of Materials Science and Metallurgy, University of Cambridge.

Strained-layer semiconductor superlattices are of potential interest for device applications. Multiple Quantum Wells (MQW) grown with InP lattice-matched barriers but biaxial compression in the wells have been shown to exhibit enhanced optical performance. However, the introduction of biaxial tensile strains in the barriers, tends to degrade the optical properties and structural regularity of the system. In this study, we compare the microstructures and composition variations for a set of $In_xGa_{1-x}As_yP_{1-y}$ multilayers with systematically varied biaxial strains as grown on InP substrates by Metalorganic Chemical Vapor Deposition (MOCVD). Various TEM probe-based and imaging techniques have been used to investigate the influence of structural features and growth temperature on the establishment of different modes of morphology-modulated relaxation mechanisms which are associated with different degrees of strain relief in the MQW system. We also find that the strains retained from layer to layer do not have the same value at the top and the bottom of the multilayer as a result of the differences in the time available for diffusional relaxation during growth.

13C2- 6

STUDY OF CHARGE-ORDERED STATES IN $LaSr_2Mn_2O_7$ BY LOW-TEMPERATURE ELECTRON DIFFRACTION

J. Q. Li, Y. Matsui, [*]T. Kimura, [*]R. Kumai and [#]Y. Tokura
National Institute for Research in Inorganic Materials,
[*]Joint Research Center for Atom Technology,
[#]Department of Applied Physics, University of Tokyo

Perovskite-related manganites with mixed valence, such as $Mn^{3.5+}$, often form ordered arrangements of Mn^{3+} and Mn^{4+} at low-temperature to form anti-ferromagnetic insulator. The authors so far reported low-temperature electron diffraction data of both $La_{0.5}Sr_{1.5}MnO_4$ with 0201-type structure [1] and $LaSr_2Mn_2O_7$ with 0212-one [2], from room temperature down to 100K by using liq.N_2 cooling holder of 1MV TEM [3]. In both materials, weak satellite reflection spots start to appear in the *hk0* patterns below about 200K, which corresponds well with a point where resistivity starts to increase. These satellite reflections were explained in terms of CE-type ordering of Mn^{3+} and Mn^{4+} within each MnO_2 sheet, associated with an orbital-ordering of 3d electrons in Mn^{3+} which possibly induce Jahn-Teller distortions.

In the present study, we extended the temperature range of our electron diffraction experiments down to 20K [4], by the use of new 300kV TEM equipped with liq.He specimen holder. The *hk0* electron diffraction patterns of $LaSr_2Mn_2O_7$ were recorded between the room temperature and 20K. It was found that the satellite reflection spots, once appear at about 200K, start to disappear by further cooling and almost vanish below 70K. When the specimen temperature was raised again, satellite reflection spots become visible above 90K. These results indicate that the CE-type ordering of Mn^{3+} and Mn^{4+} disappear below some critical temperature of 70-90K, and another type (possibly A-type) of anti-ferromagnetic structure without charge-ordering is stabilized.

REFERENCES

1 H. Moritomo et al., Phys. Rev. B51, 3297 (1995)
2 J.Q. Li et al., Phys. Rev. B 57, 3205 (1998)
3. Y. Matsui et al., Ultramicroscopy 39, 8 (1991).
4. T. Kimura et al., Phys. Rev. B, submitted.

GRAPHS REPRESENTING CRYSTAL STRUCTURES

S. J. Chung, School of Materials Science and Engineering, Seoul National University, Seoul 151-742, Korea

Crystal structure in certain classes such as silicates and borates are usually expressed by a three dimensional connected net which is also called three periodic net. This three periodic net can be assigned by a finite quotient graph[1, 2]. The repeated connections in a periodic net through translational symmetry can be expressed by labelling the edges of the quotient graph. The reversal of the process of assigning a labelled finite graph to a given three periodic net can be used to generate all the possible real and hypothetical crystal structures in a systematic fashion.

Generation of all possible three periodic nets with a given number of vertices and edges in a cell is carried out in three steps ; (i) generation of all connected graphs with a given order, (ii) labelling the edges of the graphs, (iii) partitioning the set of labelled graphs into equivalence classes by changing the coordination system and origin.
The process of generation three periodic nets and the graphs representing some real crystal structures are illustrated.

1. Chung, S. J. and Hahn, Th. (1975). Acta Cryst. A31
2. Chung, S. J., Hahn, Th. and Klee, W. E. (1984). Acta Cryst. A40, 42-50

GROWTH AND CHARACTERIZATION OF A SINGLE CRYSTAL $Bi_2Sr_2PrCu_2O_y$

T.J.Lee, T.S.Lin, C.Y.Wan, T.I.Hsu and H.C.Ku,
Department of Physics, National Tsing Hua University, Hsinchu, Taiwan 300 ROC
Y.Huang[1] and K.-W.Yeh[2] 1. Material Science Center, National Tsing Hua University, Hinchu, Taiwan 300 ROC 2. Department of Material Science,National Tsing Hua University, Taiwan 300, ROC

The bulk sample of $Bi_2Sr_2PrCu_2O_y$ is prepared using sintering method.XRD corporate with Ritveld method were used for phase confirmation. The percentage weight fractions of major and impurity phases of the bulk Bi2212 sample were calculated from the net area under the curve of individual spectrum. The result of Rietveld analysis indicates that the impurity phases are still dominated by Bi2201 phase. Single crystals of $Bi_2Sr_2PrCu_2O_y$ were grown by the traveling solvent floating zone method.The crystal growth apparatus is an infrared convergence type floating zone furnace that uses two 1.5kW halogen lamps as the radiation source.The crystal was grown at the rate of 0.2mm/h with atmosphere controlled at 3 bar total pressure (argon plus 7% oxygen, by flow rate). Single crystals in the form of film of approximately 4x8 mm^2 were selected by cleaving the crystal along the ab-plane. The diffraction patterns of *h00*, *0k0*, and *00l* were taken. Only even fundamental reflection with *h, k, l* =2n are present. Precession methods are employed to confirm the crystal symmetry and for the determination of the cell parameters. Parameters of the crystal lattice calculated from the refined diffraction data are a=5.482(2), b = 5.501(2), c = 30.214(1) Å. These results are in consistence with those obtained from the precession method. Meantime, GIX technique was applied to the thin film analysis,and the result showed that it has an incommensurate modulation along the b-axis with period of 4.264 b. The crystal symmetry belongs to space group Amaa. The crystal quality was checked by rocking curve along each direction.Characterization of this sample by electrical resistivity and magnetization has also been made.

THE BOND CHARACTER OF MO_2 (M=Si, Ge, Sn) RUTILE STRUCTURE DETERMINED BY κ–REFINEMENT AND MOLECULAR ORBITAL CALCULATION

T. Yamanaka, R. Kurashima, T. Tsuchiya and J. Mimaki
Dept. of Earth and Space Science, Osaka Univ.

In order to elucidate the bonding character of earth interiors, the covalency/ionicity and the other bonding character of rutile structure SiO_2, GeO_2, SnO_2 and α-PbO_2, high pressure form of quartz, were investigated by X-ray diffraction study using monopole refinement (κ-refinement) and molecular orbital simulation (DV-Xα). Those single crystals were synthesized using multianvil high pressure apparatus. The refinement of the charge density was undertaken by κ-parameter on the basis of the structure factor F(hkl). Electron density distribution is exposed by $\rho'\text{valence}(r)=\text{Pvalence}\cdot\kappa^3\cdot\rho\text{valence}(\kappa\cdot r)$, in consideration of the perturbed valence density.

The M-O bonding character were estimated by κ-refinement applied to the valence electrons of oxygen. Each oxygen κ-parameter was 0.91 (SiO_2), 1.06 (GeO_2), 1.14 (SnO_2). This indicates that the electron distributions are more localized with increasing the atomic number.

Molecular orbital calculation (DV-Xα) was carried out to elucidate the bonding character of these dioxides complementary to the κ-refinement. In the present study, DV-Xα results were obtained under the condition of the second neighbor cluster (M.P. ±4, ±4, ±6). The calculating total DOS (density of states) about the energy levels of main peaks for SiO_2, GeO_2, SnO_2, is in good qualitative agreement with the XPS experiment (Barr, 1991). The bond overlap populations based on Mulliken population analysis were degreased with increasing the atomic number. DOS wave function maps and deformation maps of electronic charge density interpreted that the bond character of SiO_2 is much different from GeO_2 and SnO_2. There are wide spread distributions of Si excited-3d more than Ge excited-4d and Sn excited-5d. This characteristic of Si excited-3d has a connection with the stronger covalency of d-p π-bond nature of SiO_2 compared with GeO_2 or SnO_2. However, SiO_2 rutile structure indicate more ionic than quartz lower pressure polymorph.

14A2-4

INTERACTION OF CROWN ETHER WITH LANTHANIDES : A COMPARATIVE STUDY BY X-ray CRYSTALLOGRAPHY AND PM3 AND MOLECULAR MECHANICS METHODS.

Z.Arifin, S.M.Zain and N.A.Rahman

The structures of the salt complexes formed from the interaction of dibenzydiaza-18-crown-6 and lanthanum chloride and neodymium nitrate have been determined by single crystal X-ray crystallography [1-2]. However, the conformation adopted by the crown ethers as coordinating ligand differs markedly for the lanthanum and neodymium salts, with the open, relatively relaxed structure for the former but highly strained with the dibenzyl groups pointing above and below the macrocyclic ring for the latter. In this work, we calculate the energy of the different conformations by the semi-empirical PM3 and molecular mechanics methods. This is done by taking the hkl file of the atomic positions and deleting the metal salts to give the coordinates of the atoms in cartesian format. These coordinates were then converted to MOPAC Z-matrix format for input into the MOPAC program. To calculate the energy of the ligand structures, single point calculations were carried out for the structures, leaving them as they are, without any optimization. We then optimized the ligands to obtain the minimized structure. The same procedure was repeated for the molecular mechanics calculations using the DISCOVERY suit of programs.

1. M.I.Idiris, A.Salhin, B.Saad, S.M.Zain and Z.Arifin,
J.Mol. Structure,415(1997) 71-79
2. M.I.Idiris, A.Salhin, B.Saad, S.M.Zain, N.Rahman and Z.Arifin,
J.Mol.Structure, p. 000.

14A2-5

CRYSTAL STRUCTURE STUDIES OF $CeAlO_3$ UNDER LOW TEMPERATURE

M. Tanaka[1], H. Horiuchi[2], T. Shishido[3] and T. Fukuda[3]
1 Photon Factory, High Energy Accelerator Research Organization,
2 Depart. of Natural Science, Faculty of Education, Hirosaki University
3 Institute for Materials Research,Tohoku University.

Structure of $CeAlO_3$ at the temperature range from 150K to 300K was investigated by the single crystal X-ray diffraction and structure refinements. Diffraction experiments were performed using a Mo-Kα radiation from an X-ray sealed tube, an AFC5 4-circle diffractometer (Rigaku) and a N_2 gas stream specimen cooling system, Oxford Cryostream Cooler. $CeAlO_3$ have a perovskite-type structure and its crystal system is reported to be tetragonal or trigonal at room temperature. At low temperature, the length of two axis are obviously different and the crystal system becomes orthorhombic. The difference of the two axes length decreases according to the increase of temperature and it becomes almost equivalent at 300K. The structure refinements, assuming the orthorhombic unit cell, Z=4 and space group Ibam, give the final R-factor 0.025, 0.039 and 0.039 at T = 300, 250 and 200K respectively, and no residual charge density was found in each difference Fourier map. Tanaka et al.[J. All.and Comp. 192, 87(1993)] reported that the electron distribution of oxygen atoms was remarkably deviated from spherical distribution at room temperature.

It is supposed that the true structure of $CeAlO_3$ is orthorhombic at the temperature range from 150K to 300K and the remarkable electron distribution of oxygen would be the result of an averaged electron distribution over multiplied this unit cell.

CRYSTAL STRUCTURE OF RELAXOR FERROELECTRIC $Pb(Zn_{1/3}Nb_{2/3})O_3$

H. M. Park AND S. J. Chung*, Materials Evaluation Center, KRISS, Taejon 305-600, Korea, *School of Materials Science and Engineering, Seoul National University, Seoul 151-742, Korea

Single crystal of $Pb(Zn_{1/3}Nb_{2/3})O_3$(PZN) were grown by high temperature solution growth technique. From the grown crystals, an euhedral single crystal in size of 30μm with well developed {100} face was selected for intensity measurement. The crystal structure of relaxor ferroelectric PZN as well as $Pb(Mg_{1/3}Nb_{2/3})O_3$ at room temperature was known as rhombohedral [1] with partially disordered perovskite structure. The lattice parameter of rhombohedral PZN is a=4.046(1)Å, α=89.93(2)°.

However, any detailed structure data have not been reported until now. The intensities of symmetry independent 79 reflections were measured and structure refinement of this crystal with rhombohedral as well as cubic symmetry was carried out. Various interesting anomalies in the difference Fourier maps will be reported.

1. Yokomizo, Y.,Takahashi T. and Nomura S., (1970). J. Phys. Soc. of Jpn., Vol. 28(5), 1278-1284.

14A2-7

TEMPERATURE DEPENDENCE OF INTERATOMIC DISTANCES IN THE SUPERCONDUCTIVE TRANSITIONS OF Hg-1212 AND Tl-2212 SUPERCONDUCTORS

K. Yamawaki, S. Sasaki, M. Kakihana and M. Tanaka,* Materials and Structures Laboratory, Tokyo Institute of Technology, Yokohama, Japan; *Photon Factory, KEK, Tsukuba, Japan

Single-crystal x-ray diffraction studies have been performed to interpret the superconductive transitions in Hg-1212 ($HgBa_2CaCu_2O_{6+\delta}$) and Tl-2212 ($Tl_2Ba_2CaCu_2O_8$). Both crystals are locally isostructural.

A single crystal of planar shape (0.05 × 0.02 × 0.002 mm) and a spherical single crystal (0.12 mm in diameter) were used for x-ray diffraction studies of Hg-1212 and Tl-2212, respectively. The cell dimensions for the crystals were smoothly changed through T_c. The intensity data up to $2\theta = 70°$ in one sixteenth of the reciprocal space were collected using the Mo Kα radiation ($\lambda = 0.7107$ Å). The crystal structures of Hg-1212 and Tl-2212 were analyzed for the data sets measured at 105, 110, 115, 120, 125, 130, 135, 155, 195 and 300 K and those at 100, 103, 106, 108, 112, 116, 120, 135, 175, 225 and 300 K, respectively.

Interatomic distances along out-of-planes such as Cu-O(2), Hg-O(2), Tl-O(2) and Tl-O(3) indicate a clear and systematic change against temperature. When the temperature decreases, Cu-O(2) in Hg-1212 expands until 170 K and then shortens with a convex curve, while Hg-O(2) changes to be concavely curved. On the other hand, Cu-O(2) and Tl-O(2) distances in Tl-2212 give concave and convex curves, respectively. The temperature dependence of the out-of-plane character would provide a key to the origin of superconductivity. Further details on crystallographic behavior will be discussed at the meeting.

14B2-1

DYNAMICAL DIFFRACTION AT GRAZING INCIDENCE

A. Authier, Laboratoire de Minéalogie-Cristallographie, Université. et M. Curie, 4 Place Jussieu, 75252 Paris CEDEX 05, France

X-ray specular reflection and highly asymmetric X-ray diffraction are now used quite systematically for the study of surfaces and multilayers. This has revived an interest for extensions of the dynamical theory of diffraction to situations where the angle of incidence and/or of emergence of the X-ray beam with the surface is very small. The traditional presentation of dynamical theory where the Ewald sphere is locally approximated by its tangential plane is not valid in those cases. A new derivation of the dispersion surface in those border cases is given. It is shown that the results of the dynamical theory can be obtained by solving a third-degree equation and that it is not necessary to solve a fourth-degree equation. It is also shown that for a qualitative or semi-quantitative analysis it is possible to approximate this third-degree equation by a second-degree equation.

14B2-2

UNIQUNESS OF THE COMPLEX DIFFRACTION AMPLITUDE IN X-RAY BRAGG DIFFRACTION

A. Y . Nikulin

Department of Physics, Monash University, Clayton, Vic 3168, Australia.

The concept of the complex diffraction amplitude for x-ray Bragg diffraction is discussed in terms of a unique product of its zeros, Nikulin (1998). This formalism allows the inverse scattering problem in x-ray Bragg diffraction to be solved unambiguously. The phase-retrieval technique, via a logarithmic dispersion relation, has associated with it the problem of localisation of zeros of the complex diffraction amplitude. The mathematical approach predicts an infinite number of zeros of the complex diffraction amplitude. However, a physical (discrete) representation of the inversion technique limits the number of zeros which should be considered and allows one to obtain a unique solution for the structure-factor profile. As a practical example the formalism is applied to x-ray Bragg diffraction data collected at two different radiation energies, Nikulin, Zaumseil & Petrashen' (1996), (1997).

Nikulin, A. Yu. (1998). *Phys. Rev. B*57, 11178-11183.

Nikulin, A. Yu., Zaumseil, P. & Petrashen', P. V. (1996) *J. Appl. Phys.* **80**, 6683-6688.

Nikulin, A. Yu., Zaumseil, P. & Petrashen', P. V. (1997) *J. Phys. D.: Appl. Phys.* **30**, 2373-2378.

COMPUTER SIMULATION AS A TOOL FOR THE ANALYSIS OF DIFFUSE SCATTERING

T.R.Welberry, Research School of Chemistry, Australian National University, Canberra, ACT 0200, Australia.

Conventional crystal structure analysis of disordered materials using Bragg diffraction data reveals only average one-body structural information, such as atomic positions, thermal ellipsoids and site occupancies. Diffuse scattering, on the other hand, gives two-body information and is thus potentially a rich source of information on how atoms and molecules interact with each other. However, although the presence of diffuse scattering has been known since the earliest days of X-ray crystallography, extracting such information from it is still a far from routine process and quantitative studies are rare. One of the reasons for this has certainly been, until relatively recently, that the intensity levels of diffuse scattering are typically several orders of magnitude lower than for the Bragg peaks, making measurement both difficult and time-consuming. Modern developments in X-ray sources (synchrotrons) and detectors (linear-detectors, area-detectors, image plates) have enormously increased the capability for measuring such weak data and this aspect, though still presenting challenges, is no longer the limiting factor.

The greater challenges occur in the interpretation and analysis of diffuse scattering. Traditional approaches, developed largely in the field of alloys and simple oxides, present unsurmountable difficulties when systems become more complex or when the magnitudes of atomic displacements become relatively large. More recently, progress has been made in an alternative approach to understanding the local atomic and molecular arrangements in disordered materials, which overcomes some of these difficulties[1,2]. The method consists of comparing diffraction patterns calculated from a computer model of the disordered structure with measured X–ray diffuse intensities. The advantage of the method is that it can be applied generally to all systems regardless of their complexity or the size of the atomic displacements that might be present. The computer models are generated using real-space Monte Carlo (MC) methods which employ near-neighbour effective interactions. The only requirement is the specification of the model in terms of sufficiently few parameters which nevertheless adequately describe the local physics and chemistry.

[1] T.R.Welberry & B.D. Butler (1994), *J. Appl. Cryst.,* 27, 205-231.
[2] T.R.Welberry & Th. Proffen (1998), In press *Acta Cryst.,* A.

14B2-4

STRUCTURE-PROPERTY RELATIONSHIP OF GIANT MAGNETORESISTIVE MULTILAYERS

K. Y. Kok AND J. A. Leake*, Malaysian Institute for Nuclear Technology Research (MINT). * Department of Materials Science & Metallurgy, University of Cambridge.

In this study, antiferromagnetically coupled Co/Cu multilayered films prepared by d.c. magnetron sputtering are investigated. These multilayers demonstrate pronounced giant magnetoresistance (GMR) effect at room temperature, a novel property which may be exploited to provide higher information storage densities for magnetic recording devices. We aim to characterise the average and localised microstructural features of these multilayers to establish the correlation between these microstructural features and the GMR property. Investigation of the structural features was carried out using X-ray diffraction, X-ray diffuse scattering and transmission electron microscopy techniques. Structural disorders such as uncorrelated interfacial roughness, thickness fluctuations, inhomogeneity of grain orientations and diffusion at the boundaries between the columnar grains in the multilayers, were found to degrade the GMR effect exhibited by the multilayers.

14B2-5

CORRELATED INTERFACE STRUCTURES IN $Si_{1-x}Ge_x/Si$ SUPERLATTICES DETERMINED BY X-RAY SCATTERING

Y. Yamaguchi and H. Hashizume *(Materials and Structure Laboratory, Tokyo Institute of Technology)*, N. Usami and Y. Shiraki *(Research Center for Advanced Science and Technology, University of Tokyo)*

The interface structure of $Si_{1-x}Ge_x/Si$ superlattices with $x=0.1$ (sample I) and 0.3 (sample II), both on vicinal Si(111) substrates, were investigated by grazing-angle X-ray scattering (GAXS) at synchrotron sources. The GAXS profiles show serieses of diffuse peaks in the misorientation directions, indicating the co-existent periodic and random components in the interface morphology. The periodic component is due to the bunching of surface steps at a 380 nm (sample I) and a 1000 nm interval (sample II), derived from the diffuse peak positions. The height-height correlation function shows a standard deviation of 50 nm for sample I and of a 200 nm for sample II. In a fractal model, the random component has a 20 nm in-plane correlation length in the two samples, which is much smaller than the mean terrace widths. The out-of-plane correlation length is 150 nm and 200 nm for samples I and II respectively.

14B2- 6

USE OF THE CCD AREA DETECTOR FOR LARGE SCALE SURVEYS OF MICROFIBRIL ANGLE IN WOOD SAMPLES

R. Kadirvelraj, A. Hussain, I. D. Cave, G. Smith and W. T. Robinson; Department of Chemistry, University of Canterbury, Christchurch, New Zealand

X-ray diffraction is often the best method for determining preferred orientation distributions, in powdered crystalline samples or in other materials where different crystallite orientations reflect their physical history. Metals and alloys extruded into wires are the best known examples.

When trees grow, the cellulose crystalline fibres in their cell walls may be aligned closely with the grain of the timber or well away from this direction. The angle between the two is called the Microfibril Angle (MFA). Timber with good engineering properties tends to have low microfibril angles. Furthermore angles measured in the core wood laid down at the seedling stage of growth are relatively large, but only improve with age. Thus mass screening of seedling trees provides a way of selecting those most likely to mature into good timber suitable for engineering use. This product will fetch a higher market price than boxwood.

Early attempts to assess MFA using conventional X-ray powder diffraction cameras and diffractometers were successful but slow (hours for each sample). We shall demonstrate how the experimental measurement can be made in a minute using a CCD detector, and analysed in a few more minutes. This speeds mass surveys of samples, taken from all over one tree or from similar trees or from different species grown in different climates. Useful information for the breeding and commercial forest planting programs can be made on a realistic time scale.

COMPOSITE MODULATED STRUCTURES IN WIDE-RANGE SOLID SOLUTIONS

S.Schmid, J.G.Thompson and R.L.Withers, Research School of Chemistry, The Australian National University, Canberra, Australia

A large number of recent publications reflect the importance currently attributed to composite modulated structures (van Smaalen, 1995; Yamamoto, 1996; Withers, Schmid & Thompson, 1998). It has been shown that a description as a composite modulated structure has advantages over classic crystallography in many cases. The description as a composite modulated structure is especially useful for compounds within wide-range solid solutions. Atomic modulation functions (AMFs) describe the deviation from the average of any atom based parameter at a given point in the structure. It has been proven for a few systems, *e.g.* zirconium nitride oxide fluoride, tantalum tungsten oxide and zirconium niobium oxide, that the AMFs are essentially the same for any structure within a particular solid solution field despite the variability in composition. Therefore all structures within such a solid solution can be determined once the modulation functions for one example are known and the magnitude of the primary modulation wave-vector for any composition has been defined.

All of the above systems can be described as inorganic incommensurate intergrowth compounds or more precisely inorganic misfit layer compounds. Each consists of two chemically different layers that are stacked alternately. In every case one of the layers contains the metals or metals and anions whereas the second layer contains anions only. The widths of these solid solutions are achieved by compressing the anion-only-substructure relative to the other when adding additional anions.

While the modulated structure approach is useful for all compositions within a solid solution, it is especially useful for compositions that otherwise need to be described as long-period superstructures. It is the large number of unobserved satellite reflections that cause correlations between structural parameters which make the least squares refinement of such structures in terms of a conventional superstructure difficult.

Smaalen, S. van (1995). *Cryst. Rev.* **4**, 79 - 202.
Withers, R. L., Schmid, S. & Thompson, J. G. (1998). *Prog. Solid State Chem.* **26**, 1 - 96.
Yamamoto, A. (1996). *Acta Crystallogr.* A**52**, 509 - 560.

14C2-2

THE STRUCTURES OF QUASICRYSTALS AND THEIR RELATED CRYSTALLINE PHASES

K. Hiraga, Institute for Materials Research, Tohoku University, Sendai 980-8577, Japan

Quasicrystals show diffraction patterns with noncrystallograhic symmetries but nonetheless, consisting of sharp peaks. That is, the quasicrystals have no periodicity, but some order, such as bond orientational order, producing sharp diffraction peaks. The quasicrystals found so far can be divided into two groups; three-dimensional and two-dimensional quasicrystals, which are represented by icosahedral and decagonal quasicrystals, respectively. It has also been found that some crystalline phases are formed in alloys with compositions around quasicrystalline alloys. These crystals are referred to as crystalline approximants, and their structures are valuable for understanding atomic arrangements in quasicrystals. From structural determinations of some crystalline phases and a strong resemblance of their structures to those of quasicrystals, the structures of decagonal and icosahedral quasicrystals are found to be formed by aperiodic arrangements of atom columns with decagonal symmetry and atom clusters with icosahedral symmetry, respectively.

In this paper, I will present following items,

1. One-dimensional quasiperiodicity and Fibonacci sequence in theoretical idea
2. Two-dimensional aperiodic lattice and Penrose tiling
3. Polytypes of decagonal quasicrystals and Diffraction patterns
4. Atom columns in decagonal quasicrystals and their crystalline approximants
5. Aperiodic arrangements of atom columns in decagonal quasicrystals
6. Polytypes of icosahedral quasicrystals
7. Atom clusters in icosahedral quasicrystals and their crystalline phases.

MODULATED STRUCTURE ANALYSIS OF INCOMMENSURATE COMPOSITE CRYSTAL, $(SnS)_{1.17}NbS_2$

Y. Gotoh*[1], J. Akimoto[1], Y. Oosawa[1] and M. Onoda[2]

[1]National Institute of Materials and Chemical Research, Japan
[2]National Institute for Research in Inorganic Materials, Japan

The modulated structure of mutually incommensurate composite crystal, $(SnS)_{1.17}NbS_2$ with layered substructures, has been investigated on the basis of (3+1)-dimensional superspace group approach using the X-ray diffraction data collected by A. Meetsma, G. A. Wiegers, R. J. Haange and J. L. de Boer [1]. From their average substructure analysis, it has been found that the composite crystal is built of three-atom-thick NbS_2 sandwiches with Nb atom trigonal-prismatically coordinated by six S atoms and two-atom-thick SnS double layers with NaCl-type arrangement and they are alternately stacked. In the present work, structure model with secondary harmonic modulation waves for all atomic position and anisotropic thermal parameters of SnS part was adopted. The superspace groups of subsystems employed were *L C2mm* / -1 -1 s for the NbS_2 part and *L C2mb* / -1 -1 1 for the SnS one [2]. The structure was refined by FMLSM [3] using 732 reflections with 67 parameters. The final R and Rw values have been smoothly converged to 0.044 and 0.048 respectively. The lattice stability of $(SnS)_{1.17}NbS_2$ has been investigated by the use of REMOS [4]. The interlayer interaction will be also discussed.

1. Meetsma, A., Wiegers, G. A., Haange, R. J. & de Boer, J. L. (1989). *Acta Cryst.* **A45**, 285-291.
2. van Smaalen, S. (1989). *J. Phys. Condens. Matter* **1**, 2791-2800.
3. Kato, K. (1990). *Acta Cryst.* **B46**, 39-44.
4. Yamamoto, A. (1992). *Acta Cryst.* **A48**, 476-483.

14C2-4

STRUCTURE STUDIES OF QUASICRYSTAL BY THE CONVERGENT-BEAM ELECTRON DIFFRACTION AND HIGH-ANGLE ANNUALR DARK-FIELDS

K. Saitoh[1], K. Tsuda, M. Tanaka[1] and A. P. Tsai[2]
1 Research Institute for Scientific Measurements, Tohoku Univ,
2 National Research Institute for Metals,

The HAADF method is a technique to take a structure image which is formed by high-angle scattered electrons with scattering angles of around 100 mrad using a scanning transmission electron microscope (STEM) [1, 2]. The spatial resolution of the image is about 0.2 nm. The image show atomic arrangement composed of atoms with large atomic number Z selectively.

We have taken HAADF images of Al-Ni-Co and Al-Ni-Fe decagonal quasicrystals and successfully observed the arrangement of transition metal atoms for the first time [3, 4]. $Al_{72}Ni_{20}Co_8$ water-quenched at 1173 K is a decagonal quasicrystal which shows no superlattice reflections and little diffuse scattering in the diffraction patterns. We found that the cluster column with a 2 nm diameter of the alloy, which was considered to be decagonal, has no decagonal symmetry. We also found that there exist two types of more basic structural units with radii of about 0.4 nm, pentagonal cluster columns (P) and star-shaped one (S). We constructed the atomic arrangements of P and S on the basis of the structure of the monoclinic $Al_{13}Fe_4$ approximant phase, and the tiling of the clusters.

The CBED method have been used to determine the positions of Al atoms, which are not clearly seen in the HAADF images. Intensities of CBED patterns of the quasicrystals have been calculated from the model constructed on the basis of the HAADF images and the structure of the approximant, and compared with the experimental ones. The atom positions, Debye-Waller factors and site occupancies have been determined by the least square fitting.

Furthermore, the arrangements of the 2 nm cluster columns of water-quenched $Al_{68}Ni_{20}Co_{12}$ and $Al_{70}Ni_{20}Co_{10}$, which show superlattice reflections in the diffraction patterns, have also been studied by the HAADF method. In addition, an antiphase shifts at an inversion domain boundaries of Al-Ni-Fe have been observed by the HAADF method for the first time.

References

1. S. J. Pennycook and D. E. Jesson, *Ultramicroscopy* **37** (1991) 14.
2. N. D. Browning and S. J. Pennycook, *Microbeam Analysis* **2** (1993) 81.
3. K. Saitoh *et al.*, *Jpn. J. Appl. Phys.* **36** (1997) L1400.
4. K. Saitoh, K. Tsuda and M. Tanaka, accepted to *J. Phys. Soc. Jpn.*

14C2-5

PERIODIC NODAL SURFACES, ATOMIC MODULATION FUNCTIONS AND THE THREE-DIMENSIONAL INCOMMENSURATELY MODULATED $(1\text{-}x)Bi_2O_3.xNb_2O_5$, $0.06 < x < 0.23$, SOLID SOLUTION

R.L. Withers, C.D. Ling, S. Schmid and J.G. Thompson, Research School of Chemistry, Australian National University

Integer indexation of the reciprocal lattice of the $(1\text{-}x)Bi_2O_3.xNb_2O_5$, $0.06< x <0.23$, solid solution requires six basis vectors given by $M^* = \mathbf{a}_F^*, \mathbf{b}_F^*, \mathbf{c}_F^*, \varepsilon\mathbf{a}_F^*, \varepsilon\mathbf{b}_F^*$ and $\varepsilon\mathbf{c}_F^*$ respectively, where the subscript F refers to the underlying fluorite type average structure and $\varepsilon \sim 0.35\text{-}0.39$. At any particular composition, the $(1\text{-}x)Bi_2O_3.xNb_2O_5$, $0.06 < x < 0.23$, solid solution is thus a three-dimensional incommensurately modulated structure. Characteristic extinction conditions and overall $m3m$ diffraction symmetry imply a six-dimensional superspace group symmetry of $P{:}Fm\bar{3}m{:}Fd\bar{3}m$ (1).

The form of the three-dimensional compositional and displacive Atomic Modulation Functions (AMFs), which describe the deviation of the actual crystal structure at any particular composition from its underlying fluorite-type substructure, are investigated and it shown that they are closely related to the so-called D periodic nodal surface (2). Real space compositional Bi/Nb and oxygen vacancy ordering patterns are thereby derived.

1. Ling, C.D., Withers, R.L., Schmid, S. and Thompson, J.G. (1998). *J. Solid State Chem.* **137**, 42-61.
2. von Schnering, H.G. and Nesper, R. (1991). *Z. Phys. B.* **83**, 407-412.

Pleanry-3

DIRECT DETERMINATION OF X-RAY REFLECTION PHASES USING MULTIPLE DIFFRACTION : THEORY AND EXPERIMENTS

S. L. Chang, Department of Physics, National Tsing Hua University
Hsinchu, Taiwan

The X-ray phase problem is a central theme of research in crystallography. Solutions to this problem have been developed considering the physical and statistical aspects of Bragg reflections, such as direct methods and methods involving isomorphous and molecular replacements, anomalous dispersion and entropy maximization. Very recently, multiple diffraction techniques utilizing coherent interaction of X-rays within a crystal has demonstrated its capability of directly determining the phases of reflections of small- and macro-molecular crystals. This technique has, therefore, a potential of becoming a new method for structure analysis. In this presentation, the relationship between X-ray reflection phase and multiple diffraction, as well as the phase-determination method are described. The experimental techniques of producing multiple diffraction and the theoretical grounds, both kinematical and dynamical, of the phase-determination method are presented and discussed. Experimental phase determination using multiple diffraction for single crystals of small- and macro- molecules is demonstrated. Prospective future development of this particular phasing method is also tentatively given.

REAL-TIME in situ OBSERVATION OF CHEMICAL REACTIONS

Y.Ohashi;Tokyo Institute of Technology

The process of the chemical reaction in a crystal can be observed by the stepwise crystal structure analysis if the crystallinity is kept during the reaction. Such a reaction is called as "crystalline-state reaction". Three typical examples of crystalline-state reactions and a new diffractometer designed for rapid data collection will be given.

The first example is the photoracemization of a chiral alkyl group bonded to the cobalt atom in a cobalt complex crystal. The intensity data were collected within two hours using a new diffractometer designed for rapid data collection. The two-step inversion process of the chiral alkyl group has been observed.

The second example is the photoisomerization, in which the 3-cyano-propyl group bonded to the cobalt atom is isomerized to the 2-cyanopropyl group and then the 2-cyanopropyl group is transferred to the 1-cyanopropyl group. The structure analyzed after ten hours irradiation with a xenon lamp showed a disordered structure of 3- and 1-cyanopropyl groups. The 2-cyanopropyl group produced at the intermediate stages was not observed. To examine the reaction mechanism, the structure after the irradiation was also analyzed by neutron diffraction.

The third example is the molecular oxygen insertion to a Sb=Sb double bond with retention of the single crystal form. Within ten hours the Sb=Sb bond was completely changed to the four-membered ring of -O-Sb-O-Sb- at the open air.

Recently a new on-line two-dimensional detector (MSGC) has been developed to collect the data more rapidly. The new diffractometer using the MSGC detector is now designed. The three-dimensional intensity data will be collected less than 1 msec using synchrotron radiation.

The structure of the excited molecules will be analyzed in near future.

15A1-1

THE POSSIBILITIES FOR HOMOMETRIC STRUCTURES IN A HEXAGONAL LATTICE.

A.D. Rae, Research School of Chemistry, Australian National University, Canberra, A.C.T. 0200, Australia.

Homometric structures are not crystallographically equivalent but do produce the same reflection intensities and hence the same interatomic vectors in the Patterson function. In a recent paper, P.K. Bower, K.A. Porter, A.D. Rae, A.C. Willis and S.B. Wild, *J. Chem. Soc. Chem. Commun.*, 1153-1154, (1998) reported that two homometric structures in spacegroup $P6_522$ had to be considered for $AgN_4C_{18}H_{20+}.NO_{3-}.2H_2O$ where $N_4C_{18}H_{20}$ the homochiral ligand [*R*-(*R**,*R**)]-*N,N'*-bis-(2'pyridyl methylene cyclohexane-1,2-diamine.

This provides an example of how homometric pairs of structures can be formed using three screw related substructures in a hexagonal or trigonal space group. Ligands bridge adjacent Ag atoms ($a/2 = 5.438$ Å apart) to form chains of $(AgN_4C_{18}H_{20}^+)_n$ rather than $Ag_2(N_4C_{18}H_{20})_2^{2+}$ cations with Ag atoms ≈ 3 Å apart. Ag would be coordinated to four nitrogens, two from each of two ligands, in either option. Parallel chains form layers perpendicular to **c** and these are packed in the crystal with the 6_5 screw axis relating adjacent layers. The structure can be described as three 3_2 related substructures of $C222_1$ symmetry.

A reference substructure has layers at $z = \pm 1/4$ and axes $\mathbf{a}' = \mathbf{a}$, $\mathbf{b}' = \mathbf{a}+2\mathbf{b}$, $\mathbf{c}' = \mathbf{c}$. Should the reference substructure have an **a**/2 translation repeat rather than **a**, the three individual substructures only contribute to h even, k even, and $h + k$ even reflections respectively and this is approximately the case in this structure and is exactly the case for truly homometric structures. A homometrically related structure is formed by translating the reference substructure by **b**/2 so that the screw related substructures are translated by **a**/2 and (**a** + **b**)/2 respectively. The magnitudes of all structure factors are unchanged, as are the phases of all reflections with h and k both even. However the phases of all other reflections are changed by 180 ° implying that there are two homometric structures possible. The distinction between the homometric possibilities was made using comparative refinement since the **a**/2 translation symmetry of the reference substructure (required for exact homometry) is not exact. Within the asymmetric unit of the reference $C222_1$ substructure we either have one Ag atom on a general position (constrained to be on a 2_1 screw axes parallel to **b**' if an **a**/2 translation is maintained) or two inequivalent Ag atoms on *2* fold rotation axes (with the same y' coordinates if an **a**/2 translation is maintained). The second case was found to be appropriate.

15A1-2

CLATHRATION AND CRYSTAL STRUCTURES OF SOME COORDINATION POLYMERS

X.M.Chen and M.-L.Tong, School of Chemistry and Chemical Engineering, Zhongshan University, Guangzhou 510275, China

Since the self-assembly of the supramolecular architectures of coordination polymers are influenced by the different oxidation states, the coordination preference of the metal ions, the types of ligands and solvents, and the molar ratio of the metal ions and the ligands, the exploration of the synthetic strategies and routes is therefore a long-term challenge. We have synthesized and characterized a series of one-, two- and three-dimensional coordination polymers, including trigonal, rectangular, square, ladder, and hexagonal open-networks with variable cavities or channels, in which the various metal centers (such as Co^{2+}, Ni^{2+}, Cu^{2+}, Zn^{2+}, Cd^{2+}, Mn^{2+}, Ag^{+}, *etc.*), rigid or flexible spacers (such as 4,4'-bipyridine, 2,4'-bipyridine, pyrazine, hexamethylenetetramine, Schiff bases, *etc.*), and possible bridging counter-ions (such as $CH_3CO_2^-$, SO_4^{2-}, PO_4^{3-}, *etc.*) have been used as building blocks. The influence of the added templating molecules on the construction of the host coordination polymers and the incorporation of guest molecules, as well as the role of the counterions in self-assembly of these coordination polymers have been investigated.

Acknowledgment—This work was supported by the NSFC (29625102).

15A1-3

SINGLE CRYSTAL X-RAY ANALYSIS OF SUCCESSIVE ISOMERIZATION ON A COBALT ATOM OF AN ALKYL GROUP

A.Sekine, M.Yoshiike, and Y.Ohashi ; Tokyo Institute of Technology

Recently it has been found that the 3-cyanopropyl group bonded to the cobalt atom in cobaloxime complexes is isomerized to the 2- and 1-cyanopropyl groups successively when the crystalline powder of the complexes are irradiated with visible light. In order to make clear the mechanism of the successive reaction, cobaloxime complexes with various axial base ligands were synthesized and were crystallized. Among these crystals, a complex with (*R*)-phenylethylamine as an axial base ligand was isomerized to retaining the single crystal form on exposure to a Xe lamp.

The produced 1-cyanopropyl group has about 87% of (*S*)-conformer. The product of the first step reaction, that is, the 2-cyanopropyl complex was not observed. This indicates that the isomerization rate of the second step, 2-1 isomerzation, is greater than that of 3-2 isomerzation in the crystal. The structure of the intermediate 2-cyanopropyl complex was observed as a disordered structure with 3- and 1-cyanopropyl groups in the crystal of the aniline complex after 48 hours exposure. The ratio of 3-, 2- and 1-cyanopropyl groups was 44:22:34.

THE CRYSTAL AND MOLECULAR STRUCTURES OF DI-μ-HYDROXY - BIS (DI - 2 - PYRIDYLAMINE) DINITRATODI-COPPER(II) AND AQUA - μ - FORMATO - TRIFORMATO -BIS (DI-2-PYRIDYLAMINE) DICOPPER(II) MONOHYDRATE

S. Youngme[a], W. Somjitsripunya[a], K. Chinnakali[b], S. Chantraprommaa[c] and H. K. Fun[b]; [a]Department of Chemistry, Khon Kaen University, Faculty of Science, Khon Kaen 40002, Thailand. [b]X-ray Crystallography Unit, School of Physics,Universiti Sains Malaysia, 11800 USM, Penang, Malaysia. [c]Department of Chemistry, Faculty of Science, Prince of Songkla Univeristy, Hatyai 90112, Thailand.

The crystal structures of the known copper(II) dimers have been characterised. Only a few crystal structures of the dihydroxy-bridged copper(II) dimer involving the dpyam ligand have been reported. While the corresponding dimeric complexes were obtained as the reoxygenation products,the $[Cu_2(ONO_2)_2(OH)_2(dpyam)_2]$(I) and $[Cu_2(H_2O)(O_2CH)_4(dpyam)_2].H_2O$(II) complexes were prepared directly from their components and X-ray structure determination of (I) and (II) are performed.

Compound (I) contains a dinuclear $[(dpyam)Cu(OH)_2Cu(dpyam)]^{+2}$ unit, dpyam = di-2-pyridylamine, with nearly planar CuN_2O_2 chromophores having a tetrahedral twist. An O atom from each monodentate $[NO_3]^-$ anion completes the distorted square pyramidal CuN_2O_2O' chromophores with apical Cu-O distances of 2.408(2) and 2.500(2) Å, respectively. The average Cu-O(H) bond distance is 1.940(2) Å, and the Cu-Cu distance is 2.9539(3) Å. Compound (II) contains a dinuclear $[(dpyam)(O_2CH)(OH_2)Cu(OCHO)Cu(O_2CH)_2(dpyam)]$ unit and an uncoordinated H_2O molecule. The copper atom is linked by a formate group in an anti-syn bridging arrangement. The coordination geometry around each copper atom is a distorted square pyramidal of the CuN_2O_2O' chromophores. The apical position of each chromophore is occupied by the water O atom and an O atom from the bridging formate group at distances of 2.297(2) and 2.414(2) Å, respectively. Each basal CuN_2O_2 chromophore in (II) has a tetrahedral twist with dihedral angles of 16.01 and 19.35° , respectively.

1.Wu, L. P., Keniry, M. and Hathaway, B. J. Acta Cryst. 1992. C48, 35.
2.Castro, I., Julve, M., De Munno, G., Bruno, G., Real, J. A., Lioret, F. and Faus, J. J. Chem. Soc. Dalton Trans. 1992. 1739.

15A1-5

CRYSTAL STRUCTURE OF 1,11-UNDECANEDIOL

N.Nakamura, S.Setodoi and T.Ikeya, Department of Chemistry, Faculty of Science and Engineering, Ritsumeikan University, 1-1-1, Nojihigashi, Kusatsu, Shiga 525-8577 Japan

The crystal structure analysis of 1,11-undecanediol, $C_{11}H_{24}O_2$, has been carried out by single crystal X-ray diffraction method.

All measurements were made on a Rigaku AFC-5R diffractometer with graphite monochromatized Cu-Kα radiation (λ=1.54178Å). The crystal structure is an orthorhombic system (a=7.13(1)Å, b=32.446(6)Å, c=5.141(3)Å Z=4) with a space group $P2_12_12_1$. All calculations were performed using the teXsan crystallographic software package. The structure was solved by direct methods with SAPI 91 and expanded using Fourier technique. All non-hydrogen atoms were refined anisotropically, but the refinement of hydrogen atoms was isotropically. The final cycle of full-matrix least-squares refinement was based on 697 observed reflections ($I>3\sigma(I)$). The refinement was concluded with final reliability factors R=0.037, R_W=0.047.

The hydrocarbon skeleton of the title compound has an all-*trans* conformation. One of the terminal hydroxyl groups has a *gauche* conformation with respect to the skeleton, whereas the other has a *trans*. The molecules arranged in parallel to form a layer structure. These features are same as that of 1,13-tridecanediol[1).

1) N.Nakamura, Y.Tanihara & T.Takayama. (1997). *Acta Cryst.* **C53**, 253-255.

HYDROTHERMAL SYNTHESIS AND CRYSTAL STRUCTURE OF 1-DIMENSIONAL CHAIN CLUSTER $[H_2en]_2[Mo_{8.5}V_{5.5}O_{38}(H_2PO_4)]6H_2O$

W. M. Bu[1], G. Y. Yang[2], Q. Zeng[2], L. Ye[1], J. Q. Xu[2], Y. G. Fan[1], [1]Key Laboratory of Supermolecular Structure and Spectroscopy, [2]Department of Chemistry, Jilin University, Changchun 130023

A mixture of H_2O, H_3PO_3, $BaCl_2$, H_2MoO_3, V_2O_5 and en in a mole ratio 1100:15:4:4:5:8 was heated at 160℃ for 4 days gave dark-green prism crystals.The compound have been structually characterised by single crystal X-ray diffraction studies: $[H_2en]_2[Mo_{8.5}V_{5.5}O_{38}(H_2PO_4)]6H_2O$, Monoclinic, C2/c, a=18.858(3) Å, b=11.934(3) Å, c=20.061(4) Å, β=97.47(3)°, V=4476.12(9)A, Z=4, R=0.0459. As shown in Fig.1,the compound consists of $[Mo_{8.5}V_{5.5}O_{38}(H_2PO_4)]$-cluster unit linked through inorganic bridges (oxgen atom) and form one dimensional extended chains.The cluster anion possess pseudo-Keggin structure.A distorted PO_4 tetrahedron located the center of cluster aanion, molybdenum and vanadium positions are statistical distributation.Between cluster anions and H_2en cations were attacted by hydrogen bond and electroaffinity,and formed inorganic-organic layer solid.

15A1-7

TETRANUCLEAR IRON-OXYGEN CLUSTERS IN ORGANICALLY TEMPLATED IRON PHOSPHATES

K.-H. Lii, Institute of Chemistry, Academia Sinica, Taipei, Taiwan, R.O.C. and Department of Chemistry, National Central University, Chungli, Taiwan, R.O.C.

Recently a good number of new crystalline iron phosphates with 1-D chain, 2-D layered, and 3-D framework structures have been synthesized in aqueous or predominantly nonaqueous solvents under mild hydrothermal conditions using organic amines as structure directing agents. A variety of iron-oxygen clusters have been found in these structures. The tetranuclear clusters appear most versatile. For example, topological analogue of the Fe_4O_{20} cluster in the iron phosphate mineral leucophosphite also occurs in the ferric phosphates $[H_3N(CH_2)_3NH_3]_2[Fe_4(OH)_3(HPO_4)_2(PO_4)_3]xH_2O$ [1] and $(C_4H_{12}N_2)_{1.5}[Fe_2(OH)(H_2PO_4)(HPO_4)_2(PO_4)]$ H_2O [2]. Tetramers of oxo-bridged trigonal bipyramids instead of octahedra are found in $[H_3N(CH_2)_3NH_3][Fe_2O(PO_4)_2]$ [3]. Novel Fe_4P_4 cubane-type clusters formed of trigonal bipyramidal or octahedral iron and tetrahedral phosphorus atoms with a μ_4-oxygen at the center of each cube are shown to exist in the mixed-valence compound $[H_3N(CH_2)_2NH_3]_2[Fe_4O(PO_4)_4]$ H_2O [4]. These organically templated iron phosphates greatly expands the variety of the structures of iron-oxygen clusters.

1. Lii, K.-H., Huang, Y.-F. (1997) J. Chem. Soc. Chem. Commun. 839.
2. Lii, K.-H., Huang, Y.-F., Zima, V., Huang, C.-Y., Lin, H.-M., Jiang, Y.-C., Liao, F.-L., Wang, S.-L. (1998) Chem. Mater. in press.
3. Lii, K.-H., Huang, Y.-F. (1997) J. Chem. Soc. Chem. Commun. 1311.
4. Huang, C.-Y., Wang, S.-L., Lii, K.-H. (1998) J. Porous Mater. 5, 147.

15A1-8

DIMOLYBDENUM TRIS(μ-THIOLATO) COMPLEXES

K.W. Muir, Department of Chemistry, University of Glasgow, Glasgow G12 8QQ, Great Britain, and F.Y. Pétillon & P. Schollhammer, Faculté des Sciences, Université de Bretagne Occidentale, 29285 Brest-Cédex, France.

Because the chemically robust $Mo_2(\mu\text{-}SMe)_3^+$ moiety can be stabilised by a great variety of neutral and anionic ligands the system has proved to be an excellent model for reactions of biological and catalytic importance. For example, diazenido ligands, RN_2^- derived from substituted hydrazines, can bridge either η^1 or η^2 between the molybdenum atoms. Both forms can be protonated to give cationic complexes. A review of our work on these systems will appear shortly[1].

We have now characterised six new $Mo_2(\mu\text{-}SMe)_3^+$ complexes, including the cation shown in the Figure, which contain novel carbon donor ligands. We shall present (a) our results for the new complexes, with a discussion focused on structure and bonding, (b) an attempt to systematise the extensive structural data on $Mo_2(\mu\text{-}SMe)_3^+$ complexes, much of it derived from our earlier work and (c) some comments on the crystallographic difficulties we have encountered.

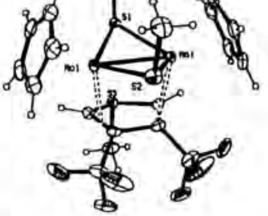

[1] Pétillon, F.Y., Schollhammer, P., Talarmin, J., & Muir, K.W., *Coordination Chem. Rev.*, (1998), in the press.

15A2-1

STRUCTURAL BASIS OF INTRASTERIC AND ALLOSTERIC CONTROLS OF PHENYLALANINE HYDROXYLASE

B. Kobe, I.G. Jennings*, C.M. House, B.J. Michell, R.G.H. Cotton* and B.E. Kemp. St. Vincent's Institute of Medical Research and *Mutation Research Centre, Fitzroy, Victoria, Australia.

Phenylalanine hydroxylase (PAH) converts phenylalanine to tyrosine as a rate limiting step in phenylalanine catabolism and protein and neurotransmitter biosynthesis (1). It is a member of the family of aromatic amino acid hydroxylases that also includes tyrosine and tryptophan hydroxylases. PAH is tightly regulated by the substrates phenylalanine and tetrahydrobiopterin, phosphorylation and other mechanisms.

We present the crystal structures of two states in its regulatory pathway, the dephosphorylated and phosphorylated forms. Truncation of the C-terminal 24 residues was necessary for reproducible crystallization (2). The difficult crystal structure determination required a combination of multiple isomorphous replacement, anomalous scattering and molecular replacement (using the structure of the catalytic domain of TyrOH); the use of maximum-likelihood refinement of heavy atom parameters and extensive density modification including solvent flipping and weighted automatic refinement protocol were imperative for obtaining interpretable electron density.

The structures show a catalytic domain flexibly linked to a regulatory domain. The latter consists of an a-b sandwich core that is structurally related to both pterin dehydratase and regulatory amino-acid binding domains of metabolic enzymes, and an amino-terminal autoregulatory sequence containing the phosphorylatable serine that extends over the active site pocket. The structures account for the remarkable functional interplay of regulatory sites that combines both intrasteric and allosteric control mechanisms; they demonstrate that intrasteric regulation is a general mechanism of enzyme regulation, and unveil evolutionary pathways yielding the highly regulated enzyme. Furthermore, the structures can serve as models for the homologous tyrosine and tryptophan hydroxylases, and provide a structural reference for the large database of mutations causing the metabolic disease phenylketonuria.

15A2-2

CRYSTAL STRUCTURE OF A *SACCHAROMYCES CEREVISIAE* PROTEIN TYROSINE PHOSPHATASE AT 2.2 Å RESOLUTION

Hyung Jun Ahn[†], Hyun Kyu Song[†], Hyeongjin Cho*, and Se Won Suh[†]
[†] Department of Chemistry, Seoul National University, Seoul, Korea
* Department of Chemistry, Inha University, Inchon, Korea

A *Saccharomyces cerevisiae* protein tyrosine phosphatase, PTP1, is involved in a signal transduction mechanism that appears to play an important role in regulation of cell proliferation and differentiation, and the cell cycle. In order to provide the structural basis for understanding the substrate specificity, its crystal structure has been determined to 2.2 Å by the multiple isomorphous replacement method. Recombinant PTP1 has been crystallized into the space group $P2_12_12$, with unit cell parameters of a=72.62 Å, b=90.74 Å, c=54.06 Å. The asymmetric unit contains one molecule with a solvent content of 45 % by volume. The crystal diffracts to about 2.0 Å with synchrotron X-rays. The structure of PTP1 has an active-site loop formed by the residues of the conserved Cys-$(X)_5$-Arg sequence and this motif forms a distinct cradle, the phosphate-binding loop in which oxyanions bind. An aspartic acid from an adjacent loop facilitates the catalysis by protonating the leaving group. In addition, variation in the recognition region and nearby residues on the active site might allow PTP1 to selectively recognize different peptide substrate sequences, compared with other PTPases.

THREE DIMENSIONAL STRUCTURE OF THE HUMAN IMMUNOGLOBULIN G RECEPTOR - FcγRII

K.F. Maxwell[1], M.S. Powell[2], D.Emmanouilidis[2], M.D. Hulett[2], P.M. Hogarth[2] and T.P.J. Garrett[1]

[1] Biomolecular Research Institute, 343 Royal Parade, Parkville 3052;

[2] Austin Research Institute, Austin Hospital, Heidelberg 3084.

The Fc receptor (FcR) family plays a critical role in maintaining immune homeostasis by binding the Fc region of antibodies to link humoral response with cell function. In particular, the low affinity IgG receptor (FcγRII) predominantly binds antigen-bound IgG and has critical roles in clearing immune complexes, phagocytosis, activation of inflammatory cells, the destruction of antibody coated pathogens and mediation of immune responses to resist infection. We have determined the three-dimensional structure of FcγRIIa to provide the first structural insight for the leukocyte FcR family. The structure reveals a novel association of the two homologous Ig domains (D1 and D2) which explains how the Fc portion can be bound at the interface between the two domains. This has allowed detailed analysis of the binding site for IgG and interpretation of structural and functional data for homologous FcRs. Furthermore, the crystal contacts suggest a plausible model for IgG binding and intracellular signalling. Sequence comparison between FcγRII, FcγRI, FcγRII and FcεRI indicate all are likely to have a similar architecture such that the FcγRIIa structure will provide a basis for design of antagonists of these receptors and possibly leading to potential treatment of FcR related diseases.

15A2-4

CRYSTAL STRUCTURE OF 20S PROTEASOME FROM BOVINE LIVER

M.Unno, Y.Tomisugi*, T.Mizushima, Y.Morimoto*, J.Yasuoka*, K.Tanaka** AND T.Tsukihara, Institute for Protein Research, Osaka University , *Department of Life Science, Himeji Institute of Technology AND **Tokyo Metropolitan Institute of Medical Science (Rinshoken)

A 20S proteasome is forms a catalytic core of the 26S proteasome. The proteasome is a central enzyme of protein degradation in both the cytosol and nucleus. The enzyme is involved in many biological processes. Especially, for the mammalian cells , this enzyme is involved in the cellular immune response. Although X-ray structures of the 20S proteasome from the archaebacterium (1) and the yeast (2) has been reported, that from mammalian has not been reported.

The 20S proteasome from bovine liver was purified and crystallized into orthorhombic space group of $P2_12_12_1$ with cell dimensions of a=122.3Å, b=193.5Å, c=317.5Å. A few crystals diffracted up to about 2.5 Å resolution using synchrotron radiation at ESRF in France, but we could not collect a full data set due to X-ray damage. We also tried to collect data using synchrotron radiation at SPring-8 in Japan. Now we have 3.5Å resolution data set with about 81% completeness and are analyzing the three dimensional structure by Molecular Replacement using archaebacterium model and yeast model.

1. Lowe,J., Huber,R. *et al. Science* **268,** 533-539 (1995)
2. Groll,M., Huber,R. *et al. Nature* **386,** 463-471 (1997)

15A2-5

THE REFINED STRUCTURES OF THE FULLY OXIDIZED AND THE FULLY REDUCED CYTOCHROME C OXIDASE FROM BOVINE HEART

M.Yao[1], N. Inoue[1], T.Mizushima[1], E.Yamashita[1], H.Yamaguchi[1], T.Tomizaki[1], T.Tsukihara[1], R.Nakashima[2], H.Shinzawa-Itoh[2], R.Yaono[2], P.L.Clare[2], S.Yoshigawa[2], [1]Institute for Protein Research , Osaka University, Japan, [2]Department of Life Science and Technology Corporation.

The cytochrome c oxidase from bovine heart is a terminal oxidase of mitochondria inner membrane. It catalyzes reduction of dioxigen to water with four-electron and four-proton coupling with pumping protons across the membrane. The 2.8Å structure in fully oxidized state of cytochrome c oxidase obtained previously (1,2) has shown the structures of the protein and active center, and possible electron and proton pathways.

The high resolution intensity data of two states was collected at Photon Factory of Japan by long-time exposure. The 2.3 Å and 2.35 Å electron density maps were calculated by extending the resolution and improving the phase with non-crystallographic symmetry averaging from the 3.0 Å MIR phase for the fully oxidized and fully reduced states, respectively. The molecular dynamic refinements were carried out in both states. Before located water molecules R factors were 24.8% and 23.3%, Rfree factors were 27.8% and 27.5% for 15Å to 2.3 Å and 15Å to 2.35 Å of resolution region in fully oxidized and fully reduced states, respectively. A molecular mechanism of proton pump has been proposed by comparing two structure (3).

1. Tsukihara, T., *et al.,* (1995). *Science*, **269**, 1069-1074
2. Tsukihara, T., *et.al.,*. (1996). *Science*, **272**, 1136-1144.
3. Yoshikawa, S., Shinzawa-Itoh, K., Nakashima, R., Yaono, R., Yamashita, E., Inoue, N., Yao, M., Fei, M.J., Clare, P.L., Mizushima, T., Yamaguchi, H., Tomizaki,T., & Tsukihara, T., (1998). *Science*, **280**, 1723-1729.

STRUCTURE OF SHEEP LIVER CYTOSOLIC ALDEHYDE DEHYDROGENASE AT 2.35Å RESOLUTION

S.A. Moore, T.J. Blythe, K.E. Kitson, T.M. Kitson, (Massey University); H.M. Baker and E.N. Baker, (University of Auckland).

Enzymes of the aldehyde dehydrogenase family are required for the clearance of potentially-toxic aldehydes, and are also essential for the production of key metabolic regulators. Cytosolic or class 1 aldehyde dehydrogenase (ALDH1) has an enhanced specificity for all-trans retinal, oxidizing it to all-trans retinoic acid, -a powerful differentiation factor. Thus ALDH1 very likely has a key role in vertebrate development.

The 3D structure of sheep liver ALDH1 has been determined by X-ray crystallography at 2.35Å resolution. ALDH1 is a homotetramer in which each subunit is folded into three domains, an NAD binding domain, a substrate binding domain and a dimerisation domain. The substrate binds in a deep tunnel leading to Cys302 at the active site. The high affinity for retinal compared with the mitochondrial enzyme ALDH2 is explained by the larger size of the tunnel. Two helices that line the tunnel seem likely to play a key role in defining substrate specificity in the wider ALDH family. The relative sizes of the tunnels also suggest why the bulky alcohol aversive drug disulfiram reacts more rapidly with ALDH1 than ALDH2.

The general base Glu268 is disordered and the nicotinamide adenine dinucleotide (NAD) cofactor binds in two distinct modes in the ALDH1 structure, thus indicating that flexibility is a key facet of the enzyme reaction mechanism.

15A2-7

CLUES AS TO DENATURATION DETECTED BY THE TEMPERATURE JUMP-LAUE METHOD IN 3-ISOPROPYLMALATE DEHYDROGENASE

T. Hori[1], H. Moriyama[2] N. Tanaka and T. Oshima[3], Faculty of Bioscience and Biotechnology, Tokyo Institute of Technology, 4259 Nagatsuta, Midori-ku, Yokohama, 226-8501 Japan

The thermophilic proteins have been investigated by the structural analysis to elucidate the factors that contribute to the thermal stability by means the temperature jump Laue method (T-jump). This method allows the dynamic detection of clues as to protein denaturation. It constitute of rapid increase in the temperature by a Yag laser of protein molecules in a crystal and Laue's method with white synchrotron X-ray radiation. TMT is a chimeric 3-isopropylmalate dehydrogenase (IMD) that has a fundamentally thermophilic structure. Approximately 20% of residues are mesophilic between residue 75 and 133 out of 345 amino acids (Mr 37.5 kD). It showed lower thermostability than thermophile T. thermophilus IMD by 20K, in spite of 6% difference in their total amino acid sequences. To obtain informations about heat denaturation, TMT crystal (P3221, a=78.9, c=158.8 Å,) was subjected to T-jump. The structural difference between at room temperature and at T-jump temperature was only 0.068 Å in r.m.s. However, the region with a residue from 109 to 112 has a large displacement. This region has a type III β-turn structure and interacts with 113 Ser OG and 110 Glu CO at room temperature. During the T-jump, the hydrogen bond was lost due to the flip of carbonyl of 110 Glu, although other structural feature does not change so much. This fact indicates that it may be a clue as to the heat denaturation in TMT.

1, Institute of physical and chemical research (RIKEN), Japan
2, Japan Synchrotron Research Institute (SPring-8), Japan
3, Tokyo University of pharmacy and life science, Japan

15A2-8

MEMBRANE ION TRANSPORT BY ANTIBIOTICS AND TOXINS

W.L. Duax, Hauptman-Woodward Institute, B.M. Burkhart, Hauptman-Woodward Institute, D. Ghosh, Hauptman-Woodward Institute, N. Li, Hauptman-Woodward Institute, and V. Pletnev, Shemyakin Institute.

Recent X-ray crystal structure determination of a Cs^+ complex of gramicidin D and an NH_4^+ complex of a virally encoded killer toxin KP6α reveal previously unsuspected modes of ion coordination that are ideally suited to facile movement of ions through membrane channels.

Our crystal structure of Cs^+ gramicidin D revealed a right-handed anti-parallel double stranded double helix (DSDH$_{\mathcal{R}}$) that is consistent with the large body of non-structural spectroscopic data. The DSDH$_{\mathcal{R}}$ structure reveals an ion channel with a single partially solvated Cs^+ ion distributed over three binding sites. The channel is relatively smooth and electrostatically negative on the interior as required for cation passage, while the exterior is electrostatically neutral, a requirement for membrane insertion. The "coordination" of the Cs^+ ion appears to be achieved by interaction with the π orbital of the carbonyls which do not bend inward or point toward the ions.

Our X-ray crystal structure determination of KP6α has revealed a trimer stabilized by salt bridges that forms a solvent filled funnel with charged residues on the inside, and tapers to an opening which is lined by three phenyl rings. The 4.2Å diameter opening at the center of the phenyl rings seems suited to NH_4^+ and K^+ ion coordination *via* the π clouds of the phenyl rings. Electron density on the symmetry axis within the barrel of the funnel surrounded by the phenyl rings is compatible with an NH_4^+ ion. The observed ion coordination is analogous to the arrangement of phenyl rings around NH_4^+ and K^+ ions in crystals of ammonium and potassium tetraphenylborate. This type of coordination for K^+ has been proposed to account for ion selectivity in insect and mammalian K^+ channels on the basis of *ab initio* calculations. This work is supported by National Institutes of Health Grant No. GM32812.

CRYSTAL STRUCTURES AND DEFORMATION ELECTRON-DENSITY DISTRIBUTIONS OF TEMPO RADICALS SHOWING MAGNETIC INTERACTIONS

F. Iwasaki, E. Kannari, D. Hashizume and M. Yasui
Department of Applied Physics and Chemistry, The University of Electro-Communications, Chofu, Tokyo 182-8585, Japan

Some of the 4-arylmethyleneamino-TEMPO radicals (4-Ar-CH_2=N-TEMPO·, hereafter abbreviated as Ar-TEMPO, TEMPO=2,2,6,6-tetramethylpiperidin-1-oxyl) were revealed to show intermolecular ferromagnetic interactions at an extremely low temperature, for example: Ph-TEMPO, Tc=0.3K, θ=0.7K and 4-Cl-Ph-TEMPO, Tc=0.4K, θ=0.7K (Nogami, et al., 1996). We determined the crystal structures of Ar-TEMPO radicals: Ar=Ph (**1**), 4-Cl-Ph (**2**), 4-I-Ph, 4-MeS-Ph and 4-Ph-Ph which show a ferromagnetic transition, Ar=4-Br-Ph, 4-Py and 3-Py with θ>0, antiferromagnetic 4-F-Ph and 4-Me-Ph derivatives and the paramagnetic 4-$MeSO_2$-Ph derivative. In the crystals showing ferromagnetic interactions, intermolecular O···β-H contacts are considered to play an important part.

Deformation electron-density distributions were investigated by the multipole refinements using intensity data at 100K in the range of $2\theta \leq 95$ and $\leq 120°$, for **1** and **2**, respectively. From these electron-density distributions, it was suggested that the unpaired electron of the O radical atom was delocalized on the π^* orbital of the N-O bond. Lone-pair electron densities of the O atom are observed in the >N-O plane with an sp^2 configuration. The intermolecular relationships between the lone-pair electrons of O atom and β-H atoms of the neighboring TEMPO rings will also be discussed.

Nogami, T., Ishida, T., Yasui, M., Iwasaki, F., Iwamura, H., Takeda, N. & Ishikawa, M. (1996). Mol. Cryst. Liq. Cryst., 279, 97-106.

15B1-2

MATERIALS DESIGN USING SUPRA- AND SUPER-MOLECULAR ASSEMBLY

Ian D. Williams, Stephen S-Y. Chui, Samuel M-F. Lo and Herman H-Y. Sung Department of Chemistry, Hong Kong University of Science and Technology, Clear Water Bay, Kowloon, Hong Kong, China
CHWILL@UST.HK

Architectural design of new materials is an important aspect for structure-property control. Due to their regularity, crystalline solids have certain advantages for example in magnetic, optical or chemical properties (sorption etc). Several examples are presented on how crystalline organic, metallo-organic or mixed organic: inorganic solids may be assembled using supra-and super-molecular principles. Even in such diverse solids, the frequent central importance of hydrogen bonding in forming inter-molecular contacts and optimization of inter-facial interactions in mixed organic-inorganic layer materials is seen. In addition the spatial influence of pendant organic groups in organising open-framework super-molecular assemblies is also demonstrated both in the 3-D mixed-metal phosphate $[FeAl(PO_4)_2(NH_2CH_2CH_2NH_3]$ and metal coordination polymers, eg for the 48-membered ring $[Cu_3(TMA)_2(py)_9]$, shown below.

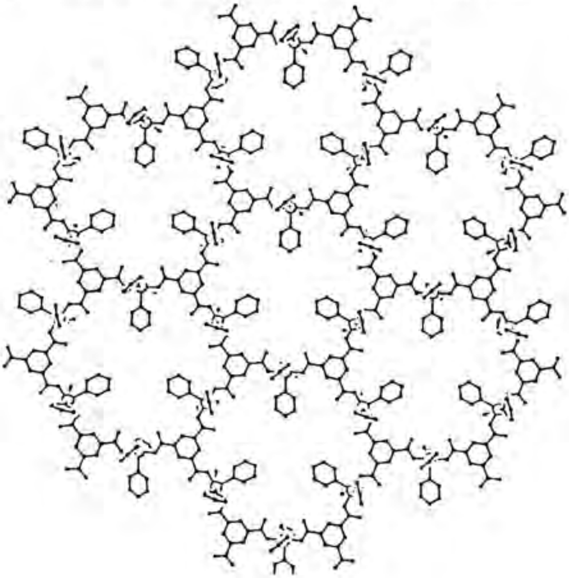

15B1-3

CRYSTAL STRUCTURE CHANGE FOR THE THERMOCHROMY OF N-SALICYLIDENEANILINES. THE FIRST OBSERVATION BY X-RAY DIFFRACTION.[1]

K. Ogawa, Y. Kasahara, Y. Ohtani, and J. Harada, Department of Chemistry, Graduate School of Arts and Sciences, The University of Tokyo, Komaba, Meguro-ku, Tokyo, 153-8902 Japan.

Reversible change in color of substances with variation of the temperature is known as thermochromism and has attracted much interest from chemists for a long time. *N*-Salicylideneanilines belong to a class of the most popular thermochromic compounds. For example, the crystals of *N*-(5-chloro-2-hydroxybenzylidene)aniline (**1**) are orange-red at room temperature and pale yellow at 77 K, and their color changes reversibly with variation of temperature. Extensive studies have revealed that the thermochromism of *N*-salicylideneanilines originates from the tautomerism between the OH and NH forms. A change in the crystal structure for their thermochromy has, however, never been observed, although an attempt to do so was reported for **1** by Bregman et al. We wish to report the first observation of a crystal structure change for the thermochromy of *N*-salicylideneanilines, using variable temperature X-ray analysis of *N*-(5-chloro-2-hydroxybenzylidene)-4-hydroxyaniline (**2**).

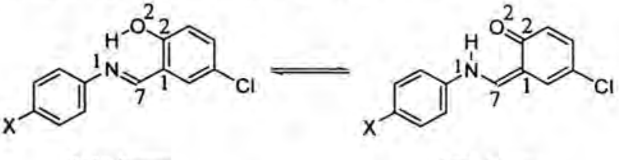

(1)

OH form **NH form**

1 : X = H **2** : X = OH

[1] Ogawa K., Kasahara, Y., Ohtani, Y. & Harada, J. (1998) *J. Am. Chem. Soc.*, **120** in press.

15B1-4

THE CRYSTAL STRUCTURES OF DIDENZYLDIAZA-18-CROWN-6 COMPLEXES WITH Cu- AND Ce-THIOCYANATES

M.I.Saleh[*], A.Salhin[*], S.A.Talipov[#], B.Saad[*]; [*]School of Chemical Sciences, Universiti Sains Malaysia, 11800, Penang, Malaysia ; [#]Institute of Bioorganic Chemistry, H.Abdullaev Str.,83, 700143 Tashkent, Uzbekistan

Dibenzyldiaza-18-crown-6 ($DD_{18}C_6$) form complexes with metal ions, where either the cavity of the macrocycle is filled by neutral salt of metal or complexed metal anion or $DD_{18}C_6$ cation form ionic type structure without coordination bonding.

We have obtained two types of complexes with thiocyanate: $[Cu(NCS)_4]^{2-} \cdot [DD_{18}C_6]^{2+}$(I) and $Ce(NCS)_3 \cdot DD_{18}C_6$ (II).

Crystal Date are:

I. $C_{26}H_{40}O_4N_2Cu(NCS)_4$, M=739.12, Monoclinic, $P2_1/m$, a=8.1089(3) Å, b=24.1065(9) Å, c=9.0172(3) Å, β=97.9107(3)°, Z=2, D=1.406 gcm^{-3}, 0.71073 , T=100 K

II. $C_{26}H_{38}O_4N_2Ce(NCS)_3$, M=758.13, Monoclinic, $P2_1/c$, a=15.597(3) Å, b=9.688(2) Å, c=21.931(4) Å, β=94.17(1)°, Z=4, D=1.523gcm^{-3}, 0.71073 Å^3, T=293 K

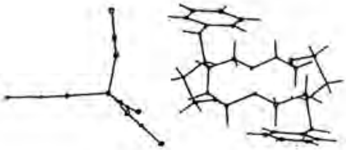

I

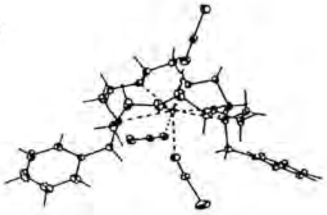

II

In the complex of type I, the atom Cu is coordinated to four thiocyanate ligands, and the cavity of crown is empty. In the second type the cerium thiocyanate salt localizes as a neutral entity in the centre of the cavity of the macrocycle.

15B1-5

GROWTH OF HIGHLY ORDERED SILICATE-ORGANIC COMPOSITE FILMS AT THE AIR-WATER INTERFACE

P.A.Reynolds, A.S.Brown, S.A.Holt, J.L.Ruggles & J.W.White, Research School of Chemistry, Australian National University.

Oriented mixed silicate-organic films may be grown at the air-water interface by hydrolysis of tetraethylorthosilicate in cetyltrimethyl ammonium bromide (CTAB) solution. We have examined the growth of these films *in situ* by X-ray and neutron reflectivity. The process can be followed over many hours from the initial film of monomolecular thickness of surfactant (CTAB), right through to the final product, an apparently highly crystalline lamellar phase consisting of hundreds of alternating CTA and silica-rich layers with repeat spacing 45 Å (Fig).[1]

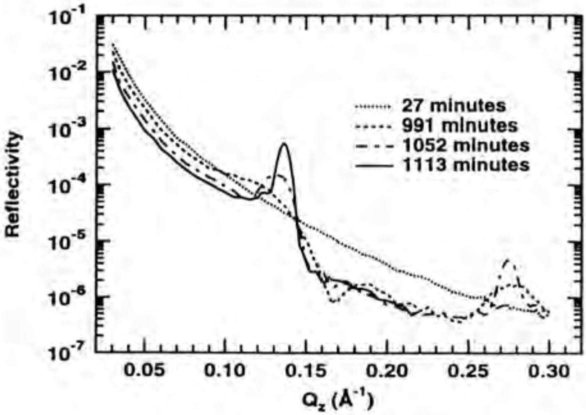

This nanocomposite material, chemical variants, and decomposition products have also been studied in other ways- by classical techniques such as NMR, by synchrotron X-ray grazing incidence and powder scattering, by SAXS and SANS. We will describe the results and attempt to relate them to other crystalline and partly crystalline materials such as the MCM macroporous zeolites.

1. Brown, A.S., Holt, S.A., Reynolds, P.A., Penfold, J., & White, J.W. (1998). *Langmuir*, in press.

15B1- 6

FROM METAL STRING COMPLEXES TO MOLECULAR METALWIRES

S. M. Peng, Department of Chemistry, National Taiwan University, Taipei, Taiwan, ROC

The nature of metal-metal multiple bonding in dinuclear metal complex is well understood. Our efforts to extend the dinuclear metal complexes to the linear oligonuclear metal complexes with all-syn conformation of oligo-(-pyridyl)amido ligands are successful1-5. The following complexes have been synthesized and characterized.

[MII3(3-dpa)4X2]	dpa = dipyridylamido anion
[MII4(4-dpda)4]	dpda = dipyridyldiamido dianion
[MII5(5-tpda)4X2]	tpda = tripyridyldiamido dianion
[MII6(6-tpta)4]	tpta = tripyridyltriamido trianion
[MII7(7-teptra)4X2]	teptra = tetrapyridyltriamido trianion

The unique feature of the structure and bonding in these complexes will be elaborated. The metal complexes [MII3(3-dpa)4(NCS)2] and [MII5(5-tpda)4(NCS)2] will bind Ag and Au [111] surface to form monolayer. The potential application of these complexes as a molecular metalwire will be discussed.

1. Sheu, J. T.; Lin, C. C.; Chao, I.; Wang, C. C.; Peng, S. M. (1996) *Chem. Commun.*, 315-316.
2. Shieh, S. J.; Chou, C. C.; Lee, G. H.; Wang, C. C.; Peng, S. M. (1997) *Angew. Chem. Int. Ed. Engl. 36*, 56-59.
3. Yang, M. H.; Lin, T.W.; Chou, C. C.; Lee, H. C.; Chang, H. C.; Lee, G. H.; Leung, M. K.; Peng. S. M. (1997) *Chem. Commun.*, 2279-2280.
4. Wang, C. C.; Lo, W. C.; Chou, C. C.; Lee, G. H.; Chen, J. M.; Peng, S. M. (1998) *Inorg. Chem.*, Accepted.
5. Lai, S. Y.; Lin, T. W.; Chen, Y. H.; Wang, C. C.; Lee, G. H.; Yang, M.; Leung, M.; Peng, S. M. (1998) submitted to *J. Am Chem. Soc.*

15C1-1

MAGNETIC NEUTRON DIFFRACTION AND COVALENCE

P.A.Reynolds, Australian National University, B.N.Figgis, University of Western Australia, D.Martin, Rutherford-Appleton Laboratory.

Metal-ligand bonding in metal complexes is poorly understood. Spin density is a fundamental property, it is much modified by bonding effects, and it has important consequences. It can be measured in detail by polarised neutron diffraction from large single crystals at reactor sources.

However many materials are available only as powders, or less detail is required. For these unpolarised diffraction using thermal neutrons has been used for decades in magnetic investigations. But for complicated magnetic structures resolution and signal can be inadequate.

Recently it has been realised that there are sufficient cold neutrons ($4 < \lambda < 25$Å) from the ISIS spallation cold source to provide high resolution, high intensity unpolarised diffraction patterns at long d-spacings ($2 < d < 12$ Å). This can resolve closely spaced magnetic diffraction peaks.

We have recently demonstrated that the IRIS spectrometer is sufficiently stable and of high enough flux that it is also now feasible to subtract, at helium temperatures, diffraction patterns from paramagnets with and without applied magnetic field, or ferro- and antiferromagnets above and below the ordering temperature. We obtain usefully defined, small, *magnetic* intensities in the presence of *nuclear* intensity ca. 100 times greater.

We have studied powders of the paramagnetic molecular metal-cluster compound $[Mn_{12}O_{12}(CD_3COO)_{16}(D_2O)_4].2CD_3COOD.4D_2O$ and the molecular antiferromagnet $ReCl_4(NHCMeNHPh)_2$ and have obtained useful information about ground state spin orientations, oxidation states and spin distribution and electron correlations within the molecules.

With greatly increased flux, and the use of polarisation, the new OSIRIS spectrometer promises a further increase in sensitivity of at least an order of magnitude in such studies.

NEUTRON AND X-RAY SCATTERING STUDY OF INORGANIC SPIN-PEIERLS COMPOUNDS

Y. Fujii, H. Nakao, K. Ohwada, T. Yosihama, N. Takesue, M. Nishi,
K. Kakurai, M. Isobe and Y. Ueda,
Institute for Solid State Physics, The University of Tokyo, Japan

Discovery of two inorganic spin-Peierls (SP) compounds $CuGeO_3$[1] and NaV_2O_5[2] has provided a great scientific opportunity to investigate spin- and lattice-dynamics of the SP phenomena by inelastic neutron scattering and to study an impurity-doping effect. In this paper we have reported neutron and x-ray scattering study of NaV_2O_5 and compared with the previous results of $CuGeO_3$.

Recent magnetic[2] and x-ray/neutron scattering[3] experiments of NaV_2O_5, in which there are $V^{4+}(S=1/2)$ linear chains along the orthorhombic b-axis, evidenced for its spin-Peierls state stabilized below T_{SP}=35K. We further carried out x-ray critical scattering (Photon Factory) and neutron HRPD (ISIS) measurements which clearly showed critical behavior of lattice dimerization with a wave vector (1/2,1/2,1/4) near T_{SP} and an anomalously large lattice strain along the c-axis below T_{SP} [4].

We also report x-ray scattering results of Na-deficient samples $Na_xV_2O_5$ (x=0.99-0.90), in which the magnetic linear chains are locally broken with an introduction of nonmagnetic $V^{5+}(S=0)$ ions. In this system, no antiferromagnetic(AF-) state is observed in contrast to the doped $CuGeO_3$ in which both the SP- and AF-states coexist in a given temperature and concentration range[5].

[1] Hase, M. et al.(1993). Phys. Rev. Lett. **70**, 3651.
[2] Isobe, M. and Ueda, Y.(1996). J. Phys. Soc. Jpn **65**, 1178.
[3] Fujii, Y. et al.(1997). J. Phys. Soc. Jpn. **66**, 326.
[4] Nakao, H. et al.(1998). Physica **B241-243**, 534.
[5] Regnault, L.P. et al.(1995). Europhys. Lett. **32**, 579.

TORSION, MIGRATION AND DISORDER: VARIABLE TEMPERATURE NEUTRON DIFFRACTION STUDIES OF HYDROGEN ATOM THERMAL PARAMETERS

C.C.Wilson, ISIS Facility, CLRC Rutherford Appleton Laboratory

The information available from structures determined at a range of temperatures can be valuable in understanding the energetics and dynamics of a system, and in revealing possible disorder. One of the most valuable aspects of an accurate neutron structural determination is the ability to analyse in detail the thermal motions of all atoms in a system, including the hydrogens. We have studied hydrogen atom parameters in a range of molecular crystals and three areas will be discussed:

- The temperature dependence of librations of terminal methyl groups, modelling the large anisotropic atomic displacement parameters (adps) in terms of torsional motions;
- Proton disorder in carboxylic acid dimer systems, where the adps can clearly indicate a disorder model to be appropriate. Temperature-dependent studies can reveal the thermodynamics of such systems;
- Thermal vibrations of hydrogen-bonded hydrogen atoms, where temperature-dependent studies can yield more information on possible proton disorder and on the possible migration of the hydrogen atoms within a hydrogen bond.

AN NEUTRON IMAGING PLATE AND ITS APPLICATION TO NEUTRON DIFFRACTOMETRY

N. Niimura AND Y. Karasawa, Advanced Science Research Center,
Japan Atomic Energy Research Institute, Ibaraki-ken, Japan

We have developed a neutron imaging plate (NIP), where the neutron converters, ^{6}Li or Gd were mixed with photostimulated luminescence materials on a flexible plastic support. The dynamic range and spatial resolution of our NIP were obtained as $1:10^5$ and less than 0.2 mm, respectively and the neutron detection efficiency of some NIP reached about 80 % at neutron wavelength 1Å.(1) These distinctive features are applicable for neutron diffraction experiments.

In this paper several examples of the application of NIP to neutron diffractometry were given.
1) Protein crystallography: Neutron quasi-Laue diffraction data (2Å resolution) from tetragonal hen egg-white lysozyme were collected in ten days with NIP. The positions of 960 hydrogen atoms in the molecule and 157 bound water molecules, were determined.(2) We have constructed a neutron diffractometer (BIX) dedicated for bio-crystallography using the NIP in the guide hall of JRR-3M. We measured the diffraction patterns from hen egg-white lysozyme crystals.
2) High resolution powder diffraction: The fine spatial resolution of the NIP provides the high resolution (0.3 %) powder diffraction, where the sample is 1 mm in diameter, camera constant is 600 mm and no collimator is used. Preliminary trial has been carried out.
3) Residual stress measurement: When finely collimated incident beam is irradiated to a residual stressed material, the distorted Debye ring is obtained with NIP and preliminary results were obtained.
4) Others: NIP could be applicable to thermal neutron small angle scattering, a single crystal diffractometry and reflectometer.

1. N.Niimura et al., Nucl. Instrum. & Methods **A349** (1994) 521-525
2. N.Niimura, et al., Nature Structural Biology , **4** (1997) 909-914

15C1-5

NEUTRON POWDER DIFFRACTION DETERMINATION OF OXYGEN POSITIONS IN METAL OXIDES

C.J. Howard, Australian Nuclear Science and Technology Organisation.

In oxides of metals of medium to high atomic number, neutron powder diffraction is generally better able to determine oxygen positions than the corresponding X-ray method. This is the basis for the very successful application of neutron powder diffraction in structural studies of oxide superconductors and cmr materials.

The sensitivity of neutron diffraction to oxygen position is critical to experimental aspects of our current work on perovskites. Our initial measurements were on strontium zirconate, $SrZrO_3$. We took the angle of rotation of the oxygen octahedron in the tetragonal phase (stable from about 1100 to 1440 K) to be the order parameter for the tetragonal to cubic transition, and measured this angle as a function of temperature. Our measurements show that the transition is effectively tricritical in nature. Measurements were also made on calcium titanate, $CaTiO_3$.

The neutron advantage has been much exploited in our studies of zirconia (ZrO_2) and zirconia ceramics, first for distinguishing the different polymorphs, and then for detailed systematic studies of structure. In respect of the tetragonal to cubic phase transition, the displacement of the oxygen atom from the position it would have in the cubic phase can be taken as the order parameter. Our measurements suggest that this phase transition is second order.

15B2-1

ATOMIC AND MAGNETIC SHORT-RANGE ORDER IN PT-8.8 AT. % Mn SPIN-GLASS ALLOY

K. Ohshima, M. Takahashi and S. Yoshimi, Institute of Applied Physics, University of Tsukuba, Tsukuba 305-8573, Japan

The X-ray and neutron diffuse scattering intensities from disordered Pt-8.8 at. % Mn alloy were measured to investigate the relationship between the physical properties and structural fluctuations. A single crystal of the alloy was grown by the bridgman technique in a high-purity almina crucible. The X-ray intensity measurement was performed at room temperature by using a four-circle goniometer attached to a rota-unit of a generator. The incident beam, CuKα radiation, from a Cu target was monochromated by a HOPG crystal. In the experiment, we have introduced a high performance X-ray detector using 3x3x2 mm^3 $Cd_{0.9}Zn_{0.1}Te$ (CZT) with preamplifier and cooler system (XR-100T-CZT, AMPTEK). The detector is so compact and light that it is easier to mount it on an usual counter arm without any improvement. There are two characteristics in compared with a conventional scintillation counter ; (1) twice better energy resolution and (2) one-tenth lower background. Therefore, the CZT detector is an effective for measuring the diffuse scattering intensity. Diffuse maxima have been observed at the 100, 110 and their equivalent positions and also found at 1/2 1/2 1/2 and equivalent positions on the pattern. A similar diffuse intensity pattern has been found in Cu-Pt and Pd-Mn alloys (1,2). The Warren-Cowley atomic short-range order (ASRO) parameters were determined up to the 50^{th} shell from the observed intensities. We have realized that the correlation length between constituent atoms is about 5 a_0 without having chain-like correlation. Neutron diffuse intensities were observed from room temperature to 13 K with the use of TOP method at FOX machine of KENS, KEK. In addition to the ASRO diffuse maxima, a maximum at around 0.7,0,0 position appeared from 100 K, which comes from magnetic short-range ordering (MSRO). No peculiar feature of the temperature dependence for MSRO intensity was observed, in particular, at the spin-glass temperature Tg (=18 K).

1.Saha, D.K. and Ohshima (1993). J. Phys.: Condens. Matter 5, 4099-4110
2.Saha, D.K. et al. (1994). Phys. Rev. B49, 15715-15722

15B2-2

LOW TEMPERATURE MAGNETIC PROPERTY AND HEAT CAPACITY OF $LiNiO_2$

O.Fujishima, H.Kawaji, M.Takematsu, T.Atake, A.Hirano[*] and R.Kanno[*]
Materials and Structures Laboratory, Tokyo Institute of Technology
[*]Department of Chemistry, Faculty of Science, Kobe University

The ternary oxide $LiNiO_2$ has attracted much interest because of its 2-dimensional structure which may form 2D triangular antiferromagnets. Although a number of studies have been made on the physical properties of the compound, the results are confused. The reason should be in the nonstoichiometry x in the sample. We have synthesized high quality samples of $Li_{(1-x)}Ni_{(1+x)}O_2$ with $0 \leq x \leq 0.1$, and studied the magnetic properties at low temperatures.

In the present study, the low temperature heat capacity of well-synthesized near-stoichiometric sample ($x \approx 0$) was measured using an adiabatic calorimeter between 4 and 300 K. Two heat capacity anomalies were observed at 6 K and 10 K, and a remarkable relaxation phenomenon was found below 6 K. The results are consistent with the spin glass like behavior observed by the magnetic susceptibility measurements. Monte Carlo simulations were carried out on an assumption of antiferromagnetic nearest neighbour interaction to clarify the mechanism of the heat capacity anomalies and spin glass like behavior.

15B2-3

CHARACTERISTICS OF ORDER-MESOSCOPIC PHASE TRANSFORMATION IN COMPOUND SEMICONDUCTER In_2Te_3

S. Abe, Y.Nakamura and O.Nittono, Department Metallurgical Engineering, Tokyo Institute of Technology, Tokyo, Japan

In_2Te_3 is one of III2VI3 compound semiconducters, which contain structural vacancies in the cation sublattice. Previously, it had shown that the phase transformation in In_2Te_3 was order - disorder. It is true that the low temperature In_2Te_3 is vacancy ordered phase. The high temperature In_2Te_3, however, is not a ideal solid solution of zincblende type. Vacancy distribution is homogeneous as a whole crystal, but it is not homogeneous on a unit cell scale. That is, structural vacancies aggregated to form {111} vacancy planes, and they arrange about every 15 {111} planes. Therefore, we have concluded that the high temperature In_2Te_3 is mesoscopic. Next, we observed the development of the vacancy ordered region during the phase transformation. As a result, the phase transformation is found to take place with two steps: the rapid ordering at the initial stage and the slow one at the follwing stage. The formar occur during even air cooling. Nevertheless, the ordering hardly develop after an annealing for a long time. The electron microscopic observations clearly show the exsistence of a small amount of the ordered regions at the intersections of the vacancy planes and the {111} vacancy planes almost unchanged. This implies that the vacancies dissolved in the regions surrounded by the vacancy planes contribute to the rapid ordering while the vacancies in the {111} vacancy planes does not. It takes appropriate time to dissolved the vacancy planes. This is a main reason why the phase transformation take place with two steps.

The phase transformation in In_2Te_3 begin with homogeneous nucleation and proceed under the supersaturation as a whole crystal. However, the phenomenon which occurs in local is different from the one as a whole crystal. At the beginning of the phase transformation, heterogeneous nucleation of the ordering occur. Only part of the ordered region, however, can grow into the low temperature phase. The ordered regions produced by the heterogeneous nucleation are not recognized as nuclei of the low temperature In_2Te_3. The phase transformation in In_2Te_3 require homogenization of vacancy concentration in local area. The size of a critical nucleus for the low temperature phase turns to be about submicron, which we consider as mesoscopic size. It is concluded that the characteristics which never appear in the order-disorder transformation originate from the internal structure of the mesoscopic phase which is homogeneous as a whole crystal but heterogeneous on a mesoscopic scale.

INCOMMENSURATE CHARGE ORDERING IN $La_{0.5}Ca_{0.5}MnO_3$

S.Mori Department of Physics, Tokyo Institute of Technology,
Meguro-ku, Tokyo 152, Japan

$La_{1-x}Ca_xMnO_3$ is one of the most typical compounds showing colossal magnetoresistance (CMR) and charge ordering. In particular, $La_{0.5}Ca_{0.5}MnO_3$ has been reported to locate on a phase boundary between two competing ground state, ferromagnetic meatallic and antiferromagnetic insulating states.[1] Recently electron and newtron diffraction experiments revealed that $La_{0.5}Ca_{0.5}MnO_3$ shows an incommensurate to commensurate transition at 135K on cooling (180K on warming) with a large thermal hysteresis.[2] In this work, we examined microstructure in the incommensurate charge ordered state of $La_{0.5}Ca_{0.5}MnO_3$ by a high resolution electron microscopy. The incommensurate charge ordered state with the wave vector of $q=(1/2-\varepsilon)a_0^*$ is characterized by fine mixture of the charge ordered and charge disordered microdomains with the size of 20-30nm. With decreasing temperature, the charge ordered microdomains grow up at the expence of the charge disordered ones and around 135K change into a macroscopic domain with the size of >100nm. High resolution lattice images taken at 200K revealed that a mixture of paired Jahn-Teller stripes [3] with two distinct spacings of $2a_0$ and $3a_0$ gives rise to the incommensurate period.

This work has been done in collaboration with Drs.C.H.Chen and S-W.Cheong at Bell Laboratories, Lucent Technologies.

[1] P.E.Schiffer et al., Phys.Rev.Lett. 75, 4042(1996).

[2] P.G.Radaelli et al., Phys.Rev.B55, 3015(1997).

[3] S.Mori, C.H.Chen and S-W.Cheong, Nature 392, 473(1998).

ANOMALOUS-X-RAY SCATTERING ASSOCIATED WITH THE ORDER-DISORDER TRANSFORMATION IN $Al_{70}Ni_{15}Co_{15}$ QUASICRYSTAL

H. Abe, N. Tamura[1], J. Bai[1], D. Le Bolloc'h[2], S.C. Moss[2] AND Y. Matsuo[3], Department of Materials Science and Engineering, National Defense Academy, Yokosuka, Japan, [1]Solid State Division, Oak Ridge National Laboratory, Tennessee, USA, [2]Department of Physics, University of Houston, Texas, USA and [3]Department of Physics, Nara Women's University, Nara, Japan

$Al_{70}Ni_{30-x}Co_x$ ($10 \leq x \leq 15$) (ANC) alloys are well known to contain a decagonal phase (two-dimensional quasicrystal). Recently many studies of ANC have been carried out in relation to an order-disorder transformation at high temperature.(1) In order to clarify the origin of the transformation mechanism, we performed an anomalous-x-ray scattering experiment in National Synchrotron Light Source (U.S.A.); each energy is 7.686 keV (near K-edge of Co), 8.098 keV ($|f_{Ni} - f_{Co}|=0$) and 8.304 keV (near K-edge of Ni), respectively. This is because the difference atomic number between Ni and Co is only one. We measured the contrast of the diffuse scattering by 3λ method, since the diffuse intensity from atomic short-range order (SRO) is proportional to the difference of the atomic scattering factor, that is, $|f_{Ni} - f_{Co}|^2$. This reflects the existence of SRO between Ni and Co atoms.

1. Hiraga, K., Lincoln, F. J. and Sun, W. (1991). Mater. Trans. JIM **32**, 308-314

15B2- 6

THERMOCHROMIC PHASE TRANSITIONS IN CRYSTALS : SINGLE CRYSTAL X-RAY INVESTIGATIONS.

B.Narayanan and M. M. Bhadbhade, Central Salt & Marine Chemicals Research Institute, Bhavnagar - 364 002, Gujarat, and National Chemical Laboratory, Pune - 411 008, India

Thermochromic phase transitions, involving colour change upon heating or cooling, exhibited by a class of metal complexes, ML_2X_2, where M=metal-ion, L=N,N-Dialkyldiamine and X=anion are found most interesting. Amongst them, only Cu-complex with L=N,N-Diethyl ethylenediamine and X=ClO_4^- exhibiting red $\rightleftharpoons$ blue colour change at ~44 °C have been extensively investigated using spectroscopic methods. Based on these, it was thought that the mechanism of color change involved increased axial interactions between the metal center and the anions. However, the variable temperature X-ray studies attributed the phase change with the dynamic disorder of the chelate ring atoms within the crystalline environment.

In our laboratory, we have undertaken structural study of a series of complexes by systematically varying the anion, metal-ion and alkyl substitutions inorder to gain insight into the structure-thermochromic behavior. Attempts will be made to correlate the intermolecular interactions, patterned by these variations, with the thermochromic behaviour of the complexes in solid state. The energetics of the molecular motions in crystals during thermochromic phase transitions computing crystal lattice energies will also be discussed.

15B2-7

PRESSURE-INDUCED PHASE TRANSITION IN RELAXOR $Pb(In_{1/2}Nb_{1/2})O_3$

K. Nomura, T. Shingai, S. Ishino, N. Yasuda[1], H. Ohwa[1] and H. Terauchi

Advanced Research Center of Science (ARCS), School of Science, Kwansei-Gakuin University

[1]Electronic and Information Engineering Department, Gifu University

The $Pb(In_{1/2}Nb_{1/2})O_3$ (PIN) crystal with disordered cation arrangement at B sites in the complex perovskite structure Pb(B,B') O_3 shows the relaxor behavior characterized by the dielectric dispersion. The pressure dependence in the relaxor-PIN single crystals (S=0.4 (type(I)), 0.2 (type(II))) were investigated by X-ray diffraction. The pressure dependence of the cell parameters and the integrated intensities of the (h/4 k/4 0) superlattice reflections associated with the antiparallel shift of lead cations were measured. The phase transition from the pseudo-cubic structure to the orhtorhombic one was observed at about 0.4GPa in the type(I) crystal. However, no phase transition was observed below 0.8GPa in the type(II) crystal. The type(I) crystal at higher pressure than 0.4GPa was isostructural with the ordered crystal at the atmospheric pressure. But with increasing pressure in the type(I) crystal, the integrated intensities of the (h/2 k/2 l/2) reflections associated with the In/Nb arrangement did not change. The antiferroelectric phase was obtained not only by changing the In/Nb arrangement with isothermal annealing but also by applying pressure above 0.4GPa in the type(I) crystal. In addition, the pressure dependence of the diffuse scattering was also measured. On the basis of the pressure dependence of the diffuse scattering, we will discuss the phase transition of the relaxor-PIN in more detail.

Poster Presentation

PHASE DETERMINATION OF FORBIDDEN REFLECTIONS

J. Kokubun, M. Kuribayashi, K. Ishida and V.E. Dmitrienko[a]
Department of Physics, Faculty of Science and Technology, Science University of Tokyo, Noda, Chiba 278, Japan
[a] A.V. Shubnikov Institute of Crystallography, Russian Academy of Sciences, 117333 Moscow, Russia

Anisotropy of X-ray tensorial susceptibility brings forth appearance of "Forbidden reflections" which is forbidden by glide or/and screw rule.[1] Indeed, forbidden reflections of this type (ATS reflections) are observed near absorption edges in several crystals.[2-4] The reflection arises from the anisotropy of local environment of the absorbing atom. Since the reflection is due to resonant scattering, the complex amplitude f_{ij} is a function of X-ray energy and the effect becomes large near the absorption edge. However, by usual diffraction method we cannot determine the phase of amplitude but only the magnitude of it.

To study the physics of the resonant X-ray scattering, it is desirable to determine the phase. The use of Renninger reflections is established method to solve the phase problem in the X-ray diffraction.[5] We extend this method to the phase determination of ATS reflections.[6] In the present report, the method is applied successfully to the FeS_2 (pyrite) crystal near the Fe K-absorption edge.

1) V.E. Dmitrienko (1983). Acta Cryst. A39, 29; (1984). A40, 89.
2) D.H. Templeton and L.K. Templeton (1986). Acta Cryst. A42, 478.
3) A. Kirfel, A. Petcov and K. Eichhorn (1991). Acta Cryst. A47, 180.
4) T. Nagano et al. (1996). J. Phys. Soc. Jpn. 65, 3060.
5) R. Colella (1992). In D.W.J. Cruickshank, H.J. Juretschke and N. Kato, editors, P.P. Ewald and his Dynamical Theory of X-ray Diffraction, p.71. Oxford: University Press.
6) J. Kokubun, K. Ishida, V.E. Dmitrienko (1998). J. Phys. Soc. Jpn. 67, 1291.

A MODEL WITH P1 SYMMETRY, WHICH SHOWS CUBIC SYMMETRY m3m IN DIFFRACTION.

T.Matsumoto, S.Hashimoto. Dept. Earth Sciences,Faculty of Science, Kanazawa University, Japan.

Enhancement of diffraction symmetry, which means the appearance of a higher Laue symmetry than normally expected has been studied by several authors. This is caused by special relations among the symmetryoperations in the unit cell, has been theoretically studied mainly in Japan.

Sadanaga and Ohsumi(1979) have shown that the symmetry of diffraction equal to the ponit group symmetry of the corresponding vector set and arrived the conclusion that an enhanced vector symmetry necessarily leads to a structure built up according to self-homometry or a certain space groupoid. Many examples and models have been reported, however, the structure model with triclinic symmetry, showing the cubic symmetry in diffraction, has not been reported. Here we show such a model. The structure is composed of the same 7x7x7 atoms. The lattice is metrically cubic, and three homometric mates on three axes (Patterson, 1944) . The atomic parameters on three axes are as follows; A:1/16{0,1,2,3,6,11,15},B:1/16{0,1,2,3,5,6,10},C:1/16{0,1,2,3,6,7,14}.

One plane configuration denoted A*B has been derived by modified convolution of A with B, where B is homometric with A.

In this case, the A*B configuration corresponds to the intersections of xj in A and yk in B, where $1 \leq j,k \leq 7$. Although this plane model is triclinic (plane group:p1, point group:1), its vector symmetry (diffraction symmetry) is not triclinic but tetragonal, 4mm. The B*C and C*A configurations are the same situation.

Moreover, a model denoted A*B*C, is obtained in the same way by group 1, however, the diffraction symmetry (vector symmetry) is convolution of A*B with C. The space group of this model is P1, point m3m. Then this structure should show the enhancement of diffraction symmetry, if anomalous dispersion can be ignored. There are special phase relations, in addition to Friedel's law, among 48 reflections (corresponding to equivalent reflections in m3m). This model shows the highest enhancement in diffraction symmetry (from 1 to m3m).

RECENT X-RAY CRYSTAL STRUCTURE ANALYSIS BY NEW DIFFRACTOMETER USING A CYLINDRICAL IMAGING PLATE

H.Uekusa, and Y. Ohashi, (Tokyo Institute of Technology, JAPAN)

Recently we have designed a new diffractometer using a cylindrical Imaging Plate (IP) for high-resolution and rapid data collection.

The new diffractometer has one large size cylindrical IP that can record the diffraction data from –60 to 140 degree on one frame. Therefore, both the usual Cu X-ray measurement (resolution 0.83Å) and high-resolution Mo X-ray measurement (0.38Å) are possible. This feature is important for the absolute structure determination study by Cu X-ray and the charge density study by Mo X-ray, thus extends the usage of IP diffractometer further. It is also equipped with a 1/4 χ three-axis goniometer for crystal alignment. The translation motion of IP makes the multi layer Weissenberg photograph possible. In order to achieve the higher completeness, the second and third axes are aligned automatically by utilizing this goniometer. In this Weissenberg mode, the total number of photographs and, therefore, the total measurement time is minimized.

All three-dimensional diffraction data (completeness 1.00 with sufficient redundancy, Mo X-ray) from a typical small-molecule crystal are recorded in 3 to 5 hours and the quality of the data is comparable to that of a four circle diffractometer. Such a rapid measurement is essential for the unstable crystals.

The results of structure analysis using this diffractometer are presented.

ON-LINE AND IN-SITU X-RAY DIFFRACTION ANALYSIS OF THE CRYSTALLISATION OF IMPORTANT PHARMACEUTICAL MATERIALS

S.Hastings, K.Roberts., Heriot-Watt University, Merrifield D., SmithKline Beecham Pharmaceuticals

The crystallisation process is an important unit operation for the separation and purification of many chemical products, particularly in the pharmaceutical industry. Variations in the conditions of crystallisation can lead to the formation of different polymorphic forms which are often meta-stable phases which results in phase conversion at different rates to the stable form. Our group, in collaboration with many industrial sponsors, have developed a number of on-line techniques which help to optimise the processing conditions of many of these specialty materials. In particular, *on-line* and *in-situ* X-ray diffraction (XRD) has been used to monitor the crystallisation of pharmaceutical materials. Several novel *in-situ* X-ray cells have been developed, in particular; a solution cell, which allows us to control and hence optimise crystallographic conditions such as temperature and pH whilst monitoring the crystal structure of the sample as it crystallises from solution. The current system being studied is the crystallisation of stearic acid, a common pharmaceutical excipient, in various polar and non-polar solvents in order to ascertain the effect that the polarity of the solvent has on the polymorphic form crystallised. Measurements of resulting particle structure enable optimisation of processes to produce optimal particle properties.

13P5

CifSieve:QUICK CREATION OF CIF INTERFACES

J. R. Hester and F. P. Okamura, National Institute for Research in Inorganic Materials, Namiki 1-1, Tsukuba, Ibaraki, Japan.

CifSieve arose from the need to find a less time--consuming and tedious method to add CIF file input capability to crystallographic programs, that is, to avoid the repetitive and unenlightening task of typing many long CIF item names together with associated library calls and checks.

CifSieve is therefore a programming tool which enables quick, trouble free addition of Cif input capability to application programs. The programmer simply adds a "_variable_name" attribute and variable name to the definitions of target CIF items in a DDL1/2 domain dictionary (eg the core CIF dictionary). CifSieve component program "BuildSiv" reads this edited dictionary file, ignoring definitions that do not have this attribute, and creates an object file containing a C or Fortran callable function "cifsiv_" .This object file can be linked with the rest of an application program. The function, when called with the name of a Cif file and Cif data block, writes the values of the chosen CIF items into the appropriate variables. It will also read data contained in a loop if the requested CIF item variable name in the DDL file has an array dimension appended.

The "cifsiv_" function is designed to be robust relative to CIF file syntax or data errors. If a syntax error occurs in the input file, the "cifsiv_" is often able to recover, and an error message is stored for the calling program. Likewise, if an incorrect number of data items is found in a loop block, a warning message is stored and processing continues.

CifSieve was developed on a Linux system, however it should run on any operating system which has a C compiler, the bison parser builder, the flex lexical analyser, and perl. It is available by anonymous ftp from "ftp://ftp.nirim.go.jp/pub/sci/cif/cifsieve_1.2.tar.gz"

XTAL3.6: NEW VERSION OF Xtal TO BE RELEASED

D.du Boulay and S.Hall, Crystallography Centre, University of Western Australia, nedlands 6907, AUSTRALIA.

XTAL3.6 is an integrated package of over 50 crystallographic programs which may be used to determine, refine and publish crystal structures. The package provides the full range of standard techniques for studying small molecule structures from X-ray, neutron and electron diffraction data, and additional calculations for use in the precise density studies. XTAL3.6 has the following new features.

(1) PIG has been changed so that there are more mouse-manipulation of the displayed image(of either a molecule or a cell) can be automatically output as an ORTEP ellipsoid plot; the output atom list can be sorted on atomic number or on label strings; newly assigned H atom sites are given U iso values based on the U values of the parent atoms.

(2) A new program BISCUT combines all direct methods phasing steps and identifies the best solution using the expected molecular geometry. This approach is similar to the iterative approach of Miller et al. (1994, JAC, 27, 613-621) and combines the algorithms of programs such as GENTAN, PATSEE, MODEL, PEKPIK, FC and FOURR.

(3) The new program GIP enables a wide variety of reciprocal space Fourier components (coefficient and phase data) to be viewed in a way similar to that used by PIG in real space.

(4) The new structure factor least squares program CRILSQ, written by Roeli Olthof, refines structural parameters using F2 and full matrix least squares. The program provides for the refinement of merohedral twin fractions and riding model constraints.

(5) A graphical front-end Tk/tcl script is available to filter the input lines so that they may be edited and toggled, and the output streamed to be viewed on the screen. The front-end can handle a multipart CIF as input, manipulating the data block for compatability with Xtal, and automatically generating an editable Xtal program control list. This also enables the Acta C structures on the IUCr web site to be browsed and viewed via the CIFs.

(6) A variety of other programs have been updated. XTAL3.6 will be demonstrated. Further details about the release and distribution may be obtained from the web site www.crystal.uwa.edu.au.

STRUCTURAL PROPERTIES INDUCED BY ANNEALING IN Al-N-M(M:Co,Fe) FILMS PREPARED BY REACTIVE SPUTTERING

A.G.Roy and O. Nittono, Department of Metallurgical Engineering, Tokyo Institute of Technology, Oh-okayama, Meguro-ku, Tokyo, JAPAN

As-sputtered alloy films exhibit unstable structures and they change their properties with respect to microstructures induced after annealing. In this study Al-N-M (M:Co,Fe) films were prepared by reactive sputtering in a two-facing-target type sputtering chamber with Al+Co(Fe) composite targets, and sputtering gas is a mixed gas of Ar and N_2 gases. The films were first examined by X-ray diffractometry, and their structural properties such as magnetization, coercive force and resistivity in the films were also examined in terms of annealing conditions. Microstructure and texture was investigated by electron diffraction and TEM.

Main results are as-follows :(1)Al-N-Co films: As-deposited films were amorphous-like, indicating that they are composed of very fine grains which are though to be heavily strained. No columnar structure was observed in the cross-section of the as-deposited films with a large amount of Co. The grain size of the films and the resistivity decrease with increasing Co content in the film. The properties drastically changes with the changes in microstructure, which can be adjusted by heat treatment. As-deposited Al-N-Co amorphous films crystallize into two distinct phases of AlN and fcc Co at higher temperatures. The phase separation dominates and the grain size increases upto about 45nm in diameter with increasing annealing temperature.

Magnetization increases with increasing annealing temperature and time. Co-based alloys dispersed in the AlN matrix result in the magnetization in the film. The resistivity for the films containing 25%Co first decreases after 12ks annealing, and increases with increasing annealing time and temperature. The decrease in resistivity at the annealing stage is probably due to the escape of nitrogen gas from the film.

(2)Al-N-Fe: As-deposited flms showed similar cross-sectional structures to those in Al-N-Co films, especially for high content of Fe. In these films Fe-N alloys were found to be formed after annealing at lower temperature, but these nitrides were decomposed at elevated temperature higher than 873K. After annealing these films showed increases in magnetization with annealing temperature but for a certain content of Fe they showed no magnetization. This is because Fe-Al compounds which are considered to be nonferromagnetic are newly formed after annealing.

13P8

SPECTROSCOPIC INVESTIGATION OF LASER DYES IN SOLID MATRICES

A.S.Farooqui and Z.H.Zaidi ; Department of Physics, Jamia Millia Islamia, New Delhi- 110025, India

In an attempt to find a suitable matrix for laser dyes where dye aggregation could be stopped or at least minimised, a spectroscopic study of some organic dyes is made in sol-gel glasses prepared by using a modified technique for silica gels.

It has been reported by various workers that in liquid solvents and in glasses,fluorescence quenching occurs in these dyes on optical pumping. Fluorescence quenching is not only concentration dependent but also varies from matrix to matrix. In fact the dye is changed from monomeric to dimeric form in many cases. This process of aggregation of the dyes can be stopped or at least minimised by controlling dye concentration provided that suitable matrices are found. Therefore a spectroscopic investigation of organic dyes in various solid matrices has been taken up including boric acid glass and silica gel prepared by using HCl as a catalyst. The present paper describes the results of these investigations and their possible interpretation.

X-RAY OPTICAL ACTIVITY AND X-RAY BIREFRINGENCE MEASURED WITH POLARIZATION-SWITCHING OPTICS

Y. Ueji[1], K. Okitsu[2], K. Sato[2] and Y. Amemiya[2], 1) Graduate Univ. for Advanced Studies, 2)Univ. of Tokyo, Japan

We have developed an x-ray optical system which enables us to switch the helicity of the circular polarization and have measured the spectra of natural circular dichroism of $NiSO_4 \cdot 6H_2O$ (c axis along the beam direction) at Ni K edge. This optical system consists of a tunable x-ray polarizer to produce a highly linear-polarized beam (I(H)/ I(V)= 108) and two successive phase retarders to convert the linear-polarized beam to circular-polarized beam of either helicity. The helicity of the circular polarization can be switched in less than a half second by rotating the diffraction angles of two phase retarders. The advantage of our system is that 1) an expensive insertion device to generate circular polarization is not required, and 2) a much higher degree of the circular polarization is obtained due to the introduction of the second phase retarder which corrects spherical aberration. The circular birefringence of the same sample was also measured with our x-ray polarimeter (1) which consists of the x-ray polarizer and analyzer. It was found that the Kramers-Kronig relation holds between the measured circular dichroism and birefringence.

This x-ray optical system also permits us to produce a high degree of vertical linear-polarized beam ((I(V)-I(H))/(I(V)+I(H))=0.97) from the horizontal linear-polarized beam which is produced with the polarizer. The spectra of linear dichroism of the $NiSO_4 \cdot 6H_2O$ (a axis along the beam direction) at Ni K edge has been successfully measured with the polarization switching between horizontal- and vertical- linear polarization. The rotation of the sample about the beam axis is not required, which is much advantageous over the conventional polarized XAFS. The Kramers-Kronig translation of the linear dichroism was in good agreement with the linear birefringence measured with our x-ray polarimeter.

(1) K. Okitsu, T.Oguchi, H.Maruyama, and Y.Amemiya, (1998), J. Synchrotron Rad., 5, 995-997.

13P10

BOTH CALCULATION OF SHIFT AND INTENSITY OF X-RAY DIFFRACTION PEAK, AND DETERMINATION OF KIND OF RESPONSE FUNCTION AND ITS PARAMETERS BY MODE ROSA IN X-RAY PROFILE BROADENING ANALYSIS

P.O.Verkhovodov, Department of X-ray Methods for Testing Materials, KCG, Box51/3, Kyiv, 252142, Ukraina.

Mode ROSA is new deconvolution method without Fourier transform. It finds solution of a Fredholm integral equation of the first kind, and calculates another parameters. Function g(x) is a convolution the function f(x) with response function $\psi(x\text{-}z)$. Function g(x) and f(x) is given by numerical value, but $\psi(x\text{-}z)$ is analytical function and it is given by the parameters. These parameters is determined by mode ROSA. Different task may be solution by this mode ROSA:*Determination of the instrument response function.* Diffraction profile g(x) is recorded from the ideal crystal. Peak of characteristic lines of X-ray tube f(x) is given by numerical value (it must be known). Mode ROSA determines the kind of instrumental response function $\psi(x\text{-}z)$ (in may be Gaussian, Lorentzian or another distribution) and calculates the parameters of this distribution. *Determination of sample broadening function containing the desired structural information.* Any changes of the structure of sample bring to bias, to the change of intensity and to the broadening of X-ray diffraction peak. Diffraction profile f(x) is recorded from the primary sample. Diffraction profile g(x) is recorded from the executed samples. Mode ROSA determines the kind of sample broadening function $\psi(x\text{-}z)$ containing the desired structural information (in may be Gaussian, Lorentzian or another distribution) and calculates the parameters of this distribution. Together, mode ROSA calculates the shift of X-ray diffraction peak g(x) with regard to peak f(x) and the relation of intensity (area under peak) diffraction peak g(x) with regard to peak f(x). Value the shift, the intensity, parameters of sample broadening function are the desired structural information.

Primary X-ray radiation may be one line or few lines. Diffraction profile f(x) may be one, two or more peaks. It is new possibility of X-ray profile broadening analysis.Of many year's standing our experience of work showed up robustness received offsprings.

13P11

RAPID AND ROUTINE STRUCTURE SOLUTION OF HIGHLY FLEXIBLE MOLECULAR CRYSTAL STRUCTURES FROM POWDER DIFFRACTION DATA

K. Shankland and W. I. F. David.
ISIS Facility, Rutherford Appleton Laboratory, Chilton, Didcot,
Oxon OX11 0QX, U.K.

A global optimisation approach to solving molecular crystal structures from powder diffraction data is presented. The approach is distinctive in

(i) its ability to solve highly flexible organic molecules
(ii) its use of correlated integrated intensities
(iii) its ability to handle multiple fragments
(iv) its computational efficiency and intrinsic parallelism

The approach is discussed in terms of the solutions of four previously unreported crystal structures of pharmaceutical interest.

13P12

CRYSTAL STRUCTURES OF A-SITE DEFICIENT PEROVSKITES $Li_xLa_{1/3}NbO_3$

R.A. Dilanian and F. Izumi, National Institute for Research in Inorganic Materials, Tsukuba, Ibaraki 305-0044, Japan
A. Yamamoto and S. Tajima, Superconductivity Research Laboratory, ISTEC, 1-10-13 Shinonome, Koto-ku, Tokyo 135-0062, Japan
T. Kamiyama, Institute of Materials Science, Tennodai, Tsukuba, Ibaraki 305-8573, Japan

Lithium-ion conductors have aroused interest widely because of their potential applications as solid electrolytes in electrochemical devices. Li^+ ions can be inserted into the channels or cavities of many transition metal oxides at ambient temperature either by chemical or electrochemical means (1). In the present study, we inserted Li^+ ions into an A-site deficient perovskite $La_{1/3}NbO_3$ and determined the crystal structures of $Li_xLa_{1/3}NbO_3$ including a sample with $x = 0$ by time-of-flight neutron powder diffraction, paying attention to their structural peculiarities. Reflections due to different superstructures appeared in their neutron powder diffraction patterns. Rietveld refinements showed that the superstructures result from tilting of NbO_3 octahedra and ordering of cations and vacancies at A sites.

1. Belous, A.G. (1996). Solid State Ionics **90**, 193–196.

13P13

RAPID STRUCTURE SOLUTION OF IBUPROFEN FROM POWDER DIFFRACTION DATA BY THE APPLICATION OF A GENETIC ALGORITHM COMBINED WITH CONFORMATIONAL ANALYSIS

L. McBride*, K. Shankland, W. I. F. David and T. Csoka
*Department of Pharmaceutical Sciences, Strathclyde University, UK
ISIS Facility, Rutherford Appleton Laboratory, U.K.

The crystal structure of ibuprofen has been solved from synchrotron X-ray powder diffraction data using a genetic algorithm (GA) based method. The performance of the algorithm has been enhanced using two methods to direct the search to low-energy regions of the ibuprofen potential energy surface :

- In method 1, the conformational flexibility of the ibuprofen molecule is analysed by crystallographic database searching and potential energy calculations. The results are used to derive hard limits which are then imposed on the values that can be assumed by flexible torsion angles within the molecule during the GA procedure.
- In method 2, molecular mechanics calculations of conformational energy are performed as part of the actual GA optimisation procedure.

In effect, both methods reduce the time spent on trial crystal structures in which the intramolecular energy is relatively high, and therefore the probability of the structure being correct is relatively low.

The results from both methods are presented and discussed in terms of the solution of the known crystal structure of ibuprofen.

13P14

PHYSICAL INTERPRETATION OF THE MARCH FUNCTION r-PARAMETER IN POWDER DIFFRACTION RIETVELD MODELLING OF PREFERRED ORIENTATION

H. Sitepu, B.H. O'Connor and D.Y. Li, Materials Research Group,
Department of Applied Physics, Curtin University of Technology.

The modelling of preferred orientation (PO) is of critical importance in powder diffraction analysis - for structure refinements and in the determination of bulk descriptors such as phase composition. The authors are conducting evaluations of the March PO pole-density distribution model using Rietveld analysis of Bragg-Brentano x-ray diffraction (XRD) and Debye-Scherrer neutron diffraction (ND) data. Extensive measurements have been performed with suites of uniaxially-pressed powders of molybdite, MoO_3, and calcite, $CaCO_3$ for which the compression has been systematically varied. The validity of the March model for these powders has been tested with a physical relationship linking the March function r-parameter and the powder bulk modulus, B. It may be shown from first principles that,

$$r = [1 - (\Delta P/B)]^n$$

where $n = 1$ and -1 for platy and acicular crystallites, respectively.

Results will be given for pressed powders involving both XRD and ND powder data, and comparisons will be made with known values of B for the materials examined. The research has been supported by the Australian Institute of Nuclear Science and Engineering - project 97/143.

STRUCTURAL PROPERTIES OF DOPED SYSTEMS: $PrBa_{2-x}Ca_xCu_3O_y$ and $PrBa_2Cu_{3-x}Ag_xO_y$

Z. Zou[1], J. Ye[2], H. Kawanaka[1], T. Minawa[1,3], H. Bando[1], Y. Nishihara[1,3]
[1]Electrotechnical Laboratory,1-1-4 Umezono,Tsukuba Ibaraki 305, Japan
[2]National Research Institute for Metals, Tsukuba, Ibaraki 305, Japan
[3]Faculty of Science, Ibaraki University, Bunkyo 2-2-1, Mito 310, Japan

The nominal $(Pr_{1-x}Ca_x)Ba_2Cu_3O_7$ and $Pr(Ba_{1-x}Ca_x)_2Cu_3O_y$ systems were wildly studied.(1) However, detailed structural analysis could not been investigated since the position of Ca ions could not be decide. In this report, the structural parameters of Ca doped $PrBa_{2-x}Ca_xCu_3O_y$(x=0~0.7) and Ag doped $PrBa_2Cu_{3-x}Ag_xO_y$(x=0,~0.3) systems are investigated with powder X-ray diffraction (XRD) and Rietveld refinements. Two doped systems are isostructural and have same tendency to become a tetragonal from orthorhombic structure when Ca=0.5, and Ag=0.1 were doped into $PrBa_2Cu_3O_7$. A changes of c lattice parameters and features in the Cu(2)-Cu(2) bond length are correlated with the unusual electronic and magnetic transitions induced by the Pr ion in these materials. Results for the two doped systems show that the c-axis lattice parameters of $PrBa_{2-x}Ca_xCu_3O_y$ (x=0~0.7) contracted with increase of the Ca doping concentration, however, the c-axis lattice parameters of $PrBa_2Cu_{3-x}Ag_xO_y$(x=0~0.3) expanded with increase of the Ag doping concentration. The structural features of these compounds are compared to similar high Tc cuprates, and related to the electronic, magnetic and superconducting transitions by the Pr ion in these materials.

1. Infante. C., Elmously. K. M., Dayal. R., Husain. M., Siddiqi. S. A., and Ganguly. P.(1990). Physica C **167**, 640-656

13P16

STRUCTURAL MODIFICATION OF BORON CARBIDE INDUCED BY INDUCTION PLASMA TREATMENT

T. Tanaka (Nisshin Flour Milling Co., Ltd.), X. Fan and T. Ishigaki (NIRIM)

Powder X-ray diffraction study revealed that the structural modification in boron carbide (B_xC) was induced by an in-flight R.F. induction plasma treatment, which was characterized by its high enthalpy and the presence of chemically active species. Boron carbide, which has a rombohedral unit cell, was known one of non-metallic hard materials and expected to the coating material in spray plasma coating process. In this study, boron carbide powders ($B_{5.25}C$) were modified by the Ar-H_2, Ar-N_2 and Ar-H_2-NH_3 R.F. induction plasma treatment and the changes of their stoichiometry and crystal structure were investigated by powder X-ray diffraction study. The formation of boron, which has a doubled ***a*** length in comparison with B_xC rombohedral cell, and remarkable change in profile intensity of rombohedral B_xC were observed in powder X-ray diffraction pattern of each plasma-treated powder. The Rietveld analysis revealed that the occupancy of boron at 1*b* site (0,0,1/2) of space group $R\bar{3}m$ were changed in those plasma-treated boron carbide. In addition, the unit cell volumes of Ar-N_2 or Ar-H-NH_3 plasma-treated boron carbide were increased rather than those of Ar-H_2 treated one. It was suggested the oxygen or nitrogen atoms took the place of boron atom through the plasma treatment, considering the atomic radii of each atom. The change of chemical composition in plasma-treated boron carbide agreed with the above results of Rietveld analysis.

EXPRESSION, PURIFICATION and CRYSTALLIZATION of BACTERIAL CMP-Neu5Ac CITIDYLYLTRANSFERASES

J.A. Carmichael1,2, R.K. Scopes2, T.P.J. Garrett1, G.G. Lilley3, M.Z Lou1 and P.A. Pilling1
1Biomolecular Research Institute, Parkville 3052 AUSTRALIA, 2Latrobe University, Bundoora 3083 AUSTRALIA, 3CSIRO Molecular Science, Parkville 3052 AUSTRALIA.

CMP-Neu5Ac citidylyltransferase is an enzyme involved in the transfer of CMP from CTP to N-acetylneuraminic acid (Neu5Ac or sialic acid). This activation of the Neu5Ac enables its utilisation by other membrane bound transferases involved in the elongation of polysaccharide chains on proteins and lipids.

The glycosylation of proteins is an important post translational modification and in this sialic acid plays a significant role. Sialic acid is commonly found as the terminal sugar on polysaccharides and is increasingly being identified as a modulator of many protein:protein and cell:cell interactions, including some evidence for homotypic binding of these sugars. Increases in the sialation of sugar residues on glycoproteins on some cancerous cells has also been used as a tumour marker and correlated with metastasis.

In bacterial infection the glycocalyx or capsule has long been identified as a virulence determinant. In particular the polysialic acid capsules of some gram negative bacteria confer a greater chance of survival of these strains due to their poor immunogenicity.

This work involves the expression, purification and crystallisation of a bacterial enzyme involved in the biosynthetic pathway of this virulence sugar. It is hoped to also determine the 3 dimensional structure of this enzyme with a view to rational drug design and a greater understanding of these novel NMP transferase enzymes.

For a general review: Biology of the Sialic Acids (1995), Edited by Abraham Rosenberg, Published by Plenum Press New York

STRUCTURES OF PENICILLOPEPSIN IN COMPLEX WITH CYCLIC AND ACYCLIC PEPTIDE INHIBITORS

A.R.Khan, J.Parrish, M.E.Fraser, A.Deacon* & M.N.G.James, Department of Biochemistry, University of Alberta, Canada & *Cornell High Energy Synchrotron Source, Ithaca, New York

A peptide-based phosphonate inhibitor of the fungal aspartic proteinase 'penicillopepsin' from *Penicillium janthinellum* was previously synthesized with a covalent amide bridge between the P2(Asn) and P1'(Phe) side chains (Smith & Bartlett, JACS 120:4622-, 1998). The 'macrocyclic' inhibitor and its acyclic analog were designed to quantify the enhancement in binding affinity upon restriction of peptide flexibility. The macrocylic inhibitor exhibited the tightest binding to penicillopepsin that has yet been achieved (Ki = 0.099 nM). In contrast, the observed binding constant Ki for the acyclic analog was 400-fold higher (41.8 nM).

We have now performed a structural comparison of the enzyme-inhibitor complexes. The structures reveal that the hydrogen-bond interactions, hydrophobic contacts, and water structures at the active site are virtually identical. We conclude that the inhibitors provide a valid comparison of the entropic cost of peptide binding to the active site, which we estimate to be 3.6 kcal/mol. Finally, the structure of the macrocycle-penicillopepsin structure has been refined using data to 0.90 Å resolution. The quality of the data is excellent considering the size of the enzyme (323 residues), thus providing unprecedented insight into its molecular structure.

PROTEIN STRUCTURE IN ORGANIC MEDIA

Q. Huang, Z. Wang, M. Qian, G. Zhu, Y. Tang, Department of Chemistry, Peking University, Beijing, People's Republic of China

Protein structure in organic solvent has been subjected to X-ray analysis because of its special behavior in nonaqeuous media. The crystals of lysozyme were studied after cross-linked with glutaraldehyde and diffraction data sets were collected to 1.93 Å, for crystals in neat water, in 90% and 95% acetonitrile-water, in neat acetonitrile and back-soaked from acetonitrile to water[1]. The diffraction data sets were refined successfully, except in neat acetonitrile. The conformations of lysozyme in acetonitrile is similar to the native except some side chain in the protein surface. One acetonitrile molecule was found in the active site cleft. We also studied the crystal structures of concanavalin A[2]. The conformation of residues in the loop and turn changed greatly in the acetonitrile. The crystal back-soaked to water also regained native conformation.

We studied two forms of non-cross-linked crystal(Vm are 2.2 and 2.9) of bovine β-trypsin in cyclohexane. The whole conformations of crystal structures were similar to the natives. Cyclohexane molecules were found, and the conformation of the side chain near the cyclohexane changed greatly. The diffraction ability are related to the packing density of crystal.

1. Wang, Z., Zhu, G., Huang, Q., Qian, M., Shao, M., Jia, Y. and Tang, Y. (1998) Biochim. Biophys. Acta, 1384, 335-344
2. Qian, M., Huang, Q., and Tang, Y. (1998) Sci. China Ser. B, in press

13P20

PROTEIN DATA BANK ACTIVITIES AT THE INSTITUTE FOR PROTEIN RESEARCH, OSAKA UNIVERSITY, JAPAN

M. Kusunoki, R. Igarashi, S. Suzuki, M. Okamoto and G. Kurisu, Institute for Protein Research, Osaka University, Osaka, Japan

The Protein Data Bank (PDB) is an archive of experimentally determined three-dimensional structures of biological macromolecules operated at Brookhaven National Laboratory (BNL), USA since 1971. The Institute for Protein Research, Osaka University, Japan, will soon start to serve as the data deposition center of the PDB for crystallographers and NMR spectroscopiests in Asia and Oceania regions. We here describe our present PDB activities and projects in the near future.

The coordinates of a biological macromolecule determined by X-ray crystallography and NMR spectroscopy are deposited with the PDB by the authors. The deposited data are validated and annotated by the PDB staff and are then released to the scientific community over the Internet. The number of PDB entries has recently increased dramatically and hence a system to catch up this tendency is needed without increasing staff number at BNL. As a scheme for overcoming this problem, the European Bioinformatics Institute (EBI) has started data deposition of PDB entries from depositors in Europe in January 1998, sharing the burden of the PDB entry processing. At present the deposited data at EBI are immediately sent to BNL for validation and annotation but in near future the validation and annotation will also be performed at EBI

The Institute for Protein Research is to participate in the operation of data deposition and validation of PDB entries at the request of and in cooperation of BNL. Our Institute founded the Research Center for Structural Biology in April 1998, in which one of the four divisions will handle the PDB archiving in the region of Asia and Oceania.

1. Abola, E.E., Sussman, J.L., Prilusky, J. and Manning, N.O.(1997), Methods in Enzymology, 277, 556-571

13P21

STRUCTURE OF A DOUBLE-HEADED SERINE PROTEASE INHIBITOR AND ITS ENZYME INTERACTIONS

D. Mukhopadhyay, S. Ravichandran, U. Sen, A. Podder, C. Chakrabarti and J.K. Dattagupta, Crystallography & Molecular Biology Division, Saha Institute of Nuclear Physics, Calcutta, India.

The crystal structure of an alpha-chymotrypsin inhibitor protein of Kunitz (STI) family, isolated from winged bean (Psophocarpus tetragonolobus) seeds, will be reported. This is a single polypeptide chain having a molecular weight of 20,244 Da with 183 amino acids. The structure of the protein has twelve antiparallel beta-strands with connecting loops arranged in a beta-trefoil fold common to other homologous serine protease inhibitors in this family like soybean trypsin inhibitor, Erythrina caffra trypsin inhibitor, proteinase K inhibitor from wheat germ and also winged bean albumin belonging to the same family, as well as to some non-homologous functionally unrelated proteins like Interleukin-1alpha, Interleukin-1beta, Human fibroblast growth factor, Abrin-a sugar complex, Interleukin-1 receptor antagonist and Amaranthin. This protein has the unique property of inhibiting bovine alpha-chymotrypsin in the molar ratio 1:2 at higher concentrations of the enzyme indicating that the inhibitor has two reactive sites. The conformation of the protruding reactive site loop in the structure is stabilized through hydrogen bonds mainly formed by the side-chain of Asn 14, which intrudes inside the cavity of the reactive site loop, with the side-chain and main-chain atoms of some residues in the loop region. The structural results have been used to understand the mechanism of inhibition against chymotrypsin at the molecular level. Analysis of the structure also led to the location of the second reactive site, a unique feature of the protein. The latter was identified mainly on the basis of a best fit structural study of the available canonical conformation of the serine protease inhibitor reactive sites. X-ray structures of the recombinant and two mutant forms of the inhibitor protein have also been determined in our laboratory.

13P22

THE CRYSTAL STRUCTURE OF THE OPEN-FORM *E. COLI* TYROSINE AMINOTRANSFERASE BOUND WITH A COFACTOR PYRIDOXAL 5'-PHOSPHATE

T.P. Ko, W.Z. Yang and H.S. Yuan, Institute of Molecular Biology, Academia Sinica, Taipei, Taiwan, ROC

Tyrosine aminotransferase catalyzes the transamination for both dicarboxylic and aromatic amino acid substrates. The crystal structure of the substrate-free *E. coli* tyrosine aminotransferase (eTAT) bound with a cofactor pyridoxal 5'-phosphate (PLP) has been determined at 3.5 Å resolution. Its overall folding resembles those of aspartate aminotransferases with two identical subunits forming a dimer that each monomer binds a PLP molecule via a covalent bond linked to the $_{\varepsilon}$-NH_2 group of Lys258. Comparison of the structure of eTAT with those of open, half-open or closed form of chicken or *E. coli* aspartate aminotransferases shows that eTAT structure is similar to the one in the open conformation. In the active site of eTAT, the side chain of Arg292* appears to associate with the nearby Asp15 and Glu141, rendering a larger space sufficient for accommodating the aromatic substrates.

13P23

TIME RESOLVED STRUCTURAL ANALYSIS FOR SOLID-STATE POLYMERIZATION OF DIACETYLENE DERIVATIVES

T.Maruo, E.Mochizuki, N.Kanehisa and Y.Kai (Dept. of Materials Chemistry, Graduated School of Engineering, Osaka Univ.)

It is well known that diacetylene derivatives undergo solid-state polymerization upon heating, irradiation or mechanical stimulation, and give single crystals of conjugated polymer. With respect to 1,6-di(*N*-carbazolyl)-2,4-hexadiyne(DCHD), Enkelmann *et al.* reported in 1977 that DCHD monomer crystals can be topochemically polymerized by heat treatment or γ-irradiation. They analyzed the crystal structures of monomer and polymers by X-ray [1].

We have investigated the correlation between monomer arrangement and polymerization process by time resolved X-ray structural analysis. The experiment was carried out by UV irradiation with a high pressure mercury lamp and analyzed by the use of newly developed imaging-plate Weissenberg camera (Rigaku RAXIS-CS). DCHD can be polymerized quantitatively by UV irradiation.

We have examined the process of polymerization by diffraction image data and residual electron density map. According to these data, lattice parameters change abruptly depending on conversion and a phase change is observed. Intemediate diffraction images indicated the mixed regions that consist of a solid solution of monomer and polymer molecule. During the polymerization, a shape of the long prismatic crystal changed according to the microscopic changes of the unit cell parameters.

1) V.Enkelmann, et al .,*Chemical Physics Letters* , 1977, **52**, 314.

13P24

INTEGRATED DIRECT METHODS WITH ANOMALOUS SCATTERING AND ISOMORPHOUS REPLACEMENT METHOD-JOINT AND CONDITIONAL PROBABILITY DISTRIBUTIONS OF THE TRIPLET, QUARTET AND SEXTET IN THEIR FIRST NEIGHBOURHOOD

D.Velmurugan and S.Banumathi
Department of Crystallography and Biophysics,
University of Madras.

In the past fifteen years, the combination of traditional direct methods with anomalous scattering /isomorphous replacement techniques has been extensively studied to improve the methods for phase determination of macromolecular structures. The results on the applications with error free data of macromolecules clearly indicated the usefulness of these integrated direct methods. Having encouraged by the results of these methods we have derived the joint and conditional probability distributions for the three phase, four phase and six phase structure invariants when Anomalous Scattering and Isomorphous Replacement data are available. In the derivations only the first neighbourhood of these invariants are considered. The crystal structure is assumed to be fixed and the reciprocal lattice vectors are assumed to be the random variables. The joint and the conditional probability distributions have been derived for the above invariants. Details of these formulae will be presented.

13P25

LIGAND BINDING BY AND STABILITY OF GENETIC VARIANTS OF BOVINE β-LACTOGLOBULIN

B.Y. Qin, Massey University
L. K. Creamer, New Zealand Dairy Research Institute
E. N. Baker, University of Auckland
G. B. Jameson, Massey University

Bovine β-lactoglobulin (BLG) is a 162-amino acid protein that is a major protein component of skim milk from cows. BLG is a member of the lipocalin family BLG and has been reported to bind a variety of mostly hydrophobic ligands. However, the site of ligand binding has not been unequivocally identified; recent reports proposed that fatty acids bind externally rather than inside the calyx formed by the 8-stranded β-barrel. We report here the structure, at 2.23 Å resolution, of a BLG-ligand complex in which 12-bromododecanoic acid is observed to bind inside the calyx.

Bovine BLG occurs in several genetic variants that have different physical and chemical properties, especially susceptibility to thermal denaturation. Variant A differs from variant B at two sites (V118A and D64G), respectively. The structures of these variants at 2.24 Å resolution reveal that minimal rearrangement of main chain and side chains occurs in the vicinity of residue 118 as a consequence of the mutation. The structural basis of the decreased thermal stability of variant B is attributed to the poorer hydrophobic packing of a partially buried Ala118 side-chain of variant B compared to the Val118 side-chain of variant A.

Functional implications of these results will be discussed

13P26

NOVEL PLASTOCYANIN WITH π-π STACKING INTERACTION AS THE KEY FACTOR FOR ACIDIC ENDURANCE.

T. Inoue[a], T. Kohzuma[c], F. Yoshizaki[b], M. Gotowda[a] and Y. Kai[a]
[a] Dept. of Materials Chemistry, Graduated School of Osaka University,
[b] Dept. of Chemistry, Faculty of Science, Ibaraki University,
[c] Dept. of Biology, Faculty of Science, Toho University.

Plastocyanin is widely distributed in the photosystems from cyanobacteria to higher plants as an essential electron-transfer protein from Photosystem II to Photosystem I. The protein has an eight-stranded β-barrel structure and a copper atom. It locates 6 Å beneath the protein surface and has four ligand residues; two histidines, a cysteine, and a methionine. In general, the ligating nitrogen of His87 accepts protonation through the reduction process and moves away from the copper atom at pH below 5.1. However, the plastocyanin from a fern plant, *Dryopteris crassirhizoma*, is recently proved to have several-fold oxidation reactivity for $[Fe(CN)_6]^{3-}$ even at low pH, which is quite rare case in other plastocyanins. The X-ray structure of the *Dryopteris* plastocyanin has been analyzed at 1.7 Å resolution. The most remarkable structural feature is a novel π-π stacking interaction adjacent to ligand His90 (Fig. 1, corresponding to His87 in higher plants). The π-π interaction is proved to be a main cause of unusual pH-dependence. We discuss the correlation between the structure and the unique properties of the fern plastocyanin.

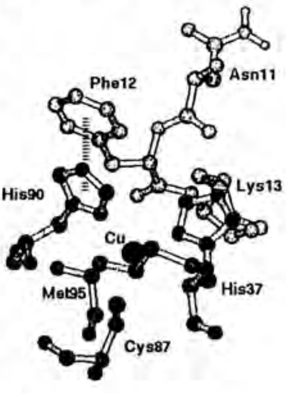

Fig.1 π-π stacking interaction

13P27

INTEGRATED DIRECT METHODS FOR MACROMOLCULAR PHASING

S. Parthasarthy and D. Velmurugan
Department of Crystallography aqng Biophysica,
University of Madras

The literature is flooded with contributions to handle phase problem in macromolecular crystallography. The improved results of the integrated direct methods where the traditional direct methods with Anomalous Scattering or Isomorphous Replacement or both on applications with error free data of macromolecules interested us to develop more formulae for higher invariants with higher neighbourhoods. In phase with this interest the joint probability distribution and conditional probability distribution functions have been derived for Triplets (second neighbourhood) with Anomalous Scattering, Triplets (second neighbourhood) with both Isomorphous Replacement and Anomalous Scattering, Quartets (second neighbourhood) with Anomalous Scattering, Quintets (second neighbourhood) with Isomorphous Replacement. This effort is in the making of generalisation process for any invariants with any neighbourhood. In all the derivations the crystal structure is considered fixed treating only the reciprocal lattice vectors as random variables. The joint probability distribution and conditional probability distribution functions of all the invariants of each one of the above derivations will be presented.

13P28

COMPUTER MODELLING OF INTERACTIONS OF α-APA WITH HIV-1 REVERSE TRANSCRIPTASE AND ITS DRUG-RESISTANT VARIANTS

V.K. Ganesh and D.Velmurugan
Department of Crystallography and Biophysics
University of Madras.

Targeting HIV-1 Reverse Transcriptase is one of the ways of developing anti-viral drugs against Human Immunodeficiency virus 1 which causes AIDS. The advantage of targeting Reverse Transcriptase (RT) is that the RT is essential for HIV replication but is not essential in normal functions of host cells. Other than few HIV protease inhibitors, HIV-1 RT inhibitors approved for therapy are Nucleoside analogs that bind at the substrate-binding site. Non-Nucleoside Reverse Transcriptase inhibitors (NNRTI) bind at a site located approximately 10Å from the substrate binding site. HIV-1 is genetically very flexible and several drug resistant variants emerge upon drug therapy using NNRTI's. α-Anilino phenyl acetamide (α-APA) is one of the potent NNRTI. Tyr181Cys mutant is common against most of the NNRTI's including α-APA. Val106Ala variant also emerge when treated with α-APA. The aim of the present work is to perform modelling studies using Molecular Mechanics (MM) on complexes of α-APA with wild type, Tyr181Cys and Val106Ala mutants to understand the structural aspects of drug resistance, which will be very useful in designing drugs that could be potent against both wild type and drug resistant variants. The results of the work will be presented.

13P29

HIGHER RESOLUTION STRUCTURE OF A DNA DODECAMER OF d(CGCGmo^{6}AATCCGCG) CONTAINING N^6-METHOXY-ADENOSINE

T. Chatake[a], A. Ono[b], Y. Ueno[c], A. Matsuda[c], and A. Takenaka[a]
[a]*Faculty of Bioscience and Biotechnology, Tokyo Institute of Technology,* [b]*Department of Chemistry, Graduate School of Science, Tokyo Metropolitan University* and [c]*Department of Medicinal Chemistry, Graduate School of Pharmaceutical Sciences, Hokkaido University*

Oxylamines such as hydroxylamine and methoxylamine are known as a mutagen which attacks amino groups of DNA bases. In order to investigate effects of such modification on base pairing, a DNA dodecamer of d(CGCGmo^{6}AATCCGCG) containing N^6-methoxyadenosine has been crytallized, and the structure has been determined at 110K by x-ray analysis. The DNA dodecamers form a double helix with B-form conformation and get in contact with other duplexes related by a 2_1 symmetry along the c-axis at the both ends by forming two extra base pairings with two N(2)-H---N(3) hydrogen bonds between guanine moieties. This packing motif is similar to that reported for d(CGCGAATTCGCG)$_2$ crystal (Dickerson *et al.*, 1981). The final electron density maps clearly indicate that the methoxyl groups of the two modified adenine bases in the duplex have a similar anti-conformation around the C(6)-N(6) bond against N(3) atom and that the adenine base forms a base pair with cytosine base on the counter chain in a manner just like a Watson-Crick type adenine:thymine pairing. To form this type of hydrogen bonds, the modified adenine base must take an imino form. The present result exhibits the real gene transition mechanism, by which not only the complementary thymidine but also cytidine residues were incorporated into the newly synthesized opposite DNA strand in duplication when this modified adenosine was introduced to the template DNA (Nishio *et al.*, 1992).

References

Dickerson, R. E. & Drew, H. R. (1981) *J. Mol. Biol.* **149**, 761-786.
Nishio, H., Ono, A., Matsuda, A. & Ueda, T. (1992) *Nucleic Acids Res.* **20**, 777-782.

WELL, HOW DO CRYSTAL PACKING EFFECTS INFLUENCE MOLECULAR GEOMETRY IN ORGANOTIN SYSTEMS?

E.R.T. Tiekink, The University of Adelaide

A fascinating aspect of the structural chemistry of main group element compounds is the observation of remarkable structural variation even when there are only small changes in remote organic substituents. Thus, several bibliographic reviews of key systems have shown that different coordination geometries and even coordination numbers may be found (*e.g.* Tiekink, 1992, 1994; Silvestru, Haiduc, 1996; Cox & Tiekink, 1997). While it is possible that electronic effects as well as steric profiles of the ligands may play a role in determining molecular structure, it is of interest to ascertain the role of intermolecular forces, *i.e.* crystal packing effects, on molecular geometry. Accordingly, we have embarked on a combined crystallographic/theoretical investigation on selected organotin systems with the aim of comparing experimental (*i.e.* crystallographic) and gas phase (*i.e.* theoretical) structures (*e.g.* Buntine, Hall, Kosovel, Tiekink, 1998). Such a study will enable a comparison of molecular geometries in the presence and absence of crystal packing effects. This presentation will highlight some of the key results obtained thus far. These clearly indicate that crystal packing effects may indeed play a significant role in influencing molecular geometry in the systems investigated.

Buntine, M.A., Hall, V.J., Kosovel, F.J. & Tiekink, E.R.T. (1998). *J. Phys. Chem. A*, **102**, 2472-2482.
Cox, M.J. & Tiekink, E.R.T. (1997). *Rev. Inorg. Chem.* **17**, 1-23.
Silvestru, C. & Haiduc, I. (1996). *Coord. Chem. Rev.* **147**, 117-146.
Tiekink, E.R.T. (1992). *Main Group Met. Chem.* **15**, 161-186.
Tiekink, E.R.T. (1994). *Trends in Organomet. Chem.* **1**, 71-116.

13P31

THE SYNTHESIS AND DEVELOPMENT OF METAL-ION ACTIVATED MOLECULAR RECEPTOR MOLECULES

S. F. Lincoln[a], C. B. Smith[b], M.R. Taylor[b], K. P. Wainwright[b] and K. S. Wallwork[b].

[a] Chemistry Department, The University of Adelaide, Adelaide, 5005.
[b] Chemistry Department, The Flinders University of South Australia,
GPO Box 2100, Adelaide, 5001

1,4,7,10-Tetrakis((S)-2-hydroxy-3-phenoxypropyl)-1,4,7,10-tetraazacyclododecane (S-thphpc12) was synthesised by the reaction of cyclen with the enantiomerically pure epoxide as seen below. This protocol has been used successfully in the past for the formation of the analogous ligands R-thpec12 and S-thpc12.[1,2] Complexation with eight coordinate metal ions such as Pb^{2+} and Cd^{2+} is expected to give rise to binary complexes where the aromatic moieties delineate a molecular basket similar to that of the calixarenes.[3] The binding of neutral or anionic guest molecules within the cavity to form ternary inclusion complexes is currently under investigation.

The crystal structures of two of these complexes have been determined. Both crystallise in space group P1, one with $Z=2$ and the other with $Z=1$. The latter has a guest tosylate ion bound in the cavity. Details of these molecules will be presented

1 Whitbread, S.L; Valente, P; Buntine, M.A; Clements, P; Lincoln, S.F; Wainwright, K.P; J.Am.Chem.Soc., in press.
2 Dhillon, R.S; Madbak, S.E; Ciccone, F.G; Buntine, M.A; Lincoln, S.F; Wainwright, K.P. J.Am.Chem.Soc. 1997, 119, 6126-6134.
3 Gutsche, D.B; Dhawan, B; No, K.H; Muthukrishnan, R. J.Am.Chem.Soc. 1981, 103, 3782-3792.

CRYSTAL AND MOLECULAR STRUCTURE OF "BIS[DIAQUA (1H-CYCLOPENTA(2,1-b:3,4-b') (DIPYRIDINE -2,5-DIONE) NICKEL(II)] MONOHYDRATE

G.Y.S.K. Swamy and K. Ravikumar,
Laboratory of Crystallography, Indian Institute of Chemical Technology, Hyderabad 500 007, India

The crystal and molecular structure of the title complex has been determined using single crystal X-ray diffractometer. The complex crystallizes in the space group P-1 with a=10.452(1), b=14.098(1), c=16.023(2)Å, α=110.13(1), β=100.63(1), γ=100.85(1)°, Z=4, Mr=1002.1. The structure has been solved by Patterson and subsequent Fourier synthesis. Anisotropic refinement of 1680 observed reflections led to R=0.051.

The ligand 1H-Cyclopenta-(2,1-b:3,4-b')dipyridine -2,5-dione, [whose synthesis and its anionic structure was reported (1)] for which no metal complex has been reported so far. The structure consists of discrete neutral units of the title complex together with uncoordinated water molecules. The asymmetric unit contains two crystallgraphycally independent molecules related by a pseudo two fold symmetry. The two bidentate ligands have a cis disposition around the metal ion forming almost perpendicular planes (N1C-Ni-N2D 94.5(6)°; N2C-Ni-N2D 175.2(6)°[for molecule2 , 91.9(5) & 172.1(6)° respectively]. The rigidity of these ligands causes the bite angles N1D-Ni-N2D 83.4(5), N1C-Ni-N2C 82.1(6)° respectively[83.6(5), 81.7(5)° for molecule2] to deviate significantly from orthogonality. This causes the geometry about the Ni(II) atom to deviate considerably from that of an ideal octahedron. The structural results has been compared with other spectral studies like UV, IR etc., Additional features of the structure will be presented.

1. Baxter,P.N.W, Connor,J.A., Wallis,J.D., Povey,D.C. and Powell,A.K. (1992). J.Chem.Soc.Perkin Trans.1. pp.1601-1605.

13P33

SEVEN CRYSTAL STRUCTURES AND CONFORMATIONS OF DRUG INTERMEDIATES OF DILTIAZEM

K.A.Nirmala, P.Kumaradhas and N.Kalyanam* ; Department of Physics, Bangalore University, Bangalore-50 056, India., *SPIC Pharmaceutical Division, R&D Centre, Maraimalai Nagar-603 209, India.

Diltiazem is an enantiomerically pure drug useful for the treatment of cardiac and coronary diseases. In order to design a pharmacologically highly potent compound a series of diltiazem drug intermediate compounds were synthesised and studied its X-ray structures. X-ray structure and molecular conformations of seven drug intermediates has been studied.

The conformational studies reveals that 1,5-benzothiazepine ring shows twist boat conformation, the benzene ring is planar and the methoxyphenyl group is significantly deviated from planarity in all the structures. The molecular structures are stabilized by hydrogen bonding. The result of this comparisons highlights the conformational changes of the molecules is mainly depend on the substituents and its orientations will be discussed.

13P34

CRYSTAL STRUCTURE ANALYSIS OF 4-PHENYL 5-CHLOROPHENYL 1,2,4-TRIAZOLE-3-THIONE

K.Puviarasan and D. Velmurugan, Department of Crystallography and Biophysics, University of Madras, and S. Shanmuga Sundara Raj and H. K. Fun, School of Physics, Universiti Sains Malaysia.

1,2,4-Triazoles and N bridged heterocycles derived from them are found to be associated with diverse pharmacological activity. Recently some new triazole derivatives have been synthesized as possible anti-convulsants, antidepressants, tranquilizers and plant growth regulators. The 1,2,4-triazole nucleus has recently been incorporated into a wide variety of therapeutically interesting drugs including H1/H2 histamine receptor blockers, choline sterase active agents, CNS stimulants, anti-anxiety agents and sedatives. Crystallographic studies of the titled compound triazole thione was carried out to determine the conformational features.

Crystal data: Molecular formula: $C_{14}H_{11}N_3ClS$, a = 6.968(1), b = 9.523(2) and c = 11.098(3)Å, $\alpha = 97.56(1)°$, $\beta = 104.30(1)°$ and $\gamma = 95.40(1)°$; Triclinic, $P\bar{1}$, $V = 701.20(3)Å^3$, Z = 2 and R = 5.8%.

The dihedral angle between the least square planes passing through the triazole ring and the phenyl ring is 58.9(1)°. The dihedral angle between the least square planes passing through the phenyl rings is 63.7(1)°. Detailed conformational features will be presented.

Program used: Structure solution: SHELXS86, Refinement: SHELXL93.

13P35

CRYSTAL AND MOLECULAR STRUCTURE DETERMINATION OF 2,4 - (BIS) 0-TOLYL-3-METHYL-3-AZABICYCLO (3.3.1) NONAN - 9 - ONE

L. Vijayalakshmi, V. Parthasarathi, R. Jayaraman and M. Venkatraj, Department of Physics and Chemistry, Bharathidasan University, Tiruchirapalli, INDIA.

Many derivatives of 3 - aza bicyclononanes are found to possess medicinal and biological activities. In order to study the conformation, X-ray diffraction study of the title compound was taken up. The compound crystallizes in the mooclinic space group $P2_1/a$ with Z = 4; Crystal data : a = 7.692(3) Å; b = 16.825(3)Å; c = 13.725(2)Å; β = 99.43(2)°; V = 1752.1(8)$Å^3$; F_{000} = 688; D_{cal} = 1.211 Mg / m^3.

The bicyclo (3.3.1) nonane ring system offers a wide range of conformational flexibilities owing to their existence in chair - chair, chair - boat and boat - boat conformations. Among them only the chair - chair conformation has been found to be the most favourable one. In the present studies, the bicyclic ring system adopts chair - chair conformations as evident by means of the torsion angles, C9-C1-C8-C7 = 54.0(3)°; C1-C8-C7-C6= -45.0(3)°; C8-C7-C6-C5 = 44.0(3)° : C7- C6-C5-C9 = -52.2(3)°; C6-C5-C9-C1= 63.3(3)°; C5-C9-C1-C8 = - 64.1(3)°; C4-N3-C2-C1 = 58.3(3)°; N3-C2-C1-C9 = -56.9(3)°; C2-C-C9-C5 = 60.8(3)°; C1-C9-C5-C4 = - 61.8(3)°; C5-C4-N3-C2 = - 58.4(2)°; C5-C4-N3- C2 = -58.9(3)°. Within the Cyclohexane ring the atoms C7 and C9 deviate from the C8 - C1 - C5 - C6 plane by - 0.537(4)Å and 0.720(3)Å, respectively. Thus there is deviation from ideal chair conformation. This deviation can also be seen in terms of the variation in bond lengths and angles of the cyclohexane ring (1.500(3) - 1.544(4)Å; 107.7(2)°- 114.4 (2)°). The phenyl rings are equatorially disposed with respect to the bicyclic ring. The torsion angles C6 - C5 - C4 - C16 = 61.6(4)°; C10 - C2 - C1 - C8 = - 60.8 (3)°. They are oriented at an angle of 29.4 (1)° to each other. The orientation of the methyl groups of the aromatic ring cause steric hindrance for the approach of the reducing agent from the side of the piperidine ring thus producing the endo alcohol predominantly.

1.Brown, W.A.C; Martin J. and Sim, G.A. (1965), J. Chem. Soc. (B), 1844 - 1857.

2. Webb, N.C. and Becker, M.R. (1967), J.Chem.Soc. (B), 1317 - 1321.

3. Bhattacharjee, S.K. and Chacko, K.K. (1979), Tetrahedron, Vol 35, 1999 - 2007.

13P36

CONFORMATIONAL ASPECTS OF SOME PIPERIDINONE DERIVATIVES

M.N.Ponnuswamy and D.Kumaran, Department of Crystallography and Biophysics, University of Madras, Guindy Campus, Chennai – 600 025, India.

The piperidine derivatives are found to be pharmacologically important but their N-nitroso derivatives are found to be carcinogens in nature. Though the unsubstituted N-nitrosopiperidines are potential carcinogens, the carcinogenicity is found to reduce when an alkyl group is substituted at the α-position(C2). Further if α-positions (C2 and C4) are substituted by methyl groups, it becomes non-carcinogens. It appears that blocking of the α-positions to the ring nitrogen atom by methyl groups in cyclic nitrosamines is responsible for reducing the carcinogenic acitiviy.

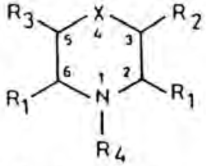

It has also been observed that the increase in bulkiness of the substituents at different positions of piperidine ring leads to the decrease in carcinogenicity. To correlate the structure with activity, a series of piperidinone derivatives have been synthesized and their conformations are derived by crystallographic methods. In N-alkyl and N-free piperidine derivatives, the piperidine ring adopts chair conformation but in N-electron withdrawing piperidine derivatives, it adopts boat conformation. The detailed conformational aspects including the energy concepts have been presented.

13P37

CRYSTAL STRUCTURE AND CONFORMATION OF THE DIPEPTIDE tboc- Aib-Ile-OMe.

M.Nilofarnissa, D.Velmurugan, Dept. of Crystallography and Biophysics,University of Madras, Chennai - 600 025, INDIA and N.Ramasubbu, Dept. of Oral Path.Biol. Diag. Sci., Newark, NJ 07103.

The wide occurrence of alpha aminoisobutyric acid (Aib) in microbial peptides, particularly in the peptaibol antibiotics has long been attributed to its role in constraining the peptide backbone, because of the two methyl substituents on the C-α atom. As a part of our continuing studies on the relationship of sequences to folding preferences of short peptides, we have synthesised and crystallized tboc-Aib-Ile-OMe, in order to understand the restriction posed by the Aib residue on peptide conformations.Crystal Data: Triclinic, space group P1, a = 9.570(9), b = 10.261(7) and c =10.610(2) Å, α =101.90, β =91.70 and γ =98.60°, V=1006.05 Å^3 and Z=2. The structure was solved by direct methods and refined to an R factor of 0.074. The backbone conformational angles for the Aib residue in molecule A, are in the left handed helical conformation while in molecule B, they are in the right handed conformation. The Ile residue in molecule A is in the folded conformation while in molecule B, it is in extended conformation. The peptide units show deviations from planarity by 14.9° in molecule A and 1.25° in molecule B.

13P38

CRYSTAL STRUCTURE OF TWO CARBAZOLE DERIVATIVES

L.Govindasamy, D.Velmurugan, Department of Crystallography and Biophysics, University of Madras, Guindy Campus, Madras – 600 025, India.

DNA intercalating property is considered as one of the potent factors for DNA binding drugs. Carbazole analogs are well known DNA intercalating agents. Carbazole compounds have pronounced biological activity due to the presence of oxygenated substituents. Benzo- and pyrrido annellated carbazoles have potential anti-tumour, anti-bacterial and anti-yeast activites.

Crystal data (I): $C_{21}H_{19}NO_5S$, Monoclinic space group I2/c, $a = 20.498(2)$, $b = 9.258(2)$, $c = 21.866(3)Å$; $\beta=116.45(1)°$, $V = 3715.2(10)Å^3$, $Z = 8$, $\lambda = 1.5418$ Å, $D_c = 1.21 Mg/m^3$.

Crystal Data (II): $C_{17}H_{13}NO_3S_2$, Triclinic, $P\bar{1}$, $a = 7.887(6)$, $b = 9.210(6)$, $c = 11.280(5)$ Å, $\alpha = 106.47(5)$ $\beta = 75.72(6)$, $\gamma = 101.57(4)°$, $V = 753.9(8)$ Å^3, $Z = 2$, $\lambda = 1.5418$ Å and $D_c = 1.513$ Mg/m^3. Both structures have been solved and refined by Direct Methods program SHELX-97 to the final R-value of 0.05 and 0.06 respectively. The sulphur atom in the phenylsulfonyl group is in distorted tetrahedral configuration. The nitrogen atom in the indole moiety exhibits a pyramidal character. The conformational details will be presented.

13P39

CRYSTAL AND MOLECULAR STRUCTURE OF AN ACRIDINEDIONE

M.S.Kumar[1], D.Kumaran[1], M.N.Ponnuswamy[1], P.Murugan[2] and V.T.Ramakrishnan[2], [1]Department of Crystallography and Biophysics, [2]Department of Organic Chemistry, University of Madras, Guindy Campus, Chennai-600 025, India

The biological activity of acridine derivatives is often manifest in their mutagenic properties. These have been attributed, at least in part to interactions with nucleic acids, particularly DNA. The hypothesis is that the planar chromophore common to the acridines involve in stacking interactions with the pyrimidine-purine base pairs. This objective has received support from a large body of physical and biological data. The crystal structure of an acridinone derivative synthesized by a novel method with chlorine and fluorine substituents has been reported. This study reveals the electronic effect of chloro and fluoro substitution on the acridinone ring system geometry and the stacking properties of the planar chromophores.

Pale yellow crystals were obtained by slow evaporation of ethanolic solution. Crystal data: a = 9.643(4), b = 15.884(4), c = 11.843(3)Å, β = 103.72(2)° . The structure was solved by direct methods with SHELXS86 and refined by full-matrix least-squares procedures to a final R of 0.05. The C-F distance differs significantly from the normal value. The central ring of the acridinedione moiety deviates from planarity. The molecules are stabilized by weak C-H...O interactions in addition to the van der Waals forces.

13P40

CRYSTAL AND MOLECULAR STRUCTURES OF PIPERAZINE DERIVATIVES

M. S. Kumar[1], D. Kumaran[1], M. N. Ponnuswamy[1], K. Chinnakali[2] and H. K. Fun[2], [1]Department of Crystallography and Biophysics, University of Madras, Guindy Campus, Chennai - 600 025, India. [2]School of Physics, Universiti Sains Malaysia, Penang, Malaysia.

The piperazine salts are very active against roundworm and pinworm infections in both humans and animals. These drugs are absorbed from the gastrointestinal tract, giving adverse effects involving both gastrointestinal and CNS side effects including nausea and vomitting, headache, muscle weakness and convulsions. In order to understand the mechanism and possibly suggest the alternate solutions, some of the piperazine compounds are synthesized and their structures are derived by crystallographic methods.

The following compounds (i) 1,4-Dinitroso 2,3,5-triphenyl 6-isopropyl piperazine and (ii) 1,4-Diacetyl 2,3-diphenyl piperazine are crystallized in alcoholic medium by slow evaporation method. The structures were solved by direct methods and refined by full-matrix least-squares procedures. In both the compounds, the piperazine ring adopts distorted boat conformation. The molecules are stabilized by N-H...O and C-H...N type of interactions in addition to van der Waals forces.

13P41

SOLID-STATE PHOTOISOMERIZATION OF COBALOXIME COMPLEXES WITH A BULKY SUBSTITUENT IN THE EQUATORIAL LIGANDS

G.Iketani, A.Sekine, H.Uekusa, and Y.Ohashi
Department of Chemistry, Tokyo Institute of Technology

It was found that the 2-cyanoethyl group bonded to cobalt atom in some cobaloxime complexes was isomerized to the 1-cyanoethyl group on exposure to visible light in the solid state. The configuration of the produced 1-cyanoethyl was strongly influenced by the structure around the 2-cyanoethyl group in the reactant crystal. In order to control the asymmetric induction, a bulky substituent, a diphenyl boron group, was introduced in the equatorial ligands as a wall to limit the motion of the 2-cyanoethyl group. Three crystals with two different axial base ligands, pyridine (**1** and **2**) and 1-cyclohexylethylamine (**3**) were prepared. The structures were analyzed by X-rays. The crystal data are shown in Table 1 and the molecular structure of **1** is shown in Fig. 1. Although the comparison of the solid state photoisomerizations among the three crystals is now in progress, the bulky substituent clearly effects on the configuration of the product.

Table 1. Crystal Data

	1	**2**	**3**
	$P2_1/c$	$P\bar{1}$	$P2_1$
a/Å	9.4117(1)	9.1591(6)	10.3559(2)
b/Å	21.3849(3)	10.9104(7)	13.1227(2)
c/Å	16.3373(2)	15.328(1)	13.7012(3)
α/°	-	102.305(1)	-
β/°	96.814(1)	100.066(2)	99.098(1)
γ/°	-	103.686(2)	-
V/Å^3	3264.95(7)	1412.5(2)	1838.53(6)
Z	4	2	2

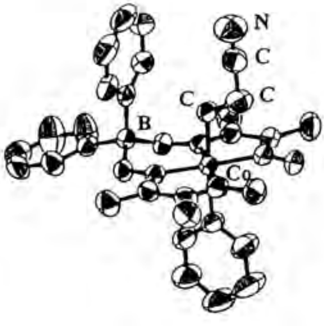

Fig. 1

13P42

RACEMIZATION PROCESS OF CHIRAL COBALOXIME COMPLEXES BY PHOTOIRRADIATION

H.Sato, and Y.Ohashi ; Tokyo Institute of Technology

It has been reported that the chiral alkyl group bonded to the cobalt atom in cobaloxime complexes is racemized retaining the single crystal form on exposure to visible light. Not only a small 1-cyanoethyl group but also a bulky 1,2-bis(allyloxycarbonyl)ethyl group have been found to be racemized. The two mechanisms were proposed on the racemization, the radical rotation and the olefin formation. The cobaloxime complexes synthesized so far always have a methylene chain or a methyl group adjacent to the chiral carbon atom, so that both of the mechanisms are acceptable since a methylene or methyl group adjacent to the chiral carbon is essential for the olefin mechanism.

In order to determine which mechanism is valid, the cobaloxime complex with (*R*)-chlorocyanoethyl group with (*R*)-1-phenylethylamine as an axial base ligand was prepared. This compound has neither methylene nor methyl group adjacent to the chiral carbon atom. The crystals were ground to powder, and they were exposed to visible light and the *R*/*S* ratio of the alkyl group was analyzed using HPLC. The diastereomer excess was significantly decreased after irradiation. This suggests that the olefin formation is not necessary for the racemization and the inversion of the radical should occur in the racemization. The analysis of the relationship between the reaction rate and the structure is in progress.

13P43

EFFECT OF SIDE CHAIN LENGTH ON MOLECULAR ASSEMBLY MODES OF CHOLIC ACID DERIVATIVES

M. Sugahara, K. Sada, and M. Miyata, Material and Life Science, Graduate School of Engineerring, Osaka University, Yamadaoka, Suita, Osaka 565-0871, Japan, Tel : +81-6-879-7406, Fax : +81-6-879-7404

We present here molecular assembly modes of four 23-nor-bile acids(norcholic acid, nordeoxycholic acid, norchenodeoxycholic acid and norlithocholic acid, Fig. 1). The acids have shortened side chains by one methylene group from normal bile acids.They formed inclusion crystals with a variety of organic substance, such as alcohols, ketones, esters, nitriles and so on. X-ray crystallographic studies revealed that all the nor-bile acids had quite similar assembly modes with various guest molecules. For example, in case of acetone as the guest, these hosts form the molecular assembly shown in Fig. 2. This contrasts with those of the normal bile acids.

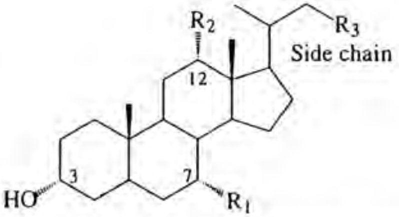

Fig. 1 Molecular structures of cholic acid (R_3=CH_2COOH), norcholic acid (R_3=COOH), and their derivatives:

Cholicacid	; R_1 and R_2=OH,
Deoxycholic acid	; R_1=H, R_2=OH,
Chenodeoxycholic acid	; R_1=OH, R_2=H,
Lithocholic acid	; R_1 and R_2=H.

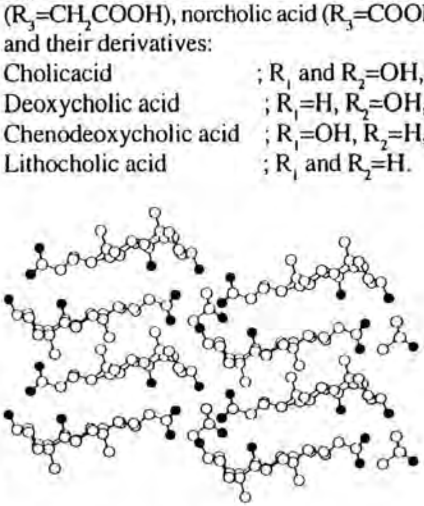

Fig. 2 Crystal structure of inclusion compound from norchenodeoxycholic acid with acetone.

13P44

CRYSTAL STRUCTURE OF ω-[4-(4-METHOXYPHENOXYCARBONYL)PHENOXYCARBONYL]ETHYL 4-FERROCENYLBENZOATE

N.Nakamura and S.Setodoi, Department of Chemistry, Faculty of Science and Engineering, Ritsumeikan University, 1-1-1, Nojihigashi, Kusatsu, Shiga 525-8577, Japan

The structure of a monosubstituted ferrocene derivative, $C_{34}H_{28}O_7Fe$, was determined by the X-ray diffraction method.
The single crystal of the title compound was obtained from a solution with a mixed solvent of benzene and methanol (1 : 5) by the slow evaporation method. All measurements were made on a Rigaku AFC-5R diffractometer with graphite monochromatized Cu-Kα radiation (λ=1.54178Å). The crystals belong to monoclinic crystal system, space group $P2_1/a$, a=8.085(4)Å, b=10.235(6)Å, c=34.257(7)Å and β=92.57(3)°. All calculations were performed using the teXsan crystallographic software package. The structure was solved by direct methods (SIR92) and expanded using the Fourier technique. All non-hydrogen atoms were refined anisotropically and the hydrogen atoms were introduced at their theoretical positions and allowed to ride with the carbon atoms to which they are attached. The final refinement was made by full-matrix least-squares based on 2784 observed reflections ($I>3.0\sigma(I)$). The refinement was concluded with final reliability factors $R = 0.049$, $R_W= 0.062$.
The molecular geometry is a rod-like feature and two cyclopentadienyl rings exhibit an eclipsed conformation rather than a staggered one. The molecules are arranged in layers which is similar to that of a smectic phase of the liquid crystals.

13P45

SOLID STATE PHOTORACEMIZATION OF COBALOXIMES IN HOST-GUEST COMPLEXES

N.Sugimoto, H.Uekusa, A.Sekine, and Y.Ohashi,
Department of Chemistry, Tokyo Institute of Technology

It was found that the chiral 1-cyanoethyl group bonded to the cobalt atom in cobaloxime complexes shows racemization in crystalline state on exposure to visible light. In the solid state reaction, the void space around the reactive group, which is called a cavity, plays an important role for the reaction rate.
In order to examine the reaction rates in various cavity sizes, the complexes of (1-cyanoethyl)(isonicotinic acid)cobaloxime and 5 different secondary amines, shown in Fig.1, were prepared. When the crystals were irradiated with visible light, the racemization of the 1-cyanoethyl group was observed with different reaction rates. The crystal structures were analyzed by X-rays. The cavity size has a good correlation with the reaction rate.

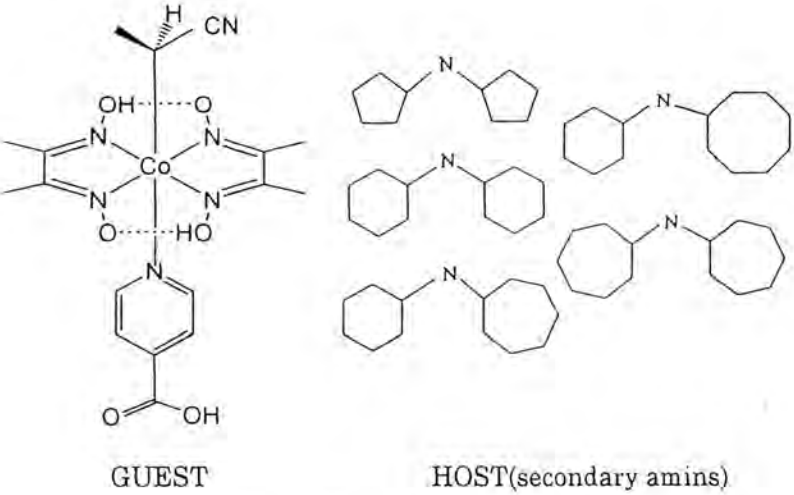

GUEST

HOST(secondary amins)

(Fig.1) Host-Guest complexes

X-RAY ABSORPTION FINE STRUCTURE STUDY IN $FeTiO_3$

R.M.F.Hsu, L. Y. Jang[1], Foo Yin Institute of Technology, Ta-Liao, Kaohsiung Hsien, Taiwan 83101, R.O.C., [1]Synchrotron Radiation Research Centre, Hsinchu, Taiwan 30077, R.O.C.

LING-YUN JANG

X-ray absorption fine structure (XAFS) spectroscopy can provide useful information on short-range interactions, thus is well suited for investigating the local environment around the constituent atoms in compounds. Synchrotron radiation has several advantages over other X-ray sources, and notably large photon intensity, a highly collimated beam, and the wide range of photon energies available. XAFS measurements were performed at the Synchrotron Radiation Research Centre (SRRC) in Taiwan. Hard X-rays in the 4 to 15 KeV range used in this study, were especially suitable for the specification of Fe atom in ilmenite, $FeTiO_3$.

The structural geometry of $FeTiO_3$ is well described in the literatures; a = 5.089 (1) and c = 14.092 (1) A, with space group R3-bar. The sequence Fe-Ti-vacancy-Ti-Fe-vacancy-Fe octahedra along the c-axis is important in determining the magnetic dipoles of antiferromagnetism in ilmenite. The magnetic dipole moment is related to both the cations' displacements and their charges. Displacements of the cations were well studied. The X-ray absorption fine structure XAFS method provides an accurate determination of atomic charges. The absorption spectra suggest that iron is in the trivalent state in ilmenite.

13P47

A REVISED DESCRIPTION OF SOME 'FLUORITE-RELATED' BINARY BISMUTH OXIDE PHASES BASED ON THE CRYSTAL STRUCTURES OF TWO BISMUTH TANTALATES

C.D. Ling, R.L. Withers, S. Schmid and J.G. Thompson, Research School of Chemistry, Australian National University

The high-temperature phase δ-Bi_2O_3 is one of the best oxygen ion conductors known. Although it cannot be quenched to room temperature, bismuth-rich phases in binary oxide systems involving certain transition metal oxides appear to approximately preserve its fluorite-related structure and ionic conduction properties. Two such phases, previously described as having fluorite-related superstructures, are $Bi_7Ta_3O_{18}$ and $Bi_4Ta_2O_{11}$ (1). During an extensive reinvestigation (2), we found the fluorite-related unit cells reported for $Bi_7Ta_3O_{18}$ and $Bi_4Ta_2O_{11}$ to be incorrect. We have now solved the structure of $Bi_7Ta_3O_{18}$using single-crystal X-ray (synchrotron) data (3). A model for the $Bi_4Ta_2O_{11}$ structure was derived and Rietveld-refined using synchrotron XRD and powder neutron diffraction data (4). Both structures are fully ordered, with columns of TaO_6 octahedra and variously coordinated Bi^{3+} ions. Metal atom arrays approximate fluorite-type with regular 'step' defects perpendicular to $[111]_f$. This structural motif is responsible for confusing electron diffraction and XRD patterns which led to their original mis-indexing as fluorite-related superstructures.

Zhou, W. (1992). *J. Solid State Chem.* 101, 1-17

Ling, C.D., Withers, R.L., Schmid, S. and Thompson, J.G. (1998). *J. Solid State Chem.* In press.

Ling, C.D., Schmid, S., Withers, R.L., Thompson, J.G., Ishizawa, N. and Kishimoto, S. (1998). *Acta Cryst.* B Submitted.

Ling, C.D., Thompson, J.G., Withers, R.L. and Schmid, S. (1998). *J. Solid State Chem.* Submitted.

SITE OCCUPANCY OF Ba AND Sm ON THE MICROWAVE DIELECTRIC $Ba_{6-3x}Sm_{8+2x}Ti_{18}O_{54}(x=0.5)$ SOLUTION

H. Ohsato, M. Imaeda, A. Komura and T. Okuda
Nagoya Institute of Technology

The microwave resonators of the $Ba_{6-3x}Sm_{8+2x}Ti_{18}O_{54}$ solid solutions with high dielectric constants have contributed to reduce the size of portable telephones. The fundamental crystal structures (subcell) of $Ba_{6-3x}Sm_{8+2x}Ti_{18}O_{54}$ with x=0.75 and 0.71, and superstructures (doubled c-axis) with x=0.71 and 0.27 were reported by Matveeva *et al.*, Ohsato *et al.* and Rawn *et al.* In this work, we refined the crystal structure of the solid solution with x=0.5 which is located on the central composition and examined the site occupancy of large cations.

The single crystals were synthesized by self-flux method. The intensity data measured by X-ray 4-circle goniometer was refined by RADY program. Crystal data: $Ba_{4.5}Sm_9Ti_{18}O_{54}$ (x=0.5); Structural formula: $[Sm_9Ba_{0.5}V_{0.5}]$ $[Ba_4]Ti_{18}O_{54}$; Orthorhombic system; Space group for the superlattice : *Pbnm* (No.62); a=12.16(4), b=22.363(8), c=7.662(2) Å, V=2083.7 Å^3; Z=2; D_x=5.897g/cm^3; R=4.49%, wR=4.99%.

It was refined as tungstenbronze related structure which has three different large cation sites: 2 by 2 perovskite blocks (A1-site), pentagonal columns (A2-site) and trigonal columns (C-site). The A1-sites were grouped in five different positions in which three positions include Sm ions and vacancies, and two positions Sm and Ba ions. A2-sites include fully Ba ions and C-sites no atoms.

Ref.: M. Imaeda *et al.*, Jpn. J. Appl. Phys., **36**(9B), 6012-6015(1997).

13P49

SINGLE CRYSTAL STUDY OF THE HYDROXYAPATITE TRANSFORMED FROM CHLORAPATITE BY THE SOLID STATE ION EXCHANGE UNDER HYDROTHERMAL CONDITIONS

H. Takase[a], N. Ishizawa[a], I. Sugiura[b], S. Oishi[b], J.C.Rendon-Angeles[c],
K. Yanagisawa[c]

a) Materials and Structures Laboratory, Tokyo Institute of Technology
b) Department of Environmental Science and Technology, Faculty of Engineering, Shinsyu University
c) Research Laboratory of Hydrothermal Chemistry, Kochi University

The solid state ion exchange in apatites has not been well studied despite its importance in various applications such as removal of heavy atoms from waste water, deterioration protection of hard tissues. This paper presents a single crystal X-ray diffraction study on the hydroxyapatite topotactically-transformed from chlorapatite crystal by the solid state ion exchange under hydrothermal conditions. Chlorapatite crystals were grown by the flux method using NaCl flux. The crystals were turned into hydroxyapatite after the hydrothermal treatment under conditions of 773 K and 100 MPa in 5 M KOH solution for 48hours. Crystals retained their original shapes after the hydrothermal treatment though the transparency looks slightly deteriorated. Crystals of the as-grown chlorapatite and as-treated hydroxyapatite were examined by the Weissenberg camera and the four-circle diffractometer. The nonstoichiometry associated with deficiencies of Cl or OH anions in apatite is commonly believed to be responsible for the stabilisation of the hexagonal $P6_3/m$ form instead of the monoclinic $P2_1/b$ form at room temperature. The hexagonal symmetry observed for the chlorapatite in the present study is consistent with the conventional understanding that the Cl-deficiency is easily introduced in the flux-grown chlorapatite. It is interesting on the other hand the hydrothermally-treated crystals were monoclinic. A detailed discussion will be given after the structure determination of both apatites being in progress.

13P50

THERMAL BEHAVIOR OF MODULATION IN Co-ÅKERMANITE AT ELEVATED TEMPERATURES.

K.Kusaka, K.Hagiya, N.Haga and M.Ohmasa, Department of Life Science, Himeji Institute of Technology, and K.Iishi, Department of Mineralogical Science and Geology, Yamaguchi University

The modulated structure of the Co-åkermanite ($Ca_2CoSi_2O_7$) at room temperature was determined based on the five-dimensional description [1]. The wave vectors are expressed as $\mathbf{k}_1=\alpha(\mathbf{a}^*+\mathbf{b}^*)$ and $\mathbf{k}_2=\alpha(-\mathbf{a}^*+\mathbf{b}^*)$, where **a*** and **b*** are the unit vectors of the reciprocal lattice for the tetragonal basic structure. The Co-åkermanite undergoes a phase transition from the incommensurate phase to the high-temperature normal phase at 493K. Recently, Riester and Böhm [2] found a lock-in phase of the Co-åkermanite which is approximately commensurate, stable up to 270K. The phase transition to the low temperature phase is characterized by a prominent hysteresis. Since a thermal behavior of modulation at the temperature range from room temperature to incommensurate-normal phase transition temperature was expected to be informative to elucidate causes of the modulation, the present studies on change of the wave vectors at elevated temperatures have been carried out. Temperature dependence of intensities of satellites and that of modulation wave vectors were examined *in situ* at elevated temperatures. A fragment of the sample synthesized by a floating zone method was mounted in a small gas blow heating system installed on an Enraf-Nonius CAD-4 diffractometer.

The hysteresis was observed at that temperature range. Upon heating from room temperature, the value α of wave vectors decreases gradually from 0.2913 at room temperature to 0.2875 at 473K. However, on cooling the value is almost constant at the temperature range from 473K to 333K and steeply increases to the value at room temperature. On the change of intensities of satellites, such phenomena was not observed.

[1] Hagiya *et al.* (1993). Acta Cryst. **B49**, 172-179.
[2] Riester and Böhm (1997). Z Krist. **212**, 506-509.

13P51

SITE PREFERENCE OF TRANSITION-METAL IONS IN FERRITES DETERMINED BY SINGLE-CRYSTAL DIFFRACTION METHODS

T. Mizobuchi, K. Matsumoto, and S. Sasaki, Materials and Structures Laboratory, Tokyo Institute of Technology, Nagatsuta, Midori-ku Yokohama, Japan.

The crystal structure and site occupancy for transition-metal ferrite, MFe_2O_4 ($M = Mn^{2+}$, Ni^{2+}, Cu^{2+}, Zn^{2+}) were studied using X-ray single-crystal diffraction methods. The anomalous scattering effect has been used to determine the cation distribution because the transition-metal ions are close in atomic number and X-ray scattering amplitude.

Transition-metal ferrite widely used as magnetic materials has a spinel structure which can be divided into extremes by the arrangement of cations in the tetrahedral A and octahedral B sites: normal spinel $[M^{2+}]^A[Fe^{3+}]_2^BO_4$ and inverse spinel $[Fe^{3+}M^{2+}]^A[M^{2+}Fe^{3+}]^BO_4$. The physical properties of spinel ferrite are strongly affected by the constituent cations and their distribution between A and B sites. Especially, the determination of the cation distribution is essential in order to understand the magnetic properties of ferrite.

Single crystals of Ni-, Cu-, Mn- and Zn-ferrites were grown hydrothermally at $T = 728$ K. Crystal structure analyses were carried out using the Mo $K\alpha$ intensity data. Synchrotron X-ray experiments were performed on anomalous scattering with a vertical-type four-circle diffractometer at BL-10A in the Photon Factory. Diffraction data were collected at $\lambda = 1.7486$ Å which is 0.005 Å longer than the Fe K edge. It was concluded in this study that the site preference on the above ferrites can be closely related to the structural quantities such as u parameter.

POSITIONAL DISORDER OF Y AND Ca ATOMS IN A MELILITE-TYPE Ce^{3+}-DOPED $YCaAl_3O_7$

M. Hayatsu, N. Ishizawa, Materials and Structures Laboratory, Tokyo Institute of Technology, and N. Kodama, Faculty of Engineering and Resource Science, Akita University

In recent years Ce^{3+}-doped crystals have attracted much attention for the potential usage for optically pumped tuneable solid state lasers in the ultraviolet and visible ranges. The melilite-type oxides are possible candidates for the host material allowing a distorted eight-fold coordination for rare-earth elements. The structure of Ce^{3+}-doped $YCaAl_3O_7$ has been thus investigated in the course of survey to characterise the behaviour of Ce^{3+} cations in various crystal fields.

Single crystals of $Y_{0.9995}Ce_{0.0005}CaAl_3O_7$ were grown by the Czochralski method in Ar atmosphere. A fragment of the crystal was ground into a sphere of 126 μm in diameter. Crystal data are tetragonal, $P\bar{4}2_1m$, a=7.6900(7) Å, c=5.050(1) Å, and Z=2. Integrated intensities of 10322 reflections in the whole reciprocal space in the range $\sin\theta/\lambda < 1.022$ were measured using an Ag Kα rotating-anode four-circle diffractometer with resultant 630 unique reflections and R_{int} of 0.019. After the least-squares procedure, relatively large accumulation and depletion of electrons were observed near the Ca(Y) position in the difference Fourier maps, suggesting possible positional disorder of Ca and Y atoms in the melilite-type structure. Subsequent refinement assuming independent atom positions for Y and Ca gave significantly smaller R factor of 0.0124. These positions are separated by about 0.16 Å, resulting in different bond distances for Ca-O and Y-O and bond valence sums of Ca and Y reflecting the difference of their valences.

13P53

X-RAY STRUCTURAL STUDY WITH THE SINGLE CRYSTAL OF A (Hg,Pb)-1223 SUPERCONDUCTOR

N. Kita, K. Yamawaki, S. Sasaki, S. R. Lee and H. Yamauchi, Materials and Structures Laboratory, Tokyo Institute of Technology, Nagatsuta, Yokohama, Japan

Site occupancy and crystal structure of a (Hg,Pb):(Ba,Sr):Ca:Cu:O superconductor, which was confirmed here to have the crystal structure of $HgBa_2Ca_2Cu_3O_{8+\delta}$ (Hg-1223), have been studied by the single-crystal x-ray diffraction method.

The Hg-1223 phase has the highest value of critical temperature of the superconducting transition (T_c = 135 K) with a promising critical current density. Because of the difficulty of homogeneous crystal growth for mercury-based superconductors, the partial substitutions of Pb for Hg and Sr for Ba were applied to enhance the stability of the Hg-1223 phase in the ampoule method. The single-crystal diffraction method has the great advantage of dealing with a single phase in the complex bulk materials.

A parallelpiped single crystal (0.10 × 0.10 × 0.03 mm) was successfully used with a Rigaku AFC-5 four-circle diffractometer and a precession camera (Mo $K\alpha$ radiation; $\lambda = 0.7107$ Å). The space group is *P4/mmm* with lattice parameters of $a = 3.819(1)$ and $c = 15.400(7)$ Å. The chemical formula obtained from the TEM/EDX analyses is $Hg_{0.5}Pb_{0.5}Ba_{0.59}Sr_{1.24}Ca_{1.83}Cu_{3.14}O_{8+\delta}$. The magnetic susceptibility measurements suggest T_c = 125 K. Integrated intensities were collected up to $2\theta = 90°$ in one fourth of the reciprocal space. The absorption correction was carried out using the program ACACA. All structural parameters including site-occupancy ones have been refined simultaneously using a full matrix least-squares program RADY (R = 4.9 %, wR = 5.6 %). The details on structural aspects will be discussed at the meeting.

13P54

SITE PREFERENCE OF CATIONS AND STRUCTURAL VARIATION IN $MgAl_{2-x}Ga_xO_4$ ($0 \leq x \leq 2$) SOLID SOLUTION WITH SPINEL STRUCTURE

T. Ito, A. Yoshiasa, A. Nakatsuka, T. Yamanaka and H. Maekawa,
Graduate school of Science, Osaka University, Osaka, Japan

$MgGa_2O_4$ has a partical inverse spinel structure (the degree of inversion, i, $\simeq 0.8$), while $MgAl_2O_4$ has a normal spinel sturucture ($i = 0.0 \sim 0.3$) depending on the temparature. The relation of the effective ionic radii is $Mg^{2+} > Ga^{3+} > Al^{3+}$ with same coordination number. The cation distribution in thier compound are expected to have the inverse spinel structure from Pauling principle. In this study, the cation distribution of $MgAl_{2-x}Ga_xO_4$ ($0 \leq x \leq 2$) solid solution are determined using the single crystal X-ray diffraction analysis and MAS-NMR analysis. The single crystals were synthesized by flux method using PbF_2. The composition of each samples were determined using the electron microprobe analyzer. The intensity data of X-ray diffraction were collected using Rigaku AFC-5 four-circle diffractometer with Mo$K\alpha$ radiation. The structure refinement was executed using the full-matrix least-squares program RADY, and provided the u-parameter, the anisotropic temparature facters, extinction parameter and the occupancy of Mg^{2+}. The occupancy of Al^{3+} was determined using NMR. The interatomic distances (Å) were determined to be T_{Mg}-O=1.92(3), T_{Al}-O=1.92(9), T_{Ga}-O=1.89(4), M_{Mg}-O=2.03(1), M_{Al}-O=1.92(1) and M_{Ga}-O=2.01(1) from the refined results using a least-square method between all data for solid solution. They correspond with the distances expected from the effective ionic radii except T_{Al}-O, which is longer about 0.15 Å. It is thought that this difference causes the different tendency of the cation distribution between $MgAl_2O_4$ and $MgGa_2O_4$.

13P55

STRUCTURAL STUDY OF PEROVSKITE-TYPE $PbZn_{1/3}Nb_{2/3}O_3$

Y. Matsushima[a], N. Ishizawa[a], N. Wakiya[b] and N. Mizutani[b]

a) Materials and Structures Laboratory, Tokyo Institute of Technology
b) Faculty of Engineering, Tokyo Institute of Technology

Perovskite-type compounds containing Pb atoms have become one of noticeable ferroelectric materials in these decades because of their various promising properties such as the low sintering temperature, the high relative dielectric constant and the high electric resistance. In this study, the crystal structure of $PbZn_{1/3}Nb_{2/3}O_3$ (**PZN**) was investigated by the single crystal X-ray diffraction. Crystals were prepared by the flux method using PbO as a flux. The diffraction experiment was carried out using a four-circle diffractometer with Ag $K\alpha$. The unit cell dimensions were determined to be $a=b=c=4.0588(3)$Å and $\alpha=89.93(1)°$. Candidates for the possible space group are $\boldsymbol{R3m}$ and $\boldsymbol{R\bar{3}m}$, though the latter was discarded in the course of an analysis. Assuming a perovskite-type atomic configuration with the rhombohedral symmetry, the **R/wR** factors became 0.094/0.048. The difference Fourier maps displayed compilations of electrons with a height of more than 10 e/Å^{-3} around Pb positions. The Pb atoms are presumably located at 9*b* sites instead of 3*a* in a statistic distribution. The fractional coordinates refined for Pb atoms were $x=-0.0227(4)$, $y=-x$ and $z=0.0189(5)$ in the hexagonal setting. Slight positional displacements for O atoms were also detected. Fractional coordinates refined for O atoms were $x=0.499(2)$, $y=-x$ and $z=-0.009(3)$. The **R/wR** factors converged to 0.050/0.030. The **PZN** crystals are likely to have rather distorted structure than was previously understood.

DEVELOPMENT OF VACUUM CAMERA X-RAY IMAGE-PLATE METHOD. EXAMPLE: ELECTRON DENSITY INVESTIGATION OF KNiF$_3$ CRYSTAL

V.V.Zhurov, Karpov' Inst. Phys. Chem. Moscow, Russia, E.A.Zhurova, Inst. Cryst. RAS, Moscow, Russia (Core Res. Evol. Sc., JSTC), K.Tanaka, Nagoya Inst. Tech., Japan

The X-ray vacuum camera image-plate (VCIP) method is convenient for investigations of inorganic crystals due to a short time of experiment. It is possible to make a precise experiment in about 7 days. The low level of background permits to make an accurate measurement of weak reflections.

For the development of VCIP method the KNiF$_3$ crystal have been chosen as a testing one. Preliminary results showed that electron density can be obtained with a good accuracy by VCIP method, but the experiment should be done very carefully. Finally, in order to get a good statistics for all the reflections, two sets of measurements have been done. Each set consisted of 18 imaging plates with 16° oscillation range for each IP and 6° sequential overlapping. These two sets were measured because of IP saturation and had a different exposure time: 2 hours and 8 min. In order to avoid powder rings from damaged surface of the crystal, sample (size=0.07 mm) have been treated in HNO$_3$ acid. To reduce the background 0.04 mm lithium-borate glass stick was used. Evacuation of the camera was done up to 70 mTorr. The average background level was about 1-3 impulses for 8 min images, and 20-30 impulses for 2 hours ones.

For interpretation of the data DENZO program (Otwinowski & Minor, 1997) was used. Also a special program for proceeding with IP data for IBM PC computer was designed. It has wide graphic capabilities and permits visualizing of images, zooming, 2D and 3D plotting of a single peak area. A number of different choices for a setting of integration area and background approximation with a best fitted plane through the center of each peak permitted to improve considerably the accuracy of integration, especially for high-angle reflections. The refinement of the atomic spherical model was done up to R=1.1%. The deformation electron density map showed a good agreement with the data obtained from the four-circle accurate X-ray experiment.

Reference:

Z.Otwinowski, W.Minor , Methods in Enzymology, Vol. 276 A: Macromolecular Crystallography, 307-326 (1997).

13P57

METAL ATOM DISPLACEMENTS IN 1T-TYPE (V,Ta)S_2

N. Ishizawa and K. Suda, Materials and Structures Laboratory, Tokyo Institute of Technology, and S. Tsubouchi and M. Wakihara, Faculty of Engineering, Tokyo Institute of Technology

Crystals of 1T-type TaS_2 has an interesting feature being the incommensurate and commensurate lattice distortions owing to the charge density waves. The commensurate phase is structurally characterised by a presence of the Ta_{13} cluster like Star of David, in which Ta atoms are displaced towards the centre of the cluster, leading to a $\sqrt{13}\mathbf{a}\times\sqrt{13}\mathbf{a}$ structure with respect to the 1T-type substructure. The present study was undertaken to investigate the effect of Ta atom replacement with V on the 1T-type TaS_2 structure.

Precession photographs of a $(V_xTa_{1-x})S_2$ single crystal with $x\approx0.3$ showed neither intense diffuse scattering nor superstructure reflections. Diffraction data of the crystal were collected by the four-circle diffractometer with Ag Kα radiation. The difference Fourier maps after the refinement of structural parameters assuming the ideal 1T-type structure revealed large accumulation and depletion of electrons near the Ta and V atoms, suggesting possible displacements of these atoms. The refinement employing a split atom model for Ta and V terminated with R/wR factors of 0.022/0.018 for 392 independent reflections. The metal atom displacement occurs along the direction towards one of the six neighbouring metal atoms within the S-Ta-S intralayer, with a magnitude of approximately 0.1 Å. Directions of the metal atom displacements essentially coincide with those in the Ta_{13} cluster if they are superimposed. The periodic lattice distortion in the present crystal is presumably rather disturbed by the presence of V atoms.

Crystal data: a=3.358(2) Å, c=5.8447(9) Å, $P\bar{3}m1$, trigonal, Z=1.

13P58

REEXAMINATION OF ELECTRON DENSITY DISTRIBUTION IN FAYALITE BY SYNCHROTRON RADIATION

F.Marumo*, Y.Tabira*, M.Okui*, N.Ishizawa** and H.Takei***
* Dept. of Geosystem Sciences, Nihon University
** Materials and Structures Laboratory, Tokyo Institute of Technology
*** Dept. of Earth and Space Science, Osaka University

X-ray determination of electron density distribution was carried out on fayalite Fe_2SiO_4 by Fujino et al. (1981). Since they used a spherical crystal with diameter of 0.20 mm in combination with Mo Kα radiation, the obtained intensity data were supposed to suffer from fairly large extinction effects. Therefore, reexamination of electron density distribution was undertaken on this, one of the most important rock-forming silicate mineral by utilizing a smaller crystal and synchrotron radiation.

Intensities were measured on a four-circle diffractometer installed on BL-14A of the Photon Factory, Tsukuba, Japan, with 0.750(1) Å radiation. The specimen was shaped into a sphere of 0.04 mm in diameter. Intensities, of 11194 reflections with 2θ values smaller than 120° were measured, of which 10118 have structure amplitudes larger than 3σ, and were used for electron density determination. The structure refinement converged to give the R value of 0.020. The difference Fourier map synthesized after the structure refinement showed a pair of prominent peaks with the height of 1.5 $e/Å^3$ at about 0.50 Å apart from the M2 site in the direction approximately along the a axis. The second highest peaks with heights 0.50 $e/Å^3$ exist near the M1 site, which coincides with a center of symmetry of the crystal, at about 0.48 Å from M1. These features closely resemble those observed by Fujino et al.

13P59

ELECTRON DENSITY IN KDP USING 60keV X-RAYS

J. Hester, NIRIM,
Y. Shiozaki, Graduate School of Science, Hokkaido University,
E. Suzuki, NIRIM, and F. P. Okamura, NIRIM

Potassium dihydrogen phosphate, KH_2PO_4 or KDP, undergoes a ferroelectric phase transition which is remarkably sensitive to substitution of hydrogen by deuterium: Tc changes by almost 100K. Therefore better understanding of the hydrogen position and state would considerably advance our understanding of the origins of ferroelectricity in this compound. Furthermore, the true ferroelectric mode has not been confirmed experimentally. Therefore more accurate knowledge of changes in the electron density distribution around the constituent atoms during the ferroelectric phase transition is desirable.

An electron density study of deuterated and undeuterated KDP has been performed by T. Hayashide and Y. Noda (J. Phys. Soc. Jpn.(1997), 66,1,pp 270--271). They note that different samples and different regions of the sample often produce data which are scattered more than would be expected from the sample deviations, a fact borne out by their own results.

As a first step, we examined electron density around the H atom by taking into account some of the factors which presumably contributed to systematic errors in the previous study, in particular by reducing extinction effects and applying a thermal diffuse scattering correction. Data were collected from a spherical crystal 0.74mm in diameter illuminated with 0.21A (WKα) radiation from a laboratory source. A multiwavelength analysis using data measured at wavelengths as short as 0.13A from the same source was also performed to check the extinction refinement.

The resulting experimental electron density in the vicinity of H resembles that of Hayashide and Noda.

13P60

ELECTRON DENSITY DISTRIBUTION IN THE HIGH TEMPERATURE PHASE OF Fe_3O_4

H. Okudera, Ceramics Research Laboratory, Nagoya Institute of Technology, Gifu, Japan.

The electron density distribution in the high temperature phase of magnetite (Fe_3O_4, space group $Fd\bar{3}m$, a (Å) = 8.3961(7), $Z = 8$) has been studied at room temperature by means of single crystal X-ray diffraction method. Deformation of an outer-shell electron cloud of oxygen atom is found in directions toward neighbouring cation site, particularly the tetrahedral *A* site, and is clearly visible in the difference Fourier maps and *X*-*X* deformation density maps. Spatial distribution of electron densities thus obtained could be interpreted as a superposition of those corresponding to vibrating atoms and Fe 3*d* - O 2*p* hybrid orbitals, in other words, covalent 'σ-' and 'π-bonding' for the FeO_4 tetrahedron and covalent 'σ-bonding' for the FeO_6 octahedron. In the FeO_6 octahedron, residual electron density map showed positive densities having cubic symmetry, which may be attributable to Fe 3*d* - O 2*p* hybrid orbital with symmetry of e_g. These results suggest highly covalent character of Fe-O bonds in magnetite. No apparent electron density attributable to metal-metal intervalence charge transfer between adjacent *B*-site Fe atoms could be found.

THREE DIMENSIONAL DIFFRACTION PHENOMENON AT A 90 DEGREE BGAGG REFLECTION

A. Y . Nikulin, J. R. Davis,

Department of Physics, Monash University, Clayton, Vic 3168, Australia.

and D. J. Cookson

Australian Synchrotron Research Program, ANSTO Building 22, Private Mail Bag 1, Menai, NSW 2234, Australia

The experimental observation of a three-dimensional diffraction phenomenon at a 90 degree Bragg reflection is reported and discussed. A novel experimental technique for the direct observation and accurate measurement of scattered intensity profiles in the vicinity of a 90 degree Bragg reflection was proposed and implemented. The detector arrangement allowed the scintillator detection of back-reflected beams via fluorescence scattering from an in-beam copper plate. This detector system has allowed a very high ratio, up to five orders of magnitude, of fluorescence back-reflection peak to the incident beam air scattering background. The experiment was performed on the Australian National Beamline Facility (ANBF), BL-20B, at the Photon Factory, KEK, Tsukuba, Japan. Three-dimensional tracking of the reciprocal lattice point of the Si(800) Bragg reflection around the 90 degree Bragg position was studied over a range of tilt angles in a plane perpendicular to the diffraction plane.

Nikulin, A. Yu., Davis J. R. & Cookson, D. J. (1998). *Phys. Stat. Sol. (a)* (submitted).

ENERGY DEPENDENCE OF ATS REFLECTIONS FOR PYRITE AND MAGNETITE

J. Kokubun, K.Hagiwara, K. Horie, M.Kuribayashi and K. Ishida
Department of Physics, Faculty of Science and Technology, Science University of Tokyo, Noda, Chiba 278, Japan

Near an absorption edge, anisotropic effect of tensorial atomic scattering factor becomes so large that reflections forbidden by screw or/and glide rule can be observed (ATS reflections).[1] ATS reflections were observed in some crystals with linearly polarized synchrotron radiations.[2-4] We measured energy dependence of ATS reflections of FeS_2 (pyrite) and magnetite (Fe_3O_4) near the Fe K-absorption edge.

For a pyrite crystal, the observed energy spectra are quite different from that of the absorption measurement. In the region above the edge, the ATS intensities for (001), (003) and (011) reflections showed the same energy dependence, two sharp peaks and one broad peak. To study nature of the scattering, we measured polarization property and azimuthal dependence of the reflections. The result can be understood on the basis of electric dipole transition. But below the edge, the energy spectra of the ATS intensity depend on the reflection plane. The azimuthal dependence of the intensity cannot be explained by the calculation based on only the dipole transition. Quadrupole transition may contribute to the scattering. While, for a magnetite crystal, there are two peaks above and below the edge, which are also different from the absorption experiment. The azimuthal dependence of the peaks can be explained by dipole transition. The energy spectrum of the scattering does not change, essentially, through the effect of the transition are observed below the temperature.

1) V.E. Dmitrienko (1983). Acta Cryst. A39, 29.; (1984). A40, 89.
2) D.H. Templeton and L.K. Templeton (1986). Acta Cryst. A42, 478.
3) A. Petcov, A. Kirfel and K. Fischer (1990). Acta Cryst. A46, 754.; (1991). A47, 180.
4) T. Nagano et al. (1996). J. Phys. Soc. Jpn. 65, 3060.

14P3

SITE-SELECTIVE EXAMINATION OF MCXD PRE-EDGE PEAKS IN TRANSITION-METAL FERRITES USING SYNCHROTRON X-RAY RESONANT SCATTERING

T. Hanashima, F. Saito, K. Matsumoto, S. Sasaki, T. Mori* and K. Hirano,* Materials and Structures Laboratory, Tokyo Institute of Technology, Nagatsuta, Midori-ku, Yokohama, Japan; *Institute of Materials Structure, High Energy Accelerator Research Organization, Oho Tsukuba, Japan.

Magnetic Circular X-ray Dichroism (MCXD) and Diffraction Anomalous Near Edge Structure (DANES) experiments for transition-metal ferrites were performed with synchrotron X-ray radiation in order to elucidate the magnetic and electronic structures of the ferrites.

The samples examined here include Mn-, Zn- and Mn-Zn-Fe-ferrites with the normal-spinel structure and Ni-, Co-, and Cu-ferrites and magnetite with the inverse-spinel structure. Our systematic studies on MCXD spectra revealed that the end-member ferrites of a normal-spinel type do not have the MCXD signal at the pre-edge region of Fe K edge, where Fe ions does not exist in the tetrahedral A sites. On the other hand, dispersion-type MCXD peaks clearly appeared in the inverse-spinel ferrites. The MCXD peak of the Mn-Zn-Fe-ferrite was reasonably observed because the A sites contain 12 % of Fe ions.

The above systematic results on MCXD were strongly supported by the observation of DANES spectra for the 220 and 222 reflections of Mn-Zn-Fe- and Ni-ferrites. The technique gives the site-specific information because the 220 and 222 intensities are mainly contributed from the A and B sites, respectively. The 220 DANES spectra of Ni-ferrite indicated that MCXD pre-edge peaks originate Fe3+ ions occupying the A sites and such ions play an important role in giving the magnetic character of ferrites.

14P4

CHARACTERIZATION OF CHEMICAL VAPOR DEPOSITION DIAMONDS BY THE MICRO-REGION LAUE METHOD

T.Osaka (Graduate School of Science, University of Tokyo), Y.Mituda (Institute of Industrial Science, University of Tokyo) and K.Ohsumi (Institute of Materials Structure Science, High Energy Accelerator Research Organization)

Diamond synthesized by chemical vapour deposition (CVD) methods is promising material in electric and optical devices,because of its outstanding properties. Recently many works on synthesis methods to improve a crystallinity of CVD diamond have been carried out. It is reported that the crystallinity is changed by synthesis conditions. In this study we have been characterizing the crystallinity of CVD diamond synthesized in three different conditions. These synthesis conditions were (A) H_2-10%/CH_4-5%/O_2 atomosphere/900°C, (B) Ar-10%/CH_4-5%/O_2 atomosphere/750°C and (C) H_2-1%/CH_4 atomosphere/750°C. Silicon (100) was used as a substrate.

Diffraction experiments by the Laue methods using polychromatic synchrotoron radiation have beed carried out at the BL-4B1 of the PF,KEK. The size of the x-ray beam is 1.6 μm in diameter. The beam was irradiated to the samples whose size are 8 to 20 μm. The diffraction patterns were recorded on an imaging plate.

Two domains related by spinel twin were included in the irradiated area in the several particles. Isotropic temperature factors were refined by a least-squares method. In all domains these values were 0.14(2) to 0.16(1) $Å^2$.These values were in agreement with that of natural diamond within standard deviation.The crystallinity analysis by the profile of Laue spot is now in progress.

14P5

STRUCTURE ANALYSIS OF SODIUM PARADODECA-TUNGSTATE USING SPRING-8 BL02B1 BEAMLINE

T.Ozeki, Department of Chemistry and Materials Science, Tokyo Institute of Technology

One of the most severe difficulties in the precise X-ray structure analysis of the crystals containing heavy elements is the absorption effect. High energy X-rays from the third generation synchrotrons, e.g. SPring-8, suffer much less absorption and are expected to provide data of high quality. As the first attempt at such an effort, the crystal structure of sodium paradodecatungstate, $Na_{10}[H_2W_{12}O_{42}].6H_2O$, was analyzed on the BL02B1 beamline of SPring-8. The X-rays from a bending magnet were monochromatized using Si(311) to the energy of 30.748 keV (λ=0.3937 Å), which reduces the absorption coefficient of the title compound to 5.25 mm^{-1}. This value is less than a quarter of the value 23.2 mm^{-1} expected for the MoKα radiation. A single crystal with the approximate size of 0.2x0.1x0.1mm was sealed in a glass capillary and mounted on the f axis of a Huber off-center 7-axis goniometer. Diffraction data, up to $(\theta/\lambda)_{max}$=0.90, were collected by imaging plates equipped in a cylindrical vacuum camera fixed on the ω axis of the goniometer. The DENZO program suit was used for the indexing and the integration of the diffraction intensities. Currently no correction is applied for the absorption effect.

However, the structure was successfully refined using the SHELXL97 program, giving the R(F) factor of 0.042 for 14592 reflections with $Fo>4\sigma(Fo)$ and the $wR(F^2)$ factor of 0.1186 for all the independent 19610 reflections. The e. s. d.'s for the W-O distances are in the range of 0.004-0.007 Å ,which are significantly smaller than those obtained by the conventional diffractometers with the MoKα radiation. With appropriate absorption corrections applied, even better results are expected.

14P6

PHASE TRANSITION AND CHARGE ORDERING OF MAGNETITE EXAMINED BY THE VALENCE-DIFFERENCE CONTRAST METHOD

T. Toyoda, S. Sasaki and M. Tanaka[*], Materials and Structures Laboratory, Tokyo Institute of Technology, Nagatsuta, Midori-ku Yokohama, Japan; *Photon Factory, Institute of Materials Structure, High Energy Accelerator Research Organization, Oho Tsukuba, Japan.

Magnetite $[\mathrm{Fe}^{3+}]^{A}[\mathrm{Fe}^{2+}\ \mathrm{Fe}^{3+}]^{B}\mathrm{O}_4$ is a mixed valence compound of an inverse-spinel structure. The high electronic conductivity of magnetite at room temperature suggests the continuous interchange of electrons between Fe^{2+} and Fe^{3+} at the B sites. As the result of freezing of the electron hopping, magnetite transforms to a lower symmetry form below the Verwey transition temperature ($T_v \cong 123$ K) with the charge ordering in the B sites. Selecting a wavelength in the XANES region, the anomalous scattering effect with a chemical shift of 5eV between Fe^{2+} and Fe^{3+} made it possible to distinguish the two kinds of ions in magnetite.

In this study, the symmetry and crystal structure of the low-temperature phase of magnetite were examined to use the synchrotron X-rays. The charge ordering in the B sites and energy dependence of superlattice reflections were studied below T_v. X-ray experiments with synthetic single crystals were performed on a vertical-type four-circle diffractometer at PF-BL-10A. Profile intensity data were collected at various wavelengths of $\lambda = 0.7$, 1.7421 and 1.7499 Å.

Half-indexed reflections and forbidden reflections on the cubic phase clearly appeared at 116 K. The energy dependence in diffracted intensity was observed at the Fe *K* edge for the 0 4 7/2 superlattice reflection. No splitting of the fundamental reflections appeared below T_v. Appearance of extra reflections has a systematic relationship with previous works, which will be presented at the meeting.

CATION DISTRIBUTION IN Mn-Zn-Fe FERRITE DETERMINED BY THE TWO-WAVELENGTHS ANOMALOUS DISPERSION METHOD

Y. Konoike, F. Saito, S. Sasaki and H. Koinuma, Materials and Structures Laboratory, Tokyo Institute of Technology, Nagatsuta, Yokohama, Japan.

Site preference of transition-metal ions in Mn-Zn-Fe ferrite, $Mn_{0.54}Zn_{0.35}Fe_{2.11}O_4$, was investigated using the two-wavelengths anomalous dispersion (TWAD) method at $\lambda = 1.7535$ and 1.2934 Å, which are 0.01 Å longer than Fe *K* and Zn *K* absorption edges, respectively. A spherical single crystal was used in a four-circle diffractometry of PF-BL-10A with tunable synchrotron X-rays; $a = 8.4727(6)$ Å, $u = 0.2609(2)$.

Mn-Zn-Fe ferrite is one of the most commercially important ferrites because of the high permeability, high magnetic-flux density, low coercive force and high wear resistance. Although the compositional dependence of the physical properties has been discussed repeatedly, there is no information on the cation distribution between the A and B sites in the ferrite. Having large differences in X-ray scattering amplitude, the TWAD method was applied to determine the site occupancy for three kinds of Mn, Zn and Fe ions in both sites.

The result shows that all Mn and Zn ions fully occupy the tetrahedral A sites within the experimental errors, suggesting that Mn-Zn-Fe ferrite has the crystal structure of a typical normal spinel. The chemical formula is $\left[Mn_{0.54}Zn_{0.34}Fe_{0.12}\right]^A\left[Zn_{0.01}Fe_{1.99}\right]^B O_4$. A superexchange interaction model between the A and B sites gives a larger magnetization of 6.8 μ_B which significantly differs from the observed 6.0 μ_B. The difference could not be explained by the partial disordering of Mn^{2+} ions to the B sites because of no occupancy. Studies on the magnetic structures are now in progress.

14P8

THE STRUCTURAL STUDY OF γ-ALUMINA(Al_2O_3) WITH SYNCHROTRON RADIATION

Y. Nakakita*, T. Ushiro*, C. Numako*, K. Koto*, T. Osaka**, K. Ohsumi**

* Faculty of Integrated Arts and Sciences, Tokushima University

** Institute of Materials Structure Sciences, High Energy Accelerator Research Organization

[Introduction] γ-alumina is an intermediate phase in the dehydration process from gibbsite (γ-$Al(OH)_3$) to corundum (α-Al_2O_3). Saalfeld (1958) and Zhou *et al*. (1991) reported that γ-alumina has a spinel-type structure. However, further investigation of the crystal structure has been limited because of its poor crystallinity and difficulty to obtain a single crystal. We applied synchrotron radiation (SR) to the single crystal of γ-alumina.

[Experimental and results] The single crystal of γ-alumina specimen was obtained by heating a synthesized single crystal of gibbsite at 600℃ in air for 24hr. The size of a platy shaped single crystal was about $2\times2\times0.5mm^3$. The X-ray diffraction patterns were recorded on IP with monochromatized (λ=1.0Å) SR at the BL-4B, PF, KEK, Japan. The Laue photographs of γ-alumina showed the broad diffraction spots so that it could be supported that the crystallinity of γ-alumina is very small. Two different types of reflections were observed. The relatively sharp and broad reflections are superimposed on the reflections contributed from the oxygen sublattice, e.g. the 222 and 440. On the other hand only isotropically broad reflections are observed for ones, e.g. the 111 and 220. The results indicate that the origin of small crystallinity is responsible for a way of ordering of aluminium atoms in the spinel structure.

14P9

DIRECT OBSERVATION OF ANISOTROPIC X-RAY FLOURESCENCE IMAGES FROM SOLID SAMPLES

C.K. Chen[*], S.L. Chang[*], T.S. Gau[*], Y.F. Hung[*], Y.N. Hung[*], J.M. Chen[#], R.G. Liu[#], and M.T. Tang[#]
[*]Department of Physics, National Tsing Hua University, Taiwan
[#]Synchrotron Radiation Research Center, Hsinchu, Taiwan , R.O.C.

X-ray emission from atoms usually exhibits a homogeneous intensity distribution except for the direction along a polarization axis. Here, we report the observation of unexpected ring-like images if X-ray emission from the constituent atoms of solid samples during the excitation of monochromatic synchrotron radiation ranging from 100ev to 7kev. The rings are found to result from the emitted X-ray fluorescence forming a solid cone along the direction of observation with a minimum in the central region. The semi-angle of the cones follow the $E^{-1/2}$ relation, where E is the transition energy involved. The images are proved to be irrespective of incident-beam polarization and independent of the samples being amorphous, polycrystalline, or mono-crystalline.

CRYSTALLOGRAPHIC STUDIES OF BIOMINERALS COMPOSING PEARL AND MARINE SHELLS

C. Numako*, T. Minomura*, K. Ohsumi**, and K. Koto*.

- * Faculty of Integrated Arts and Sciences, Univ. of Tokushima,
- ** Institute of Materials Structure Science, High Energy Accelerator Research Organization

[Introduction] Pearl is one of organic gemstones arising in bivalve molluscs with beautiful nacreous shells. There are two kinds of shell structure in the shell of the marine pearl oyster; prismatic structure consisted of calcite and nacreous structure consisted of aragonite. Calcite is more stable than aragonite under ambient pressure and temperature. However, aragonite is often arisen as a major crystalline component of biominerals. In this study, we tried to characterize these phases in the shell and pearl from crystallographic points of view by X-ray diffraction technique.

[Experimental and results] Laue photographs of prismatic and nacreous pearl specimens were taken with monochromatized synchrotron radiation (λ=1.0A) at BL-4B, PF, KEK, Japan. The photographs of a prismatic pearl specimen showed powder pattern of calcite. The photographs of a nacreous pearl specimen gave the powder pattern of aragonite when the X-rays were irradiated normal to the nacreous layer, but the elongated diffraction spots were observed on the photos parallel to the nacreous layer. The nacreous layer consists of thin plates of aragonite (0.3μm x 3μm), and these results indicate that the c-axis of aragonite is normal to the plates but the a- and b-axes are not orientated in the nacreous layer. Furthermore the elongation of the diffraction spots in the monochromatic Laue photographs suggests a small domain structure of aragonite in a thin plate of aragonite.

14P11

ENERGY-DISPERSIVE TOPOGRAPHIC OBSERVATION OF InAs LATTICE-MISMATCHED HETEROEPITAXIAL LAYER ON GaAs USING SYNCHROTRON X-RADIATION

Y. Suzuki, H. Kii, M. Yoshida, and Y. Chikaura, Department of Materials Science, Faculty of Engineering, Kyushu Institute of Technology, Tobata, Kitakyushu 804-8550, Japan

We have demonstrated an X-ray microbeam scannning type of scattering topography system involving X-ray spectroscopy(1). The spectrum at each location is measured by a energy-dispersive solid state detector (SSD) and transferred to a computer to reconstruct a physical quantity map. We call this method "X-ray Scattering Spectro-Topography".

In this paper, we have applied the method using white synchrotron radiation microbeam to an investigation of large lattice-mismatched heteroepitaxial layer InAs on GaAs, which is expected as longer wavelength light emitting devise and superconductor devise.

Experiments were carried out at Photon Factory (Tsukuba) using a white synchrotron radiation. X-ray scattering topography apparatus consists of computer controlled X-Y scanning system and a small pinhole-slit(7 μm ϕ). While a specimen was fixed at a certain Bragg angle, diffracted X-rays with the different wavelength from the specimen were simultaneously measured by the SSD. This is because considerable discrepancy between lattice constants of InAs and GaAs and different net planes cause such diffractions at the same angle position. We took four topographs of (002) and (004) InAs epitaxial layer, and of (002) and (004) GaAs substrate.

The four topographs obtained by this method reveal structural irregularities in substrate and epitaxial layer. At first sight the images confirmed the results of the previous report(2). It was found that the method provided excellent performance on the simultaneity and time required for the topographic imaging. Besides the four topographs show different contrast in detail. In order to discuss the results, we calculated computer simulation for this experiment as a white beam topography using Takagi-Taupin equations.

1. Y. Chikaura, Y. Suzuki and Y. Udagawa, J. Phys. D 26 (1993) 2212
2. Y. Suzuki, Y. Chikaura and T. Akazaki, Appl. Phys. Lett. 56 (1990) 1858

14P12

COMPUTER SIMULATION STUDY ON X-RAY DYNAMICAL PENETRATION DEPTH FOR LARGE LATTICE-MISMATCHED InAs HETROEPITAXIAL LAYER ON GaAs

M. Yoshida, Y. Suzuki and Y. Chikaura, Department of Materials Science, Faculty of Engineering, Kyushu Institute of Technology, Tobata, Kitakyushu 804-8550, Japan

Lattice-mismatched semiconductor heteroepitaxial layers, which include GaAs on Si substrates, Si-Ge and III-V compound semiconductor strain superlattices, have been fabricated by many research groups. The epitaxial layers give several hundred arcseconds in FWHM of rocking curve of diffracted intensity for double-crystal diffractometry. The present authors tried to obtain a depth-sensitive X-ray scattering topograph of InAs layer grown by molecular beam epitaxy on GaAs (1). The experimental results showed that the depth sensitivity depends on the diffraction index net plane (004), (002) and (006) used. In this report, to elucidate the mechanism, we have made a computer simulation of X-ray electro-magnetic wave field in the lattice mismatched heteroepitaxial layer by X-ray dynamical diffraction theory in Bragg case (Takagi-Taupin equation), and found a reasonable explanation for the previous1) experimental results.

The wave fields in a 1.0 μm-thick epitaxial layer were different from that in a bulk crystal. It is noted that we have to make a simulation image in order to give more exact explanation. Contrasts from a local displacement from a strain field of matrix are different from one another that of diffraction indices. Although these are dependent on a magnitude of strainfield, distribution of strain field and deviation from Bragg condition, the contrast in 004 diffraction image is longest. The surface contrast which was observed due to deeper region including a local displacement was not visible from a local displacement in shallower region. These results are capable to explain the previous scattering topography. Moreover, we'll show the study for X-ray wave field in Bragg case in large lattice mismatched heteroepitaxial layer by computer simulation using Takagi-Taupin equation.

1) Y. Suzuki, Y. Chikaura, H. Kii, Jpn. J. Appl. Phys., 35 (1996) L1311.

14P13

HIGH RESOLUTION ELECTRON MICROSCOPY WORK ON SOL-GEL DERIVED COBALT SUBSTITUTED BARIUM FERRITE

G. B. Teh , Department of Chemistry, University of Cambridge
D. A. Jefferson, Department of Chemistry, University of Cambridge,

The magnetoplumbite (M-type) $BaFe_{12}O_{19}$ has been investigated with the substitution of cobalt(II), in order to produce a quaternary system of the type BaO-Fe_2O_3-CoO. Specimens were synthesised via a sol-gel method using ethylene glycol. This synthesis route proved to be able to produce nanocrystals of cobalt substituted barium ferrite with average particle size of 26.1 nm. Hexagonal-like platelets and other morphologies of ferrites were obtained at the final stage of calcining process. The specimens were characterised using the X-ray diffraction, magnetometry measurement and high resolution electron microscopy. The different morphologies of ferrites observed are discussed. The saturation magnetisation of $BaFe_{12}O_{19}$ was found to be greatly reduced at about 50% with the cobalt doping from 47.75 emu/g in parent ferrite to 27.80 emu/g in doped ferrite. A total reduction of 74% in the value of intrinsic coercivity was recorded as the doped ferrite was recorded as 275.77 G compared to 1082.39 G in parent ferrite.

14P14

A 5-DIMENSIONAL MODEL OF DODECAGONAL Ta-Te QUASICRYSTALS

A. Yamamoto, National Institute for Research in Inorganic Materials, Japan

The consideration of two approximants of the first found stable dodecagonal Ta-Te quasicrystal (Krumeich,1994) shows that the 5-dimensional (5D) space group of the dodecagonal phase is non-centrosymmetric $P\overline{12}m2(12^5mm)$ and the structure has five atom layers within a 10 Å period. A 5D quasicrystal model leading to the two approximant structures (Conrad,1997) is proposed. The model consists of 20 Å dodecagonal clusters (DDC) as in the approximants which are arranged at each vertex of the square-triangle dodecagonal pattern (Cockayne,1994). It is the first model for real quasicrystals which has fractal occupation domains. Calculated diffraction patterns can reproduce a characteristic feature of the intensity distribution in the Ta-Te dodecagonal phase. The model suggests that the quasicrystal has the deterministic or random square-triangle packing of the DDC.

Cockayne, E. (1994). Phys. Rev., B49, 5869--5910.
Conrad, M. (1997). PhD thesis, Univ. Dortmund, Aachen.
Krumeich, F., Conrad, M. and Harbrecht, B. (1994). ICEM 13-Paris, 751--752.

14P15

LONG-RANGE ORDER AT THE SURFACE IN A MAGNETIC FLUID: AN X-RAY REFLECTIVITY STUDY UNDER MAGNETIC FIELD

K. Ueda and I. Takahashi
Advanced Research Center of Science (ARCS),
School of Science, Kwansei Gakuin University

Agglomeration of fine particles has been paid much attention to researchers who specialize solid state physics, since several resemblances between the process of forming an ordered state and crystallization have been pointed out. For example, computer simulations on the possibility of the phase transition from a gas phase as an assembly of hard spheres to an ordered phase would be the theoretical contributions to this subject. We have studied the structure of a magnetic fluid so as to clarify the ordering phenomena of fine particles experimentally.

The magnetic fluid is a colloidal system composed of magnetic fine particles. The particles with 10 nm in diameter are distributed randomly in the bulk. At the surface, however, a layering structure that has a periodicity identical to the diameter of the fine particles was found by the X-ray reflectivity (XR). After the subsequent XR measurements with elevating temperature, many remarkable properties about the long-range order (LRO) localized at the surface was revealed [1]. These interesting features in such a complex, but classical system have forced us to investigate the driving force of the LRO further.

In this presentation, we will report our recent results about relaxation of the LRO under applying alternative magnetic fields from 0 Hz to 10^5 Hz.

[1] Takahashi, I., Ueda, K., Tsukahara, Y., Ichimiya, A. & Harada, J. (1998). *J. Phys.: Condens. Matter*, **10**, 4489-4497.

COMMON PROJECTION OF INCOMMENSURATE COMPOSITE CRYSTAL $Sr_{1.145}TiS_3$ OBSERVED BY HIGH-RESOLUTION ELECTRON MICROSCOPY

M.Onoda*, G-Y.Yang#, M.Saeki* and Y.Bando*, *National Institute for Reseach in Inorganic Materials (Japan), #Tsinghua University (China)

The existence of composite crystals Sr_xTiS_3 (x=1.1-1.2) was revealed[1], and the Rietveld analysis through the four-dimensional superspace group approach was performed[2]. The structure is described as an interpenetration of two trigonal parts with common a=b=1.15nm, the TiS_3 part with c_1=0.299nm and the Sr part with c_2=0.523nm. The TiS_3 part is composed of Ti atoms on the threefold axes and remarkably twisted S atoms around the threefold axis, and Sr position is appreciably modulated in the Sr part. A high-resolution image of $Sr_{1.145}TiS_3$ has been taken with an incident beam parallel to c-axis using an electron microscope JEM-3000F. In the image, three types of contrast are observed, and they show some unusual features which can be understood based on the projected structure model along c-axis. The dark and white contrasts correspond respectively to Sr rows with displacive modulation and empty channels in the structure, and the grey contrasts with shades correspond to the projection of Ti atoms and surrounding S atoms.

1) Saeki, M. & Onoda, M., (1993) *J. Solid State Chem.*, 102, 100-105.

2) Onoda, M., Saeki, M., Yamamoto, A. & Kato, K. (1993) *Acta Cryst.*, B49, 929-936.

14P17

SUPERSPACE GROUP APPROACH OF THE ROOM-TEMPERATURE PHASE OF Cu_8GeSe_6

M.Onoda[*], M.Ishii[*], K.Shibata[#], and A.Yamamoto[*], [*]National Inst. for Res. in Inorganic Materials (Japan) ,[#]Japan Science & Technology Corp.

The low-temperature form, *i.e.* the room-temperature form, of Cu_8GeSe_6 (Cu_8GeSe_6 II, stable below 330K) has been investigated by powder X-ray diffraction method. Cu_8GeSe_6 II is hexagonal with cell dimensions A=1.265, C=1.176nm. The structure may be a superstructure of the high-temperature form, Cu_8GeSe_6 I (hexagonal, $a=0.730=A/\sqrt{3}$, c=1.176nm). A superstructure analysis using the ordinary Rietveld method is difficult, because of overlap of reflections and many unknown initial parameters. An application of the superspace group theory may overcome the difficulty, since four-dimensional approach often lead to a smooth convergence from unsatisfactory initial parameters and a superstructure is considered to be a commensurately modulated structure. Refinement of Cu_8GeSe_6 II has been successfully performed based on a four-dimensional superspace group for commensurate modulation, $P6_3mc(1/3\ 1/3\ 0)$ with basic cell constants a=0.730, c=1.176nm, through a Rietveld analysis program PREMOS. As the parameters, the cosine and sine terms of Fourier amplitudes A_0, A_1 and B_1 are adopted by considering the structural degree of freedom, where the suffixes m represent the wave vectors $m\mathbf{q}=m(\mathbf{a}^*+\mathbf{b}^*)/3$.

14P18

QUASICRYSTAL STRUCTURE AND CONDUCTIVITY OF DENTAL ENAMELS AND A SPECIAL PORCELAIN ENAMEL

Nguyen Van Tri, Institute of Engineering Physics,
Hanoi University of Technology.

From the experimental results on the temperature variation of electrical resistivity of dental enamels and of a special porcelain enamel, a special conduction effect of these enamel films was revealed : At normal room temperatures these enamels insulate very well and with rising temperature they experience a very strong increase in conductivity. Especially, once the temperature falls to below the room one these enamels transform suddenly into good conductors. This particular property of the enamels is similar to that for the typical stable quasicrystal material recently discovered, basically made of seventy atomic percent of Aluminium and of transition metals[1]. On the other hand, the careful ESR studies on these non-crystalline enamel films suggest that the films show a very outstanding angular dependence effect being exactly the same as of a single crystal sample with a typical highfold axial symmetry. The symmetry axis is perpendicular to the enamel surface. This quasicrystal effect is closely connected with the fivefold symmetry combinations distributed in the enamel film, whose planes are parallel to enamel surface. Every this fivefold structure unit is combined by fivefold (2F-2A) rhombs of four spin centers super-exchange-interacting and creating two spin couple pairs : the opposite pair A (Antiferromagnetic) with the high population density of the singlet electron state at lower temperatures and the opposite pair F (Ferromagnetic) with the high population density of the singlet electron state at higher temperatures. Evidently, the particular properties of the enamel are in close internal connection with the electronic dynamics of its quasicrystal structure.

1. J.M. Dubois, Supplement to Acta Crystallographica Vol. 52, IUCr XVII Seattle Washington USA 1996, C-3.

14P19

CRYSTALLIZATION AND PRELIMINARY CRYSTALLOGRAPHIC STUDIES ON NON-PHOTOSYNTHETIC FERREDOXINS

G.Kurisu, R.Igarashi, M.Kusunoki and T.Hase
Institute for Protein Research, Osaka University.

Ferredoxins (Fds) are well known iron-sulfur proteins. To date a large number of Fds have been isolated, sequenced and characterized. Plant-type Fds from various plants including cyanobacteria play particularly important roles as electron carriers from Photosystem I (PSI) to various Fd-dependent enzymes such as Fd-NADP reductase, nitrite reductase, sulfite reductase and glutamate synthase. Recently, Fd has been found in non-photosynthetic tissues such as roots and fruits as an isoprotein distinct from the leaf counterpart. This second type of Fd is probably involved in an electron transfer from pyridine dinucleotides supplied via the oxidative pentose phosphate pathway to some Fd-linked enzymes in plastids.

In order to compare the structures and functions of these two photosynthetic and non-photosynthetic Fds, we were interested in obtaining crystals of Fd (FdIII) from maize root. Crystals of FdIII were grown at 4°C using hanging drop vapor diffusion method by mixing equal volumes of the protein solution with a reservoir solution that contained 3.2-3.5M ammonium sulfate and 300mM NaCl in 50mM Tris-HCl buffer (pH7.5). Needle shaped dark-brown crystals appeared in 1 or 2 months. The X-ray diffraction data were collected with R-axis IIC detector, the crystals belong to the orthorhombic space group $P2_12_12_1$, with cell parameters $a = 79.93$ Å, $b = 104.56$ Å, $c = 66.40$ Å. Based on the rough estimate of Vm value, from 4 to 7 Fds were contained in the asymmetric unit. Now structure analysis with MR method is in progress.

14P20

CRYSTAL STRUCTURE OF O^6-METHYLGUANINE-DNA METHYLTRANSFERASE FROM *PYROCOCCUS KODAKARAENSIS* STRAIN KOD1

H. Hashimoto[a], M. Nishioka[b], T. Matsumoto[a], T. Yuasa[b], T. Inoue[a], S. Fujiwara[b], M. Takagi[b], T. Imanaka[c], Y. Kai[a] [a]Dept. of Materials Chemistry, and [b]Dept. of Biotechnology, Osaka University, [c]Dept. of Synthetic Chemistry and Biological Chemistry, Kyoto University

The crystal structure of the O^6-methylguanine-DNA methyltransferase from hyperthermophilic archaeon *Pyrococcus kodakaraensis* (*Pk* MGMT) was determined at 1.8 Å resolution. *Pk* MGMT with a molecular weight of 19.5 kDa repairs alkylated DNA and shows extreme thermostability (Leclere *et al.* in press). The crystal of *Pk* MGMT belongs to the space group $P2_12_12_1$ with unit-cell dimensions of $a = 53.2$, $b = 86.2$ and $c = 39.8$ Å (Hashimoto *et al.* in press). Structure determination was carried out by single isomorphous replacement method together with anomalous scatterings. Crystallographic refinement is now in progress. For present refined model, R and R_{free} factors are 17.1% and 21.8%, respectively. Recently, the crystal structure of C-terminal fragment of Ada protein, a bacterial methyltransferase from *E.coli*, was determined (Moore *et al.*, 1994). However, no structural information on eukaryotic or archaeal MGMT has ever been reported. Structural comparison of these methyltransferases has revealed large discrepancy in respect to solvent accessible surface areas and ion-pairs.

1) Leclere , M. *et al.* (1998) *Mol. Gen. Genet.*, **258**, 69-77.
2) Hashimoto, H. *et al. Acta Cryst. D*, in press.
3) Moore, M. H. *et al.* (1994). *EMBO J.* **13**, 1495-1501.

14P21

THE DEVELOPMENT OF AN EMPIRICAL PEPTIDE DRUG DESIGN SYSTEM

H. Ishida, T. Shirai, Y. Matsuda, Y. Kato and T. Yamane, *Graduate School of Engineering, Nagoya University*

We have developed a program system that designs peptide ligands being able to bond to the functional sites of target proteins. The system was named as empirical peptide ligand construction system, *EMPLICS*. Two major features of this system are: first, it evaluates stability of peptide-protein complex using empirical rules which have been obtained from three dimensional structures of known proteins; second, it designs appropriate peptides by simulating the strategy of protein evolution. This system can be applied to modify known peptide ligands and can be used to design de novo peptide ligands, when coordinates of a target protein are given.

The system was tested for four peptide-binding proteins in order to design peptide ligands. They are human class I (PDB code; 1hhg) or class II major histocompatibility complex (PDB code; 1dlh), Src homology 3 domain (PDB code; 1sem) and human immunodeficiency virus type 1 protease (PDB code; 7hvp). The peptide ligand structures designed by using *EMPLICS* were compared with those of the experimentally determined ligands in the proteins. As a result, *EMPLICS* could generate the main chain conformation and orientation of suitable peptide ligands for three out of four proteins. Some of the side chains, which are important in determining the binding specificity, were reproduced as the identical or similar ones compared with the side chains of the known ligands.

14P22

STRUCTURE OF COAGULATION FACTOR IX -BINDING PROTEIN AT 2.6Å RESOLUTION

H.Mizuno, Z.Fujimoto, M.Koizumi, H.Kano, H.Atoda § and T.Morita §
National Institute of Agrobiological Resources, Ibaraki 305-8602, Japan, and
§ Meiji Pharmaceutical University, Tokyo 188-0001, Japan

Blood coagulation factor IX-binding protein (IX-bp) from habu snake venom is a disulfide-linked heterodimer consisting of homologous subunits A and B. IX-bp is highly homologous to another anticoagulant of coagulation factors IX/X-binding protein (IX/X-bp), crystal structure of which has recently been determined at 2.5Å resolution and showed that a concave surface surrounded by two subunits is a putative binding site of factors IX and X (Mizuno et al., 1997). To understand functional difference between IX-bp and IX/X-bp on the basis of their structural comparison, we have analyzed the structure of IX-bp.

The crystals of IX-bp were obtained by vapor diffusion technique. The space group is $P2_1$, with a=58.8Å, b= 56.9Å, c=39.7Å and β=95.8° . The structure was solved at 2.6Å resolution, and refined to R=18.2%. The structure of IX-bp is very similar to but different in some places from that of IX/X-bp. One of the structural differences is in that when subunit B of IX/X-bp is superposed onto that of IX/X-bp, subunit A is required to rotate about 6° for superposition. Further structural differences between IX-bp and IX/X-bp will be discussed in connection with functional differences.

Mizuno,H., Fujimoto,Z., Koizumi,M., Kano,H., Atoda,H., and Morita,T. (1997). *Nature Struct. Biol.*, 4, 438-441.

14P23

FLAVOCETIN-A HAS A NOVEL TETRAMERIC STRUCTURE OF C-TYPE LECTIN DOMAIN HETERODIMERS

K. Fukuda§, H. Mizuno§†, Z. Fujimoto†, H. Atoda‡ and T. Morita‡, §University of Tsukuba, Ibaraki 305-0005, Japan, †National Institute of Agrobiological Resources, Ibaraki 305-8602, Japan and ‡Meiji Pharmaceutical University, Tokyo 188-0001, Japan.

Flavocetin-A (FL-A) is one of the C-type lectin-like proteins found in snake venom. Unlike other proteins, it is a high molecular mass protein (149 kDa) composed of heterodimers consisting of α-subunits of 17 kDa and β-subunits of 14 kDa. This protein binds specifically to the platelet glycoprotein (GP) Ib and acts as a blocker of von Willebrand factor (vWF)-binding in platelet aggregation under conditions of high shear stress. FL-A may therefore be useful as specific probes to elucidate the inhibitory effect on vWF binding to GPIb. In order to understand the molecular basis for the GPIb-binding specificity, we have analyzed the structure of FL-A by X-ray crystallography.

FL-A crystals were prepared by vapor diffusion method using MPD as a precipitant. These crystals belong to the tetragonal space group I4 with unit cell dimensions of $a = b = 120.4$ Å, $c = 62.9$ Å. Native data were collected at the Photon Factory in Tsukuba. A data set of 96677 measurements has been reduced to 15078 unique reflections with an R-merge of 0.082. This data set is 95.6% complete to 2.5 Å resolution. The asymmetric unit contains one α/β heterodimer, with V_m value of 3.7 Å^3/Da and solvent content of 67% by volume. The space group indicates that FL-A is a homotetramer with four identical α/β heterodimers related to crystallographic fourfold symmetry. The structure determination is now in progress by molecular replacement using the structure of coagulation factors IX/X-binding protein, a heterodimer of C-type lectin domains (Mizuno, *et al.*, 1997), as the search model.

Mizuno, H., Fujimoto, Z., Koizumi, M., Kano, H., Atoda, H. & Morita, T. (1997). *Nature Struct. Biol.*, **4**, 438-441.

14P24

CRYSTALLIZATION AND PRELIMINARY X-RAY ANALYSIS OF THERMOSTABLE ASPARTATE AMINOTRANSFEREASE FROM A THEROPHILIC CTYNOBACTERIUM

K. Hamada[1], K. Nozawa[1], H. Shibata[2] and Y. Sawa[2]
[1] Interdisciplinary Faculty of Science and Engineering, Shimane University
[2] Faculty of LIfe and Environment Science, Shimane University

Aspartate aminotransferase (AspAT) is one of the key enzymes in amino acid metabolism and catalyzes the reversible interconversion of dicarboxylic amino and keto acids. AspAT from a thermophilic cyanobacterium, *Phormidium lapideum* (*Pl*AspAT) is an thermophilic and thermostable dimeric enzyme which retains its structure and reaches maximal activity at 80 °C. The sequence homology of *Pl*AspAT is not exceeding 20% against mesophilic eukaryotic and bacterial enzymes, but that is 40% level against thermophilic bacterial enzymes. In order to obtain an atomic level of understanding of the thermostability of AspAT, we have undertaken crystallographic studies of *Pl*AspAT. *Pl*AspAT expressed in *E. coli.* containing the plasmid of *Pl*AspAT was purified, and crystallized with the essential cofactor of the pridoxal phosphate by the hanging drop technique using ammonium sulfate as precipitant. Of two different crystal shapes, crystals with plate shape belong the monoclinic space group C2 with unit cell dimensions of a = 122.13 , b = 110.82, c = 87.76 Å and β = 97.1°. A V_m value of 3.30 $Å^3$/Da indicated that a dimmer consisting of two identical subunits was contained in the asymmetric unit. Native data set was collected using synchrotron radiation at the Photon Factory, KEK, and had a R_{merge} value of 0.072 for 19,964 unique reflections with 66.3% completeness at 2.7 Å resolution. A self-rotation function calculated with the program XPLOR using 10.0-4.0 Å resolution data and 45 Å as integration radius resulted that the non-crystallographic two fold axis was indicated by a maximum at ψ = 60.0, φ = 122.5° The structure analysis by molecular replacement method is in progress.

14P25

MIR-OAS: A PROGRAM SYSTEM FOR PROTEIN STRUCTURE DETERMINATION WITH GUI

K. Hamada[1], K. Kakoi[1], N. Tanaka.[2], H. Moriyama[2] and N. Kamiya[2]
[1] Interdisciplinary Faculty of Science and Engineering, Shimane University
[2] Department of LIfe Science, Faculty of Biotechnology and Bioscience, Tokyo Institute of Technology
[3] The Institute of Physical and Chemical Research, Mihara, Hyougo

The MIR-OAS is a user-friendly software system to solve the protein structure by the multiple isomorphous replacement method with optimized anomalous scattering. The aim of the development of the system was to provide it as a part of the MIR-OAS routine analysis at the beamline for macromolecular crystallography, Spring-8. The system consists of computational and user-friendly GUI (graphical user interface) parts. Special attention was paid to make it so that users with no special knowledge about both the protein crystallography computer might solve the macromolecule structure without help of the specialist. Additionally, the software system was designed like being flexible so that each program in the system was easily maintained and replaced with more excellent program in future. Modem software technology with reusability, encapsulation, and GUI was utilized to overcome these problem. The computational part written by FORTRAN77 contains as follows; 1) data handling 2) determination of heavy atom sites 3) refinement of the heavy atom parameters 3) determination of protein phase and 4) calculation of map. Each of them was linked efficiently by the user-friendly GUI part which was developed with the Tcl/Tk macrolanguage.

The software can be run after minimal necessary parameters are typed in accordance with the direction on the widget. All the information of the computation is saved as a log file.

The software system is currently running on PCs running Linux as well as SUN workstation. It will run on Windows95/NT and Mac-OS, if the Tcl/Tk is running on them.

PRELIMINARY X-RAY CRYSTALLOGRAPHIC STUDIES OF A NOVEL ANTIOXIDANT PROTEIN FROM *Amphibacillus xylanus*

K. Kitano[a], Y. Niimura,[b] Y. Nishiyama[b] AND K. Miki[a]
[a] Department of Chemistry, Graduate School of Science, Kyoto University, Kyoto, Japan, and [b] Department of Bioscience, Tokyo University of Agriculture, Tokyo, Japan

AhpC protein (M.W.= ~20kDa), called also thiol-specific antioxidant enzyme (TSA) or peroxiredoxin (Prx), represents a family of newly discovered peroxidases, which shows no sequence homology to previously known antioxidant proteins such as superoxide dismutases, catalases and glutathione peroxidases. AhpC protects cells against oxidation damages, i.e., catalyses the reduction of organic hydroperoxides and hydrogen peroxide, in cooperation with 60kDa flavoprotein, NADH oxidase (1).
AhpC, purified from *Amphibacillus xylanus*, has two disulfide linkages between monomers, then act in the unit of dimers. Gel-filtration chromatographic study suggests further oligomerization (ca. 10-12mers) of AhpC by hydrophobic interactions. Here we report the identification of oligomeric form of *A.xylanus* AhpC by X-ray crystallographic study. AhpC was crystallized by the vapor diffusion method at 20° C, with polyethylene glycol (PEG) 6,000 and 0.1M ammonium acetate as precipitants. The crystals belong to the space group $P1$ with the cell dimensions of $a = 78.3$Å, $b = 75.0$Å, $c = 102.1$Å, $\alpha = 80.4°$, $\beta = 78.3°$, $\gamma = 82.3°$. The crystals diffract to approximately 2.8Å, and a native data set was collected up to 3.0Å using synchrotron radiation at the Photon Factory, KEK, Japan. The self-rotation function revealed the existence of fivefold and twofold axes which are located perpendicularly to each other, suggesting that AhpC protein forms a molecular assembly composed of ten monomers.

1. Niimura, Y., Pool L. B., and Massey, V.(1995). J. Biol. Chem. 270, 25645-25650.

14P27

TRIPLE-HELICAL STRUCTURE OF COLLAGEN MODEL POLYPEPTIDES

K. Okuyama, V. Nagarajan, G. Aizawa, C. Hongo, S. Kamitori,
Faculty of Technology, Tokyo University of Agriculture and Technology,
and Y. Tanaka, N. Nishino, Institute for Fundamental Research of Organic Chemistry, Kyushu University

Collagen molecule has a triple-helical structure due to the strict sequence constraints with glycine as every third residue and a high content of imino acids. For the detailed structure of collagen, two models have been generally accepted. One is the Rich and Crick model in which each strand has a 10/1-helical symmetry with a pitch of 86Å. The other is the Okuyama model in which each strand has a 7/1-helical symmetry with a pitch of 60Å. Due to the symmetry among triple strands, the repeating period along the *c*-axis becomes one third of their pitch length. Both the models could explain the fiber diffraction pattern of native collagen.

Recently, we succeeded in obtaining single crystals of collagen model peptides, (Pro-Pro-Gly)n (n=9, 10, 11) and (Pro-Hyp-Gly)n (n=10). In addition to the true repeat along the *c*-axis (80Å for n=9 and 100Å for n=10), all the diffraction data clearly show a strong 20Å repeat, which corresponds to the repeating period of the Okuyama model (Fig.1). On the other hand, the Rich and Crick model has no such supporting data other than fiber diffraction analysis of collagen.

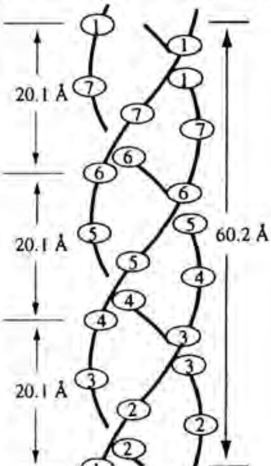

Fig. 1 Schematic illustration of the Okuyama model. Each numbered ellipse represents a Gly-X-Y triplet.

14P28

MEASUREMENT OF CRYSTAL GROWTH RATE OF TETRAGONAL HEN EGG WHITE LYSOZYME WITH ATOMIC FORCE MICROSCOPY

L. Rong[a], T. Yamane[a] and N. Niimura[b], [a]*Graduate school of Engineering, Nagoya University,* [b]*Neutron in Biology, Advanced Science Research Center, Japan Atomic Energy Research Institute*

The success in the structure analysis of biological macromolecules using either X-ray or neutron diffraction experiments depends on the availability of proper single crystals. Protein single crystals have traditionally been grown in trial-and-error methods. Rational design of the crystal growth based on basic understanding of the growth mechanism is more and more called for. One of the most effective way is the in situ observation of the crystal growth front in a molecular scale. Since an atomic force microscope(AFM) can provide a unique tool for seeing alignment of each protein molecule on the crystal surface in mother liquor, the AFM can be a good candidate to monitor whether a protein molecule is taken into the crystal lattice properly according to the crystal symmetry (1, 2).

Step growth rate (SGR) of (110) plane of a tetragonal hen egg-white lysozyme (lysozyme) crystal could be controlled and measured accurately in nanometer scale by using a specially designed sealed sample vessel of our AFM. The SGR was obtained as proportional to (C-Cs)n, where C and Cs are concentration and solubility of lysozyme, respectively. The exponent n was experimentally determined as 2.1, 2.7 and 2.3 at NaCl (precipitant) concentration of 20 mg/ml, 40 mg/ml and 60 mg/ml, respectively. The detailed experimental procedure and discussion will be given in the report.

1.Durbin, S. D. and Carlson, W. E. (1992)*J. Crystal Growth.* **122**, 71-79.
2.Konnert, J. H., D'Antonio, P. and Ward, K. B. (1994).*Acta Cryst.* **D50**, 603-613.

14P29

CRYSTAL STRUCTURE ANALYSIS OF ß-AMYLASE FROM *BACILLUS POLYMYXA*

M. Akita, H. Tasaki, F. Matsumoto, A. Suzuki, T. Yamane, and T. Ashida *Graduate School of Engineering, Nagoya University,* and N. Uozumi, *Bioscience Center, Nagoya University*

Bacterial ß-amylases could be applied industrially in the direct production of maltose from raw starch if their thermal stability can be improved. For the purpose of molecular design of ß-amylase on the basis of 3D-structure, we began the crystal structure analysis of the 51 kDa ß-amylase from *Bacillus polymyxa*.

The ß-amylase was expressed in *Bacillus subtilis* (1). Crystals were prepared by the hanging-drop vapor-diffusion method with 2.05M ammonium sulfate and 2.0% (w/v) polyethylene glycol 400 at pH 8.0, 277K. The crystals belong to orthorhombic space group $P2_12_12_1$ with cell dimensions of a=64.6, b=141.9 and c=155.1Å, and diffract up to 2.5Å resolution. Two isomorphous derivatives were prepared by soaking crystals in either 1mM solution of $Hg(CH_3COO)_2$ or K_2PtCl_4 for 1 day.

X-ray diffraction data up to 3.5Å resolution for the native and two derivative crystals were collected on a DIP-100 detector system (MAC Science) mounted on a Rigaku RU-300 generator at 293K. Oscillation images were processed with programs DENZO and SCALEPACK. Three Hg-sites and two Pt-sites were found by the Patterson vector search method with the program system PROTEIN. Protein phases were calculated with MLPHARE and improved by the solvent-flattening method with DM.

The molecular boundaries were clearly distinguished from solvent regions on an electron density map at 4.0Å resolution. Three molecules were identified in the asymmetric unit, which resulted in Vm= 2.36$Å^3$/Da. Molecular averaging is under way.

1. Uozumi, N., Matsuda, T., Tsukagoshi, N. & Udaka, S. (1991). *Biochemistry,* **30**, 4594-4599.

14P30

CRYSTAL STRUCTURE OF AZIDE BOUND CYTOCHROME C OXIDASE AT 2.9Å RESOLUTION FROM BOVINE

M.Fei, E.Yamashita, N.Inoue, T.Mizushima, H.Aoyama, T.Tomisaki, T.Tsukihara, Institute for Protein Research of Osaka University, Japan
K.Shinzawa-Itoh, R.Nakashima, R.Yaono & S.Yoshikawa, Faculty of Science, Himeji Institute for Technology, Kamigori, Hyogo, Japan

The crystal structure of azide bound cytochrome c oxidase from bovine heart has been determined at 2.9 Å resolution with a *R* factor of 0.193 and a free *R* value of 0.255. Crystals of oxidized cytochrome c oxidase were soaked with 5% sodium azide for four days to prepare azide bound crystals. Data sets used in the structure determination were collected by a Weissenberg camera for macromolecular crystals, with monochromized x-ray of 1.0 Å at the Photon Factory, Tsukuba, Japan. The crystals belong to the orthorhombic space group $P2_12_12_1$, with cell dimensions a=189.2 Å, b=210.6 Å, c=178.5 Å. The structure was determined with the multiple isomorphous replacement (MIR) method. Two possible binding sites of azide, which located between Cu_B and Fe_{a3} and at the surface of the protein, were identified respectively. In contrast to the bacterial enzyme (1), with one of the three imidazole ligands to Cu_B missing when in azide-bound fully oxidized state, the electron density of all three histidine ligands to Cu_B for bovine has been seen clearly. This is not consistent with the histidine shuttle mechanism for proton pumping proposed by previous authors (1).

1. Iwata, S., Ostermeier, C., Ludwig, B. & Michel, H. (1995). *Nature*, **376**, 660-669.

14P31

PRELIMINARY X-RAY CRYSTALLOGRAPHIC STUDIES OF FARNESYL DIPHOSPHATE SYNTHASE FROM *Bacillus stearothermophilus.*

M. Fujihashi [a], T. Koyama [b] AND K. Miki [a], [a] Department of Chemistry, Graduate School of Science, Kyoto University, Kyoto, Japan, and [b] Institute for Chemical Reaction Science, Tohoku University, Sendai, Japan

Farnesyl diphosphate synthase (FPS), one of prenyltransferases, is a key enzyme in isoprenoid biosynthesis. It catalyzes the stereospecific condensation of isopentenyl diphosphate with dimethylallyl diphosphate and with geranyl diphosphate to produce farnesyl diphosphate. The enzyme from *Bacillus stearothermophilus* is a thermostable homodimer (32kDa × 2).

Crystals of *B. stearothermophilus* FPS were obtained at 20°C in two forms. Form I crystals grown from ammonium sulfate solutions at pH 5.4 belong to the tetragonal space group $I4_122$ with unit-cell dimensions of a=b=114Å and c=247Å (1). Assuming one dimer molecule per asymmetric unit, V_M is calculated to be 3.1 Å^3/Da. Form II crystals were grown from PEG8000 solutions at pH 7.5. They belong to the monoclinic system with unit-cell dimensions of a=57Å, b=60Å, c=99Å, and β=115°. V_M is calculated to be 2.4 Å^3/Da, assuming one dimer molecule per asymmetric unit. Both the crystal forms diffract X-ray beyond 3.0 Å resolution by the use of synchrotron radiation. Structure determination is in progress by both molecular replacement and isomorphous replacement methods.

1. Nakane, H. *et al.* (1993) J. Mol. Biol., 233, 787-788.

14P32

POLYMORPHISM OF A Co(III)-SALEN SCHIFF BASE COMPLEX

S. Sato ,X-ray Research Laboratory, Rigaku Corporation, Tokyo, Japan and T.Fukuda, K.Ishii, Y. Nakano and Y. Fujii ,Faculty of Science, Ibaraki University, Mito, Japan

A complex, [N,N'-bis(salicyliden)-(2S, 3S)-[butanediaminato]-bis(pyridine)cobalt(III) tetrafluoroborate water, showed a polymorphism crystalizing in two systems: one is hexagonal[$P6_522$; a=10.422(6), c=101.433(7)Å; V=9541(6)Å^3; Z=12], and the other is monoclinic[$C2$; a=10.305(2), b=18.047(3), c= 50.764(2)Å; b=92.46°(1); V=9432(2)Å^3; Z=12]. The polymorphism was occasionally found as the two types of the crystal coexisted in the product by recrystallization from an aqueous methanol. The crystal shapes of both types were dark brown thick hexagonal plate, and very difficult to distinguish them from their appearances. The relation between both cells are: **a**(m) ≈ **a**(h), **b**(m) ≈ **a**(h)+2**b**(h) and **c**(m) ≈ **c**(h)/2. Structures were determined from intensity data by *w*-scan with Cu *Ka* radiation for the hexagonal crystal(R=0.054) and *w*-2*q* scan, Mo *Ka* radiation for the monoclinic one(R=0.054). The complex cation adopts pseudo-octahedral coordination with an approximate twofold axis of rotation comprising a tetradentate salen Schiff base ligand at equatorial and two pyridine ligands at axial positions. The geometries of the cation in both systems are quite similar.

The cations in the hexagonal cell show a spiral arrangement with a very long period along **c**(h). Two cations each in the spiral form a dimer by *p*-bonds between the pyridine rings overlapping with van der Waals contacts of about 3.5Å. Layers of the cation dimers and those of anions parallel to the (110) plane are alternately stacked in the crystal.

The spiral arrangement, dimer formation and layer structure are similarly realized in the monoclinic cell. Two spirals in the cell are not complete with only a half unit of that in the hexagonal cell . A hypothetic structure can be constructed by a simple modification of the monoclinic cells stacking along **c**(m) so that the orientations of the cells are alternately reversed by 180° rotation around **a**(m). The structure thus constructed has a close resemblance to the hexagonal one. The poly-morphism is possibly caused by slight positional differences of the anions.

STRUCTURAL STUDIES OF SOME CLONIDINE DERIVATIVES

E.M.ELSSFAH[a], H.K.Fun[a], K.Chinnakali[a], I.W.Mathison[b], E.K.Gan[c], T.W.Sam[d], C.Y.Tan[d] AND M.Zubaid[c], [a]School of Physics; [c]School of Pharmaceutical Sciences; [d]School of Chemical Sciences, Universiti Sains Malaysia, 11800 USM, Penang, Malaysia. [b]College of Pharmacy, Ferris State University, Big Rapids, MI 49307-2740, USA.

Clonidine, 2-(2,6-dichlorophenylimino)-2-imidazolidine, is one of the centrally acting antihypertensive drugs which act primarily via α-adrenoceptors in the brain. Hypotensive activity of this molecule is governed by distinct steric and electronic characteristics. Electronic interactions, charge transfer, hydrogen bonding, steric requirements of the substituents as well as the effects exerted by them play an important role in the hypotensive activity (1). Chemical manipulation of the structure of the phenyl moiety, its substitution pattern or the heterocyclic nucleus has only led to some compounds with an equal or lower hypotensive activity than clonidine. The most active compounds are those with 2,6-phenyl substituents in which rotation is restricted. As a part of our study on the search for active hypotensive drugs, we have synthesised several clonidine derivatives and X-ray structure determinations have been carried out in order to correlate the structures and pharmacological activity of these compounds. The details of the crystal structure investigation will be presented.

1. Timmermans, P.B.M.W.M & van Zwieten, P.A. (1977). J. Med. Chem. 20, 1636-1644.

CONFORMATIONAL STUDIES ON TWO XANTHENE DERIVATIVES TO CORRELATE THE STRUCTURE WITH THEIR FUNCTION.

J.Jeyakanthan, D.Velmurugan, Dept. of Crystallography and Biophysics, University of Madras, Chennai – 600 025, INDIA and S.Shanmuga Sundra Raj, Hoong-Kun Fun, X-ray Crystallography Unit, School of Physics, Universiti Sains Malaysia, 11800 USM, Penang, Malaysia.

Xanthene derivatives are known to exhibit many important biological activities. Many derivatives reduced the blood pressure gradually with long lasing action. The central ring of the xanthene moiety is planar and the two outer rings are in sofa conformations. Due to the π-conjugation, there is an electron delocalization stretch. In these compounds, the axial methyl groups are oriented in opposite directions. The phenyl ring is perpendicular to the xanthene ring system. Molecules are held together by C-H...O hydrogen bonds. **Crystal data: (I)**: $C_{17}H_{22}O_3$, a = 7.146(1), b = 9.769(1) and c = 11.886(2)Å, α = 110.78(1), β = 96.07(1) and γ = 101.30(1)°, V = 746.6(2)$Å^3$, F.W = 274.35, triclinic, P-1and Z = 2. The final R = 0.044 and R_w = 0.123 for 3331 reflections (MoKα, λ = 0.71073Å) with I > 2σ(I). **(II)**: $C_{23}H_{25}NO_5$, a = 26.581(2), b = 10.094(1) and c = 19.624(2) Å, β = 128.75(1)°, V = 4106.3(7)$Å^3$, F.W = 395.44, Monoclinic, C2/c and Z = 8. The final R = 0.043 and R_w = 0.080 for 4711 reflections (MoKα, λ = 0.71073Å) with I > 2σ(I).

Structure solution: SHELXS86, Refinement: SHELXL93. The conformational features will be presented.

14P35

CRYSTAL STRUCTURE OF (IR, 2S)-2-(N-METHYL-N-TOLUENESULFONYL)AMINO-1-PHENYL-1-PROPANOL

K.Chinnakali* AND H.K.Fun, X-ray Crystallography Unit, School of Physics, Universiti Sains Malaysia, 11800 USM, Penang, Malaysia.
K.Sriraghavan AND V.T.Ramakrishnan, Department of Organic Chemistry, University of Madras, Chennai 600 025, India.
* On leave from the Dept. of Physics, Anna University, Chennai-25, India.

The title compound is a N-tosyl derivative of (-)ephedrine. Generally, Ephedrine and its derivatives are used as sympathomimetic agent for allergic disorders, CNS stimulation, prophylaxis and treatment of hypertension and hypersensitive cartidsinus. It has also been used as nasal congestion and as mydriatis (1,2). Crystal data: a=6.0272(2), b=18.6624(8), c= 7.3642(3)Å, β=98.15(1)°, Space group $P2_1$, Z=2 and R=0.040. The sulphur atom is in a tetrahedral coordination and the nitrogen atom is in the planar configuration. The planar phenyl rings form a dihedral angle of 59.17(8)° between them. In the solid state, the phenyl rings are stacked along the c direction. One of the sulfonyl oxygen is involved in an C-H..O intramolecular hydrogen bond. The crystal structure is stabilised by van der Waals interactions.

1. The Merck Index of Chemicals and drugs.(1960) Editor. Paul.G.Steeher, p-403, Merck:USA.
2. The Merck Index, 11 th Edition (1989). Editor. Susan Budavari.

14P36

THE FIRST EXAMPLE OF THE *mer*-Oh GEOMETRY IN A SIX-COORDINATE TRIORGANOTIN COMPOUND : TRIFLUOROACETATOTRIPHENYLTIN 3, 4, 7, 8 - TETRAMETHYL -1, 10 - PHENANTHROLINE (1/1)

N.S.Weng ; Institute of Postgraduate Studies and Research, University of Malaya, 50603 Kuala Lumpur, Malaysia

$C_{36}H_{31}N_2O_2F_{39}Sn$:monoclinic $P\,21/c$ space group, a=9.170(1), b=10.372(1), c=33.041(4), β=95.05(1)° , V = 3130.3(7) Å^3. The structure was refined from the 5396 independent reflections that measured on a *CAD* -4 diffractometer(Mo-$K\,\alpha$, $2\,\theta$=50° : $0 \leq h \leq 10$, $0 \leq k \leq 12$, $-39 \leq l \leq 39$) to R =0.0433 for 3631 $I \geq 2\,\sigma\,(1)$ reflections. The tin atom is six-coordinate in a *mer* - C_3SnN_2O octahedral geometry.

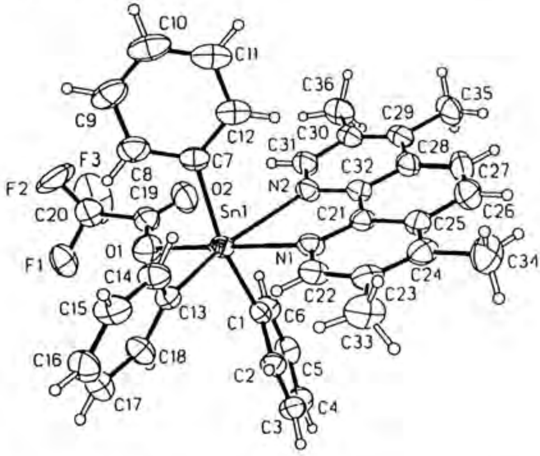

Figure 1. *ORTEP* plot of triphenyltin trifliproacetate 3,4,7,8 - tetramethyl-1, 10- phenanthroline at the 30% probability level. Selected bond distances and angles: Snl-Cl=2.145(5), Snl-C7=2.149(5), Snl-Cl3=2.175(5), Snl-Nl=2.395(4), Snl-N2=20601(4), Snl-O1=20256(4), Snl···O2=3.400(5) Å ; Cl-Snl-C7=159.0(2), Cl-Snl-C13=102.7(2), Cl-Snl-Nl=89.2(2), Cl-Snl-N2=80.5(2), Cl-Snl-Ol= 88.4(2),C7-Snl-Cl3=97.9(2), C7-Snl-Nl=93.6(2), C7-Snl-N2=81.8(2), C7-Snl-Ol= 87.7(2), Cl3-Snl-Nl=93.3(2), Cl3-Snl-N2=158.8(2), Cl3-Snl-Ol=89.8(2), Nl-Snl-N2=65.6(1), Nl-Snl-Ol=176.5(2), N2-Snl-Ol=111.4(1)°

14P37

CRYSTAL STRUCTURE DETERMINATION OF PLATYPHYLLINE

S. Ozturk* AND H. K. Fun, X-ray Crystallography Unit, School of Physics, Universiti Sains Malaysia, 11800 USM, Malaysia.

S. Ide, Department of Engineering Physics, Hacettepe University, Beytepe, Ankara-06532 Turkey.

B. Sener, Department of Pharmacognosy, Faculty of Pharmacy, Gazi University, Ankara-06330 Turkey.

*On leave from:Department of Physics, Faculty of Arts and Sciences, Erciyes University, Kayseri-38039, Turkey.

For many years, senecio species belonging to the family of *Asteraceae*, are known as a rich source of pyrrolizidine alkaloids. The hepatotoxic nature of the pyrrolizidine alkaloids from the senecio species has enjoyed wide spread interest. Platyphylline as a pyrrolizidine type alkoloid has been isolated from senecio othonnae and senecio pseudo-orientalis growing in Turkey (1,2). The work reported here is part of a project aimed at providing a better understanding of the structural properties of these bioactive natural compounds. The pyrrolizidine nucleus exhibits exo-buckling conformation. Crystal Data: $C_{18}H_{29}NO_5.0.5H_2O$, $M_r = 348.43$, Orthorhombic, $P2_12_12_1$, $a = 9.4250(2)$, $b = 13.2220(2)$, $c = 15.3326(3)$ Å, $V = 1910.71(6)$ Å^3, $Z = 4$, $T = 293(2)$ K, $R = 0.066$ for 2493 observed data with $I > 2\sigma I$.

1. Sener, B., Kusmenoglu, S., Ergun, F. & Karakaya, A. E. (1986). J. Fac. Pharm. Gazi, 3(2), 105-107.
2. Sener, B., Kusmenoglu, S., Ergun, F. & Karakaya, A. E. (1986). J. Fac. Pharm. Gazi, 5(1), 101-104.

14P38

THE STRUCTURE OF GOSSYPOL 1:2 HOST-GUEST COMPLEX WITH TROPOLONE

[a]S.A.Talipov, [b]Y.Ohashi, [a]B.T.Ibragimov, [b]J.Harada, [c]M.I.Saleh, [c]B.Saad;
[a]Institute of Bioorganic Chemistry, H.Abdullaev Str., 83, Tashkent, 700143, Uzbekistan, [b]Department of Chemistry, Tokyo Institute of Technology, Ookayama, Mesuro-ku, Tokyo 152-8551, Japan and [c]School of Chemical Sciences, Universiti Sains Malaysia, 11800 USM, Penang, Malaysia

Gossypol a bioactive polyphenolic yellow pigment of cotton seeds is a versatile host easily forming lattice inclusion complexes with a large number of organic guest species.Its all over 100 up to now known host-guest complexes are molecular crystals guest components of which are liquids under ambient conditions.Tropolone (2-hydroxy-2,4,6-cycloheptatrien-1-one), $C_7H_6O_2$, is a representative of the non-benzenoid aromatic compounds. In ordinary conditions tropolone is a solid crystalline material. Here we present the crystal structure of the 1:2 gossypol:tropolone complex.

Crystal data are: $C_{30}H_{30}O_8$ $2C_7H_6O_2$, M= 762.78, Monoclinic, C2/c, a=35.5892(10) Å, b=12.8893(2) Å, c=18.5910(2) Å, β=118.5353(6)°, V=7492.10(14) $Å^3$, Z=8, D=1.352 gcm^{-3}, λ=0.71073 Å, T=100 K

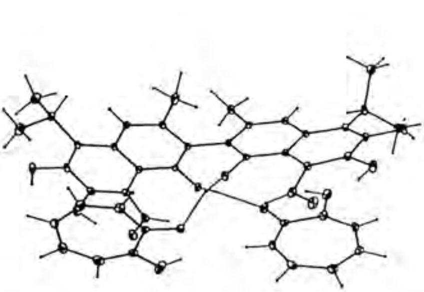

In crystal structure glide-plane-related gossypol molecules form monolayers by the two types of H-bonding. Monolayers are in contact with other ones from one side whereas from other side they contact with tropolone molecules, which assist to gossypol molecules in H-bonding as acceptor. By other words bilayers of host molecules alternate with layers of guest molecules along c-axes.

14P39

CRYSTAL STRUCTURE OF A MONOMERIC PALLADIUM (II) COMPLEX

K. Panneerselvam[a], T. -H. Lu,[a] S. -F. Tung,[b] V. K. Jain[c] and S. Narayan[c],
[a]Department of Physics, National Tsing Hua University, Hsinchu, Taiwan 300, R.O.C. [b]Southern Instrument Center, National Cheng Kung University, Tainan, Taiwan 701, R.O.C. [c]Chemistry Division, Bhabha Atomic Research Centre, Mumbai 400 085, India.

The structure of $[Pd(Spy)\{S_2P(OPr^i)_2\}(PPh_3)]$, has been investigated as part of our studies on the crystal chemistry. The high propensity of organochalcogenide ligands (S, Se, Te) to bridge two metal atoms normally makes them unsuitable for isolation of monomeric complexes. Recently we have isolated a number of palladium (II) and Platinum (II) organochacogenolates employing chelating phosphine ligands. This compound was synthesized and analyzed by x-ray diffraction in addition to the studies of mass, IR and NMR spectra. Crystals were obtained by slow evaporation of CH_2Cl_2-hexane mixture to give red crystalline solid. Crystal data: Monoclinic, $P2_1/n$ with lattice parameters $a = 14.867(4)$, $b = 10.160(1)$, $c = 21.136(4)$A, $\beta = 93.18(1)°$, Z = 4. The refinement on F^2 converged at $R = 0.0464$, $wR^2 = 0.1067$, $S = 1.09$ for 3643 reflections with $I > 2\sigma(I)$. The structure consists of discrete molecule with square planar configuration around palladium which is coordinated to an aymmetrically chelated $(OPr^i)_2\ PS_2^-$ ligand, PPh3 and pyS^- groups. The palladium atom is slightly away (0.035(1)A) from its coordination plane. The Pd - P bond lengths, as usual, less than the radius sum. The P - S bond lengths are intermediate between double and single bond values confirming partial double bond character. The pyridine plane of the Spy ligand is nearly perpendicular to the coordination plane of palladium.

14P40

STRUCTURAL CHEMISTRY OF dppe-BRIDGING DICATION $[\{(\eta^5\text{-}C_5H_5)Fe(CO)_2\}_2(\mu\text{-}\eta^1\text{:}\eta^1\text{-dppe})^{2+}]$

Ling-Kang Liu, Yuh-Sheng Wen, Cheng Peng, and Olalere Adeyemi
Institute of Chemistry, Academia Sinica, Taipei, Taiwan 11529 ROC

The phosphine exchange reaction has been employed to evaluate the fine-tuning tri(aryl)phosphine donor capability, taking advantage of a rapid establishment of equilibrium with the facile radical mechanism in the following equation: $[(\eta^5\text{-}C_5H_5)Fe(CO)_2PPh_3^+][PF_6^-] + PAr_3 = [(\eta^5\text{-}C_5H_5)Fe\text{-}(CO)_2PAr_3^+][PF_6^-] + PPh_3$ where $PAr_3 = PPh_2Py$, $PPhPy_2$, PPy_3, *etc*. The donor capability has been found in increasing order of $PPh_3 < PPh_2Py < PPhPy_2 < PPy_3$. The strategy has been extended to the preparation of $[\{(\eta^5\text{-}C_5H_5)Fe(CO)_2\}_2(\mu\text{-}\eta^1\text{:}\eta^1\text{-dppe})^{2+}][PF_6^-]_2$ whereby after treatment of trace $(\eta^5\text{-}C_5H_5)_2Co$, a 2:1 $[(\eta^5\text{-}C_5H_5)Fe(CO)_2PPh_3^+][PF_6^-]$/dppe mixture in THF produces precipitates of $[\{(\eta^5\text{-}C_5H_5)Fe(CO)_2\}_2(\mu\text{-}\eta^1\text{:}\eta^1\text{-dppe})^{2+}][PF_6^-]_2$ quantitatively. The literature preparation of $[\{(\eta^5\text{-}C_5H_5)Fe(CO)_2\}_2(\mu\text{-}\eta^1\text{:}\eta^1\text{-dppe})^{2+}]$ dication requires an oxidative cleavage of $[(\eta^5\text{-}C_5H_5)Fe(CO)_2]_2$ in acetone by $Fe(ClO_4)_3$, followed by addition of limiting dppe (0.125 equiv). The present radical pathway is apparently much easier in operation. The X-ray structure of $[\{(\eta^5\text{-}C_5H_5)Fe(CO)_2\}_2(\mu\text{-}\eta^1\text{:}\eta^1\text{-dppe})^{2+}][PF_6^-]_2$ exhibits a loosely planar P-C-C-P skeleton, to which the two $(\eta^5\text{-}C_5H_5)Fe(CO)_2$ moieties are conformationally *syn* with each other. The X-ray structure of anion-exchanged $[\{(\eta^5\text{-}C_5H_5)Fe(CO)_2\}_2(\mu\text{-}\eta^1\text{:}\eta^1\text{-dppe})^{2+}][BPh_4^-]_2$ exhibits alternatively *trans*-$(\eta^5\text{-}C_5H_5)Fe(CO)_2$-P-C-C-P-$(\eta^5\text{-}C_5H_5)Fe(CO)_2$ skeleton.

Structure in PF_6^- salt *vs.* Structure in BPh_4^- salt

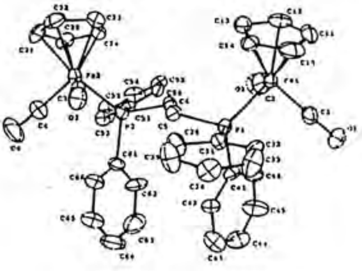

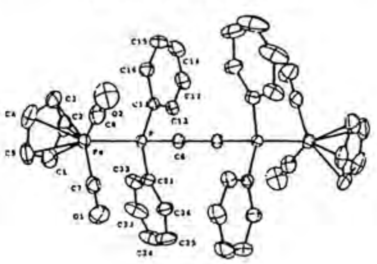

14P41

CRYSTAL AND MOLECULAR STRUCTURE OF 9-3,4,6,7,9,10-HEXAHYDRO-3,3,6,6-TETRAMETHYL-1,8(2H,5H)-ACRIDINE-DIONE

R.Sankaranarayanan, D.Velmurugan, Dept. of Crystallography and Biophysics, University of Madras, Chennai – 600 025, INDIA and S.Shanmuga Sundra Raj, Hoong-Kun Fun, X-ray Crystallography Unit, School of Physics, Universiti Sains Malaysia, 11800 USM, Penang, Malaysia.

Inspite of being an anti-tumor, anti-bacterial and anti-inflammatory agent, acridines are known to be potent DNA intercalators. The title compound is a derivative of acridine whose central ring is nearly planar and the two outer rings are in chair conformations.

Crystal data: : $C_{20}H_{23}NO_2$, a = 6.989(2), b = 10.712(2) and c = 20.420(4)Å, $\alpha = \beta = \gamma = 90°$, V = 1528.7(1)$Å^3$, orthorhombic, $P2_12_12_1$, Z = 4, λ = 0.71073 Å, D_c=1.179g-cm^{-3}. The final R = 0.054 and *w*R = 0.098 for 3495 reflections with $I > 2\sigma(I)$. The structure was solved using SHELXS-86 and refined using SHELXL-93. All the hydrogens are taken from difference Fourier map and are isotropically refined. The geometrical and conformational features will be presented in detail.

INVESTIGATION OF THE HYDROQUINONE CRYSTALLIZATION AT DIFFERENT TEMPERATURES AND CRYSTAL STRUCTURE OF THE NEW HYDROQUINONE - ACETONE COMPLEX. SIMULTANEOUSCRYSTALLIZATION OF THE α-, β- AND γ-HYDROQUINONES FROM ONE SOLUTION

K.K. Makhkamov, B.T. Ibragimov, K.M. Beketov AND G.B. Nazarov,
Institute of Bioorganic Chemistry, Tashkent, Uzbekistan

It is known that a most stable modification of hydroquinone is its α-polymorph. β-hydroquinone with empty cages is obtained from the solution in *n*-octan and γ-polymorph is prepared by rapid crystallization from solution in ether (1). We obtained single crystals of the all these three polymorphs of hydroquinone from the one solution - solution of the 1:1 hydroquinone:phenol mixture in acetone at room temperature. β-polymorph is also obtained from solution of hydroquinone in *meta-* or *orto*-xylene+acetone and CH_2Cl_2+ether at ambient conditions. At 40°C instead of β-modification α-polymorph is crystallized from solution in *o*-xylene+acetone. If phenol is added to this solution at 40°C β-polymorph continues to form.

An investigations of the hydroquinone crystallization from solutions in acetone show that below room temperature a complex of hydroquinone with acetone is formed while at high temperatures α-polymorph of hydroquinone is crystallized. Crystal data of the new complex are: *C2\c*, a=18.583 (4) Å, b=7.144 (1) Å, c=7.421 (1) Å, β=110.60 (3)°, V=922 Å^3.

In the complex acetone molecules behave as double protonoacceptors in the H-bonding and incorporate hydroquinone molecules to the endless chains running in the [101] direction. Packing of these chains to crystal structure is occurred in such manner that hydroquinone units of the two neighbouring chains is found to be in the orthogonal contacts.

1. Mak, T.C.W. and Bracke, B.R.F. (1996). Comprehensive Supramolecular Chemistry, Vol. 6, (Crystal Engineering), (Ed: J.L.Atwood, J.E.D.Davies, D.D.MacNicol & F.Vogtle), Oxford, Elsevier Science, 351 - 370

CRYSTAL STRUCTURES OF TWO COPPER(II) COMPLEXES

S. Chantrapromma[a], S. Youngmee[b], K. Poopasit[b], K. Chinnakali[c] and H.K. Fun[c]; [a]Department of Chemistry, Faculty of Science, Prince of Songkla University, Hat-Yai, Songkhla 90112, THAILAND.,[b]Department of Chemistry, Faculty of Science, Khonkaen University, Khonkaen 40002, THAILAND.[c]School of Physics, Universiti Sains Malaysia, 11800 USM, Penang, MALAYSIA.

The crystal structures of the copper(II) dimers have been well characterised (1). Only a few crystal structures of the dihydroxy-bridged copper(II) dimer involving the dpyam ligand have been reported. Here we present the crystal structure analysis of a dihydroxy-bridged copper(II) dimer, namely, Di- μ -hydroxy-bis(di-2-pyridylamine) dicopper(II) diperchlorate (a=7.5307(2), b=9.5330(3), c=9.7841(3), α=73.194(1), β = 80.950(1), γ=70.617(1), P1, z=2, R=0.037) and also the structure of Diaqua-bis (di-2-pyridylamine) copper(II) Sulfate Heptahydrate (a=10.8765(2), b=12.1197(2), c= 22.5406(4), β=98.356(1), $P2_1/c$, z=4, R=0.053). The copper atom in the dihydroxy-bridged dimer is in a square-planar geometry and if the longer coordination at 2.724(7) Å of one of the perchlorate oxygen is considered to be significant then the geometry can be explained as a square pyramidal. In the other structure the copper atom is in a square-pyramidal environment.

1. Hathaway, B. J.(1987). In Comprehensive Coordination Chemistry. The Synthesis, Reactions, Properties and Applications of Coordination Compounds. Editors: Gillard & McCleverty, Vol.5, Section 53, 533-774, Oxford: Pergamon.

A FRAMEWORK ARCHITECTURE VIA COORDINATION AND π - π INTERACTIONS: $[(VO)_2(OH)_2(C_4O_4)(Phen)_2 . H_2O]_n$

K. J. Lin, Institute of Chemistry, Academia Sinica, Taipei, Taiwan;

Supermolecules or coordination polymers with infinite two- or three-dimensional frameworks are of intense current interest because of their unique physical and chemical properties, such as magnetism, host-guest chemistry, and catalysis. Our aim is to synthesize porous coordination solid possessing open-framework structures with cavities or channels. Here we demonstrate that the squarate ligands are effective tethers for the construction of extended solids. A binuclear vanadyl (VO^{2+}) squarate chain incorporating phenanthroline ligands, $[(VO)_2(OH)_2(C_4O_4)(Phen)_2 . H_2O]_n$, was synthesized and structurally characterized by single crystal X-ray diffraction. It adopts a neutral three-dimensional framework with channels containing water molecules at the intersection of channels. This compound is of interest with respect to the supermolecular architecture via coordination and π - π Interactions. To our knowledge, cooperative π - π scaffolding is rare and has never been observed in microporous materials.

Crystal data: monoclinic system, space group C2/c, a =20.707(3) Å, b = 9.331(2) Å, c=17.050(5) Å, β= 123.85(2); V=2736(1) $Å^3$, Z=4, F(000) =1336, R_1=0.0351, $wR_2(F^2)$ =0.0897 and *GOF*=0.955; residual density: max =0.27, min =-0.36 e$Å^{-3}$.

14P45

PROTONATION AND OLIGOMERIZATION OF TETRAALKYLAMMONIUM DECAVANADATES

S.Nakamura & T.Ozeki, Tokyo Institute of Technology

Many polyoxoanions protonate in aqueous solution in multiple steps depending on the acidity of surroundings. We have a special interest in the protonation sites and the hydrogen-bond acceptor sites of polyoxoanions, since these sites are considered to be basic and can easily attract electrophilic compounds. This provides a first step toward understanding the various reactivities of these species. In this study, in order to clarify the charge distribution and the nature of decavanadate anion, we carried out X-ray structure analyses and IR spectroscopic investigations on 11 kinds of tetraalkylammonium salts $[R_4N]_{6-n}[H_nV_{10}O_{28}]$, where $R=CH_3 \sim C_6H_{13}$, which were obtained from aqueous and non aqueous solutions.

Di-, tri- and tetraprotonated species crystallized from aqueous solutions. Diprotonated anions $[H_2V_{10}O_{28}]^{4-}$ form hydrogen-bonded dimers $([H_2V_{10}O_{28}]_2)^{8-}$. Triprotonated ones $[H_3V_{10}O_{28}]^{3-}$ also aggregate, forming two types of dimers. Tetraprotonated anions build a hydrogen-bonded polymer $([H_4V_{10}O_{28}]^{2-})_\infty$. From the nonpolar protophilic solvents, both tri- and tetraprotonated anions were crystallized. While the triprotonated anions form dimers, the tetraprotonated ones do not aggregate, but are hydrogen-bonded to solvent molecules, in contrast to the polymeric structure in the salts obtained from aqueous solution. In the salts recrystallized from the polar protophobic solvents, only the triprotonated dimers $([H_3V_{10}O_{28}]_2)^{6-}$ were observed, which interacts electrostaticically with solvent molecules located midway between anions and cations.

The protonation occur at the oxygen atoms bridging equatorial and apical vanadium atoms, giving rise to surface OH groups. Most of the other oxygen atoms can play the hydrogen-bond acceptors. The OH groups show various kinds of geometries with respect to the decavanadate framework. The versatility in the directions of the O-H bonds allows the protonated anions to form various kinds of hydrogen bonds to the other anions or solvents.

14P46

THE CHEMISTRY AND STRUCTURAL PROPERTIES OF PALLADIUM-OSMIUM MIXED-METAL CARBONYL CLUSTERS

W.T. Wong, Department of Chemistry, The University of Hong Kong, Pokfulam Road, Hong Kong, P.R. China

The chemistry of bimetallic clusters has received much current attention because of their potential for cooperative reactivity in the activation of small molecules and in catalysis. Recent studies have shown that mixed-metal cluster complexes are capable of catalysing a variety of organic transformations. Molecular mixed-metal clusters have been used to prepare bimetallic supported nanoparticles that are active catalysts. It is believed that bimetallic clusters of palladium and osmium are of interest as the palladium ion can attain either a 16- or an 18-electron configuration which is an important feature for catalytic processes. On the other hand, osmium clusters display very rich chemistry and are kinetically stable, thus allowing for easy isolation and characterization. Interaction of the unsaturated cluster $[Os_3(\mu\text{-}H)_2(CO)_{10}]$ with trans-$[Pd(py)_2Cl_2]$ and trans-$[Pd(py)_2Cl_2]$ and trans-$[Pd(py)_2I_2]$ (py = pyridine) was found to yield a series of hydrido heterometallic complexes with a common $\{Os_3Pd\}$ tetrahedron unit. Palladium reagents containing phosphorus donor ligands have also been used to construct mixed-metal clusters of Os-Pd. Reactions of pentaosmium carbide cluster $[Os_5C(CO)_{15}]$ with $[Pd(PPh_3)_4]$ and $[PdCl_2(PPh_3)_2]$ gave $[Os_5PdC(CO)_{12}(\mu\text{-}CO)_2(PPh_3)_2]$ and $[OsPd(CO)_{15}(\mu\text{-}Cl_2)(PPh_3)]$. Both of them contain a novel metal core.

14P47

SYNTHESIS AND CRYSTAL STRUCTURE OF A NEW MOLYBDENUM OXALATE COMPLEX $K6[Mo_2(\mu\text{-}O)(\mu\text{-}S)O_2(ClPO_3)_2(C_2O_4)_2] \cdot 3H_2O$

Y.-H.Xing[a], W.-M.Bu[b], L.Ye[b], Y.G.Fan[b], J.-Q.Xu[a] ;
[a]Department of Chemistry, Jilin University, Changchun 130023, China
[b]Key Laboratory for Supramolecular Structure and Spectroscopy, Jinlin University, Changchun 130023, China

The oxalate is an important organic ligand, which is coordinated to many metals, exhibiting different structural characterisation complexes. Therefore, much attention has been focused on the synthesis and study of a variety of metal-oxalate complexs, especially contained molybdenum oxalate complexes[1,2]. Although numerous Mo-oxalate complexes have been reported, to our knowledge, there appear to be no reports on Mo-oxalate complexes with sulphur bridge or unsymmetry bridge(O and S). We here reported the structure of a new Mo-oxalate complex $K6[Mo_2(\mu\text{-}O)(\mu\text{-}S)O_2(ClPO_3)_2(C_2O_4)_2] \cdot 3H_2O$.

Synthetic manipulations were carried out under an atmosphere of purified nitrogen at room temperature. The compound was obtained from $(NH_4)_2MoS_4$, $K_2C_2O_4 \cdot H_2O$, KCl,(molar ratio:1:2.5:6.7) in the system of methanol-water, the pH value is in range 7.2-7.8.

A complete X-ray structural determination revealed that the crystal structure of the title compound consists of six K^+ cations and on$[Mo_2O_3S(ClPO_3)_2(C_2O_4)_2]^{6-}$ anion, with three lattice water, showing in Fig1. In the anion, two molybdenum atoms are linked by two different unsymmetry bridging oxygen and sulphur atoms, and each molybdenum atom is also coordinated to a terminal atom, a Cl atom of ligand $ClPO_3$ and oxalate ligand through two carboxylato-oxygen atom, leading to a stable five membered ring. Two oxalate ligands are in cis configuration, trans to terminal oxo groups. The presence of $ClPO_3^{2-}$ ligand in the complex, releaved by X-ray crystallography, is somewhat intriguing, intially, no external source P was suppplied. It appears that the P is supplied by the starting material impurity. It is in progess for its reaction mechanism and detail structure.

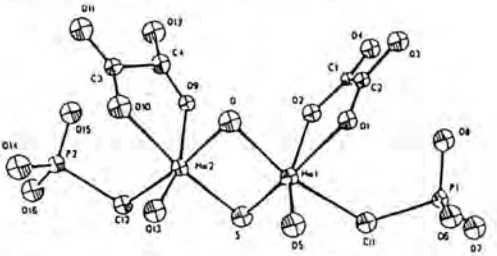

Fig.1 A Perspective View of the Anion of the Complex $K_6[Mo_2(\mu\text{-}O)(\mu\text{-}S)O_2(ClPO_3)_2(C_2O_4)_2] \cdot 3H_2O$

14P48

CRYSTAL STRUCTURES OF DABCO SALTS WITH LONG ALKYL CHAINS – ANALYSES OF THE HIGH TEMPERATURE PHASE USING POWDER X-RAY DIFFRACTION DATA

M. Sudo, H. Sato, D. Hashizume, M. Yasui, and F. Iwasaki, Dept. of Applied physics and Chemistry, The Univ. of Electro-Communications.

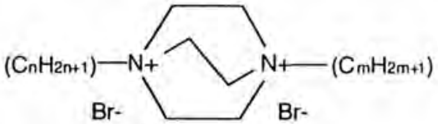

(1), n=13,14,15, m=n
(2), n=12,13,14, m=n+2
(3), n=10, m=16,18

A series of DABCO (1,4-diazabicyclo[2.2.2]octane) salts quaternarized by two long n-alkyl groups, C_nH_{2n+1}-DABCO-$C_mH_{2m+1}{}^{2+}\cdot 2Br^-$, exhibits phase transitions at *ca.* 100°C, and shows the anion conductivity at a high temperature phase. Crystal structures at the room temperature phase were determined by the X-ray analyses. To clarify the mechanism of the phase transition, crystal structures of high temperature phases were simulated based on the powder diffraction patterns because the crystals became polycrystallines during the phase transition. For (2), it was revealed that the alkyl chains rotate around the molecular axis and the bromide ions are disordered along the longest axis of the unit cell at high temperature phase. But, this model could not apply to (3) since the crystal structures at room temperature are quite different from those of (2). A new model which interpret the structure at high temperature phase of (3) is now investigated.

14P49

CRITICAL BEHAVIOR ON $SrTiO_3(001)$ SURFACE WITH THE STRUCTURAL PHASE TRANSITION

S.Doi and I.Takahashi, Advanced Research Center of Science(ARCS), School of Science, Kwansei Gakuin University

Dielectric substances that exhibit structural phase transitions have been investigated intensively. However, it remains unclear what distinct features the surface displays and how these manifest with respect to its physical properties and structures, when the bulk undergoes structural phase transition.

$SrTiO_3$, a perovskite, undergoes the cubic-tetragonal phase transition at $T_c \approx 105K$. The phase transition can be described simply by the soft mode concept as the condensation of optical transverse phonon at R point. In the tetragonal phase, a complex twin microstructure comprising three kinds of domains which match each other in so-called tetragonal manner occur. As a result, the surface is expected to be tilt from the crystal surface plane reflecting the tetragonality c/a, where a and c are contracted and elongated cubic unit cell parameters in the tetragonal phase respectively.

We performed X-ray reflectivity measurements on $SrTiO_3(001)$ surface with varying temperature through T_c. Characteristic behaviors on the surface connected to the spontaneous strain were observed. We will report several aspects of these behaviors compared with the bulk ones which show good agreement with Landau phenomenological theory.

14P50

CO DOPING EFFECT ON THE STRUCTURE AND MAGNETIC PROPERTIES OF $La_{0.7}Sr_{0.3}Mn_{1-x}Co_xO_3$ SYSTEM

T.J.Lee, C.Y.Wan and H.C.Ku, Department of Physics, The National Tsing Hua University, 300 Taiwan
X.-G.Li, W.B.Wu, X.J.Fan and G.Ji, Structure Research Laboratory, University of China 230026 Heifei

The effect of Co substitutions on the structure and magnetic properties of highly magnetoresistive compounds $La_{0.7}Sr_{0.3}Mn_{1-x}Co_xO_3$(x=0, 0.01, 0.03, 0.05, 0.1, 0.3, 0.5, 1)has been studied systematically. It was found that the crystal structure of thecompounds belongs to an orthorhombically distorted perovskite structure with space group Pbnm. With the increase of Co content, the lattice parameters decrease in the range $0 < x < 0.03$, then increase in the range $0.03 < x < 0.1$, and then decrease gradually again. DC susceptibility measurements indicate that the spontaneous magnetization is of antiferromagnetic ctate. The compounds show(AFP) transitions from antiferromagnetic to ferromagnetic then to paramagnetic states in zero field cooled process, while the ferromagnetic to paramagnetic(FP) transition occurs only in field cooled case. The FP transition temperature decreases with the increase of Co content, which has some relation to the Mn-O bond length.

(Work supported by National Science Council of ROC under Grant No. NSC-87-2112-M-007-028)

14P51

PYRENE II ↔ PYRENE I : THE HIGH-RESOLUTION VIEW

K. S. Knight[a], K. Shankland[a], N. Shankland[b], S. W. Love[b] and C. S. Frampton[c]

[a]ISIS Facility, Rutherford Appleton Laboratory, UK
[b]Department of Pharmaceutical Sciences, Strathclyde University, UK
[c]Roche Research Centre, Welwyn Garden City, UK

Crystals of pyrene I undergo a first-order phase transition to pyrene II when cooled to below *ca.* 105 K. Powder diffraction data were collected from 3 g of perdeuterated pyrene on the High Resolution Powder Diffractometer at the ISIS spallation neutron source, and the unit cell refined at each of a series of temperatures either side of the transition. These data were then used to determine the thermal expansion tensor and its temperature dependence in both phases. The magnitudes of the principal axes for the tensor of pyrene II over the temperature range $50 < T < 105$ K are very similar to those of pyrene I over the temperature range $105 < T < 185$ K, consistent with the similarity in the crystal structures. In addition, and by way of confirming the crystal structure of pyrene II, we have determined the previously unreported single-crystal X-ray structure of pyrene II.

14P52

STRUCTURAL PHASE TRANSITIONS IN TRIAMMONIUM HYDROGEN DISULFATE

K.Sooryanayana and T.N.Guru Row
Solid State and Structural Chemistry Unit, Indian Institute of Science

Structural phase transitions in triammonium hydrogen disulfate have been characterized by determining crystal structures at -90, -110°C by single crystal X-ray diffraction and at +140°C by X-ray powder diffraction. The room temperature structure is monoclinic, C2/c. On cooling the space group changes to P2/n at -90°C and reverts to C2/c at -110°C. These changes in the symmetry are characterized by carefully analyzing the hydrogen bonding patterns at these temperatures and a mechanism is proposed for this transition. On the other hand, using X-ray powder diffraction, crystal structure of the high temperature phase was refined using Rietveld refinement. The starting model for the refinement was derived from the structure of the selenium analogue. The high temperature is rhombohedral (R-3m) with the sulfate tetrahedra in this phase envisaged as a rigid rotor.

14P53

CRYSTAL STRUCTURE OF SPINEL $CuIr_2S_4$ AT LOW TEMPERATURE

H. Ishibashi, K. Tanioka, K. Nakahigashi, College of Integrated Arts and Sciences, Osaka Prefecture University, Japan; and R. Oshima, Research Institute for Advanced Science and Technology, Osaka Prefecture University, Japan

Recently a spinel-type compound $CuIr_2S_4$ was discovered to exhibit a metal-insulator transition (MIT) at $T_C = 230$ K accompanied by a structural transition from cubic spinel structure to tetragonally distorted one. The space group of the tetragonal phase (below T_C) was assumed to be $I4_1/amd$(1), however, some weak reflections that cannot be explained by the assumed structure were found. Therefore, the crystal structure below T_C has not been determined completely. The purpose of this study is to determine the crystal structure of $CuIr_2S_4$ at low temperature by using X-ray and electron diffraction methods.

The $CuIr_2S_4$ powder used was prepared by heating the mixture of Cu, Ir and S powders in evacuated quartz tubes. The powder x-ray diffraction data at temperatures from 10 K to 295 K were collected using CuKα radiation. The electron diffraction pattern at temperatures near T_C were obtained using a transmission electron microscopy.

The results of the x-ray powder pattern at 10 K are follows:
All weak reflections can be indexed by h, k, l = (all half integer) such as (1/2 1/2 1/2) and h, k, l = (all integer), where the basis vectors $\boldsymbol{a}$, $\boldsymbol{b}$, $\boldsymbol{c}$ are corresponding to the cubic axes in the high temperature phase. Furthermore, some strong reflections such as (400) and (511), each of which is single peak in assuming the tetragonal symmetry, are clearly splitting. This result suggests that the symmetry is lower than tetragonal.

These result are consistent with those of electron diffraction below T_C because the 'half integer indices' reflections were observed and the diffraction pattern with an incident along the [001] direction shows not four-fold symmetry but two-fold one.

Consequently, we assumed that the crystal structure of $CuIr_2S_4$ below T_C is orthorhombic as a fundamental structure, and has a commensurate superstructure with the wave vector of $\boldsymbol{q} = \boldsymbol{a}^*$ and $\boldsymbol{q} = 1/2\boldsymbol{a}^* + 1/2\boldsymbol{b}^* + 1/2\boldsymbol{c}^*$. Detailed results will be presented and discussed.

1. Furubayashi, T., Matsumoto, T., Hagino, T. & Nagata, S. (1994). *J. Phys. Soc. Jpn.*, **63**, 3333-3339.

IMPROVEMENT OF CRYSTAL HABIT FOR X-RAY DIFFRACTION OF MALTOOLIGOSYL TREHALOSE SYNTHASE BY REDUCTIVE METHYLATION OF LYSINE RESIDUES

M.Kobayashi[a], M.Kubota[b] & Y.Matsuura[a], [a]Institute for Protein Research, Osaka University,Suita,Osaka,Japan; [b]Hayashibara Biochemical Lab. Inc, Amase-minami,Okayama,Japan

Maltooligosyl trehalose synthase(MTSase) is enzyme which is produced from *Arthrobacter sp* .Q36.The enzymatic synthesis of trehalose involves two kinds of enzymes,MTSase and MTHase(maltooligosyl trehalose trehalohydrolase).

First crystallization experiments were performed with using intact purified enzyme of MTSase.The crystals grew by using 20 % PEG2000 in the presence of 0.2 M $MgCl_2$,and protein concentration of 30 mg/ml buffered with 0.1 M Tris-HCl at pH 8.5. In this case we obtained needle-shaped crystals which are not suitable for X-ray diffraction experiments,but diffracted up to 3.5 Å resolution. Thus we tried a chemical modification of this enzyme by using reductive methylation of lysine residues as described previously (1,2).After the reaction the modified enzyme was salted-out by ammonium sulfate and dialysed against the same buffer.The crystallization was performed with the same conditions described above,and crystals grew to 2.8 Å resolution by using rotating anode X-ray generator,and up to 2.4 Å by using synchrotron radiation The crystals belong to the space group $P2_12_12_1$,with unit cell dimensions of a=56.70,b=140.1,c= 205.2 Å with one molecule in the asymmetric unit.We collected intensity data by using the SPring-8 facility (BL41XU) for native crystal.The heavy atom derivative searches are now underway.

1.Means,G.E.(1968).Biochemistry 7,2192-2201

2.Rypniewski,W.R., Holden,H.M. &Rayment,I.(1993).Biochemistry 32 ,9851-9858

15P2

THREE-DIMENSIONAL STRUCTURE OF GLUTATHIONE S-TRANSFERASE FROM *Escherichia coli*.

M. Nishida[1], S. Harada[2], Y.Satow[2], H. Inoue[3] and K. Takahashi[3]
[1] Department of Molecular Physiology, Tokyo Meteropolitan Institute of Medical Science
[2] Graduate School of Pharmaceutical Sciences, University of Tokyo
[3] School of Life Science, Tokyo University of Pharmacy and Life Science.

The crystal structure of *E. coli* Glutathione *S*-Transferase (GST) complexed with glutathione sulfonate, a competitive inhibitor with GSH was determined by the multiple isomorphous replacement, and was refined to a crystallographic *R*-factor of 0.183 at 2.1 Å resolution. The structural model consists of one dimer of two 201 amino-acid polypeptides, two inhibitors, and 174 water molecules. Although its sequence identity to eukaryotic GSTs is less than 20 %, the folding topology is mostly identical. *E. coli* GST consists of N-terminal (residues 1-80) and C-terminal (residues 89-201) domains, and the GSH-binding site possesses the common architectures with those of eukaryotic enzymes. But the side chains of Tyr 5 and Ser 11, positionally corresponding to the catalytic residues in eukaryotic GSTs, are not located in proximity to the sulfonate group of the inhibitor molecule in the *E. coli* enzyme/inhibitor complex. Alternatively, Cys 10 N and His 106 Nε hydrogen-bond to the sulfonate group and are supposed to induce the thiolate form of GSH in the catalysis. These results indicate *E. coli* GST has a novel catalytic apparatus distinct from those of eukaryotic enzymes.

15P3

THE CRYSTAL STRUCTURE OF 1-AMINOCYCLOPROPANE-1-CARBOXYLIC ACID DEAMINASE FROM YEAST

M. Yao[2,1], T. Sugimoto[1], A. Horiuchi[1], T. Ose[1], A. Nakagawa[1], I. Tanaka[1], S. Wakatsuki[3], D.Yokoi[4], T.Murakami[4] and M. Honma[4], [1]Graduate School of Science, Hokkaida University, Japan., [2]Institute for Protein Research, Osaka University, Japan., [3]ESRF, France, [4]Graduate School of Agriculture, Hokkaida University, Japan.

A pyridoxal phosphate (PLP) -dependent enzyme, 1-Aminocyclopropane-1-carboxylic acid (ACC) deaminase found only in microorganisms catalyzes a reaction of cleavage ACC to α-ketobutyrate and ammonia by cyclopropane ring-opening. ACC is a key intermediate in the biosynthesis of a plant hormone ethylene which affects diverse growing and fruit ripening. Interestingly, introduction of ACC deaminase gene in plants was reported to reduce the production of ethylene and delay ripening progression of fruits, although ACC deaminase has never been found in highter plants with the exception of transgenic plants. The three dimensional structure of ACC deaminase from yeast *Hansenula saturnus* (yACCD) was determined by MAD method using mercury atoms as anomalous scatterer.

The two crystal forms were obtained for mercury derivative of yACCD by co-crystallization. The 2.0 Å nativedata and 2.8 Å MAD data of the orthorhombic form and 2.5 Å MAD data of the trigonal form were collected using synchrotron radiation at the ESRF of France and Photon Factory of Japan, respectively. Initial phasing was done independently at 2.8 Å for the orthorhombic and 2.5 Å for the trigonal form by MAD data of mercury atom using remote wavelength data as 'native' data. The model was built based on 2.8 Å electon density map after improvement by non-crystallographic symmetry averaging of multiple crystal forms. The molecular dynamic refinement are currently underway at 2.0 Å resolution using native data.

15P4

CRYSTALLOGRAPHIC STUDY OF PHOSPHOLIPASE D FROM *STREPTOMYCES ANTIBIOTICUS*

A.Suzuki[a], K.Kakuno[a], Y.Iwasaki[b], T.Yamane[b], and T.Yamane[a], [a]Graduate School of Engineering, Nagoya University, [b]Graduate School of Bio- and Agro- Sciences, Nagoya University

Phospholipase D (PLD, E.C. 3.1.4.4.) hydrolyzes phospholipids to phosphatidic acids and alcohols. In mammalian cells, PLD plays an important role in signal transduction. However, the tertiary structure is not yet known, because most animal PLDs are membrane-bound and consist of more than 1,000 amino acids.

Tsuneo Yamane et al. have been studying PLD from *Streptomyces antibioticus*. The bacterial PLD is a soluble protein consisting of 509 amino acid residues and contains the "HKD motif", which is highly conserved in other eukaryotic PLDs.

The preparation and purification of PLD was performed as described previously (1). PLD has been crystallized in six crystal forms using the hanging-drop vapor-diffusion method. The Type III and V crystals belong to monoclinic and hexagonal systems, respectively. All of the other crystal forms, Type I, II, IV and VI, belong to space group $P2_12_12_1$. Of these four types, the Type VI crystals are suitable for X-ray structure determination. Crystal data for Type VI crystals are: a=50.1, b=98.7, c=107.6Å, V=532,100$Å^3$, Z=4, and Vm=2.47$Å^3$/Dalton. Type VI crystals diffract to at least 2.3Å resolution.

A total of 11,295 independent reflections to 3Å resolution from a Type VI native crystal and 3438 reflections to 4.5Å resolution from a $Hg(CH_3COO)_2$ derivative have been collected, using a conventional X-ray source. Structural analysis of Type VI crystals is underway using the isomorphous replacement method.

1. Mishima, N., Mizumoto, K., Iwasaki, Y., Nakano, H. & Yamane, T. (1997). *Biotechnol. Prog.* 13, 864-868.

15P5

CRYSTALLOGRAPHIC ANALYSIS OF THE CATALYTIC MECHANISM OF L-2-HALOACID DEHALOGENASE

Y. Hata, Y.-F. Li, T. Fujii, T. Akutagawa and N. Esaki, Institute for Chemical Research, Kyoto University, Kyoto, Japan

L-2-Haloacid dehalogenase from *Pseudomonas* sp. YL catalyzes the dehalogenation of L-2-haloalkanoic acid to yield the corresponding D-2-hydroxyalkanoic acid. Crystal structures of the dimeric enzyme were determined in the native, intermediate (1) and product-bound forms, and the catalysis which proceeds by a two-step mechanism has been crystallographically analysed based on structural changes between them. The subunit has the active site in the cleft between a core domain of α/β-structure and a subdomain of four-helix-bundle structure. The substrate is taken into the enzyme by Arg-41 which fluctuates at the active site entrance in the native state and then dehalogenated by its guanigino group which projects to the C2 atom of the substrate in the complex. The carboxyl group of the substrate is fixed through the hydrogen bond to the side chain of Ser-118, and the alkyl group of the substrate is stabilized by the hydrophobic pocket which may play an important role in determining the stereospecificity of the enzyme. Concurrently with the dehalogenation, Asp-10 nucleophilically attacks the C2 atom to form the ester intermediate by covarently bonding to the substrate moiety. In this course, the Walden's inversion occurs, and the substrate moiety adopts a D-configuration at the C2 atom. In the intermediate, a new water molecule is present in the vicinities of Asp-10 and Ser-175. The water molecule may be activated by Ser-175 and Glu-180 and serve as the nucleophile for hydrolysis of the ester intermediate to yield the product, and finally the enzyme is restored to the original state.

1. Li, Y.-F., Hata, Y., Fujii, T., Hisano, T., Nishihara, M., Kurihara, T. & Esaki, N. (1998). *J. Biol. Chem.* **273**, 15035–15044.

15P6

THE CRYSTAL STRUCTURE OF FOLYLPOLYGLUTAMATE SYNTHETASE TO 2.4Å RESOLUTION: STRUCTURAL HOMOLOGIES WITH ATP- AND FOLATE-BINDING ENZYMES.

C.A. Smith, X. Sun, E.N. Baker (University of Auckland)
and A.L. Bognar (University of Toronto).

Folylpolyglutamate synthetase (FPGS), responsible for the addition of a polyglutamate tail to folate and folate derivatives, is an ATP-dependent enzyme isolated from eukaryotic and bacterial sources where it plays a key role in the retention of the intracellular folate pool. Here we report the 2.4Å resolution crystal structure of the MgATP complex of the enzyme from *Lactobacillus casei*. The structural analysis reveals that FPGS is a modular protein consisting of two domains, one with a typical mononucleotide-binding fold, and the other strikingly similar to the folate-binding enzyme dihydrofolate reductase. We have located the active site of the enzyme in a large interdomain cleft, adjacent to an ATP-binding P-loop motif. Opposite this site, in the C-domain, a cavity likely to be the folate binding site has been identified and inspection of this cavity and the surrounding protein structure suggests that the glutamate tail of the substrate may project into the active site. A further feature of the structure is a well-defined Ω-loop which contributes both to the active site and to interdomain interactions. The determination of the structure of this enzyme represents the first step toward the elucidation of the molecular mechanism of polyglutamylation of folates and antifolates.

DIRECT PHASE DETERMINATION FOR MACROMOLECULAR CRYSTALS BY STEREOSCOPIC MULTI-BEAM IMAGING

C.H Chao[*], Y.S Huang[*], F.J Liang[*], H.C Chien[*], C.K Chen[*], S.L Chang[*], Y.C. Jean[#], H.S Sheu[#], and H.S. Yuan[$],
[*]Department of Physics, National Tsing Hua University, Hsinchu, Taiwan,
[#]Synchrotron Radiation Research Center, Hsinchu, Taiwan, R.O.C.
[$]Institute of Molecular Biology, Academia Sinica, Taipei, Taiwan, R.O.C.

Phase information necessary for determining single-crystal structure is lost in the intensity measurement of x-ray reflection. For macromolecular crystals, anomalous dispersion(AD) and heavy atom derivatives are usually employed in phase determination. Here, without invoking AD and derivatives, we demonstrate the direct phase determination of a large number of reflection collected in a short time from macromolecular crystals using a stereoscopic oscillation-crystal imaging technique in a multi-bean diffraction geometry, where two crystallographic axes in opposite directions are employed as the rotation axes. The intensity contrast of the diffraction profile (distribution) versus the varying tilt Bragg angle of the rotation axis in the stereoscopically-related two images yields qualitative and quantitative phase information, respectively. More than 100 multiple diffraction profiles of tetragonal lysozyme and of a crystal of unknown structure are obtained, respectively, in total 30 minutes x-ray exposures and more than 100 phases are determined accordingly. This technique thus provides a new practical way for direct phase determination of macromolecular crystals.

15P8

CRYSTALLOGRAPHIC STUDY OF A PORCINE HEMOGLOBN AT 1.8Å RESOLUTION - A POTENTIAL ARTIFICIAL HUMAN BLOOD

T.-H. Lu,[1] K. Panneerselvam,[1] Y.-C. Liaw,[2] C.-M. Tsai,[1] P. Kan[3] AND C.-J. Lee[3]. [1]Department of Physics, [3]Department of Chemical Engineering, National Tsing Hua University, Hsinchu, Taiwan 30043, ROC. [2]Crystallography Laboratory, Institute of Molecular Biology, Academia Sinica, Nankang, Taipei 11529, ROC

To investigate a potential candidate material for making artificial red blood cells for supplement blood transfusion, X-ray structure of porcine hemoglobin (pHb) was determined as a partial research toward making human blood. Porcine hemoglobin was crystallized by the vapor diffusion method to a size of 0.3~0.5 mm after succesive seeding. The crystals of pHb are orthorhombic, with space group $P2_12_12_1$ and unit-cell dimensions a=68.10, b=72.27 and c=114.85Å and diffract x-rays beyond 1.8Å resolution. Initial solution by molecular replacement method using human oxyhemoglobin. The solution agrees well with the self-rotaion function of pHb. Fourier analysis, electron density fit, least-squares fit and other data calculations were processed by using the programs of XPLOR, QUANTA, O, PROCHECK, CCP4, GRASP and MolScript. The final R factor was reduced to 19.5% for 36820 reflections, after 762 water molecules were validated. The r.m.s deviations of bond lengths, angles, torsion angles and improper angles from their ideal values are 0.014Å, 2.9, 21.6 and 2.7° respectively. The average B-factor is 33.99Å^2 for the hemoglobin molecule and 53.07Å^2 for the water molecules. The structure could be superimposed on 2.8Å resolution with an r.m.s difference in main-chain atomic position of 0.57Å and in side-chain of 1.27Å. Detail tables and colorful figures will be presented for the comparison of porcine and human hemoglobins.

PROTEIN CRYSTALLIZATION AND LAB. AUTOMATION

F. Han, Structure, Analytical & Medicinal Chemistry, Pharmacia & Upjohn Inc., USA

Crystallization is a critical step for protein structure determination. The common approach is so called "Vapor Diffusion Method" using multiple well trays. This method requires time consuming steps to setup the trays: grease the well lips; transfer different liquids to the wells; dispense 1-2 µl microprotein drop on the cover slips; mix the well solution with the protein drop; and finally seal the wells with cover slips. Becauuse of the "Trial and Error" nature, it could take many attemps to optimize the crystallization conditions. During the last decade, many commercial company and research institutions spent years and multimillion dollars trying to automate these steps with computer controlled robotics. Until recently, there was no robot available for this purpose. Last year, we purchased one robot from CyberLab, which is designed for "Vapor Diffusion Crystallization", and modified another old Tecan robot for preparing buffers and adjust pH for the crystallization experiments. All of the basic functions of these two robots are currently running.

To improve the CyberLab robot for our needs, some software and hardware modifications have been made: 1). Rewrite the tray setup program: The old software had a DOS like interface. The new one we wrote was a GUI (Graphic User Interface) program, which is much easy to use. This program can generate the special command file for running the robot. 2). Some of the screening experiments require handling very small amount (< 50µl) liquid. To evaluate the precision of this robot, we calrated its liquid handling tools. The results were not quite satisfaction specially for those viscous solutions (PEG etc.). Several improvements are underway. We also did the following to the Tecan robot: 1). Replace the old computer with a Pentium PC; 2). Write a new program to control the Tecan; 3). Connect a pH meter to the robot; 4). A vacuum cover handling function was added to it; 5). A motor driving stirrer was attached to the robot arm; 6). A three steps wash station can thoroughly wash the probe was installed. 7). A disposable tip exchange station was added to it. The whole system has been thoroughly tested, all of the functions seemed working well.

15P10

THE STRUCTURE OF THE FIRST 3 DOMAINS OF THE TYPE 1 IGF RECEPTOR.

T.P.J. Garrett[1], N.M. McKern[2], M. Lou[1], M.J. Frenkel[2], J.D. Bentley[2], G.O. Lovrecz[2], T.C. Elleman[2], L.J. Cosgrove[2,3] and C.W. Ward[2]. Biomolecular Research Institute[1] and CSIRO Division of Molecular Science[2],343 Royal Parade, Parkville, Victoria, 3052, Australia,

The type 1 insulin-like growth factor receptor (IGF-1R) belongs to a family of vertebrate cell surface receptors which also include insulin receptor. However homologues have also been found in many invertebrates, including some of the simplest multicellular animals. The ligands for this family are protein hormones which induce a variety of metabolic and mitogenic responses. IGF-I and IGF-II are primarily produced as a consequence of growth hormone signalling and are essential for normal growth and development . They also seem necessary in malignant transformation of cells. Insulin is a major mediator in glucose homeostasis and induces lipid, protein and glucose metabolism in a variety of tissues. Although many other cell-surface receptors dimerize upon binding their ligands the mature IGF-1R pre-exists as a disulfide-linked homodimer. Thus binding of the hormone to the extracellular portion is believed to induce a structural change in the receptor which is transmitted across the membrane to allow transphosphorylation of the tyrosine kinase domains.

We have determined the structure of the first three domains of the type 1 insulin-like growth factor receptor (L1-cys rich-L2 domains) to 2.6 Å resolution by X-ray diffraction. This corresponds to the first half of the extracellular portion and it contains two regions which have been implicated in ligand specificity. L1 and L2 are homologous and adopt the a fold which represent a new type of structural domain. The cys-rich region also shows unique structural features, being composed of small disulfide-bonded modules associated in a novel manner. At the centre of the molecule is a space of sufficient size to accommodate a hormone ligand. Two regions of the receptor which are involved in hormone-binding map to this site. Thus this structure gives a first view of how members of the insulin receptor family might interact with their ligands.

CRYSTAL STRUCTURE OF RIBULOSE 1,5-BISPHOSPHATE CARBOXYLASE/OXYGENASE FROM A RED ALGA, *GALDIERIA PARTITA*, WITH HIGH SPECIFICITY FACTOR

H. Yamamoto[a], H. Sugawara[a], N. Shibata[a], C Miyake[b], A. Yokota[b] & Y. Kai[a]
([a]Dept. of Materials Chemistry, Osaka Univ., [b]Graduate School of Biological Science, Nara Institute of Science and Technology)

Ribulose 1,5-bisphosphate carboxylase/oxygenase (RuBisCO) catalyzes the competing reactions of carboxylation and oxygenation of ribulose 1,5-bisphosphate. The oxygenation reaction reduces the rate of photosynthesis. Consequently, the enhancement of the carboxylation/oxygenation ratio is one of the most important factors for creating RuBisCOs with more useful properties for current global problems. Recently, a strongly carboxylase-specific RuBisCO was found in a red alga, *Galdieria partita*. Thus, we have determined the crystal structure of *Galdieria* RuBisCO complexed with 2-carboxyarabinitol bisphosphate (2-CABP) at 2.4Å resolution.

Crystallization and data collection were already reported[1)]. The crystal structure analysis has been performed by Patterson search method with the structure of spinach RuBisCO as a starting model. The crystallographic R-factor and R_{free}-factor for the current structure refined are 17.1% and 19.3%, respectively. *Galdieria* RuBisCO forms L_8S_8 hexadecameric complex, and the amino acid residues interacting with P5 phosphate of 2-CABP showed significant structural difference in comparison with the spinach RuBisCO. Small subunit of *Galdieria* RuBisCO has 32 prolonged amino residues on C-terminus, which make up hairpin loop structure.

1) Shibata, N. *et al.* (1996). *J. Biochem.*, **120**, 1064-1066.

15P12

CRYSTAL STRUCTURE OF COPPER COMPLEXES AND ITS HYDROGEN BONDINGS

T. Nemoto, S. Terada, T. Ogawa, S. Isoda and T. Kobayashi
Institute for Chemical Research, Gokasho, Uji 611-0011, Japan

Copper oxinate crystallizes in various crystal structures depending on its formation process or conditions. In this report, the relationship between hydrogen bonding network and morphology of pyridine copper oxinates and others are discussed.

Dark green crystals were obtained from pyridine solution of copper oxinate dihydrate. Space group is Pbca, Z=8. One pyridine was coordinated with copper, and the copper oxinate plane bent to pyridine. Dihedral angle between these oxines is 8.6 degree. The water molecules make hydrogen bond chain between the oxines of two molecules. Molecules were aligned along a-axis by this hydrogen bond chain.

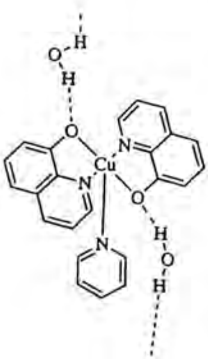

Fig. 1. Structural formula

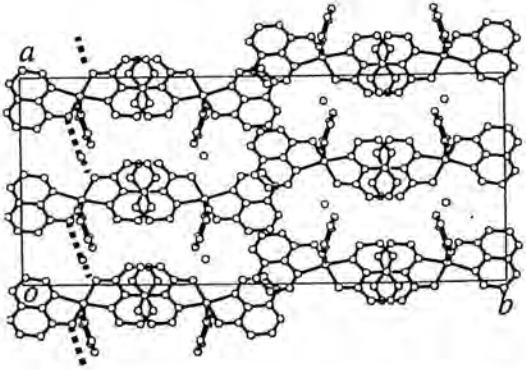

Fig. 2. Crystal structure viewed along c axis

15P13

CRYSTAL STRUCTURE OF 4-METHYL-(2-FORMYL-6-MORPHOLINO-1-YL-METHYL)PHENOL (I) AND BIS [2 - HYDROXY - 3 - (MORPHOLINO - 1 -YL- METHYL)-5-METHYL BENZYL] ETHYLENEDIIMINE (II)

S. S. S. Raj[b], R.Thirumurugan[a], G. Shanmugam[a] and H-K. Fun[b], [a]Department of Crystallography and Biophysics, University of Madras, Guindy Campus, Chennai - 600 025, India, [b]X-ray Crystallography Unit, School of Physics, Universiti Sains Malaysia, 11800 USM, Penang, Malaysia.

The knowledge of the molecular skeleton of binucleating ligands are extremely essential for preparing metal complexes and due to their significance in bio-inorganic chemistry as simple models for magnetically coupled binuclear metalloproteins. Both the compounds crystallize in monoclinic system $P2_1/c$ space group with Z=4 and 2 respectively.The cell parameters are: a=5.3172(1)[11.1356(5)], b=15.3099(3) [9.5825(5)], c=15.3406(1)Å[12.4721(6)Å], β=91.846(1)[98.828(2)], V=1248.17(3)$Å^3$ [1315.1(1)$Å^3$]. In compound II, the molcules lie at the crystallographic centre of inversion. The morpholine ring in both the title compounds adopt chair conformation. The methelene substituent at the morpholine ring lie in the equatorial conformation in both the compounds. The structure is stabilized by intramolecular O-H...N type of hydrogen bonds.

15P14

FERROCENIUM TETRABROMOTIN STRUCTURAL STUDY OF A COMPLEX OF FERROCENIUM AND TETRABROMOTIN

I.A.Razak AND H.K Fun, X-ray Crystallography Unit, School of Physics, Universiti Sains Malaysia, 11800 USM, Penang, Malaysia.
B.M.Yamin, Department of Chemistry, University Kebangsaan Malaysia, 43600 Bangi, Selangor, Malaysia.

Although the structures of several ferrocenium salts with halogeno-metal anions such as tetrachloroferrate (1) and tetrachloroantimonate (2) have been reported, not many others have been successfully studied because of the hygroscopic nature. Here we report the crystal structure of a complex of ferrocenium and tetrabromotin. Crystal data: a=17.792(1), b=8.569(1), c=12.464(1)Å space group P2/c, Z=4 and R=0.055.
The two cyclopentadienyl rings of the ferrocenium cation are planar with a staggered configuration and with a torsion angle of 24.
The coordination around the tin atom is octahedral. In the solid state, the anion form infinite chain along the b axis.

(1) Paulus, E. F. & Schafer, L. (1978). J. Organomet. Chem. 144, 205-213.
(2) Yamin, B.,M., Fun, H. K., Sivakumar, K., Yip, B. C. & Shawkataly, O. B. (1996). Acta Cryst. C52, 600-602.

15P15

HYDROTHERMAL SYNTHESIS AND CRYSTAL STRUCTURE OF A CLUSTER $[Co(en)_3]$ $[Co(en)_2$ $(H_2O)_2$ $][Mo_8V_8O_{40}(HAsO_4)]$

W. M. Bu[1], G. Y. Yang[2], Q. Zeng[2], L. Ye[1], J. Q. Xu[2], Y. G. Fan[1]; [1]Key Laboratory of Supermolecular Structure and Spectroscopy, [2]Department of Chemistry, Jilin University, Changchun 130023

The dark crystals $[Co(en)_3]$ $[Co(en)_2$ $(H_2O)_2$ $][Mo_8V_8O_{40}$ $(HAsO_4)]$ were prepared in the system of H_2O-V_2O_5-H_2MoO_4-$H_2C_2O_4$-CoC_2O_4.The crystal maxium size is 1.0mm. Crystal data: Monoclinc C2/c, a=14.583(2) Å, b=21.741(3) Å, c=18.932(2) Å, β=91.532(7)° , V=6000.2(10), Z=2. X-ray single crystal diffraction analysis reveals that the cluster contains two types of $[Co(en)_3]^{2+}$ and $[Co(en)_2$ $(H_2O)_2]^{2+}$ cations.The $[Mo_8V_8O_{40}$ $(HAsO_4)]^{6-}$ anion possess four-capping structure.Within the structure by sharing side-on and vertices.Between cations and anions were connected by supramolecular forces.In the center of cluster,there is a AsO_4 tetrahedron.

15P16

HYDROTHERMAL SYNTHESIS AND CRYSTAL STRUCTURE OF A SUPRAMOLECULAR INORGANIC-ORGANIC CLUSTER $[Co(enMe)_2]_3\ [As_6V_{15}O_{42}\ (H_2O)]_2H_2O$

W. M. Bu[1], G. Y. Yang[2], Q. Zeng[2], L. Ye[1], J. Q. Xu[2], Y. G. Fan[1]; [1]Key Liaboratory of Supermolecular Structure and Spectroscopy, [2]Department of Chemistry, Jilin University, Changchun 130023

A mixture of H_2O,$H_2C_2O_4$,$CoSO_4$,As_2O_3,V_2O_5 and enMe in a mole ratio 1000:6:3:2:6:8 was heated at 160℃ for 4-days, give dark-green crystals $[Co(enMe)_2]_3\ [As_6V_{15}O_{42}(H_2O)]_2H_2O$. Crystal data: Triclinic, P-1, a=13.2976(3) Å ,b=15.0583(3) Å , c=20.166(4) Å , α=85.620(8)° , β=79.553(3)° , γ=65.087(9)° , V=3606.6(9) A, Z= 2,R=0.0469. X-ray single crystal diffraction reveals that the compound possess two-dimensional extended framework linked through inorganic bridging ligands $[Co(enMe)_2]^{2+}$ and constructed from cluster anion subunits $[As_6V_{15}O_{42}(H_2O)]^{6-}$. Fig.1 indicates the bridging gorm is diffetent along two directions.There are one inorganic bridging ligand along one direction and two inorganic bridging ligand along another direction.The subunit of cluster consists of six AsO_4 trigonal and fifteen VO_5 square pyramid with corer-sharing.In the cluster there is a water molecule.

15P17

HYDROTHERMAL SYNTHESIS AND CRYSTAL STRUCTURE OF SUPRAMOLECULAR INORGANIC-ORGANIC CLUSTER $[Ni(en)_2]\ [Ni_2(en)_4\ As_8V_{14}O_{42}\ (HPO_3)]5H_2O$

W. M. Bu[1], G. Y. Yang[2], L. S. Chen[2], L. Ye[1], J. Q. Xu[2], Y. G. Fan[1]; [1]Key Laboratory of Supermolecular Structure and Spectroscopy, [2]Department of Chemistry, Jilin University, Changchun 130023

A mixture of H_2O, H_3PO_3, Ni, $Ni(CH_3COO)_2$. $4H_2O$, V_2O_5, As_2O_3 and $H_2NCH_2CH_2NH_2$ in a mole eatio 800:30:5:3:8:6:6 was heated at 160℃ for 4 days gave dark-green prism crystals of $[Ni(en)_2]\ [Ni_2(en)_4As_8V_{14}O_{42}$ $(HPO_3)]$ $5H_2O$ (Ca. 28% yield based on anadium). Anal. Caled for $C_{12}H_{59}N_{12}O_{50}Ni_3PV_{14}As_8$: C, 5.35; H.2.21; N: 6.25; Ni: 6.54; V: 26.50; As: 22.27; Found: C: 5.06; H: 2.16; N: 5.83;P:1.34; Ni:7.19; V: 26.60; As: 23.10. Crystal data: Triclinic P-1, a=12.934(3) Å, b=13.413(3) Å, c=21.182(4) Å, α=87.17(3)°, β=77.52(3)°, γ=68.48(3)°, V=3335.9(12), z=2, Dc=2.6658/ml, R=0.0459, wR=0.0883.

As shown in Fig.1, the crystal structure of 1 is a As-V-O cluster three dimensional extended network. Linked through inorganic bridging ligands. It consists of a discrete $[Ni(en)_2]^{2+}$ cation, a subunit $[Ni_2(en)_4As_8V_{14}O_{42}$ $(HPO_3)]^{2-}$ anion containing cluster anion $[As_8V_{14}O_{42}(HPO_3)]^{6-}$ linked by coordination compound $[Ni(en)_2]^{2+}$, and water of crystallization. The Ni atom of Ni(4) site is statistical distribntion. In crystal structure, subunit $[As_8V_{14}O_{42}(HPO_3)]^{6-}$ cluster anion linked two coordination complexes, such as Ni(1)and Ni(3), which formed two-dimensional extended framework via symmetric operation, while another inorganic bridging ligand Ni(2) site located out of 2-dimensional network, So the structure is a three-dimensional imrganic/orgauic solids. Between cluster anions of compound 1 exhibit only weak interactions because axial O- Ni-O distance is 4.154(13) and 4.212(10) Å. The As-Odistances range from 1.747(8) to 1.793(9)A, V-O from 1.581(9) to 2.466(14)A, P-O from 1.45(4)to 1.56(2) Å, and Ni-V from 1.923(14) to 2.093(9) Å, respectively. The distance of Ni(4)-Ni(4í) is 1.243(8) Å.

15P18

COMPLEXES OF DIMETHYLTIN(IV) DICHLORIDE WITH HYDRAZONE AND AZINE LIGANDS —THE CRYSTAL STRUCTURES OF $[Sn(Me)_2(Ph_2CNNC(Me)(C_5H_4N)Cl_2]$ AND $[PhNHHNC(Me)(C_5H_4N)][Me_2SnCl_3]$.

Ramli b. Hitam, Md. Abu Affan and Mustaffa b. Shansuddin, Department of Chemistry, Faculty of Science, Universiti Teknologi Malaysia, Locked Bag 791,80990 Johor Bahru, Malaysia
Bohari M. Yamin, Department of Chemistry, Faculty of Physical Sciences, Universiti Kebangsaan Malaysia,43000 Bangi, Selangor, Malaysia
Fun Hoong Kun and A. Razak Ibrahim, School of Chemical Sciences, Universiti Sains Malaysia, 11800 Pulau Pinang, Malaysia

Dimethyltin(IV) dichloride complexes with 2-acetylpyridinephenylhydrazon (apph) and 2-acetylpyridinebenzophenoneazine(apba) have been prepared and characterised by X-ray crystallography. The crystal system of $[SnMe_2(apba)Cl_2]$ is monoclinic with space group P2(1)/n, a=10.1819(3) Å, b=18.313(5) Å, c=12.645(4) Å, and ß=105.03(1). In this complex, the (apba) ligand acts as a NN bidentate donor. The tin(IV) is in a distorted octahedral geometry with the two methyl groups occupy the *trans* position. However, the later complex is ionic in nature with molecular formula $[PhNHHNC(Me)(C_5H_4N)][Me_2SnCl_3]$. The crysatal system is monoclinic with space group P2(1)/n, a=6.94820(10) Å, b=20.5694(3) Å,c=13.592 Å, and ß=104.33(1).

15P19

STRUCTURES OF CALIX[n]ARENES

PARK Y.J., LEE B.H. AND CHO S.H.

Department of Chemistry
Sook Myung Women's University,
Seoul, Korea

Two calix[n]arenes have been determined by X-ray diffraction method.
(1) P-Tert-butylcalix[4]arene hexanoate, $C_{68}H_{96}O_8 \cdot 2CHCl_3$, $Pca2_1$, Z=4, a=34.599(5), b=10.208(3), c=20.358(4) Å. The molecule is in the 1,3-alternate conformation. The structural analysis of an another conformational isomer, a symmetric cone, is in progress.
(2) P-Benzylcalix[5]arene, $C_{65}H_{60}O_5 \cdot 2CHCl_3$, $P2_1/n$, Z=4, a=18.981(4), b=18.043(3), c=17.488(4) Å, β=109.95(2)°. The molecule has the symmetric conformation. Five hydroxyl groups are involved five intramolecular hydrogen bonds.

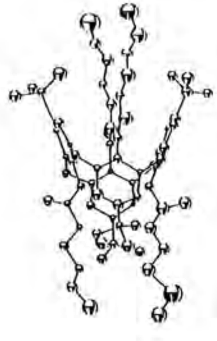

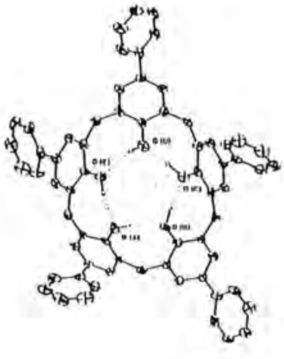

15P20

STRUCTURE OF TETRACYCLO-μ-(*N*-ETHYLENETHIOUREA)-TRIS(IODOCOPPER(I)) MONOHYDRATE

Y. Thanyasirikul and C. Pakawatchai and S. Pansook and T. Saepae, Department of Chemistry, Prince of Songkhla University, Hat Yai 90112, Thailand, and H. K. Fun and K. Chinnakali, X-ray Crystallography Unit, School of Physics, Universiti Sains Malaysia, 1180 USM, Penang, Malaysia.

The crystal structure of the complex of copper(I) iodide : *N*-ethylthiourea (ettu) in 1 : 1.5 stoichiometric ratio has been determined. This complex is a tetracycle with four six-membered ring of molecular formula$[Cu_4I_4(ettu)_6].H_2O$ exhibiting a $Cu_4S_6I_4$ "adamantane" type cluster. Each copper atom has tetrahedral geometry coordinated to an iodide atom and three bridging ettu ligands. The Cu-I distances vary from 2.623(2) to 3.087(2) Å and the Cu-S distances range from 2.253(9) to 2.386(3) Å.

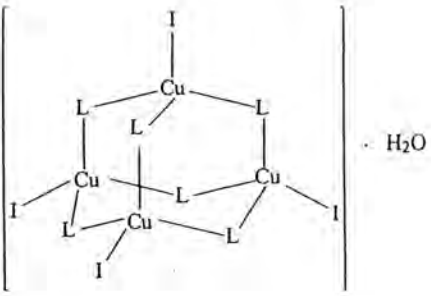

Fig. 1 $[Cu_4I_4L_6].H_2O$, L = ettu

STRUCTURES OF COPPER(I) AND SILVER(I) NITRATES WITH ETHYLENETHIOUREA

C. Pakawatchai and W. Ratchawee, Department of Chemistry, Prince of Songkla University, Hat Yai 90112, Thailand, and B. W. Skelton and A. H. White, Department of Chemistry, University of Western Australia, Nedlands 6907, Australia.

Copper(I) and silver(I) are known to form complexes with substituted thioureas with various stoichiometries and structural types. The complexes of copper(I) and silver(I) nitrates with ethylenethiourea(etu) have been prepared and structurally reported in this work. In the copper system, it has been found that the copper atom in the 1 : 4 ionic complex is quasi-tetrahadral with four sulphur atoms of from the etu ligands. Cu-S distances range between 2.3322(9) and 2.366(1) Å, and S-Cu-S 98.76(3) - 117.83(3)°. In the silver system, the binuclear ionic 1 : 3 complex has been formed. The structure contains discrete $[(etu)_2Ag(\mu\text{-}etu)_2Ag(etu)_2]$ cations and NO_3 ions. The asymmetric unit consists of one half of the dimer where the other half is generated by the center of symmetry. Each silver atom is in a distorted tetrahedral coordination, being bonded to two bridging and two terminal sulphurs of etu ligands. The Ag-S distances vary from 2.5333(9) to 2.725(1) Å and the Ag...Ag distance is 3.3062(7) Å.

1. Bowmaker G. A., et. al., (1994). *Aust. J. Chem.*, 47, 15-24.

15P22

THE STRUCTURAL CHARACTERIZATION OF $[L_2CdI_2]$ COMPLEXES

F.Fariati*, S.I. Rahayu*, B.W. Skelton[1] and A. H. White[1], *Department of Chemistry, Institut Teknologi Bandung, Bandung-40132, Indonesia,
[1] Department of Physical and Inorganic Chemistry, University of Western Australia, Nedlands, W.A. 6009

A Previous report has described the structural characterization of the $[(py)_2CdC_{12}]$[1] complexes as its $[(py)_2ZnCl_2]$[2] and $[(py)_2ZnI_2]$[3] complexes. In the present work, $[L_2CdI_2]$ complexes have been prepared {with L being: pyridine (py), 2-methyl pyridine (mp) and quinoline(qu)} as their $[(py)_2ZnX_2$]complexes (X = Cl and I). All are isomorphous with $[(py)_2CdCl_2]$[1],$[(py)_2ZnCl_2]$[2], and $[(py)_2ZnI_2]$[3].

	(I)	(II)	(III)
cell parameter	$[(py)_2CdCl_2]$	$[(py)_2ZnCl_2]$	$[(py)_2ZnI_2]$
a (Å)	17.889 (6)	14.155 (3)	15.756 (4)
b (Å)	18.747 (5)	7.754 (3)	8.284 (3)
c (Å)	8.626 (6)	15.939 (3)	7.717 (3)
α (°)	90	90	113.75 (3)
β (°)	90	109.19 (2)	93.14 (3)
γ (°)	90	90	92.06 (2)
system	orthorhombic	monoclinic	triclinic
space group	Pbca	P21/n	P1
Z	8	2	4
R	0.045	0.042	0.0275
No	1269	2574	2966

In all three of these complexes, each Cd atoms is tetrahedraly coordinated by two iodide atoms and two monodentat ligands nitrogen atoms. Cadmium to nitrogen bond lengths Generally assume a constant value of c, 2.31 Å and c,2.28 Å, respectively. The value of the I(1)-Cd-I(2) angle appears to decrease in I>II>III complexes but the N(11)-Cd-N(21) angle increases in I<II<III.

1. H. Paulus, Z. Anorg.Allg.Chem., 1969, 369, 38
2. W.L Steffen, G.J. Palenik, Acta Crystallogr. , Sect.B, 1976, 32, 298
3. J.F. Le Querler, M.M Borel, A. Leclaire, Acta Crystallogr. , Sect.B, 1977, 33, 2299

15P23

IMPROVING THE RATE OF CRYSTALLISATION OF CONFECTIONERY FATS.

S.D.MacMillan and K.J.Roberts, Heriot-Watt University M Wells, M Polgreen & I Smith, Cadbury Ltd.

Understanding and refining the molecular-scale processes involved in the manufacture of structured materials such as long-chain hydrocarbon compounds is important in many commercial areas such as the food, pharmaceutical and soap industries. In such processes crystallisation is an important separation, purification and preparation method. Despite this our knowledge of crystallisation itself is surprisingly limited.

In order to improve the crystallisation of confectionery fats, the crystallisation of it's main component, cocoa butter fat, must be properly understood. Cocoa butter fat can exhibit up to 6 polymorphic forms of different crystallographic structures with melting points varying from 17.3°C to 36.3°C. During the production of chocolate it is essential to control the polymorphic form of fats present, in order to produce a final product with the correct physical and rheological properties. Both shear rate and temperature are thought to play a crucial role in this process.

The relationship between crystallisation rate, polymorphic form, shear and the fat composition has for the first time been quantified, which will enable more accurate control of the polymorhic form in chocolate production. This has been achieved by developing an improved *in-situ* cell for X-ray studies. The X-ray studies are necessary for the examination of *on-line* studies under well controlled conditions of temperature and stirring rate (shear rate). The X-rays used are from a high intensity synchrotron radiation source, enabling polymorphic phase transformations for a variety of fat mixtures to observed.

15P24

N-H...π(INDOLE) INTERMOLECULAR INTERACTION IN 3,3' DI INDOLYL PHENYL METHANE

R. Krishna and D.Velmurugan
Department of Crystallography and Biophysics, University of Madras.

Indoles possess many interesting chemical and biological properties. Pharmacological studies of numerous indole derivatives have shown that most of them display anti-inflammatory and anti-microbial properties. The interaction of indole with DNA molecule has been reported. The title compound C23 H18 N2 crystallizes in monoclinic system with space group P21/c and its three dimensional structure has been determined. **Crystal data**: a = 10.187(1)Å , b = 9.759(2)Å , c = 17.778(1) Å, β = 94.01(1)° and R = 0.053. Both indoles are at right angles to each other. The structure has two N-H....π(Indole) intermolecular interactions: H1'...Cg1 = 2.35Å ; N1'-H1'...Cg1 = 172°; H1...Cg2 = 2.60Å ; N1-H1...Cg2 = 158°. This type of amino or amide N-H...π hydrogen bonding (aromatic) interactions have recently been theoretically postulated in model systems and experimentally described in globular proteins. It has been suggested that such interactions may provide stability, contribute to the folding process and / or have a functional role in proteins.

Programs used : Structure solution, SHELXS86;
Structure Refinement, SHELXL93.

A detailed report on the conformation of the molecule and the interactions will be presented.

CRYSTAL AND MOLECULAR STRUCTURES OF DIAZAPINES

M.Suresh Kumar[1], D.Kumaran[1], M.N.Ponnuswamy[1], K.Chinnakali[2] and H.K.Fun[2], [1]Department of Crystallography and Biophysics, University of Madras, Guindy Campus, Chennai – 600 025, India. [2]School of Physics, Universiti Sains Malaysia, Penang, Malaysia.

Many compounds of the benzodiazapine series display pharmacological properties such as tranquilizing, muscle relaxant, anticonvulsant and sedative effects. Benzodiazapines are in general not depressants of the CNS but they affect only discrete areas of the brain. The crystallographic studies of following compounds (i) N-Formyl 2,7-diphenyl 3-isopropyl 1,4-diazapin-5-one [IDPN] and (ii) N-Formyl 2,7-diphenyl 3-methyl 1,4-diazapin-5-one [MDPN], have been studied to understand the Structure Activity Relationships (SAR).

Both the structures are solved by direct methods and refined by full-matrix least-squares procedures. The diazapine ring in both the structures adopt distorted boat conformation. In IDPN, the two phenyl rings are in equatorial and axial positions whereas the isopropyl group is in equatorial orientation. In MDPN, the methyl group is in equatorial orientation. The structures are stabilized by C-H...O and C-H...N type of interactions in addition to van der Waals forces.

CONFORMATIONAL ANALYSIS OF AZA AND DIAZA BICYCLIC RING SYSTEMS

D.Kumaran[1], M.N.Ponnuswamy[1], G.Shanmugam[1] K.Sivakumar[2] and H.K.Fun[2], [1]Department of Crystallography and Biophysics, University of Madras, Guindy Campus, Chennai –600 025, India. [2]School of Physicis, Universiti Sains Malaysia, Penang, Malaysia.

Several 3-azabicyclononanes have been synthesized and studied widely in view of their conformational flexibilities and intermolecular interactions. In addition they also posses many medicinal properties. The effect and orientation of the substituents on the conformations of the bicyclic ring system are analysed and presented here.

The crystallographic studies on 2,4-diaryl azabicyclononanes show that the bicyclic ring sytems predominantly adopt chair-chair conformation. When electron withdrawing groups such as acetyl, nitroso and ester groups are substituted at the nitrogen atom, the piperidine ring gets distorted.

The detailed conformational analysis on the diazabicyclo [5.3.0] decanone derivatives indicate that the bicyclic ring system adopts chair-envelope conformation with slight distortion. The conformational restriction is imposed due to the presence of two torsional constraints in the seven membered ring, namely, the planar rigid lactam group (N-C-O) and the fusion to a five membered ring. The energy calculations have also been carried out and presented.

15P27

GROWTH OF HOKUTOLITE CRYSTAL WITH FLUX PROCESSES AND ITS IMPLICATIONS

S. C. Yu and H.R. Wang, Department of Earth Sciences National Cheng-Kung University Tainan, Taiwan 70100, ROC

Natural hokutolite is a radioactive sulfate mineral, $(Pb,Ba)SO_4$, occurring in hot-spring deposit. An attempt to synthesize hokutolite crystal with a flux-growth process was made in this study. $PbSO_4$ and $BaSO_4$ in various proportions were used as precursor materials with Na_2SO_4 as a flux agent. The growth was carried out in a platinum crucible at 750-850° C and ambient pressure conditions. The nucleation and growth were activated by a slow-cooling process at 2° /hr cooling rate.

The flux-grown hokutolite crystals up to 1mm in dimension were obtained and their chemical compositions were found to cover the entire range between $PbSO_4$ and $BaSO_4$. It is thus that there does exist a complete solid solution series between the anglesite($PbSO_4$) and barite($BaSO_4$) binary system. This result is consistent with that reported for hokutolite synthesized with a hydrothermal method . Both natural and hydrothermally synthesized hokutolite crystals display a distinct domain structure in which the Pb/Ba ratios varied among different domains. This type of chemical zoning is recognized under an optical microscope to be a banded texture in which bright bands(Pb-rich area) alternating with dark bands(Ba-rich area). In contrast, the hokutolite samples synthesized in this work contain no detectable optical bands, and this dramatic difference is believed to be a direct consequence of different growth kinetics. Similar to natural and hydrothermal samples, the flux-grown hokutolite crystals were determined to be a barite type of structure with Pb and Ba atoms in a fully disordered arrangement. The cell parameters vary continuously and systematically from the Pb-rich end toward the Ba-rich end as dictated by an ideal solid solution series. The Raman spectra of the ν_1, ν_2, ν_3 vibrational modes were recorded for the flux-grown hokutolite samples and their variations as a function of composition were investigated.

15P28

CRYSTAL STRUCTURE OF A MIXED-VALENCE COPPER CHLORIDE COMPLEX WITH TRIETHANOLAMINE

L. A. Kovbasyuk-Mokhir[a], O. Y. Vassilyeva[a], V. N. Kokozay[a], I. Bernal[b] and H. Chun[b], [a]Department of Chemistry, Kyiv Shevchenko University, Volodimirska St. 64, Kyiv 252033, Ukraine,
E-mail : kokozay@chem.kiev.ua, [b]Department of Chemistry, University of Houston, Houston TX 77204-5641

We have succeeded in preparation of a mixed-valence Cu(I)Cu(II) chloride containing triethanolamine (HL) from zerovalent copper. Crystal data: $C_6H_{14}ClNO_3Cu$, M = 247.17, hexagonal, a = 8.132(1), c = 8.235(2) Å, V = 471.6(1) Å^3, T=293 K, space group P-3, Z = 2, 268 reflections measured, 261 unique (R_{int} = 0.0077), $wR(F^2)$ = 0.1168, R1 = 0.0447.

The HL forms four bonds with the Cu atom, the coordination polyhedron of which is a bipyramid with a trigonal base. The Cu-O, Cu-N and Cu-Cl distances are 2.069(6), 2.02(1), 2.236(4)Å respectively, the N-Cu-Cl angle is 180°. The molecules are linked together by O-H···O hydrogen bonds to give layers parallel to the ac plane. The crystallographic results represent an average of indistinguishable copper(I) and copper(II) ions in identical trigonal bipyramidal sites.

The magnetic susceptibility of the complex displays normal Curie behaviour between 5 and 295 K with μ_{eff} = 1.07(5) μ_B, making the % Cu(II) about 40%.

15P29

PHASE ANALYSIS OF NIOBIUM DOPED HEXAGONAL POTASSIUM TUNGSTEN BRONZES

A. Hussain and A.U. Monir, Department of Chemistry, University of Dhaka, Dhaka-1000, Bangladesh.

Tungsten bronzes, M_xWO_3, have attracted much attention since its discovery because of its remarkable properties such as metallic luster, intense colour, inertness towards chemical attack. Attempts are now been made to prepare mixed alkali metal tungsten bronzes, $M_xM'_yWO_3$(1, 2) where M, M' are two different alkali metals or partial substitution of W atom of bronzes with suitable pentavalent atom, $M_xM'_yW_{1-y}O_3$,(3)where M' =Nb, V or Ta.

The present study was undertaken to replace tungsten atom by niobium atom in the potassium hexagonal tungsten bronzes, K-HTB phases, $K_xNb_yW_{1-y}O_3$. Samples were prepared from intimate mixtures of appropriate amount of different oxides at 600-800℃ in vacuum. The prepared bronzes were examined by optical microscope and characterised by X-ray powder diffraction method.

The well ordered niobium doped K-HTB was found to form at 700℃ or above. It was observed that a pure single phase could be prepared only if the oxidation state of tungsten atom ranges from +5.67 to +5.81. The cell parameters, a and c, decrease as the niobium content increases.

1. Banks,E. and Goldstein,A. (1968) Inorg. Chem.7, 966-969
2.Hussain,A. and Kihlborg,L. (1987) Acta. Chem. Scand. A41, 18-23
3.Kihlborg,L. and Sharma,R. (1982) J.Microsc.Spectrosc.Elect.7, 387-396

NEW HIGH PRESSURE PHASE OF $FeGeO_3$ CLINOPYROXENE

T.Hattori[1], G.Yagyu[1], T.Nagai[1], T.Yamanaka[1], S.Werner[2] and H.Schulz[2]
Department of Earth and Space Science, Graduate school of Science, [1]Osaka University, Toyonaka, Osaka, [2]Institut fur Kristallographie und Angewandte mineralogie der Universitat Munchen, Theresienter.41, Munchen

High-pressure clinopyroxene (high-P cpx), one of the most important constituents of the upper mantle, is based on the cubic closed packing (ccp) of oxygen and constructed by the highly-kinked tetrahedral chains. Generally the compression of pyroxenes is performed by kinking of tetrahedral chains. From the fact that the tetrahedral chains of high-P cpx are highly kinked even at ambient pressure, it can be predicted that the high-P cpx has the different compression mechanism and will transform into high pressure phase readily. In order to clarify its compression process and the structure of high pressure phase of $FeGeO_3$ high-P cpx, we have tried in-situ powder and single crystal X-ray diffraction measurements at pressures up to 20GPa and 7.4GPa, respectively. With increasing the pressure up to 7.4GPa, the ccp arrangement of oxygen approached into an ideal one. The O3-O3'-O3" angle indicating the kink of tetrahedral chains was not changed by compression. On the other hand the cation in the M2 octahedral site slightly shifted away from the center of the octahedra toward the adjacent void space with keeping (100) oxygen stacking layer. The same thing is also observed in the cation in tetrahedral (T) site. At about 13GPa, a new reversible high pressure phase appeared in the powder X-ray diffraction pattern. The structure remained to be seen. The transformation into the high pressure phase would be explainable by the successive movements of the cations in M and T sites into the adjacent void spaces.

15P31

A STUDY ON ZSM-5 ZEOLITES SYNTHESISED WITH AND WITHOUT THE AID OF TEMPLATE

Fakhry Seyedeyn-Azad and Dongke Zhang
Chemical Engineering Department, The University of Adelaide

ZSM-5 zeolites compositions and properties are compared using synthesised ZSM-5 zeolites using two different methods, with and without a template. From the two methods, zeolites with 100% crystallinity are synthesised with different silica alumina molar ratio (SiO_2/Al_2O_3) from 34 to 180. For each SiO_2/Al_2O_3 ratio, zeolites with different amounts of alkaline inclusion are also synthesised. Surface area and pore size of a series of synthesised zeolites are measured using BET and Langmuir Methods and the results are compared with literature. Direct observation of typical samples synthesised using different methods and conditions are established by scanning electron microscopy (SEM). It is observed that many variables such as ratios of the starting materials and the condition of the process affects the crystal topology i.e. the shape of the crystals but not the shape of the zeolite framework. A short detail of the each method used for ZSM-5 zeolite synthesis will be introduced. The influence of the synthesis procedures and initial composition on the structure and property of the final products is discussed. Comparison with literature data is also made where possible.

POLYMORPHISM, TWINNING, STRUCTURAL MODULATION, AND CHEMISTRY OF SARTORITE, $PbAs_2S_4$(?)

T.Ozawa and O.Tachikawa, (Mineralogical Institute, University of Tokyo)

Sartorite is rather common among 'rathite (dufrenoysite) group' minerals in its type locality (Lengenbach quarry, Binntal, Switzerland). Bannister et al.(1939) reported it has an orthorhombic subcell with unit cell dimensions a 19.46, b 7.79, c 4.17Å, and a true-cell of 3a, b and 20c; whereas Nowacki et al.(1961) described a true-cell of 3a, b and 11c, and possible complex disordering. Then, Ozawa and Takeuchi(1993) cofirmed the periodicity proposed by Nowacki et al. and revealed that the complex disordering is due to the coexistence of two probably polymorphic phases, as well as due to fine twinning. On the other hand, Pring et al.(1993) recorded some electron diffraction patterns and the corresponding lattice images as well exhibiting a different periodicity from those in previous reports, and put some other interpritation on the modulation in sartorite. Though we have not encountered the periodicity Pring et al. observed, we have also recorded plural different periodicities. Several ordered states appear to coexist in this mineral. We will display the diffraction patterns and TEM images to confirm and supplement our previous report.

We have also accumulated chemical analysis data of sartorite. First EPMA of sartorite was performed in about 1960 (Nowacki and Bahezre, 1963), which apparently confirmed $PbAs_2S_4$, the formula assigned to this mineral since the first of this century. Then, Laroussi et al.(1989) yielded the composition of ~$Pb_5As_8S_{17}$ to a sartorite-like new species(?). Our accumulation of chemical analysis data indicates that the species with the composition of ~$Pb_5As_8S_{17}$ is no doubt sartorite itself.

Bannister,F.A., Pabst,A. & Vaux,G. (1939) Mineral.Mag., 25, 264-270. ; Laroussi,A., Moelo,Y., Ohnenstetter,D. & Ginderow,D. (1989) C.R.Acad.Sci.Paris. 308,Ser.II, 927-933. ; Nowacki,W. & Bahezre,C. (1963) Schweiz.Mineralog.Petrog.Mitt. 43, 407-411 ; Nowacki,W., Iitaka,Y., Burki,H.&Kunz,V. (1961)Schweiz.Mineralog.Petrog.Mitt. 41, 103-116. ; Ozawa,T. & Takeuchi,Y. (1993) Mineral.J. 16, 358-370. ; Pring,A., Williams,T. & Withers,R. (1993) Am.Mineral., 78, 619-626.

15P33

INFLUENCES OF DOPED - MATERIALS ON STRUCTURES AND PROPERTIES OF THE SnO_x - THIN FILMS

V. Vong[1], N-T. Huong[2], [1]Laboratory of Electron Microscopy, Vietnam National Centre for Natural Science and Technology, Nghiado Caugiay Hanoi, [2]National University of Hanoi, Faculty of Physics, 90 Nguyen Trai str. Dongda Hanoi

The $Sn(Y)O_x$ films are widly used not only in many optoelectronic devices but also in the field of gas sensor materials. Where Y is doped-materials. These films are prepared by various methods. In the paper the films were made by evaporating tin (Sn) and silver (Ag) as well as doped-material from the tungsten boats in high vacuum of $2x10^{-6}$ to $2x10^{-5}$ Torr.

Tin and silver, which have mass-rate 6:1, pure 99,999%, were put on the boat together and then materials were evaporated (method two temperatures). The other experiment, tin and silver were put on two differential boats and then both boats were simultaniously heated to evaporate (method three temperatures).

The films were simultaniously grown on the surfaces of two substrates : optical glass and (110)-NaCl monocrystall. The temperature of both substrates is always fixed at the 150^0C. The deposited films were then annealed in atmosphere, which is rich oxygen, at the following temperatures : 200 - 300 - 400 - 450 and 500^0C.

With two differential methods of preparation we received the films, in which silver was distributed very differently.

In each stage of film-preparations, the changes of structure, the changes of size-grain, the creation of clusters etc... were studied by transmission electron microscope (TEM) and X-ray diffraction (XRD). Optical properties as well as transparency, absorption; electrical resistivity and properties of gas-sensitivity were investigated.

[1]. J.Zhang ,B.K.Miremadi ,K.Colbow , Journal of Materials Science Letters 13 (1994) 1048 -1050

[2]. Vo Vong, Nguyen An, Nguyen thi Huong, Proceedings of the 2nd International Workshop on Materials Science (IWOM'95) Hanoi Oct. 1995 Part 1. p. 232 -235

15P34

CRYSTAL MORPHOLOGY OF $Y_3Fe_5O_{12}$ GROWN BY TSSG TECHNIQUE AND BY LPE METHOD.

S. J. Chung, H. M. Park* and D. Y. Choi, School of Materials Science and Engineering, Seoul National University, Seoul 151-742, *Materials Evaluation Center, KRISS, Taejon 305-600, Korea

Single crystals of YIG were grown from high temperature solution by TSSG technique and YIG films were grown on GGG substrates by LPE method.

For the growth of single crystals, the slow cooling method as well as the temperature gradient transfort method were used.

The relative growth rates between {211} faces and {100} faces which are depended on the flux compositions and cooling rates were reported in the previous work[1]. By plotting the cooling rate versus the relative growth rate, it was observed that the {110} faces developed predominently in a low supersaturated solution, whereas the {211} faces developed well in a high supersaturated solution.

The {211} and {110} facets were also well developed at the edges of the YIG film grown by LPE method. The measured growth rate ratio in direction of <211>, <110> and <111> at a supercooling of 50¡É was 1 : 1.2 : 8. This result fit well to the previous plot of the relative growth rates. The growth form of YIG depended on the relative growth rate of the {211} faces against the {110} faces can be predicted in a given measure.

1. Park H.M., Seo K. I., and Chung S.J. (1993) J. Crystal Growth 134, 43-50.

15P35

TWINNING AND ORIENTATION CHARACTERISTICS OF HTSC EPITAXIAL THIN FILMS

I.K.Bdkin ; Institute of Solid State Physics, Chernogolovka, Moscow dist. 142432, Russia A.D.Mashtakov, G.A.Ovsyannikov ; Institute of Radio Engineering and Electronics, Moscow, 103907, Russia

Using X-ray diffraction methods, we have studied the structure of epitaxial(001) YBCO thin films on (110) $NdGaO_3$ substrates and (001) YBCO/(100)CeO_2 thin films on (10-12) Al_2O_3 substrates. The YBCO/CeO_2 films were produced successively. The growth of the CeO_2 buffer layer on r-cut sapphire substrate preceded the growth of the YBCO film. The epitaxial (100) CeO_2 buffer layers were deposited using RF-magnetron sputtering technique at growth temperatures 620-770℃. The thickness of these layers is 300 Å. The (001) YBCO films (the thickness is 1300 Å) were grown with high oxygen pressure DC-sputtering technique. The structural parameter (c=11.65 Å) of YBCO films is corresponded to superconducting $YBa_2Cu_3O_7$.

Twinning structure of these films from analysis (103) and (113) YBCO reflections were investigated. Disorientation between films and $NdGaO_3$ substrates were found. YBCO films on Al_2O_3 substrates have part twinning structure.

Disorientation of CeO_2 and YBCO grains about the direction in the surface of the substrate is 0.7° and 0.8° correspondingly. It shows a correlation in the disorientation of YBCO and CeO_2 grains in this direction.

Topographies in asymmetrical geometry demonstrate different disorientation in the direction in the plan of the surface and in the prependicular direction of the surface for CeO_2 and YBCO. The disorientation in the plan of the surface fpr CeO_2 is 1.2° and for YBCO is 0.8° . It means that grains of YBCO grow on determinably orientation grains of CeO_2 or its disorientates are realized in opposite direction to disorientation of CeO_2 grains.

These results illustrate that these multiple films may have not only interesting physical characteristics but quality of these films may be better when single layer films.

Very strong interaction across CeO_2 buffer between film and Al_2O_3 substrate was studied on complex and part growth films. The part with YBCO films shows increase X-ray diffraction on reflections from Al_2O_3. This is reflect influence YBCO film on substrate. It is possible because use dynamical perfect substrates. The nature of this interaction now is not understand.

15P36

STRUCTURAL CHARACTERIZATION OF SOME NEW IONIC AND MIXED CONDUCTORS BASED ON Li_4GeO_4

R.P. Gunawardane, M.A.K.L. Dissanayake and H.H. Sumathipala
Faculty of Science, University of Peradeniya, Peradeniya, Sri Lanka.

Three new types of Li_4GeO_4 based solid solutions with γ-LISICON structure have been found. In the Li_4GeO_4-Li_3CrO_4 binary system[1], an extensive range of solid solutions $Li_{3+x}Cr_{1-x}Ge_xO_4$ with γ-LISICON structure has been found for $0.30<x<0.92$ with probable solid solution mechanism Cr^{5+} $Li^{+}+Ge^{4+}$. These solid solutions are unusual in containing Cr in the +5 oxidation state. X-ray powder diffraction data for the γ solid solution can be indexed on an orthorhombic unit cell, space group Pmnb, and are very similar to those of other γ -phases such as γ-Li_3PO_4 and LISICON. Li^{+}ion conductivity increases with x; at x=0.90, σ (bulk)~1.4×10^{-5}S cm^{-1} at 27°C rising to 0.044 S cm^{-1} at 300°C. These ionic conductivities are among the highest found for solid Li^{+}ion conductors in the LISICON/ γ family.

In the Li_4GeO_4-Li_2CoGeO_4 system[2], a new LISICON type γ-solid solution range with formula $Li_{4-2x}Co_xGeO_4$ has been found for $0.15<x<0.8$. Powder X-ray diffraction data for the γ -solid solution can be indexed on an orthorhomsic unit cell, space group Pmnb, similar to γ-Li_3PO_4 structure. The highest net conductivity, 8.4×10^{-6} Scm^{-1}, was observed for x=0.25 at 27°C, Charge/discharge polarization measurements and low frequency a.c. impedance measurements show the occurrence of mixed Li^{+} ion and electronic conductivity in the material. The relative amounts of each type vary with composition:

In the Li_4GeO_4-Li_2SO_4 binary system, a new LISICON type γ solid solution range with formula $Li_{4-2x}Ge_{1-x}S_xO_4$ has been found for $0.08<x<0.42$. The γ -solid solutions are structurally related to orthorhombic γ-Li_3PO_4 and contain interstitial Li^{+}ions.

1. M.A.K.L. Dissanayake, R.P. Gunawardane, H.H. Sumathipala and A.R. West, (1995), Solid State Ionics 76, 215.
2. H.H. Sumathipala, M.A.K.L. Dissanayake and A.R. West, (1996), Solid State Ionics, 86-88, 719.

INTERATOMIC INTERACTION OF THE RUTILE-TYPE DIFLUORIDES OF FIRST-ROW TRANSITION METALS BY EXTENDED X-RAY ABSORPTION FINE STRUCTURE

K. Murai[1], A. Yoshiasa[1], O. Kamishima[2], K. Nakajima[1] and T. Yamanaka[1]
[1]Dept. of Earth and Space Science, Faculty of Science, Osaka University
[2]Faculty of Science, Tohoku University

The rutile-type structure is found in many dioxides. The rutile samples in this study, difluorides of the first-row transition-metals, MF_2 (M=Mn, Fe, Co,Ni), are important materials from the view point of electronic and magnetic properties.

In general, MF_2 except such as FeF_2 is characterized by four shorter coplanar M-F than two axial bonds in MF_2 octahedron. The second- and third- neighbors surrounding the M cations are two and eight cations, respectively. In this study, we could obtain a detailed information about the thermal vibration of atoms by the analysis of Extended X-ray Absorption Fine Structure (EXAFS) Debye-Waller factor. We discuss on the atomic momentum in the local structure of the difluorides. The Debye-Waller factor by EXAFS is sensitive to short-range correlation of the mutual atomic motions.

The Mn, Fe, Co and Ni K-edge EXAFS spectra were measured in the temperature range 20K~800K, at the Photon Factory in the National Laboratory for High Energy Physics, Tsukuba. A X-ray mirror was used in order to eliminate the higher order harmonics. Ionization chambers were applied as transmission beam intensity detectors.

The displacement correlation functions (DCF) for each neighbor atom were determined by using both the mean square relative displacement (MSRD) and the mean square displacement (MSD) by X-ray diffraction. In FeF_6 octahedron in FeF_2, two apical bonds exhibit the vibration with strong correlation (DCF/MSD:75%). On the other hand, four equatorial bonds have the weak correlation (DCF/MSD: 30%).

The lattice constants a and c are calculated from the second- and the third- neighbor cation-cation distances. Thermal expansion of c-axis of MnF_2, CoF_2, NiF_2 is larger than that of their a-axis, while the expansion along c-axis in FeF_2 is smaller. Furthermore the parameter in FeF_2 decreases with higher temperature. These are consistent with the results from the force constants obtained by EXAFS Debye-Waller factor.

15P38

STRUCTURAL STUDIES OF SOME INCLUSION COMPLEXES INVOLVING β-CYCLODEXTRIN AND ALKYL(AQUA) COBALOXIME

H.K.Fun AND K.Chinnakali X-ray Crystallography Unit, School of Physics, Universiti Sains Malaysia, Penang, Malaysia.
X.Ping, Y.Chen AND H.L.Chen, Coordination Chemistry Institute, State Key Lab of Coordination Chemistry, Nanjing University, Nanjing, P.R.China.

Cyclodextrins (CD) are amongst the most fascinating naturally occuring molecular receptors to a variety of inorganic and organic molecules. Since the non-covalent host-guest interactions have been widely accepted in substrate-enzyme interaction model, CD's and their derivatives have been developed as artificial enzymes to catalyze many reactions. The alkyl(aqua)cobaloxime can form inclusion complexes with α and β-CD's both in aqueous solution and in solid. From the crystal structure study, it has been found that the structure and conformation changes of the alkylcobaloxime induced by cyclodextrin are similar to that between 5'-deoxyadenosylcobalamin and protein in the B_{12}-dependent enzyme system (1). In continuation of this study, the crystal strucures of four inclusion complexes involving β-CD and alkyl(aqua)cobaloxime have been determined and their results will be presented.

1. Luo, L.B., Chen, H.L., Tang, W.X., Zhang, Z.Y. & Mak, C.W.(1996) J.Chem.Soc. Dalton Trans., 4425-4430.

CLATHRATE COMPOUNDS OF MONOALKYLTRIMETHYL-AMMONIUM SALT AND NON-PLANAR AROMATIC MOLECULES

K. Noguchi, Y. Sumimoto, and K. Okuyama, Faculty of Technology, Tokyo University of Agriculture & Technology

Monoalkyltrimethylammonium salts form clathrates with various aromatic compounds not only by recrystallization from their solution, but also by grinding host and guest crystalline powders in a mortar. Normally, host surfactant molecules arrange parallely and build a smectic layer structure, in which alkyl chains interdigitated mutually with the nitrogen atoms found at the layer surfaces. In their clathrate crystals, planar aromatic compounds (guest) are incorporated into the cavities generated by loosening of this mutual interdigitation of alkyl chains. In these cases, the zigzag planes of alkyl chains and the ring planes of aromatic molecules are arranged almost parallel to each other.

Recently, a different type of host–guest interaction was found in the monoalkyltrimethylammonium salt clathrates with 2,2'-dihydroxydiphenyl. Although the guest molecules were located in the cavities that were formed between the alkyl chains, the zigzag planes of alkyl chains and the phenyl planes were nearly perpendicular in these clathrate crystals. 2,2'-dihydroxydiphenyl molecule can not take a planar conformation because of the steric hindrance between the hydroxyl groups at the 2-position of phenyl rings. The host molecules are aligned along the phenyl rings of the guest molecule. With the dihedral angle between the phenyl rings of the guest molecule being about 30°, the alkyl chains of these clathrates exhibit a zigzag arrangement within the layer, which is dissimilar to the earlier findings.

15P40

COMPLEX FORMATIONS BETWEEN SURFACTANT AND AROMATIC COMPOUNDS WITH HETERO-RING

K. Sawada and Y. Ohashi Kokyo Institute of Technology

The micelle structures between the surfactants and the aromatic compounds have been studied on the basis of the crystal structures analyzed by X-rays. Various complexes were obtained from aqueous solutions with cationic surfactants, such as hexadecyl-, tetradecyl-, dodecyl- and decyl-trimethyl-ammonium bromide, and aromatic compounds. The grinding of the two compounds in a mortar gave the same complexes as obtain in the solution. One of the driving forces to form the complexes is the weak interaction between the two kinds of these molecules, alkyl chains - aromatic rings interaction (alkyl-pi interaction).

In this study the complexes between the aromatic compounds with hetero-ring, 2-phenylpyridine and 4-phenylpyridine, and the cationic surfactant, hexadecyltrimethylammonium bromide, were obtained from aqueous-methanol solutions. These complexes were recrystallized several times and washed with the cold water. The single crystals were analyzed using the X-ray analysis. These complexes have the same structures as those of the complexes without the hetero-ring. These aromatic compounds also formed the complexes with the surfactants only by grinding in the mortar without any solution. This shows that the alkyl-pi interaction is formed between the hetero atoms and alkyl chains.

15P41

CRYSTAL STRUCTURES OF PHENANTHRIDINE AND ACRIDINE DERIVATIVES WITH MAGNETIC INTERACTIONS

M. Suzuki, D. Hashizume, M. Yasui, T. Ishida, T. Nogami, and F. Iwasaki
(Dept. of Applied Phys. and Chem., The Univ. of Electro-Communications.)

Crystal structures of phenanthridine and acridine derivatives were investigated by the X-ray method. By the magnetic measurements, the crystals of **1b**, **1c**, and **2c** showed a ferromagnetic interaction, while those of **1a**, **2a**, and **2b** showed an antiferromagnetic interaction.

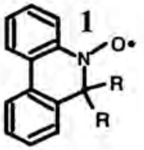

1

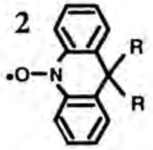

2

1a, 2a : R=*p*-tolyl
1b, 2b: R= *p*-ethylphenyl
1c, 2c : R= propyl

Molecular Structures : The dimension of the phenanthridine skeletons of **1a**, **1b**, and **1c** are similar to each other, while the bond length of N-O radical of **1a** is much longer than those of the other N-O radicals. The acridine skeletons and the lengths of N-O bonds of **2a**, **2b**, and **2c** resemble each other.

Crystal structures : In the crystal of **1a**, the intermolecular O···O distance between the nearest radical O atoms is 2.77Å. This interaction may cause the strong antiferromagnetic interaction and the elongation of the N-O bond. In the crystals of **1b** and **2a**, the overlappings of skeltons are found. These overlappings can interpret a ferromagnetic interaction by using the spin model. The crystals of **1c**, **2b**, and **2c** do not have the overlappings of skeltons and the direct interactions of radical O atoms. The investigation of the electron dencity distribution of **1a** by the multipole expansion method is undergoing.

15P42

STUDY ON A NEW TETRAGONAL PHASE OF NB-DOPED $PB(ZR_XTI_{1-X})O_3$ BY SYNCHROTRON X-RAY POWDER DIFFRACTION

H.C. Liu and H. Toraya, Ceramics Research Laboratory, Nagoya Institute of Technology, Asahigaoka, Tajimi 507, Japan

The crystal structure of a new ferroelectric phase of Nb-doped $Pb(Zr_xTi_{1-x})O_3(x\cong0.97)$ ceramic materials was studied by synchrotron X-ray powder diffraction. It was found that this phase has supperlattice reflections. When these supperlattice reflections were disregarded, it has a tetragonal symmetry with space group P4mm, the cell parameters of a=4.08401(2)Å and c=4.06738(2)Å. The crystal structural parameters of this phase were initially obtained by the direct methods, then refined by the Rietveld method. The structure of this phase is still a distorted ABO_3 perovskite-type. Three structure models with different stoichiometries have been tested in the Rietveld refinement procedure; the results showed that Nb atoms replaced part of Zr/Ti atoms in B site. The chemical formula for this phase should be $Pb_{0.987}Zr_{0.945}Ti_{0.029}Nb_{0.026}O_3$, vacancies occur at A site. The appearance of supperlattice reflections indicates that modulation also exists in this phase. The results of indexing these supperlattice reflections showed that the modulation is along the *c* axis and supper lattice is 10 times of original simple tetragonal cell. Crystal structure and its relationship with ferroelectricity will be described in detail.

15P43

SYNTHESIS AND STRUCTURES OF POLYNUCLEAR COPPER(II)-LANTHANOID(III) COMPLEXES WITH CARBOXYLATE-BRIDGES

Y. Y. Yang, Y-L. Wu and X-M. Chen, School of Chemistry and Chemical Engineering, Zhongshan University, Guangzhou 510275, China

Polynuclear mixed-metal complexes are of current interest in chemistry and are of potential application in material science. We report herewith the synthesis and crystal structures of one dinuclear and one pentanuclear copper(II)-lanthaniod(III) complexes containing pyridinioacetate (pyb, $C_5H_5N^+CH_2CO_2^-$), namely $[CuLa(pyb)_5(H_2O)_5](ClO_4)_5{\cdot}2H_2O$ (1) and $[Cu_3Nd_2(pyb)_{10}(NO_3)_2(H_2O)_8](ClO_4)_{10}{\cdot}4H_2O$ (2). Complex 1 features a dinuclear CuLa cation, in which the Cu and La atoms are bridged by a tetrakis(μ_2-carbxoylate) bridge, the Cu atom is coordinated in a square-pyramidal geometry with the apical position being occupied by an aqua ligand and, the La atom is coordinated in a distorted square-antiprism. In complex **2**, there are two similar dinuclear cores, and the two Cu atoms in two centrosymmetrically-related dinuclear cores are each linked to the central Cu atom by a single *syn-anti* carbxoylate group, resulting in formation of a pentanuclear cation.

Acknowledgment–This work was supported by the NSFC (29625102) and NSF of Guangdong.

15P44

SOLVOTHERMAL CRYSTALLIZATION OF METAL COORDINATION POLYMERS

Samuel M-F. Lo, Stephen S-Y. Chui, Herman H-Y. Sung and
Ian D. Williams* Department of Chemistry, Hong Kong University of Science and Technology, Clear Water Bay, Kowloon, Hong Kong, China
CHWILL@UST.HK

The use of high temperature on of metal coordination polymers is explored. Details are given for several representative examples including [M / TMA]; M = Sr, Cu, Er (TMA = $C_6H_3(COO)_3$) and the mixed-ligand system [M/ 1245 / 4,4'-bipy] M = Zn, Co. (1245 = $C_6H_2(COO)_4$) Coordination polymers of higher dimensionality are formed at higher temperature due to lower ancillary ligation by water or solvent co-ligands. For example the porous 3-D network polymer [Zn_2(1245)(4,4-bipy)] shown below is formed at 180°C over 10 days, lesser times or temperatures leading to 2-D sheet polymers.

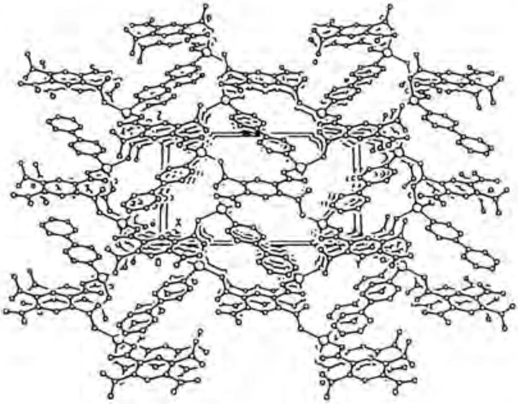

Similar to zeolite syntheses, meta-stable kinetically formed polymers can often be isolated after intermediate crystallization times of 1-2 days. Enhanced crystal growth can be found for thermodynamically favoured products through higher reagent loading or use of longer crystallization times up to one month. The control of these conditions is important for formation of microporous solids which may be regarded as zeolite analogues for absorption or catalysis.

15P45

DIMENSIONAL CONTROL OF INORGANIC SOLIDS: 1-D, 2-D AND 3-D ORGANO-TEMPLATED ZrPOS

Herman H-Y. Sung, Jihong Yu and Ian D. Williams* Department of Chemistry, Hong Kong University of Science and Technology, Clear Water Bay, Kowloon, Hong Kong, China CHWILL@UST.HK

Low dimensional zirconium phosphates have been much studied as systems for intercalation, organic derivatization and proton conductivity. Compared to aluminium phosphates, relatively few organically templated zirconium phosphates have been crystallized. We have now succeeded in synthesizing 1-D, 2-D and 3-D mixed organic ZrPO phases through use of ethylene diamine (en) as a structure directing organic base. [1] Hydrothermal reaction of $Zr(OPr)_4$ with H_3PO_4 in presence of en and HF yields three crystalline phases; the 1-D $[enH_2][Zr(HPO4)_3]$ **1**, which grows as needles up to 1mm in length, the 2-D $0.5[enH_2][Zr(PO_4)(HPO_4)]$ **2**, which is found as thin plates, and the fluorinated 3-D open-framework $0.5[enH_2][Zr_2(PO_4)_2(HPO_4)F].H_2O$ 3. [2]

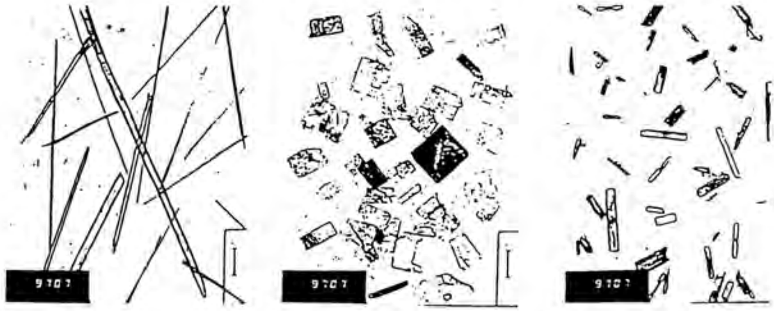

Vari-dimensional Crystals of the 1-D and 2-D and 3-D ZrPOs **1**, **2** and **3**

1.Sung,H.H-Y., Yu,J. Williams, I.D. (1998) J. Solid State Chem., in press
2.Kemnitz, E.Wloka, M., Trojanov, S., Stiewe, A (1996), Angew. Chemie, Int. Ed. Engl. 35, 2677.

15P46

CRYSTAL ENGINEERING OF NLO PROPERTIES OF ORGANIC CRYSTALS USING SACCHARIDE MOIETIES

John A.K. Cha, Kin-ning Hui, Vivian M-F. Chen and Ian D. Williams*
Department of Chemistry, Hong Kong University of Science and Technology, Clear Water Bay, Kowloon, Hong Kong, China
CHWILL@UST.HK

There is much recent interest in the use of supra-molecular chemistry to design crystalline organic materials through control of inter-molecular interactions.[1] One practical application is the orientation of molecular hyperpolarisabilities β to give effective bulk susceptibilities, χ^2 for SHG. Our previous investigations [2,3] reveal that certain sugar acids and related materials such as glucurono-6,3-lactone (GAL) to be potentially useful sub-micron frequency doublers.[3] In addition to these transparent materials we also have been interested in the orientation of high β NLO chromophores such as p-nitroaniline (PNA) and their extended π-system analogues such as stilbenes, through formation of N-glycoside derivatives. We wished to see if in addition to introducing chirality, the hydrogen bonding from the saccharides would assist in overcoming dipole-dipole cancellation and anti-parallel packing tendencies. Whilst we have shown this to be possible for PNA itself, examination of several families of saccharide-derivatised chromophores and more than 100 compounds reveals some intriguing patterns of materials structure-property relationship. It is noteworthy that all 'optimal' SHG materials were found to be derivatised by sugars bearing only 3 rather than 4 hydroxyl groups. Too many H-bonding alternatives may allow an arrangement which also leads to dipole-dipole cancellation and thus a lower energy for the solid. We believe this finding has general implications for crystal engineering when such competing inter-molecular interactions are involved.

1.Desiraju, G., Crystal engineering: the design of organic solids, (1989) Elsevier
2.Bourhill, G., Perry, K., Mansour, K., Khundkar, L., Kern, R.G., Perry, J.W., Williams, I.D., Kurtz, S.K., Chem. Mater., (1993), 5, 802.
3. Chen, J., Li, X., Yang, F., Wang, J., Williams, I.D., J. Cryst. Growth, (1997), 172, 508.

15P47

(BEDT-TTF)-BASED ORGANIC CONDUCTOR SURFACES CHARACTERIZED BY STM

K.Hashimoto[a,b], T.Nakayama[a,c], N.Yoshimoto[d], M.Yoshizawa[d], M.Hara[a], M.Aono[a,e], and I.Yamaguchi[a,b], [a]The Institute of Physical and Chemical Research (RIKEN), [b]Graduate School of Science and Engineering, Saitama University, [c]Core Research for Evolutional Science and Technology (CREST) Program, Japan Science and Technology Corporation (JSTC), [d]Faculty of Engineering, Iwate University, [e]Department of Precision Science and Technology, Osaka University

The organic conductor BEDT-TTF [bis(ethylenedithio)tetrathiafulvalene] (Referred to as ET, hereinafter) salt has a layered structure comprising an anion and a cation (ET). Depending on the kind of anion in the ET salt, the conduction properties of the ET salt are expected to change.

First of all, we observed a surface corresponding to ab plane of a single crystal β-ET_2I_3 by scanning tunneling microscopy (STM). Fig. 1 shows an STM image containing three terraces of different kinds as indicated by A (A'), B and C. The first and the second distinct terraces are identified as an I_3 layer and an ET layer, respectively. As for the third distinct terrace, we propose a model of molecular relaxation in the ET layer.

Experiments, on the deposition of anion molecules on the terraces of ET layer, are being proceeded.

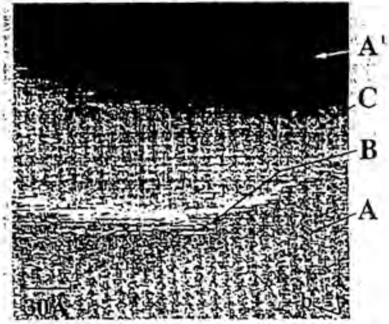

Fig. 1 STM image of β-ET_2I_3 surface

15P48

NEUTRON DIFFRACTION STUDY OF 3-1 PHOTOISOMERIZATION OF THE 3-CYANOPROPYL GROUP IN A COBALOXIME COMPLEX

T. Ohhara, J. Harada, Y. Ohashi (Tokyo Institute of Technolpgy)
I. Tanaka, S. Kumazawa, N. Niimura (JASRI)

It was found that the (3-cyanopropyl)[(*R*)-1-phenylethylamine] cobaloxime complex isomerized to the 1-cyanopropyl cobaloxime on exposure to visible light with retention of the single crystal form. In addition, the produced 1-cyanopropyl group in this isomerization revealed high enantioselectivity.

The X-ray structure analyses before and after the isomerization made clear the reason why the produced 1-cyanopropyl group showed high selectivity. However, the mechanism of this crystalline-state 3-1 isomerization remains equivocal. It must be made clear the intermediate structure, and the relationship between the enantio-selectivity and the hydrogen transfer in the process of the isomerization. The complex of (3-cyanopropyl-d^{α},d^{α})[(*R*)-1-phenylethylamine]cobaloxime was prepared. To reduce the background of neutron scattering, the hydrogen atoms of (*R*)-1-phenylethylamine and cobaloxime moieties were replaced with the deuterium atoms. A crystal with dimension 3.5 x 3.5 x 0.7 mm was irradiated with a xenon lamp for 7 days and the crystal structure was analyzed by neutron diffraction at JAERI.

The analyzed structure indicated that the conversion ratio of the 3-1 isomerization was about 90%, and the 2-cyanopropyl group must be produced as an intermediate structure in the process of the isomerization.

15P49

NEW 4-CIRCLE NEUTRON DIFFRACTOMETER AT JRR3M

Y. Noda Research Institute for Scientific Measurements Tohoku University, A.Kojima and H. Sawa ,Faculty of Science Chiba University, H.Yoshizawa , ISSP The University of Tokyo, and Y. Morii , JAERI Advanced Science Research Center

Neutron 4-circle diffractometer is constructed in the guide hall of the JRR3M reactor at Japan Atomic Energy Research Institute. The system is still under construction and testing. The purpose of this new diffractometer is to carry out a structural physics such as phase transition phenomena and detailed structure analysis of hydrogen and oxide materials, especially by using a single crystal. The components of each circles of the diffractometer are Huber 440 for 2theta- and omega-tables, 420 for phi-table, and 480 for chi-table. The characteristic point of this diffractometer is that the large chi-cradle with the size of 820mm diameter is used in order to mount a heavy accessory such as low temperature cryostat and photographic devices. Mocnochromator is specially designed to focus the beam to horizontal and vertical directions. We use nine Si553 crystals for the monochromator. Each crystal is bent by using metal wire to focus the horizontal beam divergence, and nine crystals mounted on the goniomater head is tilted to focus the vertical direction. The reason to use Si553 is that the diffraction angle for 1 angstrom neutron beam is 90 degree and this angle gives a large advantage for the neutron guide beam line. We plan to develop an asymmetrical monochromator in future to use the advantage of the 90 degree diffraction further more. The scientific activities planed are the structure analysis of a hydrogen-bonded material to study the large isotope effect on the transition temperature, detect a small distortion of oxygen atoms associated with the phase transition of oxide materials such as LaSrCuO and others, and the phase transition of metal-organic compounds.

15P50

INTRAMOLECULAR HYDROGEN BRIDGES AND INTERMOLECULAR INTERACTIONS

U. Englert, G. Heger, E. Kuemmerle and R. Wang
RWTH Aachen and IFF Juelich, Germany

Motivation for the precise determination of the intramolecular hydrogen bridge geometry in compounds of the type $Co(Hdmg)_2L_1L_2$ (left) stems from the fact that the donor-acceptor distance amounts to ca. 2.5 Å, a value quoted in the literature [1] as the critical distance for possible occurence of symmetric hydrogen bonds.

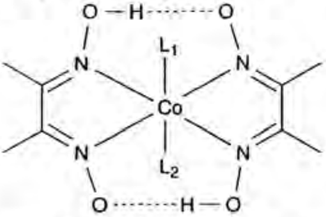

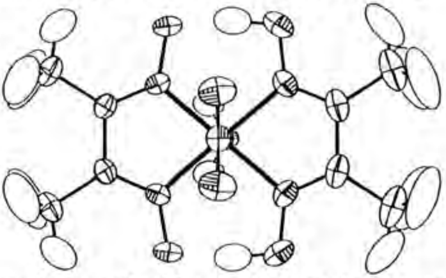

Complexes of the above type have been studied by single crystal x-ray and neutron diffraction, and close correlation between *intra* and *inter*molecular hydrogen bridges has been observed. Intermolecular interactions are responsible for the unexpected hydrogen bridge geometry in the complex $Co(Hdmg)_2(NO_2)(H_2O)$ (PLATON [2] of the neutron data refinement on the right).

[1] Ellison, R. D.; Levy, H. A.: A centered hydrogen bond in potassium hydrogen chloromaleate: a neutron diffraction structure determination. *Acta Crystallogr.* **19** (1965) 260-268.

[2] Spek, A. L.: PLATON-94. University of Utrecht, The Netherlands, 1994.

15P51

Ni$_2$[(m-S)CH$_2$CH$_2$NC(CH$_3$)CHC(CH$_3$)NH]$_2$ DIMER: AN UNEXPECTED N-DEALKYLATION REACTION PRODUCT

K.J. Haller
School of Chemistry, Suranaree University of Technology
Nakhon Ratchasima 30000 Thailand
T. Tuntulani and B. Tomapatanaget
Department of Chemistry, Chulalongkorn University
Bangkok 10330 Thailand

Installation of a Bruker Analytical X-Ray Systems P4 single crystal diffractometer has just been completed at Suranaree University of Technology. SUT ís P4 is the third single crystal x-ray system to be purchased in Thailand.

The condensation reaction of acetylacetonate and 2-aminoethanethiol in the presence of nickel was carried out in an attempt to produce an inexpensive nickel Ni$_2$S$_2$ complex for further reactions. Spectra of the isolated product did not match the anticipated product.

X-ray structural analysis showed the product to be the square planar dimeric nickel Ni$_4$S$_2$ title complex of this report. In addition to the unexpected loss of one of the ethanethiols, one of the bridging methylene protons of the acetylacetonate is also lost as shown by the planarity of the N2 chelate rings (maximum deviation 0.016%). The Ni-Ni distance is 2.757(1)Å, the butterfly angle of the Ni$_2$S$_2$ core is 69.4° and the angle between the two coordination planes is 73.8°. Further details of the structure and a proposed reaction scheme will be given.

Recrystallized by liquid diffusion of diethyl ether into a methanol solution as red plate crystals. Crystal Data: $C_{14}H_{24}N_4S_2Ni_2$, MW=429.91, orthorhombic Pbca (No.†61), a=13.555 (3), b=11.206 (2), c=23.501(5) Å, V=3569.9 Å^3, T=295±1 K, z=8, d_{calc}=1.60 Mg m-3, μ=2.34 mm^{-1}, MoKα radiation, F(000)=1792., sinq/l$_{max}$=0.557 Å^{-1}, R_{int}=0.034, 2566 unique data, 2215 Fo>4σ(Fo), R1=0.043, wR2=0.087.

Author Index

The Smart
Heat Capacity System
by Quantum Design:

We listened.

The QD Heat Capacity System's fully automated measurement/data analysis capabilities save countless hours and eliminate analytical errors.

A sophisticated fitting technique enables the system to accurately model the effect of heat flow between the micro calorimeter chip and the sample (tau1), as well as the heat flow between the chip and the sample mount (tau2).

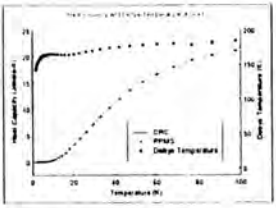

Heat capacity of a gold sample on the PPMS in comparison with CRC values. Each triangle is three overlapping symbols; there has been no averaging.

- **Automated relaxation micro-calorimetry**
- **Easy sample mounting**

Introducing the world's first Smart Heat Capacity System, built on the proven architecture of Quantum Design's popular Physical Property Measurement System (PPMS). This system is designed with three things in mind: extraordinary functionality, a high degree of accuracy, and unprecedented ease of use.

Sample mount with the micro calorimeter chip

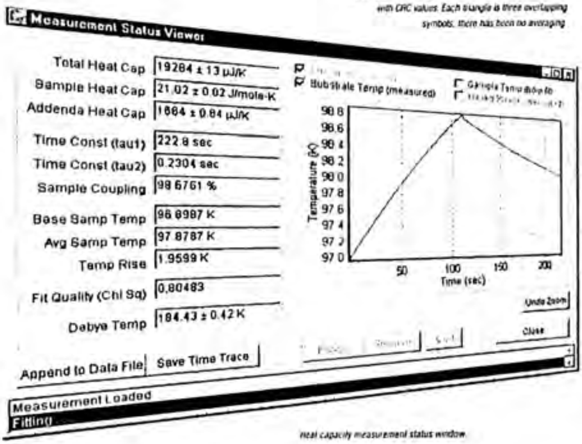

Total Heat Cap 19284 ± 13 µJ/K
Sample Heat Cap 21.02 ± 0.02 J/mole-K
Addenda Heat Cap 1664 ± 0.84 µJ/K
Time Const (tau1) 222.8 sec
Time Const (tau2) 0.2304 sec
Sample Coupling 98.6761 %
Base Samp Temp 96.8987 K
Avg Samp Temp 97.8787 K
Temp Rise 1.9599 K
Fit Quality (Chi Sq) 0.80483
Debye Temp 184.43 ± 0.42 K
Append to Data File
Measurement Loaded
Fitting

Heat capacity measurement status window

The Heat Capacity System includes an intelligent, user-friendly software package with built-in data subtraction to correct for the contribution of elements extraneous to the sample.

Temperature Range: <0.5 - 350K
Fields up to 14 Tesla

- **Two quantitative values (curve fit and sample coupling) for data quality assurance**
- **Automatic calculation of the Debye temperature at each point**
- **Auto-calibration and built-in addenda subtraction**

You asked for an accurate, flexible heat capacity system. As usual, Quantum Design was listening.

Quantum Design

Phone: 1-619-481-4400
Fax: 1-619-481-7410
www.quandsn.com
Email: info@quandsn.com

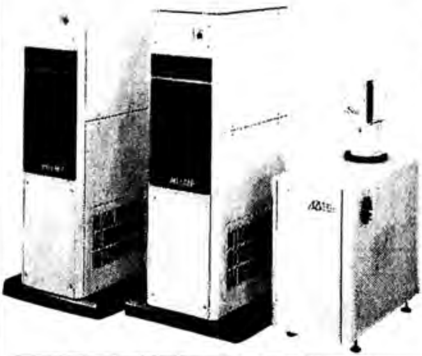

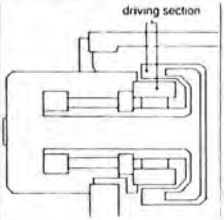
driving section

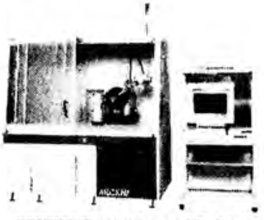

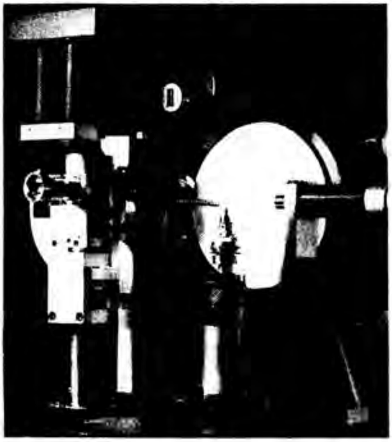

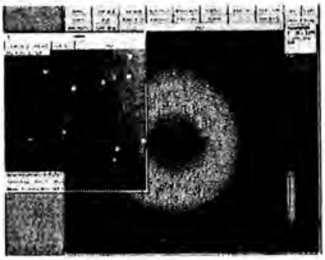

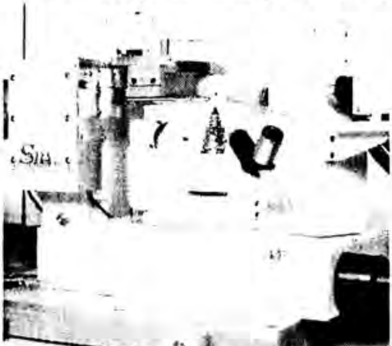

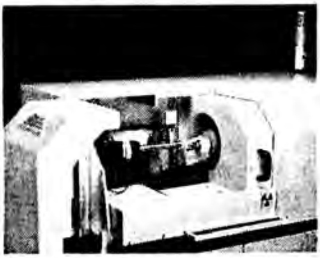

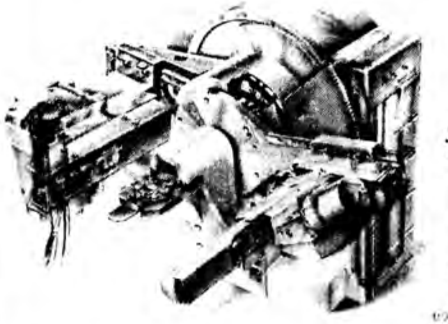

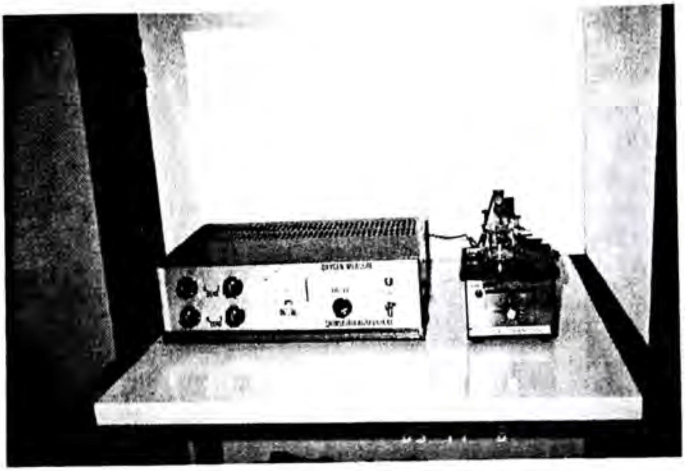
FUJICOLOR HR 65

Rigaku

High performance and simple operation in a compact configuration

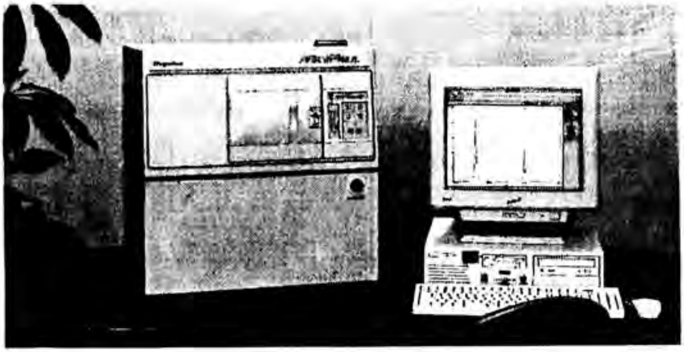

MiniFlex

Rigaku/Desktop X-ray Diffractometer

Application Example

- Quantitative analysis of asbestos and free silicic acid
- Quantitative analysis of cristobalite contained in concrete skeleton material
- Quality control of pharmaceuticals
- Pattern measurement of crystals, noncrystals and polycrystals
- Experimental tool for high school and college students
- etc.

Standard Measurement Software

The Miniflex software with multiple functions is easy to use.

Standard Data Processing Software includes the following:

- Profile smoothing
- Background subtraction
- $K\alpha_2$ removal
- Peak search
- Calculation of integrated intensity

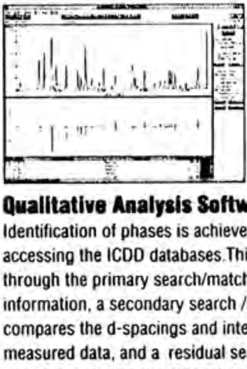

Qualitative Analysis Software (option)

Identification of phases is achieved through accessing the ICDD databases.This is accomplished through the primary search/match to ICDD card information, a secondary search /match which compares the d-spacings and intensities with the measured data, and a residual search/match which is performed after excluding the major components.

Quantitative Analysis Software (option)

Jade*(option)

- Each software works in a Windows environment.

*Jade is a product of MDI

Rigaku International Corporation
Rigaku Corporation
3-9-12, Matsubara-cho, Akishima-shi, Tokyo 196-8666, Japan Phone 81-42-545-8189 Fax 81-42-545-7985 e-mail rinttyo@rigaku.co.jp Telex J26418 RINT


NEW

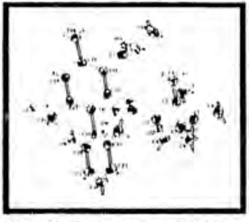

BANDAR BARU BANGI

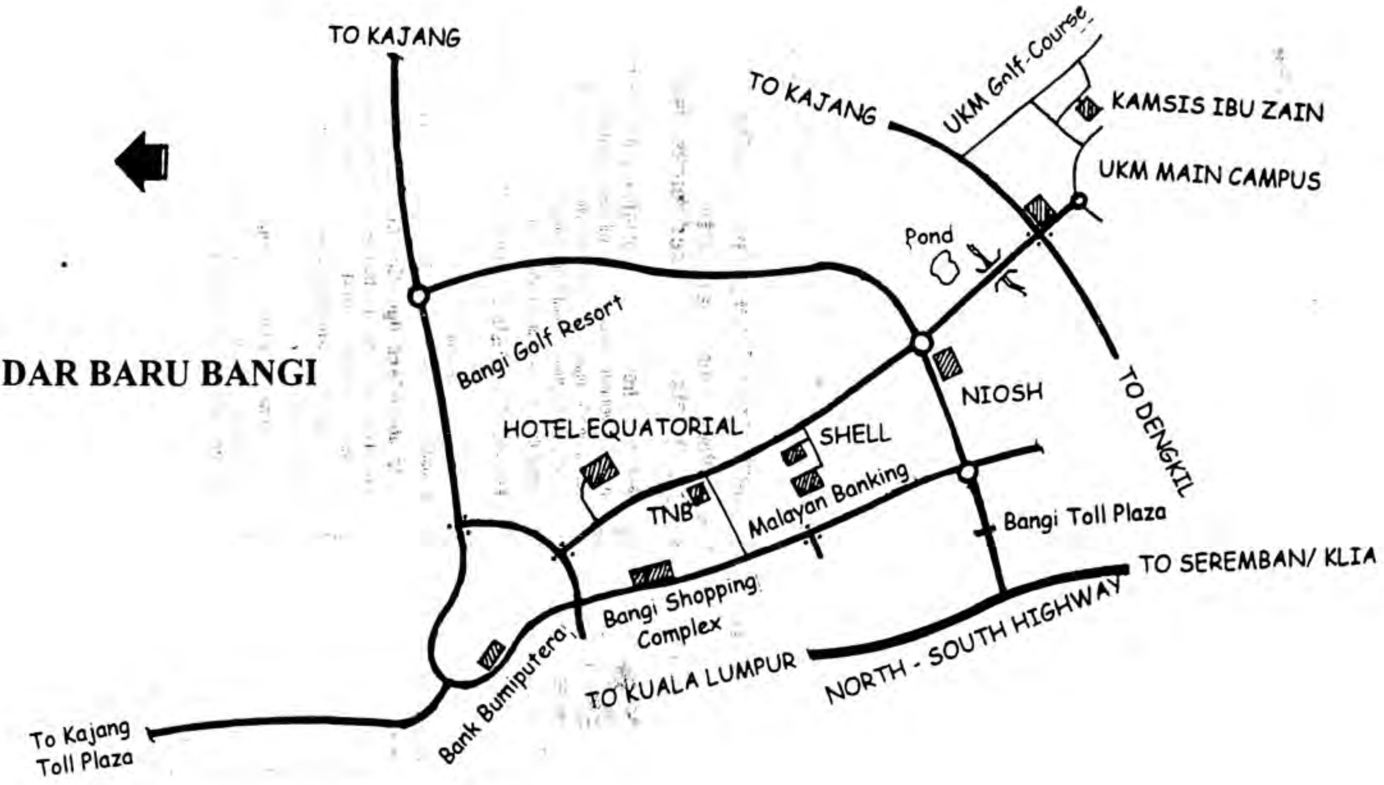

DESIGN AND PRINTED BY CENTRE FOR EDUCATIONAL TECHNOLOGY , UKM •1998